

Alma Mater Studiorum – Università di Bologna

DOTTORATO DI RICERCA IN

**Scienze Farmacologiche, Tossicologiche, dello
Sviluppo e del Movimento Umano**

Ciclo XXIX

Settore Concorsuale di afferenza: 03/D1

Settore Scientifico disciplinare: CHIM/08

Design, synthesis, and biological evaluation of new agents for the
treatments of chronic degenerative diseases

Presentata da: Nibal Betari

Coordinatore Dottorato

Prof. Patrizia Hrelia

Relatore

Prof. Vincenzo Tumiatti

Correlatore

Dr. Andrea Milelli

Esame finale anno 2017

Acknowledgments

I left Syria when the war erupted, and left behind all my memories, took with me nothing but my masters, my father taught in my early childhood, that whatever you achieve in your life, your scientific achievement is the only thing that will secure you in the future.

When I arrived to Italy, I was full of fear, the fear of future and the unknown, but it didn't took me long, to realize that I am in the right place, blessed by having new people in my life, who became close to me as my family, and because of them I became the person that I am now.

First and foremost, I would like to thank my Professor Vincenzo Tumiatti for his help and support during these three years spent together. I appreciate all his contributions of time, his patience, enthusiasm, immense knowledge and his guidance supported me through this long journey of PhD.

A special thank goes to Dr. Andrea Milelli, who helped me a lot to achieve what I am presenting in my PhD, Dr. Andrea was always there for me, providing me with all the experience he has to be a good example for foreign students.

A special thank goes to Professor Diego Muñoz-Torrero López-Ibarra, I'll never forget the days I spent in Spain, and the way Prof. Diego and his team treated me, they just made me feel I'm home, the trust Prof. Diego gave me helped me to increase my self confidence and to become a better researcher, he supported me with the whole needed academic experience that's required to complete my trip in PhD.

My gratitude goes also to my friends, the research team, the admiration of the university and the scholarship administration, for the continues help and support, for the prompt replies to my needs and questions, for all the efforts they put to facilitate my life here.

The greatest thank goes to my family, to my parents in Damascus, who are living the war in Syria, but their thoughts are always with me. My siblings Nidal, Nor and Nael, my nieces Alma and Ritta, who the war spread them all over the world, but this never stopped them from being with me giving me all the courage and support I need.

Last but not least, thanks from all my heart goes to the person who showed up accidentally in my life, and turned to be the closet person to me, my spring of strength and hope, to my person Dr. kristoffer Sahlholm, all the appreciation and thanks for your neverending support and encouragement and for drawing the smile in my life and face.

Contents

Preface	5
Abstract	6
Chapter 1. Introduction to Alzheimer's disease	10
1.1 Theories on the Causes of Alzheimer's Disease	12
1.2 Therapeutical Approaches to AD	25
1.2.1 Cholinomimetic Therapy	26
1.2.2 Anti-amyloid Strategies	28
1.2.3 Antioxidant therapy	33
1.2.4 Targeting NMDAR-mediated neurotoxicity	34
1.2.5 Cholesterol-reducing approach	35
1.2.6 Metal-chelating approach	35
Chapter 2. Glycogen synthase kinase 3 (GSK-3) functions and structure	38
2.1 Crystal structure of GSK-3	38
2.2 Regulation of GSK-3 activity	40
2.3 GSK-3 substrates	41
2.4 Involvement of GSK-3 in human diseases	43
2.4.1 GSK-3 and diabetes Type 2	44
2.4.2 GSK-3 and Cancer	44
2.4.3 GSK3 and inflammation	45
2.4.4 GSK3 and Nervous system disorders	45
2.4.4.1 Prion diseases	46
2.4.4.2 Parkinson's disease (PD)	46
2.4.4.3 Huntington's disease (HD)	46
2.4.4.4 Ischemic stroke	46
2.4.4.5 Human immunodeficiency virus type 1 (HIV-1)	46
2.4.4.6 GSK3 signaling in Alzheimer's disease pathogenesis	47
2.5 Targeting GSK3 in drug discovery	49
2.5.1 ATP-competitive GSK-3 inhibitors	51

2.5.2 Non-ATP competitive GSK-3 β inhibitors	52
2.6 Drug Design	55
2.7 Methods	59
2.8 Results and Discussion	67
2.8.1 The evaluation of GSK-3 β inhibition	67
2.8.2 Results and Discussion for the compounds (1-13)	67
2.8.3 Mechanism of action for the compound 13	68
2.8.4 In vivo Evaluation for the compound 13 by using zebrafish model	69
2.8.5 Results and Discussion for the compounds (14-23)	70
2.9 Conclusion	72
2.10 Experimental Section	73
Chapter 3. The “Multi-Target- Directed Ligand” approach in AD	83
3.1 Multi-target-directed ligands developed in Diego Muñoz-Torrero group	91
3.2 Drug design	96
3.3 Methods	98
3.4 Results and discussion	103
3.4.1 Activity toward cholinesterases	103
3.4.2 A β 42 aggregation inhibition assay in intact <i>Escherichia colic</i> cells overexpressing A β 42 and tau	104
3.4.2.1 Activity toward A β 42 aggregation	105
3.4.2.2 Activity toward tau protein aggregation	106
3.4.3 Activity toward BACE-1	107
3.4.4 Antioxidant activity	108
3.4.5 In vitro BBB permeation assay	110
3.5 Experimental Section	112
3.6 Conclusion	113
Chapter 4. Epigenetic modifications and AD diseases	122
4.1 The biological role of Histone Acetylases and Histone Deacetylases	123
4.1.1 Histone Acetylases (HATs)	123
4.1.2 Histone deacetylases (HDACs)	124
4.2 The role of HDAC in the development of AD	126

4.3 HDAC inhibitors in therapy	127
4.4 Drug Design	133
4.5 Methods	135
4.6 Results and discussion	138
4.7 Conclusion	141
4.8 Experimental Section	142
Chapter 5 DNA as target: Topoisomerases structures	147
5.1 Introduction to cancer therapy	147
5.2 DNA-Topoisomerases	148
5.2.1 DNA topoisomerases I	149
5.2.2 DNA topoisomerases II	151
5.3 Topoisomerases as Targets for Cancer Chemotherapy	153
5.3.1 Anticancer topoisomerase I-targeted drugs	153
5.3.2 Anticancer topoisomerase II-targeted drugs	155
5.4 Drug design	159
5.5 Methods	161
5.6 Conclusion	165
5.7 Experimental Section	166
Biography	170

Preface

This PhD thesis has been carried out at the Department of Life Quality Studies, Alma Mater Studiorum-University of Bologna (Italy), under the supervision of Prof. Vincenzo Tumiatti and Dr. Andrea Milelli.

The whole PhD thesis is devoted to the study of new agents for the treatments of chronic degenerative diseases, in particular for the treatment of Alzheimer and cancer's diseases. This thesis describes four main projects: the first project is focused on the development of new non-ATP competitive GSK-3 β inhibitors for Alzheimer disease treatment. The second was carried out at Barcelona University in Diego Muñoz-Torrero López-Ibarra's group and this project focused on the development of novel family of rhein-huprine hybrids as MTDLs for AD. While the third project regards design and synthesis of new GSK-3 β -HDAC inhibitors agents as MTDLs for AD. And the fourth one is the development of new topoisomerase inhibitors as potential for the treatment of cancer diseases.

The thesis is organized in different chapters: the first chapter is a brief introduction about Alzheimer's disease. Chapter 2 describes design, synthesis and the biological studies for the new non-ATP competitive GSK-3 β inhibitors. While chapter 3 and 4 contain the drug design approaches used in each project of the new MTDLs agents for AD, including the synthetic methods and the biological evaluation assays of the new synthesized compounds. Results and discussions section and experimental procedures are also reported. Finally chapter 5 describes the drug design approach for the new topoisomerase inhibitors, and explains the synthetic methods and experimental procedures.

Abstract

Alzheimer's disease (AD) is the most common form of dementia, and the one with the strongest societal impact for what concerns incidence, prevalence, and cost of care, it is the sixth leading cause of death, currently it affecting more than 44 million people worldwide, due to its debilitating nature it causes enormous financial and emotional stress on patients and caregivers. Against this backdrop, the governments and industries have increased their support for drug discovery and development. The current FDA-approved therapies for moderate to severe AD provide only temporary and incomplete symptomatic relief and only represent a palliative tool to slow down the clinical course of the disease. The cause for the incredible high attrition rate for AD drug discovery has been attributed to several factors, including the fact that the AD pathogenesis is not yet fully understood. Nevertheless, what is increasingly recognized is that AD is a multifactorial syndrome, characterized by massive deposits of amyloid- β ($A\beta$) peptide, neurofibrillary tangles (NFT) of the hyper-phosphorylated τ protein (P- τ), inflammatory mediators, and reactive oxygen species (ROS), which may lead to neuronal death.

Glycogen synthase kinase-3 β (GSK-3 β), is serine/threonine kinase largely expressed in the central nervous system (CNS), it proved to play a significant role in regulating tau phosphorylation under both physiological and pathological conditions. In particular, GSK-3 β dysregulation is believed to contribute to the etiology of chronic conditions such as cancer, and AD. GSK-3 β , the major kinase responsible for τ hyper-phosphorylation, it is implicated in the formation of $A\beta$ plaques and NFTs. Further, GSK-3 β modulates inflammatory response, axonal transport and microtubule dynamics impairment, apoptosis, cell cycle deregulation, and adult hippocampal neurogenesis impairment.

However, most the available GSK-3 β inhibitors bind to the ATP-binding site which is highly conserved in all the kinome; therefore, such agents indicated low selectivity being able to block the actions of other kinases leading to severe adverse effects. Nowadays, only few non-ATP competitive GSK-3 β inhibitors could reach the clinical investigations, in light of these considerations, the discovery of non-ATP competitive GSK-3 β inhibitors is highly desirable.

This thesis deals with the design and synthesis of new non-ATP competitive GSK-3 β inhibitors; The present study allowed identifying a new GSK-3 β inhibitor in micromolar range, the Study of the mechanisms of action for this synthesised compound revealed that

it behaves as non-ATP competitive GSK-3 β inhibitor, this compound have become an interesting lead-compound, and in order to estimate its toxicity and the bioavailability, it was evaluated in vivo using zebrafish model. This new lead compound was subjected to a structure-activity relationships campaign and further optimization in order to increase its inhibitory potency and the lipophilicity for better pharmacokinetic properties.

In this thesis, we also describe the design of new “Multi-Target-Directed Ligand” able to tackle the multifactorial nature of AD, since AD is a complex multifactorial disease whose insurgence is due to a dys-regulation of different pathways, and various biochemical targets have been indicated to have a fundamental role in their development. Based on their complex nature, MTDLs has been emerged as a promising therapeutical approach able hit several targets responsible for the onset and/or progression of the pathology.

Therefore, having developed a new GSK-3 β inhibitor we used this scaffold to develop GSK-3 β - HDAC inhibitors agents as MTDLs for AD. A study by Sharma et al reported that sub-effective dose combination of lithium chloride (GSK-3 β inhibitor) and Valproic acid (HDAC inhibitor) produced a synergistic neuroprotection against streptozotocin-induced cognitive deficits in rats. Based on this we designed and synthesized new MTDLs able to simultaneously inhibit GSK-3 β and HDAC. The synthesized compounds have been evaluated for their ability to inhibit GSK-3 β by using a luminescence assay, and HDAC by using fluorimetric assay, one of the synthesized compounds turned out to be the best of the series in terms of inhibition of both targets. For this reason, it has been selected for further biological evaluations, in particular, to test its HDAC inhibitory potential in cell, promising results was observed after performing Western blotting analyses in neuroblastoma (SH-SY5Y) cell lines.

A second project related to develop new MTDLs was carried out during research stage at Barcelona University in Diego Muñoz-Torrero López-Ibarra's group; In 2014 Muñoz's group developed novel family of rhein-huprine hybrids as MTDLs for AD, and these compounds endowed ablitly to inhibit AChE and BchE enzymes and A β aggregation, with the aim of increasing the potency of the activity for rhein-huprine hybrids family, and enhance the ablitly to hit several key targets for AD, we synthesised new modified series of rhein-huprine hybrids. The biological screening for the activity of the synthesized compounds performed in vitro and in Escherichia coli cells, they have been shown that these hybrids exhibit good level of inhibitory activities against human acetylcholinesterase, butyrylcholinesterase, and dual A β 42 and tau antiaggregating

activity, and brain permeability, and potent activity as antioxidant, the new synthesized compounds indicated a promising disease-modifying anti-Alzheimer drug candidates.

Cancer is a very complex pathology characterized by a very complex etiology and several biochemical targets have been recognized to play a fundamental role in its development. In particular, in cancer therapy, DNA topoisomerase inhibitors are amongst the most widely used and effective, anticancer drugs target either type I or type II enzymes, have been raised as potential anticancer targets

The principal aim of this research is design and synthesis of new topoisomerase inhibitors as potential new anticancer agents. Scope of this project is the modification of the tryptanthrin scaffold, a natural product that show anticancer properties by inhibit Topoisomerases I and II, to develop more potent and selective agents. Such modifications are achieved by linking several different positively charged chains with the aim of increasing the affinity towards topoisomerases and the cytotoxic activity, the synthesized compounds are currently under biological evaluation towards topoisomerases I and II.

In conclusion, all these studies may represent a promising starting point for the development of new interesting molecules useful for the treatment of cancer and AD diseases.

Chapter 1. Introduction to Alzheimer's disease

Alzheimer's disease (AD) is the most common and well-known cause of dementia affecting the increasingly elderly population. AD is characterized by behavioral, psychological and cognitive degeneration and memory loss, influences the lives of patients and their families.

The countries and regions of the world which are most affected by AD are Western Europe, USA and China. According to the World Health Organization, more than 37 million people worldwide have dementia and AD affects 18 million of them (Mount 2006), it is expected to raise to 81.1 million in 2040 (Ferri 2005). The expansion of dementia elevates with age, increasing from 1% in the 60-64 to between 24 and 33% in those 85 years or older (Blennow. 2006, Ferri 2005).

AD was firstly described by Alois Alzheimer in 1907 during the 37th Conference of South-West German Psychiatrists in Tübingen when he gave a lecture on his 55 year old patient Mrs. Auguste Deter (Alzheimer 1907). He described the observation of the neuropathological lesions, neurofibrillary tangles in the brain of the patient, and her case has showed memory impairment, aphasia, psychosocial incompetence and disorientation, which developed gradually over the remaining years of her life, including experiencing hallucinations and worsening cognitive function. The disease is known today as AD based on describing the work done by Alois Alzheimer in the 8th edition of the book *Psychiatrie* (Emil Kraepelin 1910). The case of Auguste Deter was interesting due to her younger age, as previous patients with such cognitive decline were in 70 years old. After her death, Alzheimer examined tissue sections in her brain using a silver staining technique, from these microscopic analyses, he noticed and reported the presence of fibrillary bundles and small miliary foci, nowadays recognized as neurofibrillary tangles (NFT) and senile plaques (SP) (Lage 2006, Alzheimer 1907).

AD was considered a disease different from dementia in the late 1960's, after the demonstration of some studies (Blessed 1968) that there is relationship between the characteristic hallmarks, SP and NFT, and cognitive decline (Lage 2006). Other researchers suggested that AD was separated from normal aging (Kay 1964) and identified mutations implicated in hereditary forms of the disease (Tanzi.1996). AD is classified into two types: Familial AD (FAD) and Sporadic AD (SAD), epidemiological studies suggest that more than 80% of AD cases are familial caused by mutations in genes and having an early age of onset before 65 years (van der Flier et al. 2011, Miyoshi 2009).

At the opposite, sporadic version has not commonly acknowledged, and causes and risks which are related to the disease are not well understood.

The type of FAD is inherited in an autosomal dominant fashion; it is identified by genetic mutations in the amyloid precursor protein (APP) or presenilin-1 and -2 (PS1 and PS2) genes (Levy 1995; Bayer TA 1999), a family of multi-pass transmembrane proteins constituting the catalytic subunits of the α -secretase intramembrane protease complex. In AD the mutations occurring on PS1 lead to extra amounts of toxic forms of A β peptide, which may aggregate into SP and, probably, damage neuronal messaging leading to neuronal death (Zhang. 2001).

The other type of AD is SAD, in which few members of a family have the disease, it is described as multifactorial disease where various risk factors add up to promote the dysfunction that leads to the symptoms of AD (Grundke 2010). The most relevant genetic factor is the inheritance of the ϵ 4 allele of the apolipoprotein E (ApoE), which enhances the proteolytic breakdown of A β peptide within and between cells. At least one allele is present in 40-80% of SAD cases (Mahley RW 2006), its presence increases the risk of AD by three times in heterozygosis, and by 15 times in homozygosis (Blennow K 2006). Other risk factors linked to SAD include head trauma and vascular-related diseases such as high blood pressure, heart diseases, stroke, and diabetes or high cholesterol levels. In addition, environmental agents such as diet, aluminium and viruses have also been reported as factors involved in the etiology of AD (Grant WB 2002). Since Alois Alzheimer reported the description AD disease (Alzheimer 1907), various theories has been described the cause of AD. In the 1960's, it was reported the relationships between SP and NFT and cognitive decline, attracting the attention of the scientists to intensive research on the causes behind these neuropathological lesions (Lage 2006). The discovery of metal aluminum observed in NFT in AD patients' brains (Perl 1980, Terry, Pena 1965) led to theories that excess of this metal may resulted in AD. Nowadays, this theory is generally outcast due to circumstantial evidences. Currently, theories about AD pathogenesis include the identification of abnormal or large amounts of molecules, such as A β peptide within AD patients' brains. Other studies have indicated that the variations in the brain's homeostatic environment could lead to AD (Crouch, 2007), along with viruses and bacteria (Kamer.2008, Itzhaki 2004) that are able to cross the blood-brain-barrier, as well as the possibility that the immune system loses the ability to proceed efficiently (Giunta 2008, Miklossy 2008).

1.1 Theories on the Causes of Alzheimer's Disease

The following sections discuss some of the foremost theories thought to cause the brain to degenerate and develop AD.

The cholinergic hypothesis:

AD brains are characterized by low levels of acetylcholine (ACh), which is a main neurotransmitter in the brain (Martorana 2010, Contestabile 2010), from this observation it is derived the so-called “cholinergic hypothesis” of AD which states that damaging of the cholinergic pathway in the basal forebrain leading to decrease the cholinergic neurons (Bartus, 2000, Terry 2003), memory disruption and cognitive symptoms (Bartus, 2000). This theory justifies the use of drugs such as donepezil, rivastigmine, and galantamine, together with N-methyl-D-aspartate receptors (NMDA’s) antagonist memantine for the treatment of AD. Unfortunately, these compounds are Cholinesterases (ChE) inhibitors and are only palliative drugs, therefore, acting on the symptoms of the disease and are not able to slow the decline associated with the disease, these drugs act by blocking the activity of Acetylcholinesterase (AChE) leading to maintain ACh concentration in the synaptic cleft and its activity.

The cholinergic hypothesis and cholinesterases:

ChE belongs to family of serine hydrolases; it is implicated in many important physiological processes, e.g. digestion (Whitcomb 2007), blood coagulation (Flemmig 2012) and neurotransmission (Pohanka 2011), which are linked to various diseases such as pancreatitis, thrombosis, and AD.

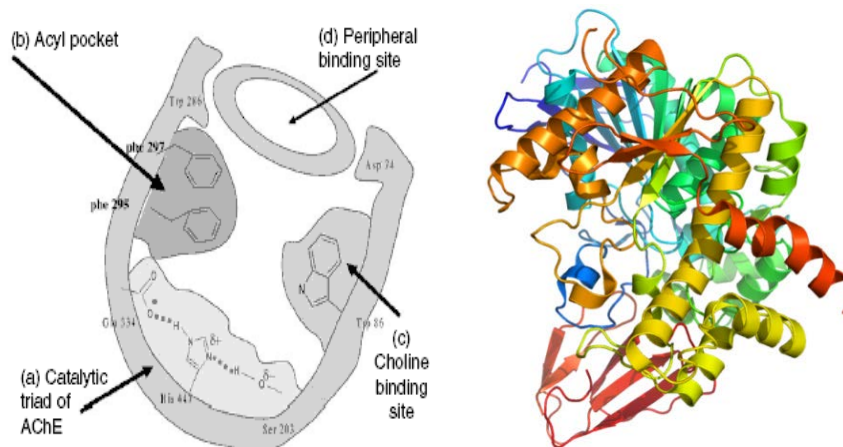


Figure 1: Structure of AChE (Cheung 2012).

The cholinesterases consist of AChE and butyrylcholinesterase (BChE), AChE is considered the main enzyme in the cholinesterase family, in humans, AChE is encoded by a single gene, which localized on the long arm of chromosome 7 at position 7q22 (Getman 1992). Crystallization of AChE has identified the residues involving the substrate binding pocket as well as the catalytic domain, which is responsible for the hydrolase activity. AChE acts as modulator of neurotransmission at cholinergic synapses by hydrolyzing ACh in both central and peripheral nervous system. Keeping the balance of ACh activity is crucial, since it was demonstrated that the lack of ACh decreases receptor stimulation which can be seen for example as the cognitive deficit occurring in AD (Garcia 2005).

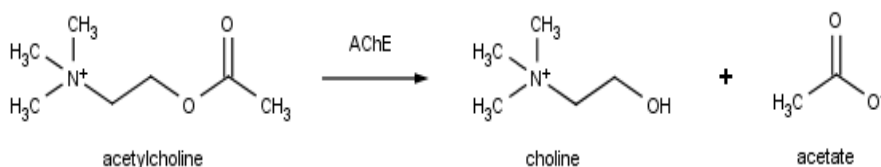


Figure 2: Reaction cascade of acetylcholinesterase hydrolysing acetylcholine.

BChE is a glycoprotein of 340 kDa (Asojo 2011), it has long half-life due to its high amount of glycosylation (Nachon 2002), and it is localized on the long arm of chromosome 3 at position 3q26.1-q26.2 (Gaughan 1991). BChE is more active in the

peripheral tissue than in the brain (Liston 2004), it exists in serum, glial cells, and neurons (Darvesh 1998; Darvesh 2003). BChE is involved in many physiological processes, mainly in the hydrolysis of several choline and non-choline esters, such as ACh (Mesulam 2002), succinylcholine (Kaufman 2011), cocaine (Xue 2011) and aspirin (Masson 1998), thus, it has an important role in neurotransmission, anaesthesia and drug abuse.

The cholinergic hypothesis arose from the fact that there is a significant loss of cholinergic neurons in the brain of AD patients as well as a decreased activity of choline acetyltransferase which catalyzes the production of acetylcholine, leading to decrease neurotransmission and cognitive dysfunction (Whitehouse 1982; Francis 1999; Gauthier, 2002), furthermore, a reduction of the nicotinic and muscarinic receptors has also been reported (Francis 2010).

A strategy of AD therapy is based on the inhibition of AChE and BChE which can contribute to elevate the amount of free ACh, resulting in interact with neuronal receptors (Lane 2006). ChEs inhibitors, by restoring the levels of ACh, play an important role in enhancing the cognitive functions (Liston 2004). AChE has usually been the main drug target even if recently the research has been also focused in the discovery of BChE inhibitors (Darvesh 2007, Decker 2008, Carolan 2010, Nawaz 2011).

Amyloid hypothesis:

β -Amyloid ($A\beta$) peptide derived from APP, the gene encoding for this protein is located on chromosome 21. The amyloid hypothesis suggests that there is a primary imbalance between $A\beta$ production and its subsequent clearance, with enhancing $A\beta$ production in familial disease and reduced $A\beta$ clearance in sporadic disease. $A\beta$ oligomers may block hippocampus activity and damage the synaptic action, resulting in inflammation and oxidative stress caused by the aggregation and depositing of $A\beta$. These pathways together can impair neuronal and synaptic activity causing neurotransmitter deficits and cognitive symptoms. $A\beta$ senile plaques are composed by $A\beta$ insoluble peptides which derived from APP, it consists of 39-43 amino acid residues proteolytically derived from the sequential enzymatic action of β - and γ -secretases of transmembrane APP (Coulson EJ 2000).

App is expressed in cells throughout the body, its amount is influenced by the physiological state of the cells, there are several isoforms of APP, and most of abundant form in brain is constituted APP695. APP could be processed following two different pathways: amyloidogenic and non-amyloidogenic pathway.

- Non-amyloidogenic pathway: It includes the enzyme α -secretase, while amyloidogenic contains two other secretases, β - and γ -secretase, APP cleavage by α -secretase releases a large soluble fragment (α -APP) and the retention of an 83 amino acids fragment.
- Amyloidogenic pathway: β -secretase (BACE) cleaves APP producing an extracellular soluble fragment called β -APP and an intracellular COOH-terminal fragment called C99 that further processed by γ -secretase to generate peptides of different length such as $A\beta_{1-40}$ and the pathogenic $A\beta_{1-42}$, the length of $A\beta$ peptides varies at C-terminal according to the cleavage pattern of APP, being the $A\beta_{1-40}$ the most prevalent form followed by $A\beta_{1-42}$, an hydrophobic form that aggregates faster (Perl DP 2010). Within plaques, $A\beta$ peptides can assume different conformations and polymerize into structurally distinct forms such as fibrillar, protofibrils and polymorphic oligomers (Selkoe DJ 1994).

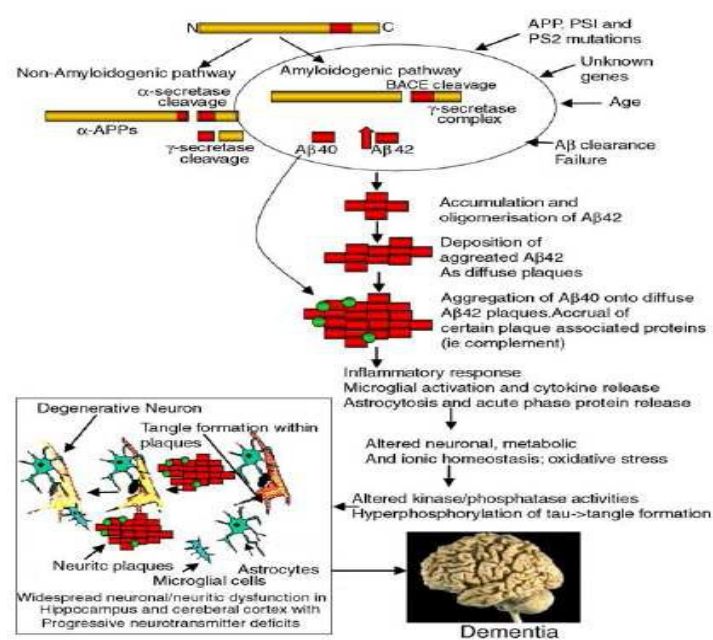


Figure3: The amyloid cascade hypothesis, (VerdileG. 2006).

In normal brain, most of the $A\beta$ peptides consist of 40 amino acids and only about 10% of $A\beta_{1-42}$ peptide, in the brains of AD patients the production of $A\beta_{1-42}$ peptide is increased, and this form is more hydrophobic and more neurotoxic than the $A\beta_{1-40}$ peptide (Selkoe 2001, Findeis 2007), it can be found as monomers, oligomers, protofibrils, fibrils and in the latter stages form of the SP. The presenilin proteins (PS1 and PS2) are essential in the

enzymatic cleavage of the APP, in subsequent it releases β -APP, the mutations in the presenilin genes leading to familial AD, through raising APP cleavage, which results in enhancing the production of β - amyloid (Mudher 2002).

Studies indicated the role of apolipoprotein E type 4 (APOE ϵ 4) in enhancing the risk of late onset AD (Mattson 2004), experiments carried out on transgenic gene knockout animal models, characterized by mutations on APP and PS1 and PS2, illustrated the molecular mechanisms underlying plaque pathology (Mattson 2004, Mudher 2002, Oddo 2003). There is suggestion that amyloid cascade theory contribute to genetically inherit or predisposed people, whereby a ready mutation is present (Mudher 2002).

Other factors could contribute to $A\beta$ formation such as sortilin (SORL1), a neuronal sorting receptor, which monitoring APP processing. Levels of SORL1 have been shown to be reduced in the brains of SAD patients (Rogaeva 2007) and in the brains of individuals with mild cognitive impairment (Sager 2007). SORL1 acts by directing APP into the recycling pathway from enzymatic cleaving by BACE1 and the presenilin proteins. Therefore, BACE1 and the presenilin proteins can not work on APP, can lead to decrease $A\beta$ production; whereas the low levels of SORL1 lead to a direct transit of APP to BACE, resulting in increasing $A\beta$ production.

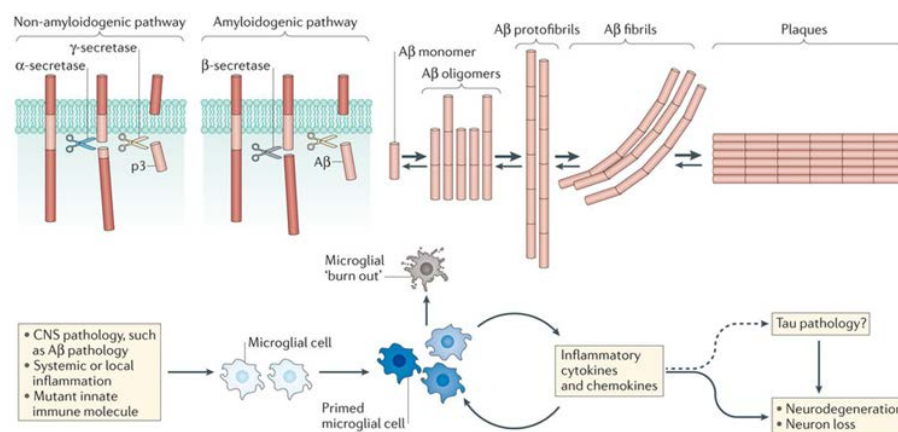


Figure 4: Role of APP cleavage processing in AD and microglial activation (Heppner FL 2015).

Clusterin is chaperone protein implicates in the production of $A\beta$, recent genome-wide association studies in patients with AD, demonstrated that this protein is correlated with the severity and progression of the disease (Thambisetty 2010).

Lipid/cholesterol metabolism is also involved in AD pathogenesis, by influencing the activity of enzymes which contribute in the metabolism of APP and in the production of A β . Studies including AD patients treated with Statins, well-known cholesterol lowering drugs, showed decreasing in the risk of the development of dementia (Jick 2000), but it did not show any improvement in recover cognitive impairment has been observed (Jones 2008). APOE ϵ 4 is involved in the transporting of cholesterolis which are linked to the production of tau, A β and dysfunction of cholinergic neurotransmission (Reiman 2009, Holtzman 2000).

β -Secretase (BACE1):

β -Secretase (BACE-1) is a transmembrane human aspartic protease, known as β -site amyloid precursor protein cleaving enzyme, which exists in high levels in the brain, mostly in neurons, peripheral tissues and in pancreas (L.Katz 1999). BACE-1 enzymatic functions are displayed only in the brain (S.D.Hanton 2001), where it is implicated in the early stage of formation of A β plaques characterized as the major symptoms of AD. In AD neurotoxic A β ₁₋₄₀ and A β ₁₋₄₂ are generated from the APP, which is cleaved by BACE-1, initiating an amyloidogenic pathway. APP can be cleaved by BACE-1 at the M-D bond including in the sequence KMDAE, producing two fragments: an A β N-terminus soluble fragment, called APPs β , and a C-terminus fragment, called CTF99, (S.L.Cole 2008), the last one is then heterogeneously cleaved by γ -secretase, giving neurotoxic peptides A β ₁₋₄₀ and A β ₁₋₄₂.

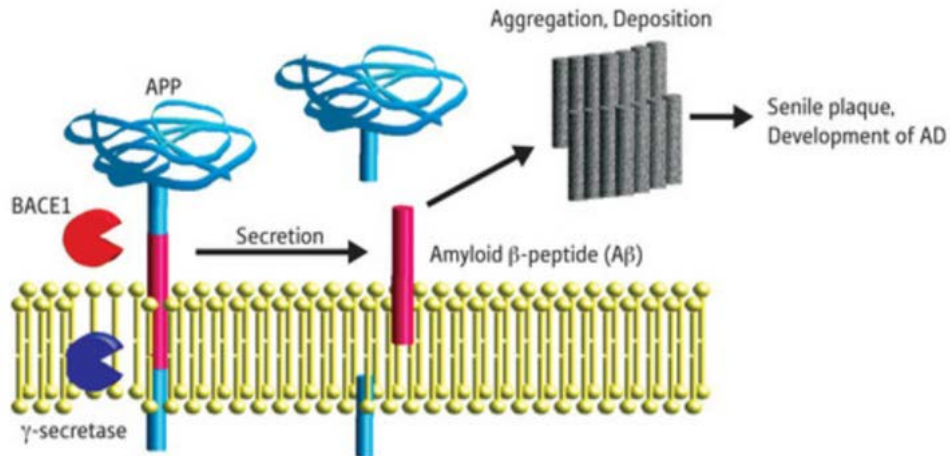


Figure 5: APP is cleaved by BACE1 and secreted as A β , which is thought to be associated with amyloid fibres aggregation and deposition, leading to AD (John 2003).

In the metabolism of APP there is another alternative and non-amyloidogenic pathway, it starts by zinc metallo proteinase α -secretase; this pathway dominates in most cell types. It has been revealed that BACE-1 inhibition decreases A β peptide levels in mouse brain, and up-regulates the α -secretase non amyloidogenic pathway (S. Sankaranarayanan 2008). Since BACE-1 is important for certain hippocampal memory processes (D. De Pietri 2004), its partial blocking may not impact normal learning and memory processes. Therefore, BACE-1 inhibitors have been suggested to have therapeutic advantages in AD.

Tau phosphorylation theory:

Neuropathologically, AD is defined as the presence of intraneuronal neurofibrillary lesions consisting of tau proteins (Forman MS 2004). Tau proteins are mainly found in the axons of neurons, it belongs to the family of microtubule-associated proteins (Tucker RP 1990). Tau protein has six isoforms ranging from 352–441 amino acids in length, formed from MAPT gene which localizes on chromosome 17 (Lace 2007, Brown 1992), these isoforms differ in the numbers of binding domains; recent studies suggested that all tau forms are present in AD (Iqbal 2009, Lace 2007, Andrea 1992).

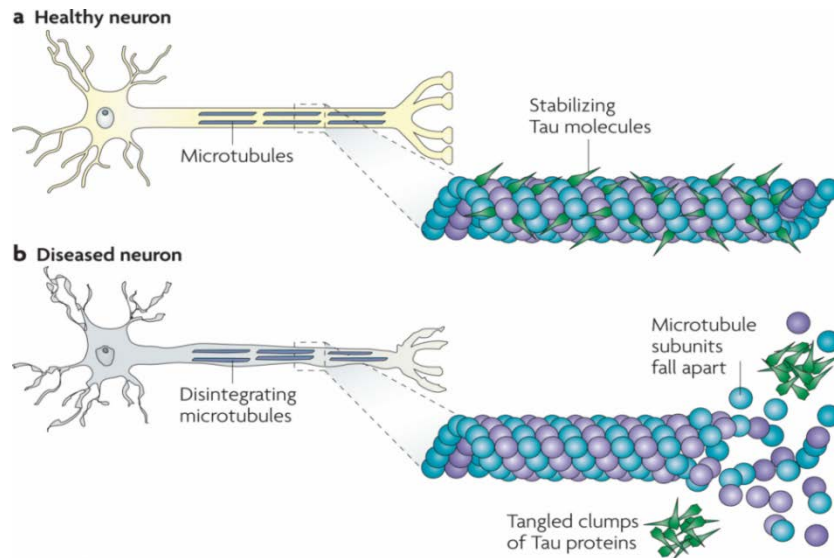


Figure 6: (A) Tau facilitates microtubule stabilisation within cells and is particularly abundant in neurons. (B) In AD the loss of tau function leads to microtubule instability and reduced axonal transport, which could contribute to neuropathology (Brunden KR 2009).

In AD, tau protein is abnormally phosphorylated, that resulting from the imbalance between kinases and phosphatase activities. This phosphorylation occurs at serine and threonine by protein kinases cyclin-dependent kinase-5 (CDK-5), glycogen synthase kinase-3 (GSK-3) and mitogen-activated protein kinase (MAPK). Other kinases including Akt, Fyn, protein kinase A (PKA), calcium-calmodulin protein kinase-2 (CaMKII) and microtubule affinity-regulating kinase (MARK), are also involved in the tau phosphorylation process.

Hyperphosphorylation of Tau; leads to the production of NFTs which are the second major hallmarks of AD. NFTs consist of paired helical filaments PHF- τ , the main component of the NFTs is the protein tau, and microtubule associated protein (MAP) (Grundke 1986) under normal conditions, tau, which is a soluble protein, undergoes phosphorylation and dephosphorylation, forming insoluble aggregates; dysregulation of this process leads to increase the levels of abnormally hyperphosphorylated tau (P-tau 181, P-tau 199, P-tau 231, P-tau 396, P-tau 404), which in turn aggregates into PHF- τ and induces neurotoxicity through the formation of NFT and the disassembly of microtubules (Blennow 2007).

Inflammation:

Inflammation is a defensive mechanism of the body against multiple threats such as infections and injury. It is a complex event that involves both soluble factors and specialized cells (Brown KL 2007). Similar inflammatory processes occur both in the brain and peripheral tissues; in the brain astrocytes and microglia, the activation undergoes under pro-inflammatory conditions, by increasing the production of inflammatory cytokines in CNS, which becomes deleterious leading to progressive tissue damage in degenerative diseases.

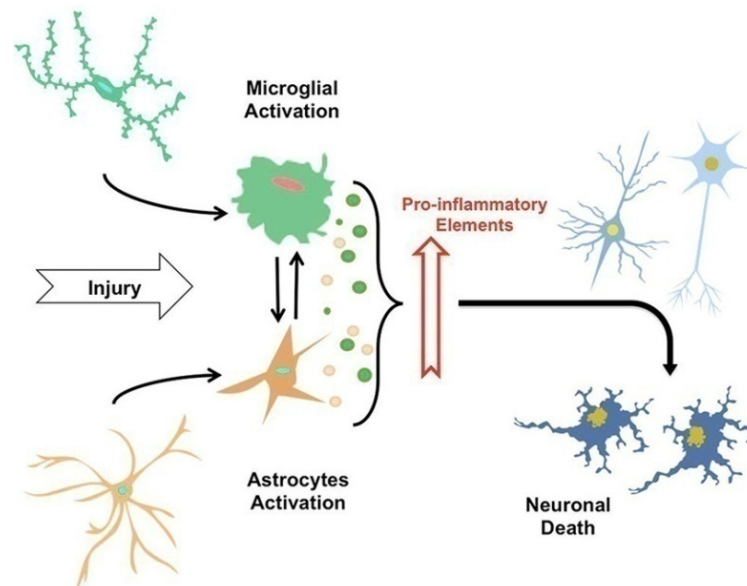


Figure 7: The neuroinflammatory process (Morales I 2014).

Both astrocytes and microglia suffer from gradual activation triggered by damage or injury leading to secretion of pro-inflammatory elements such as cytokines, cytotoxic elements or ROS. The constant exposure to factors causing injuries induces a neuro inflammatory process that eventually triggers neuronal death (Morales I, 2014).

In chronic disorders such as AD, inflammation plays a critical role; indeed, increased neuronal inflammatory mediators such as cytokines and microglia have been observed in AD brains (Wyss-Coray 2002), it has been reported that insoluble fibrillar A β surrounding microglia, reactive astrocytes and dystrophic neurites contributes to the neuronal process of degeneration by initiating a series of cellular events which are able to elicit an immune

response; furthermore, it was suggested that chronic inflammation is a risk factor which plays the major role in AD brain injury (Guo 2000, Mayeux 1995).

Cyclooxygenase (COX), key mediator of the inflammatory cascade, is targeted by non-steroidal antiinflammatory drugs (NSAIDs); some studies showed that anti-inflammatory drugs (more specifically with NSAIDs) did not decrease the risk or delay of AD in patients treated with these drugs (Van Gool 2001), while in other animal models it was observed that NSAIDs lead to decrement of A β deposits without inhibition of COX (Weggen 2001).

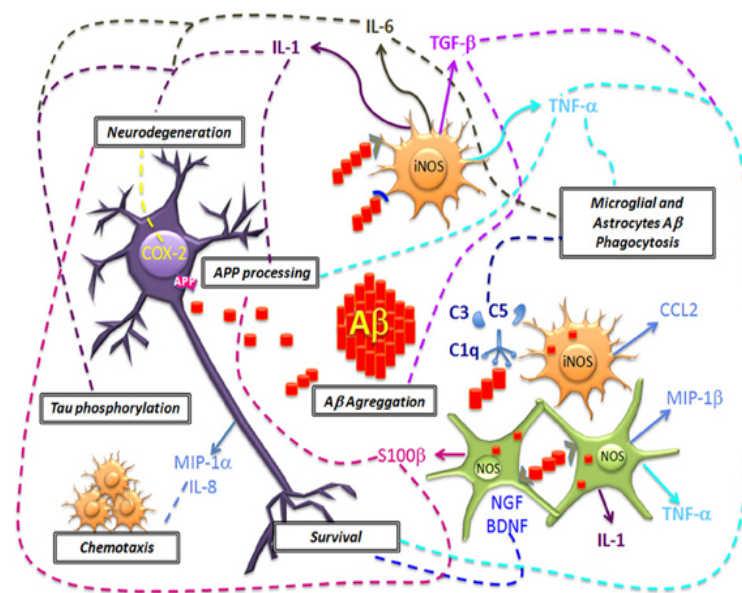


Figure 8: Neuroinflammation in AD condition (Meraz 2013).

Multiple inflammatory mediators are observed in postmortem AD brains (Finch 2007, McGeer 2007). A β deposition in parenchyma and blood vessels has been described to trigger microglial migration and mediate acute and chronic inflammatory response against the aggregates, thus inducing the production of nitric oxide (NO), ROS, pro-inflammatory cytokines such as tumour necrotic factor α (TNF α) or inter leukins-1 β and -6 (IL-1 β , IL-6) and prostaglandin E2 (PGE2), which eventually may promote neuronal death (Kitazawa M2004, Graeber 2010). Microglia makes up 12% of brain cells and they are normally in a 'resting' state controlling the brain (Zilka, 2006), it was suggested that it may have an essential role in synaptic disruption and early event in memory impairment and participation in disease etiology of AD (Cagnin 2001).

Other studies showed that microglia cluster exists around A β peptide aggregation sites, which suggested the role of A β peptide deposits in this microglia activation (Tuppo 2005).

Microglia produces pro-inflammatory molecules such as interleukin-1 β , interleukin-6 and (TNF α), which recruits lymphocytes to inflamed parts by modifying vascular cell adhesion (Ghoshal 2007).

Oxidation and Mitochondrial dysfunction:

Redox reactions are necessary for the generation of ATP and free radical intermediates; they are produced via the establishment of proton gradient in oxidative phosphorylation. Multiple damaging mechanisms coexist in AD pathology, affecting each other at multiple levels (Bernhardi R 2012). Oxidative stress (OS) involves in the impairment of many biological macromolecules, it is considered being a hallmark of neurodegenerative diseases. OS resulting from the imbalance in prooxidant/antioxidant homeostasis leads to the production of toxic reactive oxygen species (ROS), such as hydrogen peroxide, nitric oxide, superoxide and the highly reactive hydroxyl radicals. Constant evidence reported that ROS and reactive nitrogen species (RNS) mediated injury, are observed in AD (Praticò D 2008). Studies in animal models indicated that oxidative damage precedes the pathological modifying correlated with AD (Nunomura 2001).

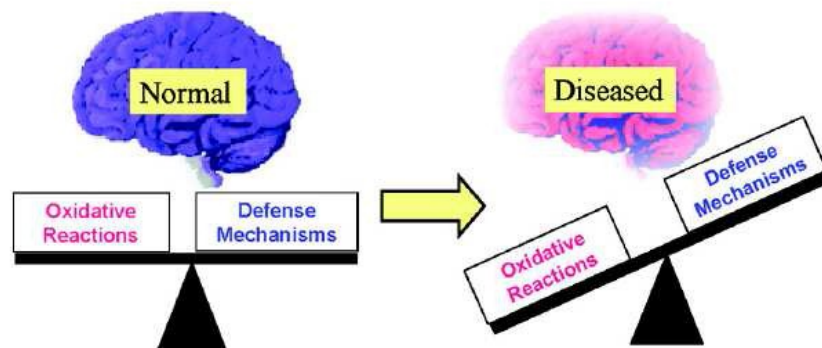


Figure 9: Imbalance in pro-oxidant/antioxidant in normal and pathological condition (Sayre, L.M.2008).

ROS can directly oxidize and destroy DNA, lipids and proteins and enhance stress-responses, resulting in apoptosis through mitochondrial process (Altman 2010, Casadesus 2007). Based on these observations, the “oxidative stress hypothesis of AD” stated that oxidative stress is a key event in both the onset and progression of this disease. OS is a wide spread cellular process that currently lacks specific biochemical targets for

atreatment, such as a receptor or a single major metabolic pathway (Galasko DR 2012). In AD, there are established connections between OS and other key AD events, which amplify its complexity.

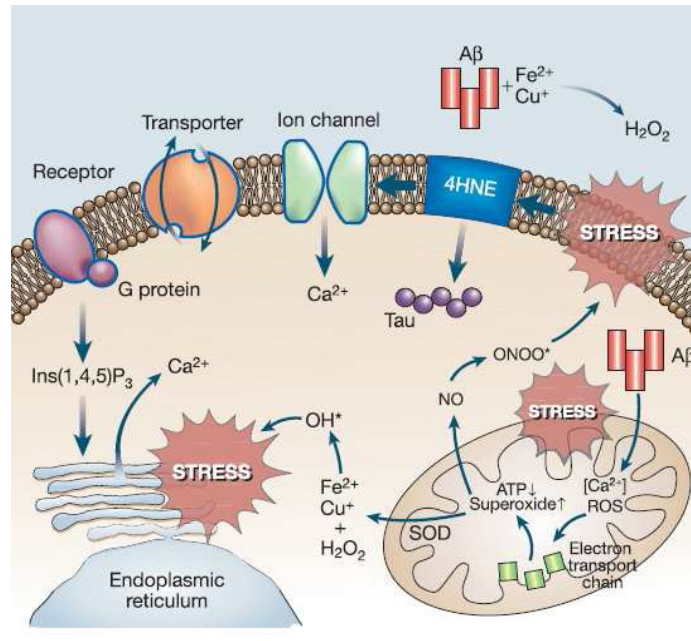


Figure 10: Prevailing connections between OS and other key players in AD (Mattson MP 2004).

Mitochondrial abnormalities, initially caused by gradual oxidative disturbances are enormous contributor of ROS to the cell (Bonda DJ 2010). In elderly people these pathways become less effective, and mitochondrial dysfunction is suggested to be associated to AD (Gibson 1998, Onyango 2010, Swerdlow 2009, Hyde 2008). The increase of ROS and other oxidized molecules, such as lipids and glucose, may lead to the impairment of the memory, long term potentiation (LTP), and AD pathogenesis (Cheng 2010). The primary role of OS in AD onset and progression has been overwhelmingly confirmed, offering the chance to develop specific disease-modifying antioxidant approaches to confronting the disease.

Biometal hypothesis:

Several studies in AD and other neurodegenerative disorders have described increase the levels of oxidative stress reflected by dysregulated content of metals, such as iron, copper and zinc in the brain of patients. Recent discoveries have strongly pointed to brain oxidative stress as one of the earliest changes in AD pathogenesis that might play a central

role in the disease progression (Guglielmotto M 2010, Lee HP 2010). Redox-active metals, especially Fe^{2+} , Cu^{2+} and Zn^{2+} , are capable of stimulating free radical formation via Fenton reaction increasing protein and DNA oxidation and enhancing lipid peroxidation.

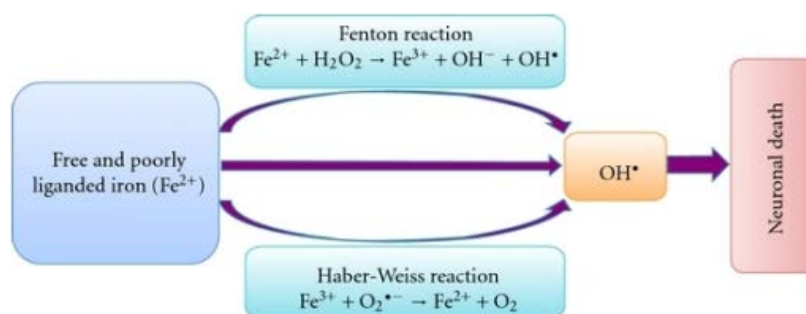


Figure 11: The highly hydroxyl radicals lead to OS-induced lipid peroxidation, mitochondrial dysfunction and increase in intracellular free-calcium concentration, causing neuronal death (Khalil M 2011).

Metals are required in the body especially in the brain; they are components of some enzymes that play crucial role in proceeding biological functions such as redox reactions (Crouch 2007). The imbalance in metals can lead to oxidative stress and neurodegeneration (Crouch 2007), which could involve in the initial cause of AD.

Metals, such as iron, zinc, and copper have been identified in AD brains to be in dyshomeostasis (Crouch 2007, Adlard 2008). Aggregation of $\text{A}\beta$ peptide can lead to reducing copper and zinc resulting in the production of ROS which in role can react with a multitude of different molecules damaging cellular functions, forming toxic species, and neuronal cell death (Curtain 2001).

1.2 Therapeutical Approaches to AD

The above-mentioned complexity of AD pathology has encouraged the development of multiple therapeutic approaches targeting several pathological events that occur in this multifaceted pathology.

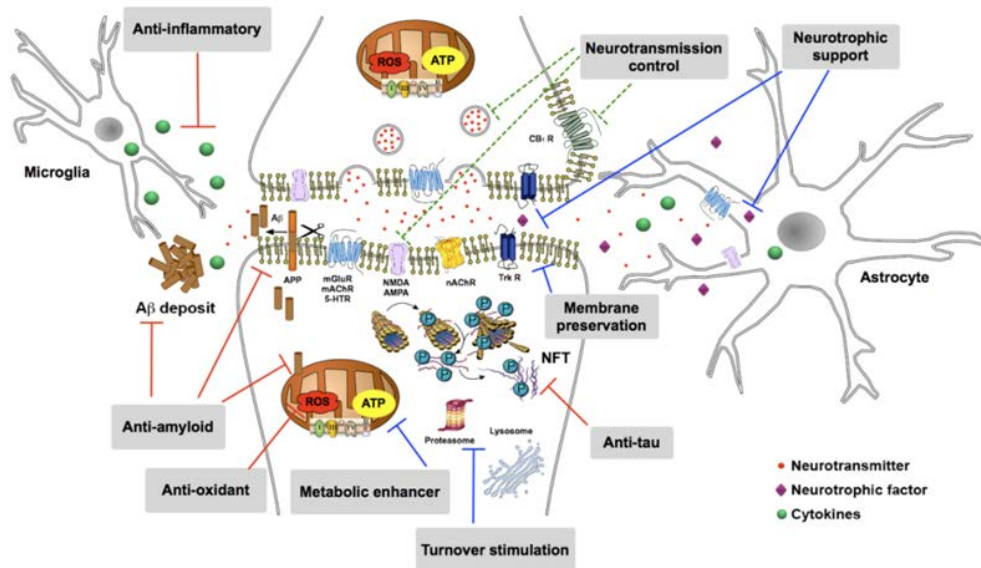


Figure 12: Schematic representation of the main cellular targets that are currently under development to prevent and/or delay the progression of AD (Aso E 2013).

In the recent years, the appearance of several hypotheses explaining AD pathogenesis, allowed the scientist to develop different therapeutic strategy to try to prevent or block the development of AD. To date, only five drugs have been approved by the U.S. Food and Drug Administration (FDA- USA) for the treatment of AD. The first class successfully used for AD treatment is the inhibitors of Acetylcholinesterase (AChEIs); tacrine was the first AChEI approved drug in 1993, but recently it has been withdrawn because of its hepatotoxicity. Other AChEIs are available in the market for the treatment of AD such as donepezil, rivastigmine, and galantamine. More recently, the role of an overactivation of glutamate receptors in neuronal death has been definitely cleared out, and the NMDA antagonist Memantine has been approved in the US in the late 2003, Figure (13).

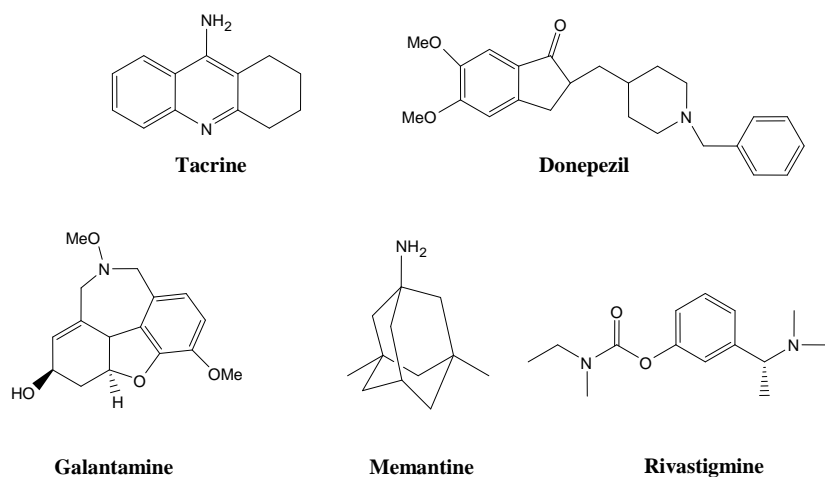


Figure 13: Chemical structures of approved drugs for AD treatment

1.2.1 Cholinomimetic Therapy:

The “cholinergic hypothesis” was the first theory postulated to describe the onset of AD. These findings led to the development of drugs specifically designed to treat the distinctive hallmarks of this neurologic disorder by increasing the reduced levels of the neurotransmitter ACh in AD through the use of AChEIs (Bartus RT 2000, Bartus RT 1982).

Tacrine or tetrahydroaminoacridine (THA), is the first drug for AD treatment, it has been approved by the FDA in 1993 marketed as Cognex®, it is competitive AChEI with high lipid solubility (Nielsen JA 1989), which able to interact with muscarinic receptors (Adem A 1993) and MAO A and B (Adem A 1989). Tacrine suffers from several disadvantages, such as poor oral bioavailability and considerable side effects, which led to be withdrawn from the market. In particular, its hepatotoxic effects seem to be related to toxic quinone-type metabolites produced by the hepatic oxidative metabolism (Qizilbash N 1998).

Donepezil (Aricept®) which is reversible AChEI was approved by FDA in 1997. In many clinical trials of donepezil beneficial effects were observed on standard measures of cognitive function, activities of daily living, behavioral and neuropsychiatric symptoms, such as hallucinations, distractibility, aberrant motor behavior and apathy in patients with mild to moderate or severe AD. Rivastigmine (Exelon®) is another selective, reversible AChE and BChE inhibitor; it was approved by FDA in 2000. Rivastigmine transdermal patch proved to be efficient, in terms of improving cognitive and global function,

generally it presents good tolerability in patients with mild to moderate dementia of the Alzheimer's type in large well designed trial.

Galantamine (Reminyl®) selectively and reversibly inhibits AChE, it was approved by FDA in 2001 for the treatment of mild to moderate AD. It has dual mechanism of action able to attenuate the symptoms of cognitive decline in AD. It is, indeed, reversible selective competitive AChEI (Greenblatt HM 1999) able to modulate simultaneously nicotinic receptors (nAChERs) (Dajas 2003). The main mechanism of action of this molecule is the ability to increase the content of ACh, enhancing the cholinergic neurotransmission and, therefore, improving cognition in AD patients. Moreover, galantamine has also demonstrated to interact directly with nAChER as low-affinity agonist allosterically binding to a distinct binding site from that of classical nicotinic agonists, such as ACh, choline or carbachol, (Akk G 2005).

One of the recent approaches for the modulation of cholinergic receptors is based on targeting M1 muscarinic receptor in AD brain, since it was reported that M1 muscarinic receptor activation could mediate many of cognition promoting effects. Unfortunately, M1 agonists lack of M1 selectivity with resultant intolerable effects, which limited their use in AD treatment.

Studies also focused on M2 muscarinic receptor subtypes in AD treatment, since this receptor subtype has important role in learning, memory and neuronal plasticity. Developed drugs such as SCH 57790, SCH 57790, and BIBN-99, are emerging as selective M2 antagonists able to raise the extracellular levels of ACh and cognitive function. Unfortunately, these drugs showed poor pharmacokinetic profile, and limiting the potential use in AD treatment.

Other drugs such as SIB1553A, and ABT418 were developed to target nAChR since AD patients are defined by a remarkable decrease in the number of nAChR; different studies illustrated strong connections between AD and such receptors, but unfortunately the use of these drugs in the treatment of AD are limited because of the fast desensitization of nAChR to the effect of these agonists.

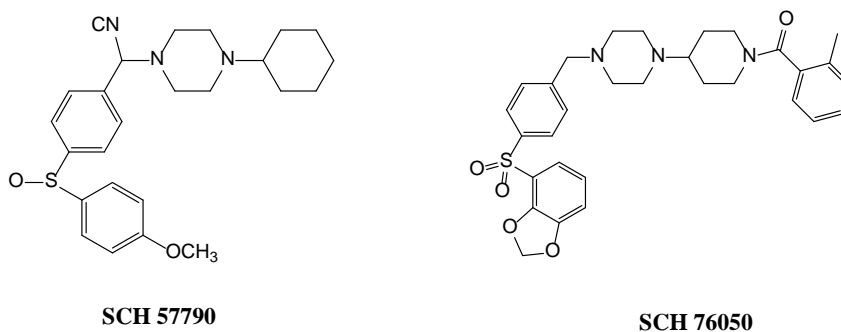


Figure 14: Chemical structure of M2 mAChR antagonists

Studies revealed that clinical use of AChE inhibitors are temporary stabilization of cognitive deficits, other recent studies have reported apparent retardation of the progression of neurodegenerative process, and interfere with the accumulation and precipitation of A β in patients treated with AChEIs. This led the scientists to reconsider this enzyme as a target mediates two important effects in the neurotoxic cascade, that is, A β fibrils formation and ACh breakdown. Therefore, it seems that cholinergic hypothesis will continue to drive drug discovery with the aim to design and synthesize new multipotent AChEIs combining the ability to increase the cholinergic response with inhibition of the A β -aggregation deposition.

1.2.2 Anti-amyloid Strategies:

In the recent years the amyloid cascade hypothesis allowed the scientists to understand the mechanism of neuronal death, the attention of researchers was mainly focused on the modulation of A β -production by using α -secretase stimulators, BACE1 inhibitors, γ -secretase inhibitors and modulators, aggregation blockers, catabolism inducers with the aim to decrease A β in the brain, which may lead to ameliorate the symptoms of A β -induced neurotoxicity.

- *Secretase inhibition:*

γ -Secretase is implicated in the cleavage of APP leading to the production and formation of β -amyloid plaques. Inhibition of BACE1 has emerged as attractive target to design safe anti-amyloid agents, the exploration of BACE-1 as a target derived from a study reported that transgenic mice lacking BACE gene does not produce A β (Luo, Y., 2001).

Several peptidomimetics and non-peptidomimetics compounds have been synthesized as BACE1-inhibitors, such as OM99-2, which represents the first generation of BACE1 peptidomimetic inhibitors, with an IC_{50} of 0.002 μ M. However, it is well known that peptidomimetic inhibitors suffer from difficulties typical of polypeptides, such as poor blood–brain barrier crossing and poor oral bioavailability. In order to enhance the potency and to increase blood-brain barrier crossing ability, further developing has been developed by using X-Ray structure-based modification in order to obtain new low molecular weight peptidomimetics BACE1 inhibitor, such as compound **I** in figure 15.

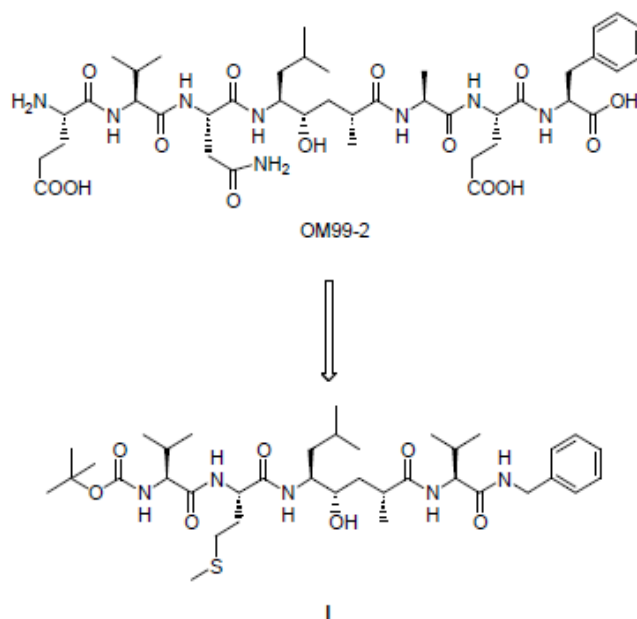


Figure 15: Chemical structure of peptide mimetic BACE1 inhibitors OM99-2 and I

The lead compound **II** has been developed by Elan/Pharmacia showed an IC_{50} = 0.03 μ M; further development carried out on compound **II** by the truncation of the *N*-terminus and *C*-terminus led to the compound **III**, with an IC_{50} of 0.3 μ M. Further structural modification of **III** led to the discovery of **IV** as potent and cell-permeable BACE1 inhibitor, with an IC_{50} of 0.12 μ M; the corresponding diacide **V** is more potent (IC_{50} = 0.02 μ M), but it showed no inhibition of $A\beta$ in HEK cell due to the poor cell permeability.

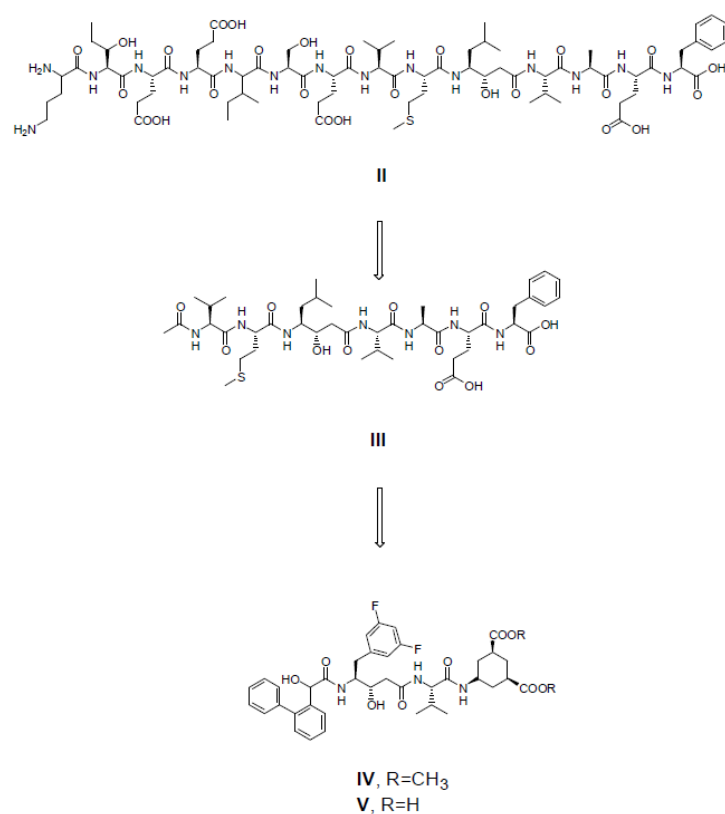


Figure: 16

Further, the developments led to the compound **VI** with an IC₅₀ of 4.8 and compound **VII** characterized by an IC₅₀ of 1.2 nM, in order to obtain better pharmacokinetic profile, the compounds which are characterized by hydroxyethylamino residue, were deeply investigated leading to **VIII** and **IX**, which displayed an IC₅₀ of 5 nM and 20 nM, respectively.

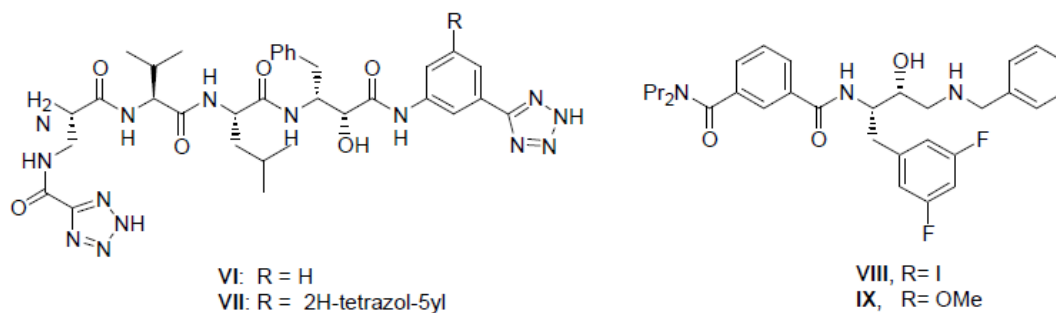


Figure 17: Chemical structures of **VI-VII** and hydroxyethyl amino-based BACE1 inhibitors **VIII-IX**.

Aminoethyl-substituted tetraline have been discovered in 2001 as BACE1 inhibitors, the compound **X** in the figure (18) was the most potent inhibitor in this series with an IC_{50} of 0.35 μ M, Furthermore, the compound **XI** displayed high BACE1 inhibitor activity in micromolar range.

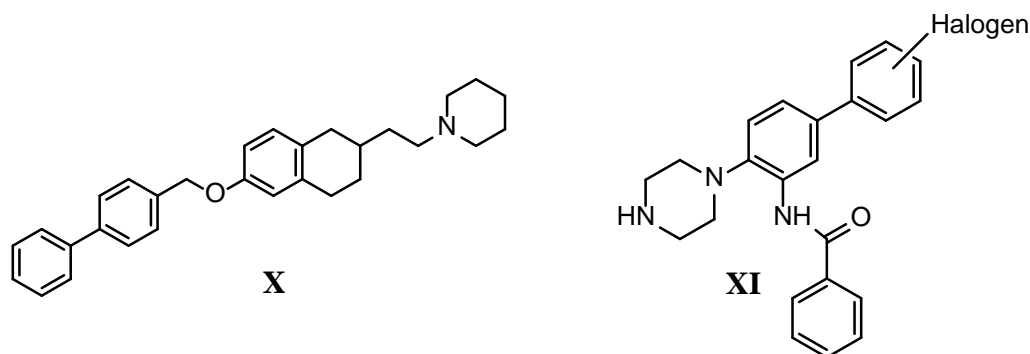


Figure 18: Most potent BACE inhibitors based on the aminoethyl-substituted tetraline scaffold **X**, and Vertex's inhibitor **XI**

γ -secretase is responsible for the final cleavage of the APP to produce the A β peptide and, therefore, it is implicated in the pathogenesis of AD. Thus, this protease is considered a promising target for the development of AD therapeutics in spite of the interferences of γ -secretase inhibitors with Notch signaling that may lead to several side effects. However, compounds that inhibit γ -secretase with little effect on Notch could be useful in AD therapy. For instance, DAPT has advanced into late-phase clinical trials for the treatment of AD: it inhibits A β production with an IC_{50} of 115 nM, the most potent γ -secretase inhibitor was LY-411575 with an IC_{50} of 119 pM. But unfortunately, this compound showed the ability to interfere with maturation of B- and T-lymphocytes in mice due to the inhibition of Notch signaling.

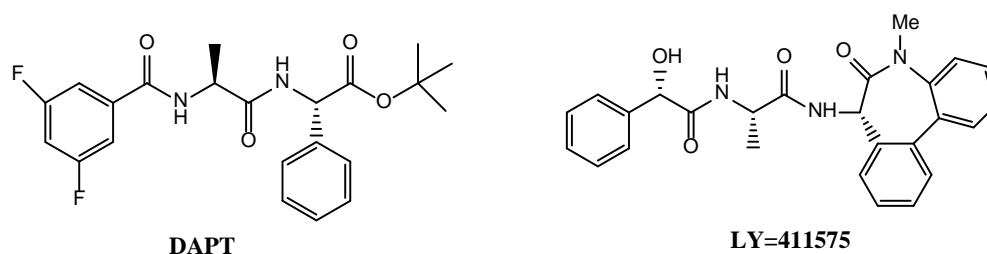


Figure19: Chemical structures of γ -secretase inhibitors

Interesting studies reported that some NSAIDs, such as ibuprofen, indomethacin, are able to decrease the release of A β ₁₋₄₂ and enhancing the release of less amyloidogenic A β without interfering with the Notch. The effect of NSAIDs on amyloidogenic-pathway is not mediated by interaction with COX, but they interact directly with the γ -secretase complex; currently *R*-flurbiprofen (Tarenflurbil[®]) is in Phase III clinical trials for AD treatment.

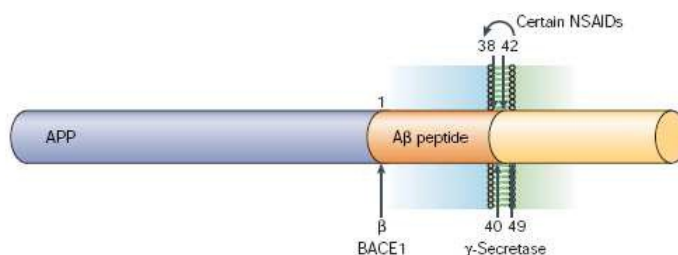


Figure 20: Modulation of γ -secretase cleavage by NSAIDs (Citron, 2004).

- *β -sheet breakers:*

Amyloid plaques are important hallmarks of AD, which could be considered as potential target candidates in AD treatment. Agents able to interfere with the formation of A β -aggregates may have neuroprotective effects through promoting the disaggregation of A β -fibrils. It was reported that the developed compound **XII** in the figure (21) is able to bind to A β and to form a complex stabilized by hydrophobic interaction, and it enhances the changes in the β -sheet structure. Unfortunately, the use of these peptides in AD treatment is limited because of the poor drug-like profile, due to their pharmacokinetic characteristics.

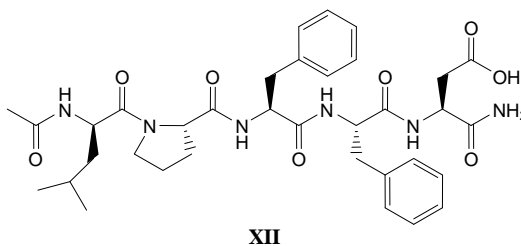


Figure 21: Structure of **XII** pentapeptide compound

- *A β immune therapy:*

This strategy in AD therapy has received considerable attention for its ability to decrease the APP levels. Several theories have been proposed to clarify the mechanism of how the reduction of the APP levels can be achieved by using A β antibodies. The first one says that antibodies link to A β in the brain and trigger microglia to A β phagocytose via Fc-receptors; the second one supposes that the antibodies can act as chaperone and block the A β aggregation, and may sequester A β in the plasma promoting fast efflux of A β from the brain.

- *τ -hyperphosphorylation directed strategies:*

The presence of NFTs is important hallmark of AD and dementia. It has been suggested that reducing tau phosphorylation via inhibition of kinases is major therapeutic strategy based on the presence of hyperphosphorylated tau protein in the brain. Studies reported the important involvement of the inhibition of both glycogen synthase kinase-3 β (GSK-3 β) and cyclin-dependent protein kinase 5 (cdk5) in blocking AD neurofibrillary degeneration. Furthermore, the activation of phosphatases could result in the restoration of correct tau functionality; an example of this approach was verified during the use of Memantine, it can make restoration of protein Phosphatases PP2A activity, leading to the inhibition of tau hyperphosphorylation.

Several small molecules have been developed as tau-aggregation inhibitors such as rhodanine and its derivatives, which were developed by Waldmann group. Also Phenothiazine derivatives showed inhibitory activity toward tau-aggregation such as Thionin which displayed IC₅₀ of 12 μ M, moreover, Porphyrins such as Hemin, are organometallic example of tau-aggregation inhibitor.

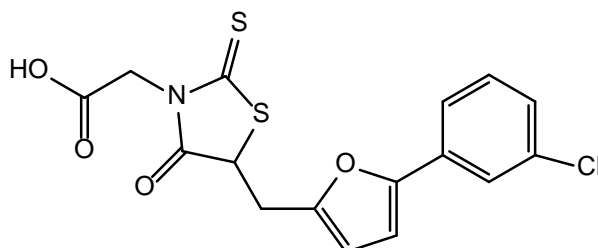


Figure 22: Structure of the hit compound Rhodanine

1.2.3 Antioxidant therapy:

Oxidative stress is suggested to have causative role in the pathogenesis of AD. ROS and other radical species are implicated in the cellular damage leading to neuronal death. Potential antioxidants which could be used to contrast oxidative stress include mitoquinone, vitamin E, and natural polyphenols, such as asextracts from Ginkgo biloba, green tea, wine, blueberries, and curcumin. These agents protect cells from free radicals because they are able to accept radical or free electron. Fortunately; none of them is reported to show any serious toxic effects.

Among antioxidant agent, Lipoic acid chelates redox-active transition metals and shows relevant antioxidant activities by inhibiting the formation of hydroxyl radicals and scavenges ROS. And melatonin is the most promising radical scavenger; it is a hormone able to react with hydroxyradical forming non-toxic derivatives that are easily metabolized. Furthermore, melatonin reacts with peroxytrile and ROS, displaying other interesting activities such as the inhibition of amyloid fibril formation and anti-apoptotic effects.

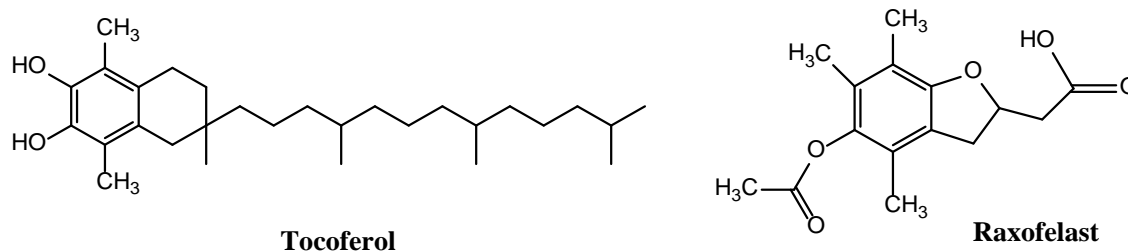


Figure 23: antioxidants examples used in AD

1.2.4 Targeting NMDAR-mediated neurotoxicity:

NMDAR plays an important role in neuronal death in AD; the use of NMDAR antagonist is emerged as useful therapeutic approach to treat AD. For instance, Memantine, which derived from the antiinfluenza drug amantadine, is the only NMDAR antagonist approved for the treatment of moderate to severe form of AD. It binds near the Mg²⁺ binding site within the ion receptor channel.

1.2.5 Cholesterol-reducing approach:

The mechanism of how cholesterol can influence A β production in AD is not yet well understood, several studies have been reported that cholesterol modulated the A β production, and indicated that the high levels of cholesterol can induce the BACE-mediate APP proteolysis (the amyloidogenic pathway). Drugs able to decrease the cholesterol concentration, such as statins, showed the ability to reduce the level of A β in mice and guinea pigs. A promising approach could be the use of inhibitors of acyl-coenzyme, cholesterol acyltransferase; this enzyme catalyzes the formation of cholesteryl-esters from cholesterol, its inhibition result in reducing A β formation.

1.2.6 Metal-chelating approach:

High concentrations of metal ions, such as Cu²⁺, Fe²⁺, and Zn²⁺, have been found within A β deposits in AD brains, there are studies indicate that metals are able to enhance A β aggregation in AD. It was reported that metal-chelators, such as diethylenetriaminepentaacetic acid (DTPA), triethylenetetraamine (TETA), and desferrioxamine (DFO), may solubilize A β in AD brains and reduce the production of hydrogen peroxide derived from the interaction of Cu²⁺ and Fe³⁺ with A β 1-42.

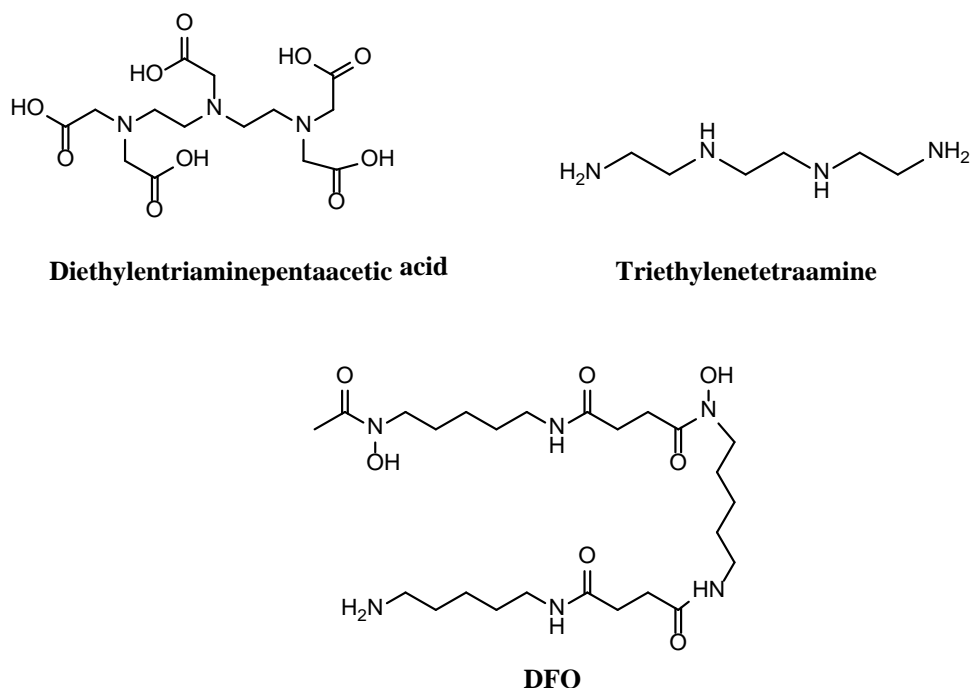


Figure 24: Chemical structure of some metal-chelators used in AD treatment

However, it should be considered that, despite the metal chelator could represent therapeutic benefits in decreasing metal-mediated brain injury; their protracted use could present serious side effects by interfering with the normal function of physiological metal enzymes.

Chapter 2. Glycogen synthase kinase 3 (GSK-3) functions and structure

Glycogen synthase kinase 3 (GSK-3) is a serine/threonine kinase involved in the regulation of glycogen synthase (Embi 1980, Hemmings 1981, Woodgett 1990, Woodgett 1982). It was primarily found in skeletal muscles, then it was discovered that it is ubiquitously distributed in all tissue; in particular, it is present in high levels in the brain (Leroy 1999). GSK-3 is one of the first kinases discovered and studied for its important role in various biological processes such as gene transcription regulation, cell survival and cell division cycle, stem cell renewal and differentiation, insulin action, apoptosis, Wnt and hedgehog signaling pathway, and DNA damage responses (Meijer 2004). Dysregulation in GSK-3 activity is involved in the development of several human diseases, such as diabetes mellitus, AD, bipolar disease, and many types of cancers (Doble 2003). Given to its implication in the pathophysiology of various human diseases; in the last 25 years GSK-3 attracted the attention of the researchers as an important target for developing therapies to treat, through its inhibition, different diseases such as neurodegenerative disorders (Meijer 2004, Doble 2003).

2.1 Crystal structure of GSK-3

In mammals there are two conserved GSK-3 isoforms, GSK-3 α (51 kDa) and GSK-3 β (47 kDa), (Hansen 1997, Woodgett 1990). The two isoforms share 98% similarities within their catalytic domains and the difference between them is due to the extra Glycine-rich in the *N*-terminal region of GSK-3 α .

GSK-3 α and GSK-3 β have high similarity in the structure, but they are functionally different, furthermore they have some diverse substrate specificities, a study demonstrated that mice carrying a selective deletion of exon 2 of GSK3- β undergo embryonic death due to extensive hepatocyte apoptosis despite the presence of GSK-3 α (Hoeflich 2000).

GSK-3 β activity is central for TNF α enhance NF-kappa B activation in hepatocytes while GSK-3 α knockout mice are able to stay alive, with the ability to promote glucose and insulin sensitivity and decrease fat mass. Other studies indicated that GSK-3 α knock-

out mice induced defects in metabolic and neuronal developmental (MacAulay 2007, Kaidanovich 2009).

The crystal structure of GSK-3 β was solved in 2001 figure (25) (Bax 2001, Dajani 2001, Haar 2001) GSK-3 β structure consists of a small *N*-terminal domain, a large *C*-terminal domain, ATP binding site and the activation loop (Dehmelt L2004). The *N*-terminal lobe (25 to 134 residues) comprises of seven antiparallel β -strands which intermittent by the α -C helix and this domain, the entrance of this domain localize ATP binding site which is enclosed by the glycine-rich loop (residues 60 to 70) and the hinge (residues 134 to 139). The *C*-terminal lobe (residues 135 to 380) involves the activation domain, which is essential for the kinase activity (Baas P.W 2005, Lucas F.R 1997).The activation loop begins with the DFG motif (Asp 200 to Gly 202), terminates with the APE motif (Ala 224 to Glu 226) and sets up one edge of the substrate-binding groove. The other edge is founded by the loop that connects β strand five with the α -C helix. The last 55 residues after the kinase domain (residues 330 to 384) compose a cluster of loops and helices that gathers against the C-terminal domain (Alessi D.R 1996).

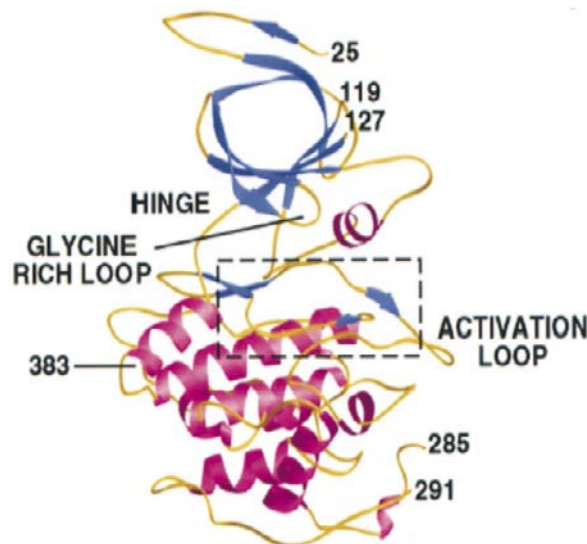


Figure 25: The different regions of GSK-3 β (Haar 2001).

2.2 Regulation of GSK-3 activity

The crystal structure of GSK-3 β has provided the researchers with important information illustrating the regulation of GSK-3 β (Dajani 2001, Haar 2001). GSK-3 β kinase activity is mainly regulated at varied levels, first by post translational phosphorylation, second by interaction with other proteins, third through its intracellular distribution and finally GSK-3 β action requires priming phosphorylation to its substrates.

- *Post translation phosphorylation of Serine and Tyrosine:*

Phosphorylation of serine and tyrosine is an important physiological process that regulates the activity of GSK-3: the inhibition of GSK-3 is caused by the phosphorylation of an *N*-terminal serine 9 in the GSK-3 β and serine-21 in the GSK-3 α (Frame S. 2001) forming an intramolecular association which acts as a pseudo-substrate that prevents the access of substrates to the catalytic domains of GSK-3 resulting in its inhibition (Dajani R. 2001).

This inhibition of GSK-3 through serine-phosphorylation is catalyzed by various protein kinases such as protein kinase-A (cyclic AMP-dependent protein kinase), protein kinase B (Akt), and protein kinase C.

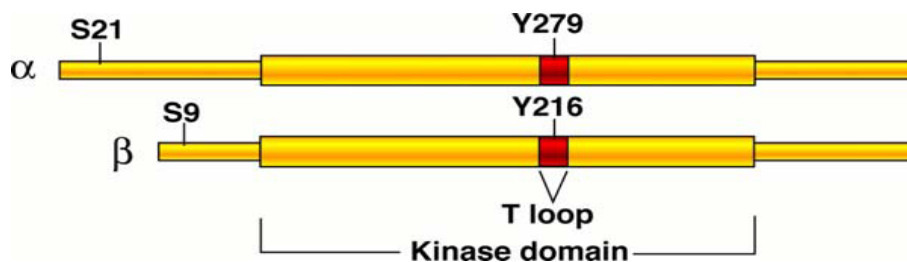


Figure 26: Sites of Phosphorylation of GSK-3beta which regulate its Activity
(James R Woodget 2001).

The activity of GSK-3 is also regulated by the phosphorylation of tyrosine-216 in GSK-3 β and tyrosine-279 in GSK-3 α (Takahashi 2004) and several nonreceptor tyrosine kinases such as src (Kotova 2006). It is reported that the inhibition of tyrosine phosphorylation blocks the access of primed substrates which is essential for GSK-3 activity (Dajani 2001).

- *protein-protein interactions:*

GSK-3 is central to many signaling pathways and its activity can be regulated by interactions with many other proteins. The canonical Wnt signaling pathway is an example of regulating GSK3 activity through complex formation. GSK-3 is regulated through protein-protein interaction by binding to the scaffolding protein Axin, which associates with other proteins including adenomatous polyposis coli (APC), Casein kinase1 (CK-1), and β -catenin. Under basal conditions, CK-1 phosphorylates β -catenin Ser45 resulting in a primary site for GSK-3 phosphorylation (Culbert 2001, Hagen 2002). Phosphorylation of β -catenin leads to its degradation through the ubiquity in proteosome pathway (Amit 2002, Liu 2002).

- *Intracellular distribution:*

GSK-3 is a cytoplasmic protein, but it has been discovered also in the nucleus and mitochondria where it is more active compared to its cytoplasmic forms (Bijur 2003). GSK-3 activity is increased during apoptosis and considerable part of GSK-3 is subjected to intracellular distribution (King 2001, Meares 2007). For instance, it has been shown that nuclear levels of GSK3 are decreased by the activation of the PKB/Akt (Bijur 2001), as well as binding of FRAT1 to GSK-3 assists nuclear release (Franca 2002).

A study has been revealed (Azoulay 2011) that extra glycine-rich stretch in *N*-terminal of GSK-3 leads to block the nuclear translocation (Azoulay2011). Notably, the *N*-terminal of GSK-3 β contains a potential nuclear localization signal, and cancellation of the nine aminoacids on *N*-terminal of GSK-3 β leads to decrease the aggregation in the nucleus (Meares 2007).

2.3 GSK-3 substrates

In mammalian cells GSK-3 is ubiquitously expressed, and it is essential to several signaling pathways. Requisition of GSK-3 to various signaling modules and pathways let the specificity of the stimulus giving the effect. GSK-3 activity is regulated by inhibiting the phosphorylation at their serine 9/21 or *via* Wnt pathway, and based on the upstream signal the cellular consequences are changeable. GSK-3 phosphorylates over than 100 putative substrates, only few of them have been confirmed as physiological substrate of

GSK-3. Since the discussion in details about GSK-3 regulation of its substrates is outside the field of this summarized introduction, we will highlight only some of these targets.

GSK-3 acts as a negative regulator of glycogen synthesis and glycogen synthase is the first discovered substrate of GSK-3. It has been proved that GSK-3 is able to phosphorylate three serine residues of glycogen synthase, which results in decreasing of its activity (Embi 1980, Rylatt 1980). GSK-3 activity inhibition via insulin stimulation results in reducing the phosphorylation, enhancing glycogen synthase activation and increasing glucose uptake due to the increasing in the expression of glucose transporter1 (GLUT1). This important role in glucose metabolism emerged as a promising path to treat insulin resistance in Type II Diabetes via small molecules able to act as pharmacological inhibitors of GSK-3 (Buller 2008).

GSK-3 is involved in synaptic plasticity through the phosphorylation of MAP (Sanchez 2000). It was also reported that GSK-3 is implicated in the phosphorylation of tau in more than ten sites (Hanger 1998); therefore, GSK-3 might be responsible for tau hyperphosphorylation causing its aggregation and precipitation to form NFT in AD brains (Lucas 2001, Spittaels 2000).

Other studies revealed that GSK-3 is a negative regulator in Wnt signaling. Wnt contains a series of 19 different secreted proteins, which have important role in early embryonic development (Miller JR. 2002, Dann CE 2001). During embryonic development, Wnt family enhances cell growth, differentiation, migration, and cell fate. In the lack of Wnt signals, it results a complete activation of GSK-3 which binds and phosphorylates β -catenin (Lagna G 1999, Winston. JT1999). Before the interaction with GSK-3, cytoplasmic β -catenin is primed phosphorylated by CK-1 at Ser45, then GSK-3 phosphorylates β -catenin, at residues Thr41, Ser37 and Ser33 (Luo. J 2009, Lagna G 1999, Winston JT 1999).

Other recent studies explained the role of GSK-3 in self-renewal and differentiation of stem cells, various experiments have been performed in the human and mouse embryonic (HESC and MESC respectively), demonstrated that GSK-3 inhibition results in enhancing pluripotency and deficiency of differentiation through activation of Wnt signaling pathway (Sato N 2004). A study by Sato showed that leukemia inhibitory factor (LIF)/Stat-3 has function in retaining pluripotent status in mouse embryonic stem cells (MESC) but does not have the same influence on HESCs (Sato N 2004, Smith AG 2001). LIF/Stat-3 signaling pathway functions through activating both JAK/STAT and MAPK

signaling pathways which can subsequently result in the activation of PI3K-Akt cascade and block the activity of GSK-3 (Paling NR 2004).

GSK-3 participation in regulating the gene transcription and expression is of fundamental importance. GSK-3 does not link DNA itself, but it phosphorylates and activates a wide range of transcription factors, and extending its regulatory action in gene expression. GSK-3 is involved in the phosphorylation of several transcription factors, including AP-1, CREB, β catenin, Hif1, NFAT, STAT, driving the gene transcription involved in cell survival, cell growth, toxin response, stress, and inflammation (Beurel 2008, Grimes 2001). It is clear that GSK-3 reacts to numerous various stimuli, which in turn has important role in genes transcription engaged in cell growth, survival, toxin response, stress, and inflammation.

2.4 Involvement of GSK-3 in human diseases

GSK-3 β is one of the principal regulators of several cellular processes. The dysregulation of GSK-3 β activity is correlated with various human diseases. To date, GSK-3 was implicated in the pathophysiology of various diseases, including type2 diabetes, bipolar disorder, schizophrenia, AD, PD, developmental disorders, and cancer. For example, GSK-3 has central role in the Wnt and Hedgehog pathways, which promotes cell fate determination and morphology changes (Hart 1998, Jia2002). These pathways are both implicated in different types of human cancer (Polakis, 2000, Taipale 2001). Furthermore, there are plenty of studies aim to understand the role of the overexpression of GSK-3 activity in AD, and the involvement of GSK-3 in tau hyperphosphorylation which is important pathological hallmarks in the development AD (Aghdam 2007).

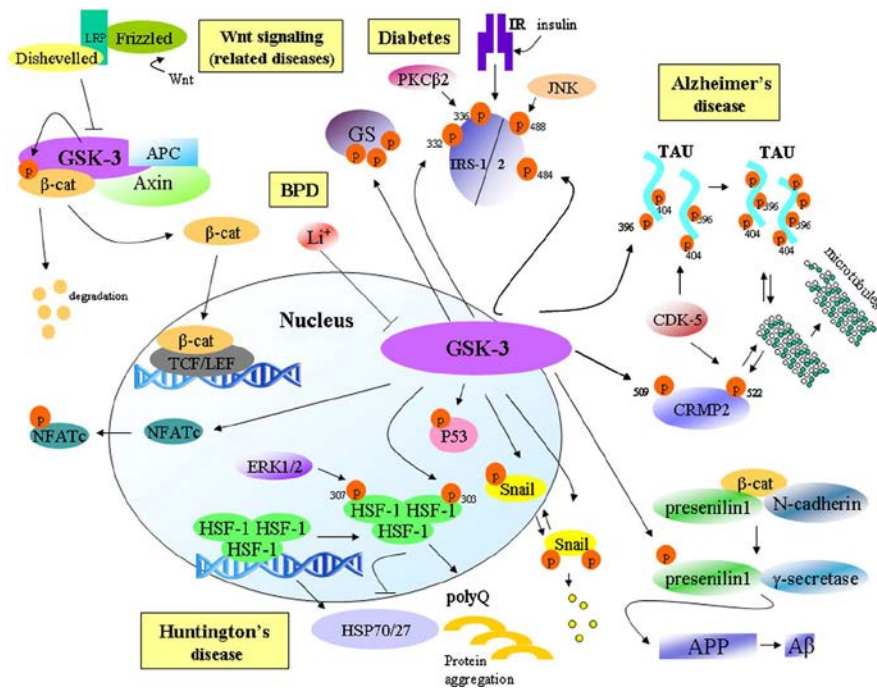


Figure 27: Role of GSK-3 in multiple cellular pathways (Eldar 2010).

2.4.1 GSK-3 and diabetes Type 2:

GSK-3 is engaged in Type 2 diabetes disorder which correlated with insulin resistance in peripheral tissues and chronic inhibition of muscle glycogen synthase leading to hyper insulinemia (Wagman 2004, Lee 2007). It has also been demonstrated that overexpression of GSK-3 in the diabetic patient muscle is implicated in insulin signaling (Conde. S 2003), and designing small molecules able to inhibit GSK-3 might be beneficial to treat non-insulin dependent diabetes mellitus through their ability to mimic insulin function in enhancing glycogen synthase activation, converting glucose to glycogen and raising the glucose uptake in various cell cultures.

2.4.2 GSK-3 and Cancer:

Different types of cancers, especially colorectal cancers, have impairment in elements of the Wnt pathway that result in the abnormal activation of Wnt signaling and accumulation of β -catenin whose overexpression contributed totumorigenesis. GSK-3 inhibition is expected to mimic Wnt signaling and stabilize three cell-cycle regulators, namely cyclin D1, cyclin E and c-Myc.

GSK-3 is a negative regulator of Wnt signaling pathway, it phosphorylates and targets β -catenin for ubiquitination and degradation, it also contributes in the phosphorylation and

activation of the Wnt co-receptor LRP6. Axin and APC are substrates of GSK-3 in this pathway as their phosphorylation induces the interactions within the β -catenin destructing multi-protein complex. By maintenance β -catenin levels in the cytosol, GSK-3 blocks the nuclear translocation and the activation of target genes such as c-myc and cyclin D1, which would finally result in raising cell proliferation. Moreover, GSK-3 has central role in the dynamics of the mitotic spindle. GSK-3 inhibitors prohibit chromosome movements and result in the stabilization of microtubules and a pro- metaphase- like arrest. Therefore, GSK-3 inhibitors emerged as potential therapeutic treatment thanks to the potential role of aberrant GSK3 in malignancy development.

2.4.3 GSK3 and inflammation:

Studies indicated that inflammation is a frequent component in mood disorders, neurodegenerative diseases, diabetes, and various cancers (Beurel 2010, Jope 2007). Whether inflammation occurs to protect or harm the host that is still controversial, the capacity to stimulate an inflammatory response is critical for keeping the general wellness of the organism, GSK-3 has important role in the inflammatory signals (Jope 2007, Martin 2005). GSK-3 is involved in the production of pro-inflammatory cytokines inclusive interleukin-6 (IL-6), interleukin-1 β (IL-1 β), and tumor necrosis factor (TNF) (Beurel 2008, Yuskaitis 2009). On the contrary, GSK-3 blocks the production of anti-inflammatory cytokine IL-10. Consequently, inhibition of GSK-3 was discovered to have anti-inflammatory effects, some studies indicated that GSK-3 inhibitors are able to protect against endotoxin shock in mice (Martin 2005), other studies demonstrated that treating various systemic inflammation mice models with GSK-3 inhibitors able to produce anti-inflammatory effect, that confirm the role of GSK-3 in the inflammation.

2.4.4 GSK3 and Nervous system disorders:

Latest data using pharmacological and genetic approaches have led to propose a central role for GSK-3 in the array of neural developmental activities including neural progenitor homeostasis, neuronal migration, neurite growth/specification, and synapse development. Furthermore, various studies suggested that dysregulation of GSK-3 activity contributed to the pathogenesis of nervous system disorders such as Prion diseases, Parkinson's disease, Huntington's disease (HD), AD, and others. In this introduction it will be briefly

described the role of GSK-3 in the development of some of these diseases and it will be provide more details to describe the contribution of GSK3 in AD.

2.4.4.1 Prion diseases: Dysregulation of the prion protein (PrP) has essential role in neurodegeneration. It was reported that the activation of GSK-3 is critical in prion peptide-enhancing neuronal cell death and neurodegeneration (Perez, M. 2003).

2.4.4.2 Parkinson's disease (PD): PD is age-related disorder, characterized by degeneration of dopaminergic neurons. Recently, it was proved that GSK-3 inhibition can protect dopaminergic neurons against several degenerations (Smith, P.D 2003); therefore, GSK-3 inhibitors might be a therapeutic advantage in the treatment of PD.

2.4.4.3 Huntington's disease (HD): HD is an inherited neurodegenerative disease characterized by the extension of Huntington protein by polyglutamine. The resulting protein is toxic, makes intracellular accumulation and reducing in β -catenin level. Studies performed in cells and invertebrate animal models showed that using GSK-3 inhibitors results in reducing the overexpression of GSK-3, suggested that these agents may be new therapeutic appropriateness for HD treatment (Carmichael, J 2002).

2.4.4.4 Ischemic stroke: It was revealed that activation of GSK-3 contributes to the development of excite toxicity phenomenon in Ischemic insults, which results in the death of particular neurons and causing stroke. This was further supported by a study reported that treatment with Lithium in rat model of stroke decreases the neurological impairments and reduces the brain-infarct size that supported the suggestion of designing selective GSK-3 inhibitors might be useful in the therapy of stroke (Yan 2007).

2.4.4.5 Human immunodeficiency virus type 1 (HIV-1): HIV-1 pervades the CNS and induces cognitive deficits (Cherner 2002). There is much benefit in the potential therapeutic use of GSK-3 inhibitors in HIV patients because of their neuroprotective and anti-inflammatory actions. A study in eight patients with HIV-1 correlated neurocognitive deficits is reported that lithium treatment for 12 weeks enhanced cognitive performance in all patients and cognitive deficits which reduced in six patients (Letendre 2006).

2.4.4.6 GSK3 signaling in Alzheimer's disease pathogenesis: There are epidemiological analyses that supported important relationships between overexpression of GSK-3 and increase of its activity and neuropathological developments in AD (Leroy 2002, Mateo 2006). Immunohistochemical data demonstrated that GSK-3 co-localizes to neuronal inclusions generated by neuritic plaques, NFT, and dysfunctional neurons. These feed backs suggest that GSK-3 may be implicated in the processes resulting into neuropathological changes (Baum 1996, Pei 1999).

- *GSK-3 mediated tau hyperphosphorylation:*

Tau is a neuronal microtubule-associated protein, plentifully expressed in the brain whose pharmacological function is regulated through phosphorylation process by several protein kinases at tyrosine, threonine, or serine residues. Tau kinases are classified in proline- (PDPK) and nonproline- (NPPDK) directed protein kinases (Morishima 1995).

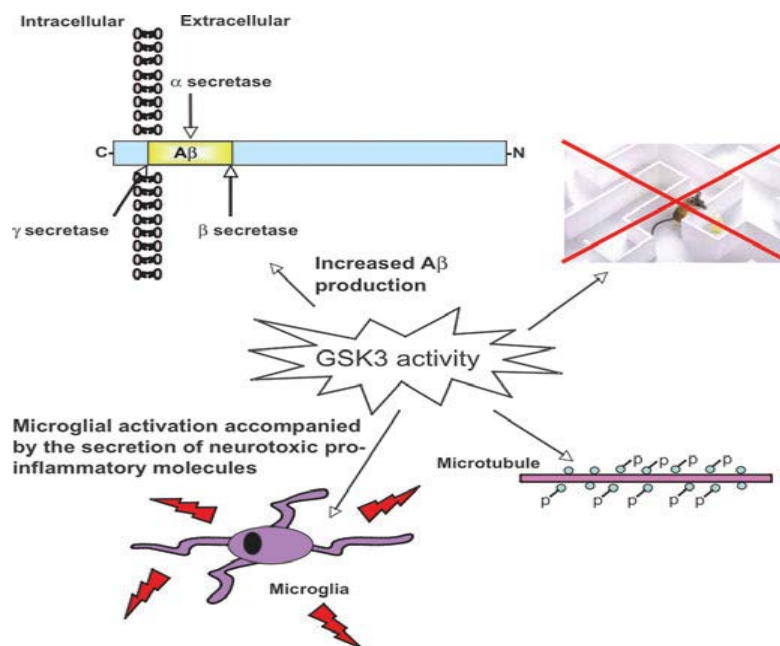


Figure 28: GSK3 hypothesis of Alzheimer's disease (Hooper C 2008)

In AD, tau protein is hyperphosphorylated and could be found in aggregated form and can be congregated into paired helical filaments (PHF) which result in the aberrant structure known as NFTs. Tau protein links to C-terminal end of tubulin protein through three or four repeat sequences which is critical for microtubule aggregation (Cho 2004).

GSK-3 β is known as tau kinase for its important role in tau hyperphosphorylation (Hoshi, 1996; Ishiguro, 1993). GSK-3 β inhibitors may have a beneficial effect in AD since they may decrease tau hyperphosphorylation. For instance, transgenic mice having overexpressed GSK-3 β and tau were treated with Lithium an inhibition of tau hyperphosphorylation and NTF formation was observed (Engel 2004).

- *GSK-3 mediated A β production:*

A β formation and aggregation have essential role in the development of AD; A β is generated from sequential cleavage of APP via two different cleavages, the first one by BACE-1 and second one by γ -secretase. Alteration in the expression or in the activity in anyone of these two enzymes results in modification in APP processing pathway and enhances the production of A β .

Various studies reported the role of GSK-3 in A β production and aggregation. One of the studies revealed that GSK-3 may contribute to the phosphorylation of Thr668 site in APP (Aplin 1996, Sun 2002), and promotes the association of APP with BACE-1 (Lee 2007). Other researchers demonstrated that GSK-3 could behave as a γ -secretase modulator; a research by Phiel reported that lithium, well known GSK-3 inhibitor, induced the inhibition of γ -secretase and the reduction of A β production without affecting other signal transduction pathways such as Notch cleavage (Wolfe 2008). Furthermore Qing and colleagues proved that the use of GSK-3 inhibitor valproate resulted in preventing γ -secretase activity and inhibited the formation of A β (Qing 2008).

Moreover, GSK-3 may regulate several members of γ -secretase complex (presenilin-1/2, APH-1, PEN-2, nicastrin, TMP21), for example, phosphorylation of presenilin-1 by GSK3 regulates the interaction with APP protein, and mutations in this process links to FAD (De Strooper 2003). However, more experiments and studies should be carried out in order to shed light in the role of GSK-3 in γ -secretase complex and A β production, surprisingly, one of recent studies including GSK-3 α and GSK-3 β knockout animals, showed that neither GSK-3 α nor GSK-3 β isoforms are involved in APP processing by

acting on γ -secretase activity. Furthermore, the authors reported that there are no changes in the levels of APP gene or A β production (Jaworski 2011).

- *GSK-3 and neuronal cell death:*

AD is characterized by cell death and the neurons are loosed via apoptotic mechanism through two different apoptotic pathways, the intrinsic one that involves intracellular impairments, and the extrinsic one promoted by cell death receptors. GSK-3 is involved in promoting the apoptotic intrinsic pathway in AD (Meijer 2003).

Studies demonstrated that GSK-3 has major role in neuronal cell death, through its role in forming overexpression of shaggy (*Drosophila* homolog of GSK-3) and increasing Tau hyperphosphorylation, which leads to enhance the neurodegeneration (Jackson 2002), studies performed by using kinase with dead mutant shaggy resulted in enhancing neuronal death (Jackson 2002), conferring the important role of GSK-3 in neuronal cell death.

- *GSK-3 and memory:*

The damage in Long term potentiation (LTP) is associated with memory failure in AD progresses and results from the inhibition of Wnt and PI3, which are both also negative regulators for GSK-3 (Sanna 2002). A study on mice with aberrant GSK-3 showed inhibition in LTP induction and reduce in spatial learning, while the treatment of mice with GSK-3 β inhibitor results in enhancing the learning and inhibits long term depression (LTD). That demonstrates the crucial role of GSK-3 inhibitors in improving the memory formation in AD (Hamilton 2007, Reiman 2007).

2.5 Targeting GSK3 in drug discovery

The contribution of GSK-3 in the important biological functions and in the pathogenesis of various diseases, made it an important target in drug discovery since agents able to inhibit this enzyme could have therapeutic potential for the treatment of various disorders including cancer, diabetes, bipolar disorder, AD, PD, schizophrenia.

To date, more than 30 molecules have been described as GSK-3 inhibitors with wide various chemical types, including cations and compounds isolated from natural sources and synthetic compounds. The crystal structure of GSK-3 β was obtained, and this was a

key to clarify the binding sites within the enzyme and to classify the inhibitors based on their mechanism of action. The inhibitors could be divided in ATP-competitive, non ATP-competitive and substrate- competitive inhibitors. Recently, Palomo et al. figure (29) explained the map of the GSK-3 surface by using the geometry-based algorithm fpocket, and hpocket programs. They declared that it is characterized with seven conserved binding sites; three of them are ATP substrate, and peptides axin/FRATide-binding sites. The other four sites are non ATP binding: one of them is localized on the C-terminal domain of GSK-3, the second one is located on hinge region, and the other two sites are situated on the N-terminal domain of GSK-3.

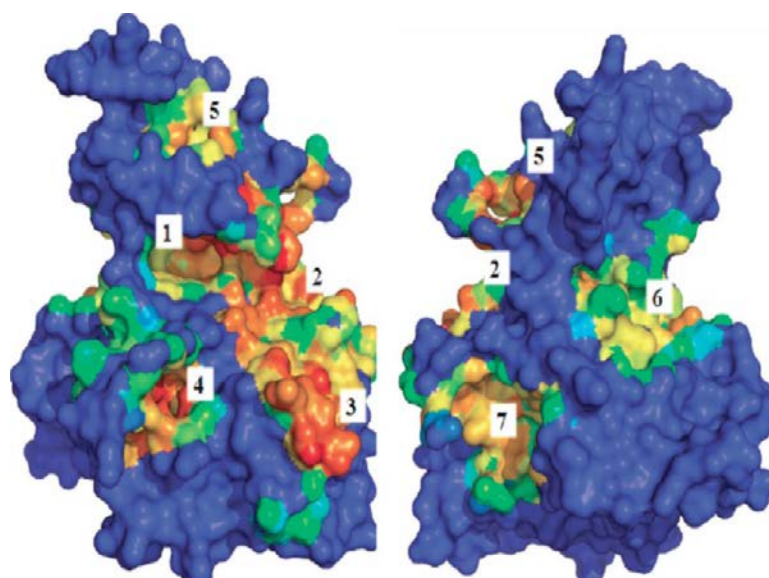


Figure 29: The binding sites available on the surface of GSK-3 (Palomo2011)

The selectivity and safety are important challenges in the design and synthesis of GSK-3 inhibitors to produce effective drug useful to treat the human diseases. The common properties for all GSK-3 inhibitors include: low molecular weights, flat planar structures, most of them are hydrophobic and contain cyclic ring moieties. Additionally, since GSK-3 is essential for life, smooth or moderate inhibitors are requested to avoid the toxicity, since high values for IC_{50} can prevent the cells from acting normally. Another important challenge for GSK-3 inhibitors to turn into in an efficient drug for AD treatment is the ability to cross the blood brain barrier in order to regulate the exacerbated GSK-3 brain levels. To date only a few GSK-3 inhibitors reached the clinical trials in human subjects. Most of them are ATP-competitive inhibitors targeting cancer and diabetes disorders, and

only two compounds are non ATP - competitive inhibitors including lithium chloride and Tideglusib.

Lithium is the first natural identified cation as GSK-3 inhibitor, it has been used for long time as a clinical treatment of bipolar disorder, it acts as GSK-3 inhibitor directly by competing with magnesium cation and indirectly by increasing the auto regulation and the phosphorylation on the serine site, a study by Davies et al. demonstrated the selectivity of the lithium as GSK-3 inhibitor, the study included 24 different kinases and displayed an inhibition of GSK-3 more than the other kinases.

Clinical studies have been widely developed to investigate the therapeutic effect of lithium on AD, some studies reported that treating transgenic mice with Lithium, resulted in APP inhibition, and decreasing in A β and tau phosphorylation, some other investigations revealed toxic side effects in old patients, so the clinical studies on Lithium were stopped, and currently it is used just as reference compound for bipolar disorders.

2.5.1 ATP-competitive GSK-3 inhibitors:

Many compounds has been identified as ATP-competitive GSK-3 inhibitors, most of them show low specificity and high toxicity since the human body has more than 500 proten kinases which have high similarity of homology in the catalytic domain; for this reason most of the tested compounds failed in the preclinical studies.

Some of GSK-3 ATP-competitive inhibitors were isolated from natural resources, in particular from Marine organisms, such as Indirubins, they showed selectivity toward GSK-3 over CDKS, 6-bromoindirubin 3-oxime was studied at 1.5 μ M concentration in transgenic mice, proved neuroprotection properties and axon formation in addition to decrease of tau phosphorylation. On the contrary, studies carried out on rat brain with the same compound, showed no effect in reducing tau phosphorylation because of its poor bioavailability which due to its limited water solubility (Selenica 2007, Leclercetal 2001). Hymenialdisine (HD) is potent protein kinase inhibitor targeting GSK-3 β , CDKs, MEK, CK-1, and Chk1 functions in competition with ATP (Wanetal 2004), it induced the reduction in tau phosphorylation and the neuroprotective effect already at 10nM concentrations and currently it is evaluated in preclinical studies.

Purine group, including compounds CT98014, CT98023, CT99021, represents one of the first synthetic ATP competitive GSK-3 β inhibitors with high selectivity toward this isoform and IC₅₀ in nanomolar range concentrations (Alabed2011). AR-A014418 is another ATP-competitive GSK-3 β inhibitor showed decrease in tau phosphorylation and

NFT formation in transgenic mouse model (Bhat 2003). SB-216763 is a synthetic ATP-competitive GSK-3 β inhibitor that showed advantages in AD therapy; for instance, it decreased A β aggregation and tau phosphorylation in mice (Hu 2009, Selenica 2007).

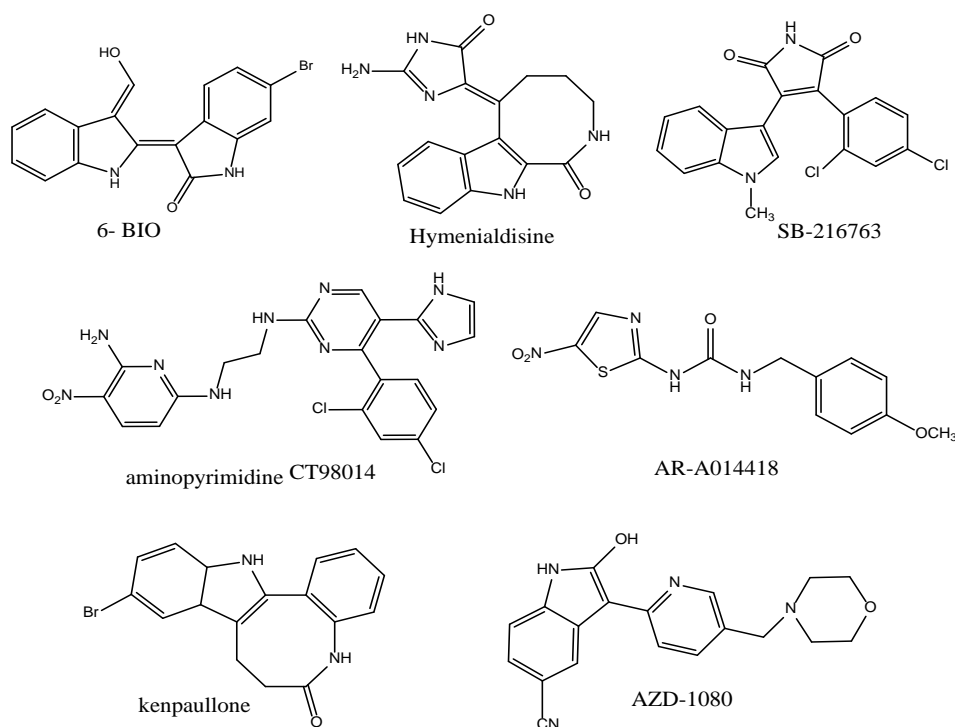


Figure 30: Structures of ATP-competitive GSK-3 inhibitors

2.5.2 Non-ATP competitive GSK-3 β inhibitors:

Kinase selectivity is one of the major challenges in design and synthesis of protein kinases inhibitors (Eglen 2009), ATP -competitive GSK-3 β inhibitors are emerged as distinct real potential drugs with more selectivity than ATP-competitive GSK-3 β inhibitors, since they should bind to unique regions within the kinase producing more subtle modulation of kinase activity than only blocking ATP entrance, they act as covalent inhibitors, substrate competitive inhibitors or allosteric modulators. Non ATP-competitive GSK-3 β inhibitors are promising potential drugs which could provide important benefits in therapeutic for various disorders with a safer use in the clinic.

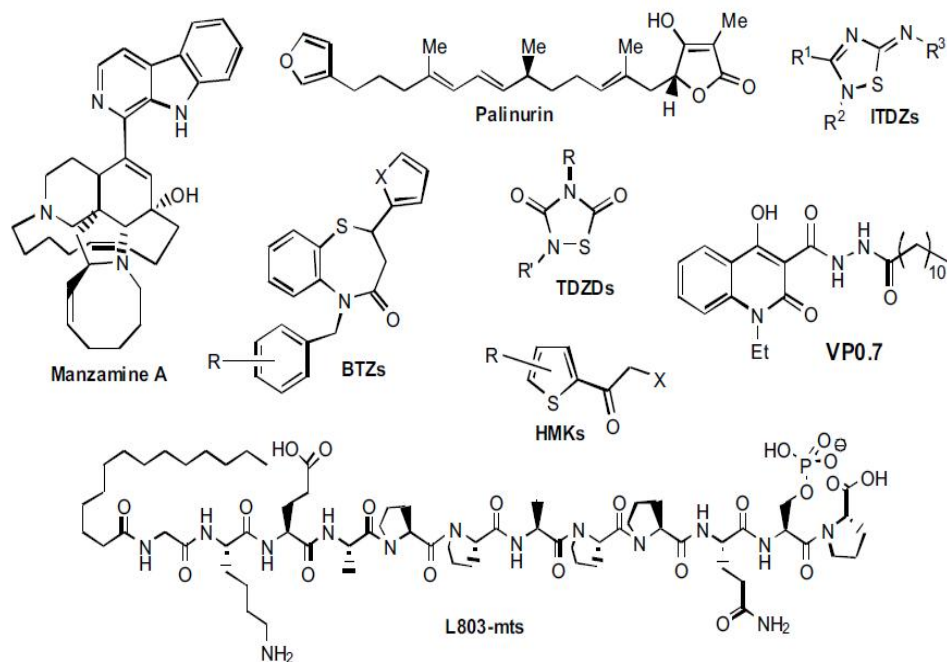


Figure 31: Structures of ATP non-competitive GSK-3 inhibitors (Martinez A 2013)

In 2002, Martinez et al. have reported cyclic thiadiazolidinones (TDZD) as first group of synthetic non ATP-competitive GSK-3 β inhibitors, through its interaction with the oxyanion binding site of GSK-3 β , several derivatives were synthesized and evaluated for inhibiting GSK-3 β , and one of these synthesized compound currently known as Tideglusib, showed high selectivity toward GSK-3 β over a panel of several protein kinases including Protein Kinase A, Protein kinase C, casein kinase II (CK-2), and cyclin-dependent kinase 1 (CDK1/cyclin B). Tideglusib was investigated for treatment of AD and progressive supranuclear palsy (PSP). It demonstrated positive results after several studies in different animal models, it showed enhanced in cognitive performance, reducing in tau phosphorylation and decreasing in A β production, furthermore, it showed the ability to cross the BBB, currently, Tideglusib is under clinical studies to investigate the safety and efficacy characteristics in human patients.

Emodin was reported by Gebhardt as non-ATP competitive GSK-3 β inhibitor and its analogue, carrying an ethylenediamine chain, showed an insulin sensitizing influence mediated by an increase in hepatocellular glycogen and in the biosynthesis of fatty acids.

Other compound is 5-imino-1, 2, 4- thiadiazoles (ITDZs), it was demonstrated by Polomo et al. as a first class able to block reversible GSK-3 β acting as substrate competitive inhibitor.

Chloromethylthienyl ketones and Halomethyl phenyl ketones were reported by Condeas irreversible non ATP-competitive inhibitors toward GSK-3 β : these two classes showed cell permeability and reduced tau phosphorylation and are highly selective (Perez 2009).

Other ATP non-competitive GSK-3 inhibitors from natural resources were reported, such as Manzamine, which was isolated from an Indopacific sponge, and Palinurin and Tricantin isolated from Mediterranean sponges. These compounds showed reducing in tau phosphorylation, but no clinical studies were developed on these compounds.

2.6 Drug Design

As largely discussed in the introduction, GSK-3 β enzyme is involved in the development of AD. Some GSK-3 β inhibitors are currently evaluated in clinical trials for the treatment of AD and other pathologies, such as diabetes and cancer. Most of these inhibitors interacting with the ATP-binding site which is, as already reported, highly conserved in all the different kinases. The human kinome is known to be about 500 kinases and all these enzyme share high homology in the catalytic domain. Therefore, agents that bind to this site are characterized by low selectivity, which may lead to toxic side effects. One of the main challenges in these years in GSK-3 β inhibitors research is to develop non-ATP competitive GSK-3 β inhibitors, binding in other sites such as substrate-binding or allosteric binding sites.

The aim of the present work is the development of new non-ATP competitive GSK-3 β inhibitors. In medicinal chemistry different strategies can be followed to discover biologically active compounds (hit) which may represent a starting point for a new drug discovery program. One of the most promising strategies is based on the screening of collections of small molecules towards a given biological target. Following this strategy, we screened our in-house collections towards GSK3 β with the aim of discover a potential new hit compound. The compounds were assayed at 10 μ M concentrations, and those which showed a degree of inhibition at least 40% were considered for further IC₅₀ determination. Among all the compounds, only compound **1** met the criteria for further development and it was subjected to IC₅₀ determination (IC₅₀ = 1.56 \pm 0.05 μ M) (Figure 32).

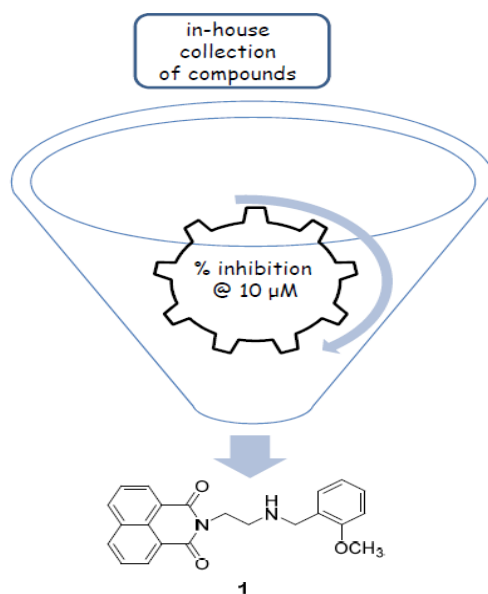


Figure 32: Schematic representation of the screen strategy leading to compound **1**

Compound **1** is structurally characterized by a naphthalendiimide scaffold and an *o*-methoxybenzyl moiety linked by a two-methylene spacer. Compound **1** is characterized by a diimide moiety, which is characteristic of phthalimide-based compounds, such as SB-216763, which are known to behave as ATP-competitive inhibitors. SAR studies performed on these inhibitors reported that the -NH engage a critical interaction with the carbonylic oxygen of Asp133 located in the ATP binding site and that the replacement of the H atom with an alkyl moiety induces a loss of the activity. Therefore, based on these considerations and on the structure of tideglusib, we hypothesize that compound **1** may be able to inhibit GSK-3 β by interacting with different sites out of ATP binding site.

Based on these results, we started a campaign of SAR evaluations and hit to lead optimization with the goal of discovering potent and selective GSK-3 β inhibitor (Figure 33 and Figure 34).

We started synthesizing compounds **2-4** characterized by alkyl chain of different length in order to evaluate the importance of the distance between the two aromatic moieties for a good interaction with the enzyme. Then, we focused our attention on the evaluation of the methoxy group in *ortho* position of the aromatic ring (**5-8**) together with the elimination of the chain (**9**), in one of the aromatic ring (**10** and **18**) and other of carbonyl group (**11**). Then we evaluated the effects of the replacement of the methoxybenzylamine group with

a dimethylamino (**12-13**), morpholino (**14**), piperazine (**15**), hydroxyl (**16**) and benzyl (**17**) groups, methoxyphenyl-methanamine (**18**) (Figure 33).

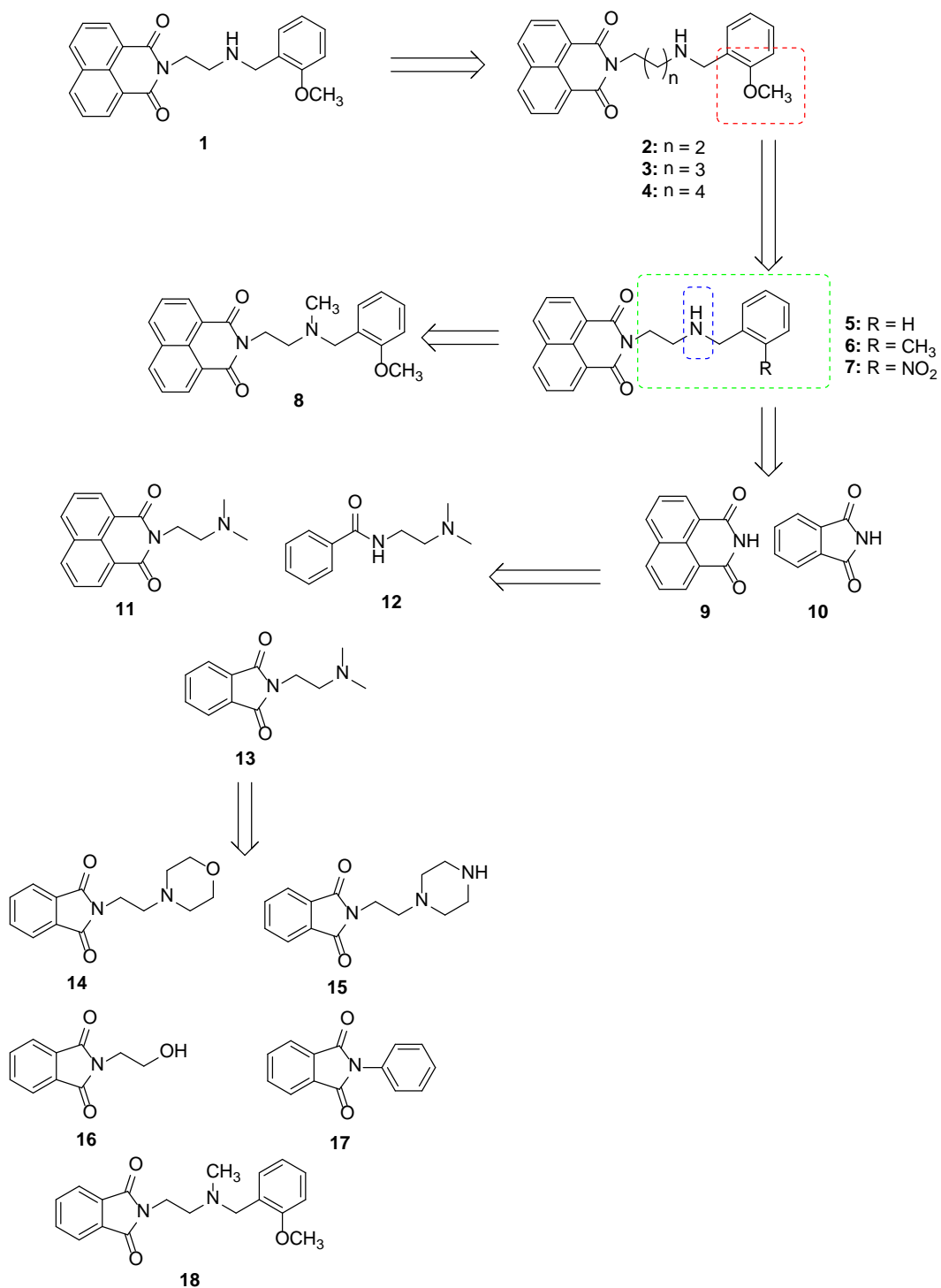


Figure 33: Structure-Activity Relationships of compound **1**.

Lastly, the most interesting structure obtained through this study compound (**18**) was further modified in order to increase the lipophilicity to improve its pharmacokinetic properties (**19-23**) (Figure 34).

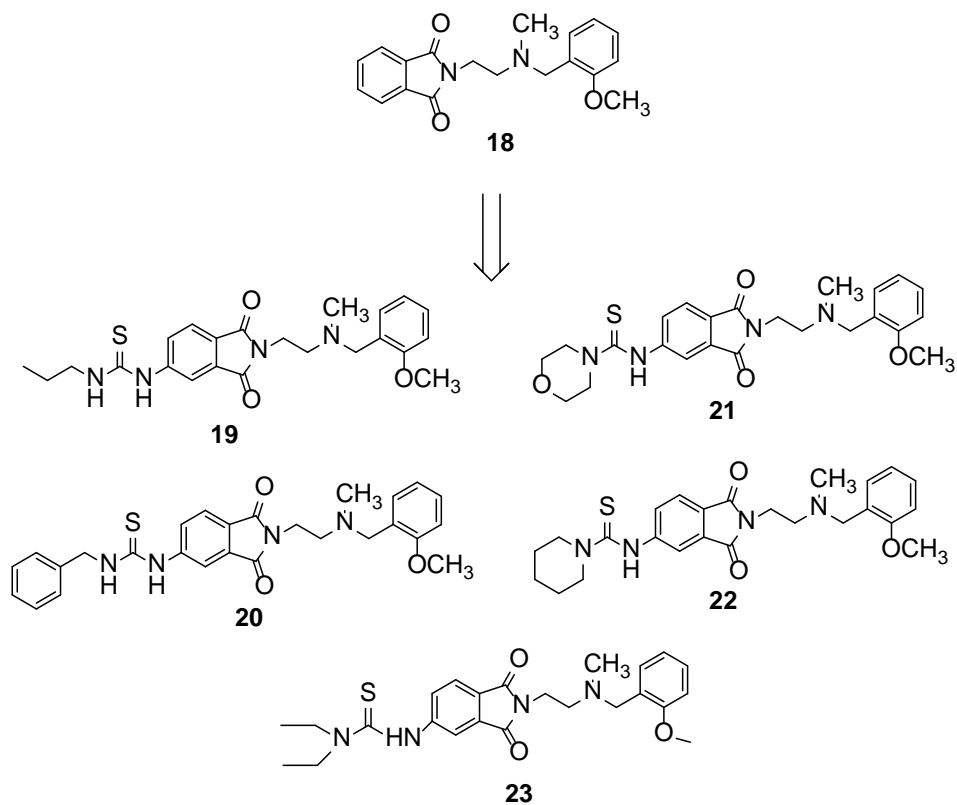


Figure 34: Drug design leading to **19-23**.

2.7 Methods

2.7.1 Synthesis:

1-4 were obtained by reacting 1, 8-Naphthalic anhydride with the corresponding diamines (**n=1-4**) leading to **41-44** following the procedure reported in literature (Braña 2002); then **41-44** were condensate with 2-methoxybenzaldehyde and then reduced by sodium borohydride giving the products **1-4** (Scheme 1).

The compounds **5-8** were obtained following the procedure reported in Scheme 2, by reacting 1, 8-Naphthalic anhydride with the corresponding amine (**51-54**). The compounds **51-54** were obtained reacting the Boc diamine **45-46** with the corresponding aldehyde to give **47-50** which were followed by treatment with HCl and then worked up to give **51-54** which, finally, reacted with 1, 8-Naphthalic anhydride to give the final compounds **5-8**.

The compounds **9-10** were obtained by dissolving the corresponding anhydride in ammonium hydroxide, in particular, 1,8-naphthalic anhydride or phthalic anhydride, respectively, and leaving the reaction under reflux for 6 hours (Scheme 3).

Compound **11** was synthesized by dissolving benzoic acid and Dimethylethylenediamine in dichloromethane in the presence of EDCI, HOBt and triethylamine, the reaction stirred at room temperature for 12h (Scheme 4).

Compounds **12-13** were obtained by the condensation of dimethylethylenediamine with the corresponding anhydride, 1,8-naphthalic anhydride or phthalic anhydride, respectively, dissolved in ethanol (Scheme 5).

The compounds **61** and **62** were synthesized following the procedure described in (scheme 6), starting from 2-chloroethylamine hydrochloride which was treated with Boc₂O to have the compound **56**, then **56** was treated with **57** and **58** under reflux to give **59** and **60** followed with deprotection to give the corresponding compounds **61** and **62**,

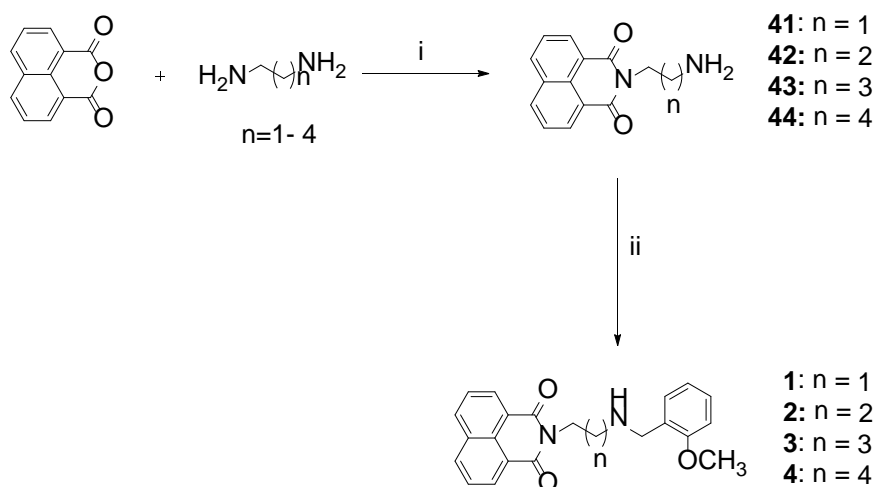
The synthesis of the final compounds **14-17** was carried out following the procedure described in (Scheme 7), phthalic anhydride was suspended in water then glacial acetic acid and the reported side chains were added to the suspension, **61** for the compound **15**, **62** for the compound **15**, ethanolamine and benzylamine for **16** and **17**. Then the mixture was stirred under reflux for 4 hours. The amines and phthalic anhydride are used in ratio (1:1). The work-up was different for the reactions based on the nature of the side chains. Compounds **16-17** were obtained by adding water, and then filtering the precipitated solid

in water, followed by crystallization. To note that compounds **14-15** were purified directly by flash chromatography.

Compound **18** was obtained by dissolving phthalic anhydride with diamine **65** in ethanol and stirred under reflux for 3 hours (Scheme 8). Compound **65** was obtained by reacting the compound **62** with the reagent EtOCOCF₃ in methanol to give the compound **63**, which furthered with metalation reaction by reacting with formic acid 85% and form aldehyde 40% to give the compound **64**, and after removing the protection group we obtained **65** (Scheme 8).

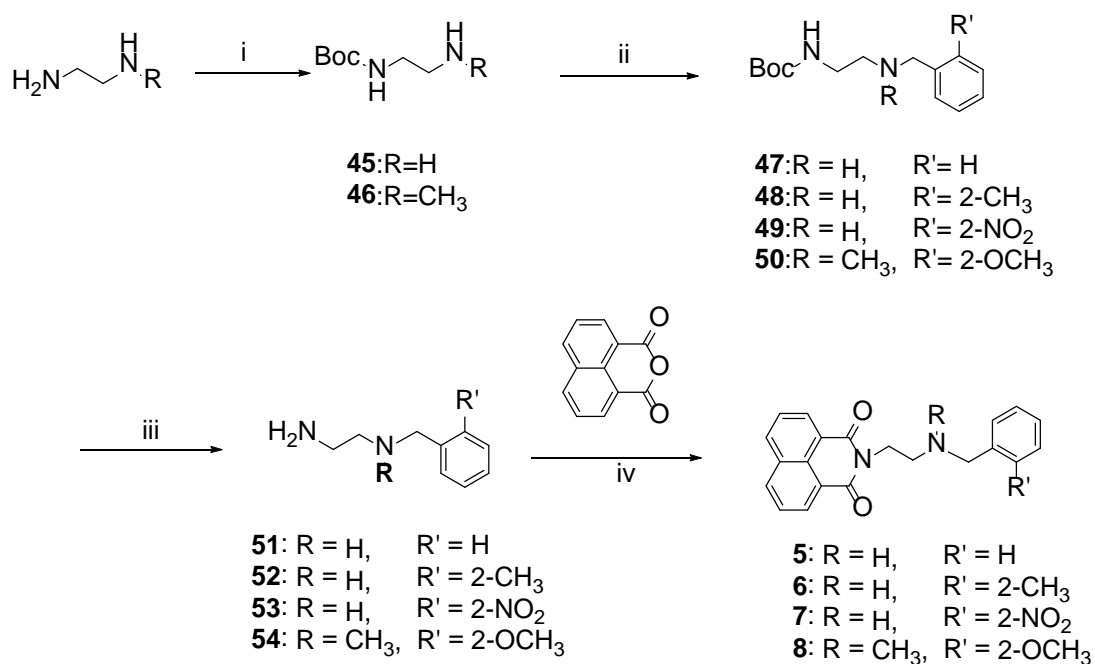
The synthesis of the final compounds **19-23** was carried out following the procedure described in (scheme10) by react the compound **68** with the corresponding amine. The synthesis of the compound **68** is described in (scheme 9), it was obtained by reacting the compound **65** with Nitroptalic amide to give the compound **66**, which was subjected to reduction reaction using Fe under acidic condition and using ultra sonic for 2 hours, to give the compound to give **67** which was reduced to into isothiocyanate group using Tiocarbonyl dipyridine, to give the compound **68**.

Scheme 1:



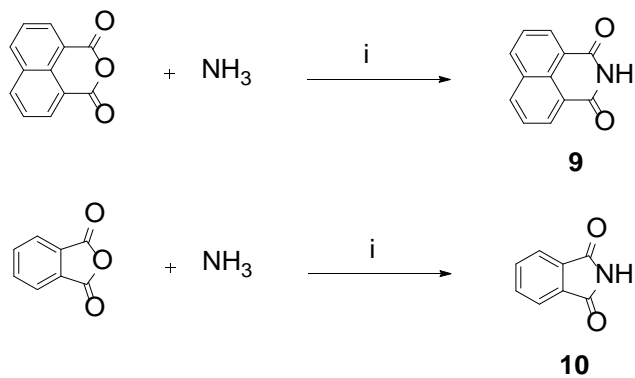
Condition: (i) EtOH, reflux; (ii) 2-MeOC₆H₄CHO, Toluene, reflux, (b) NaBH₄, EtOH, room temperature.

Scheme 2:



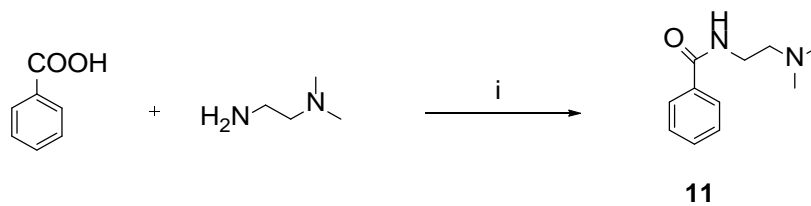
Condition: (i) Boc₂O, DMF, room temperature, 12h (ii) aldehyde, toluene, reflux, 5h (iii) HCl 6N, MeOH, room temperature, 12 h (iv) EtOH, reflux, 4h.

Scheme 3:



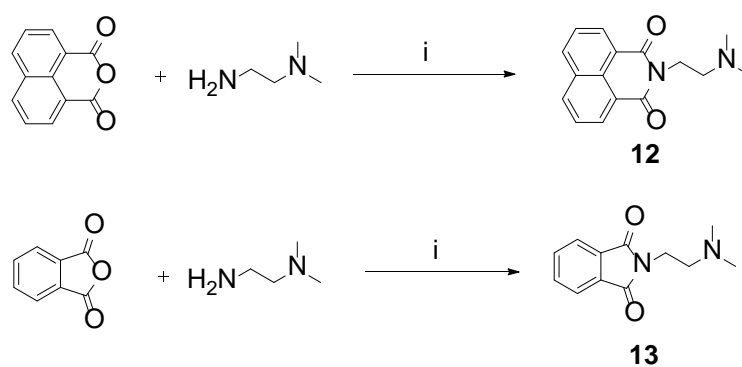
Condition: (i) reflux 6h.

Scheme 4:



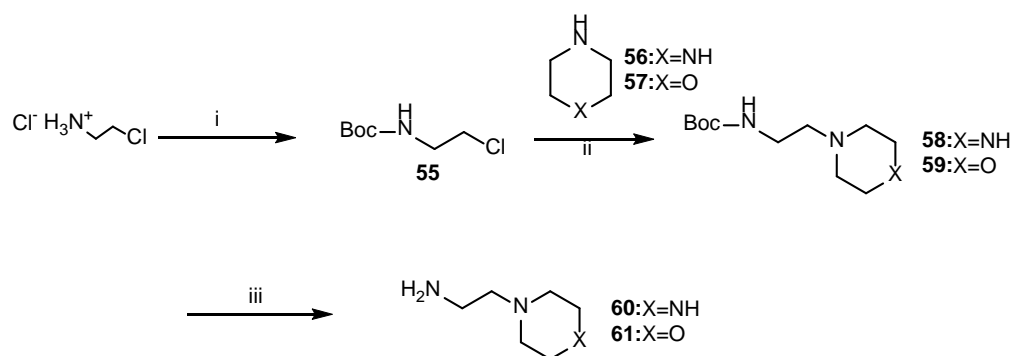
Condition: (i) EDC, HOBT, Et₃N, DCM, room temperature, 12 h

Scheme 5:



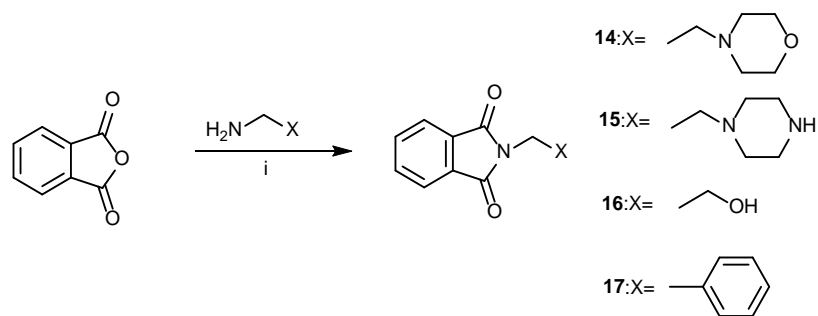
Condition: (i) EtOH, reflux 4h

Scheme 6:



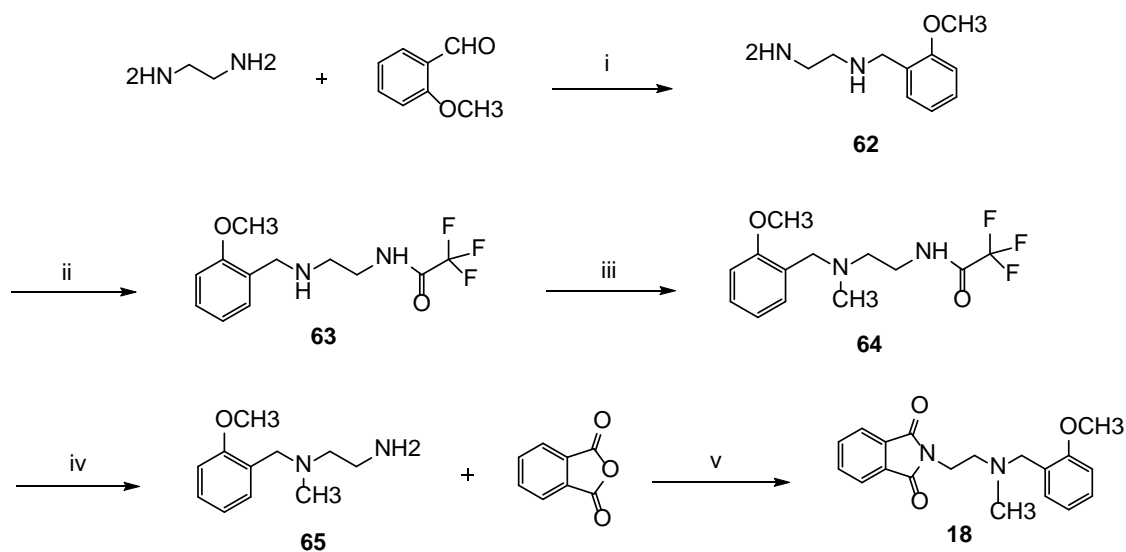
Condition: (i) Boc_2O , Et_3N , H_2O , room temperature, overnight (ii) Et_3N , DMF, reflux, 12 h (iii) HCl 3N, room temperature, overnight

Scheme 7:



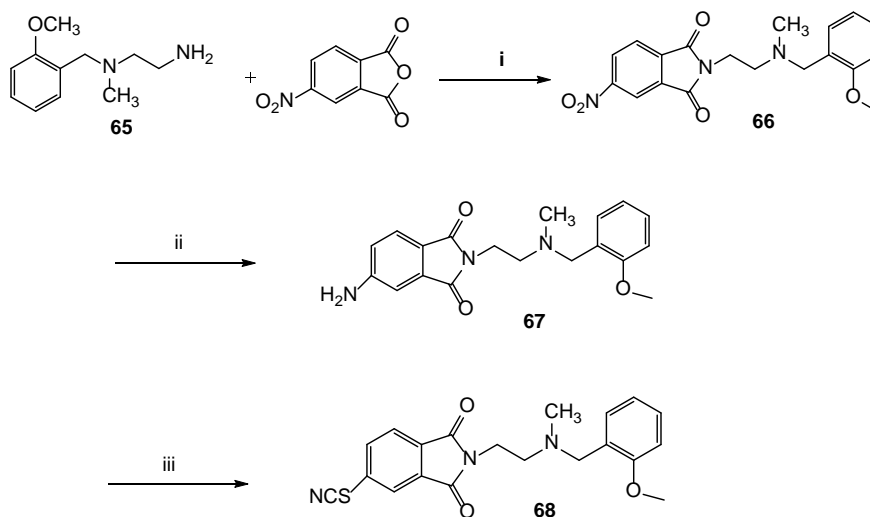
Condition: (i) H_2O , CH_3COOH , reflux, 4h

Scheme 8:



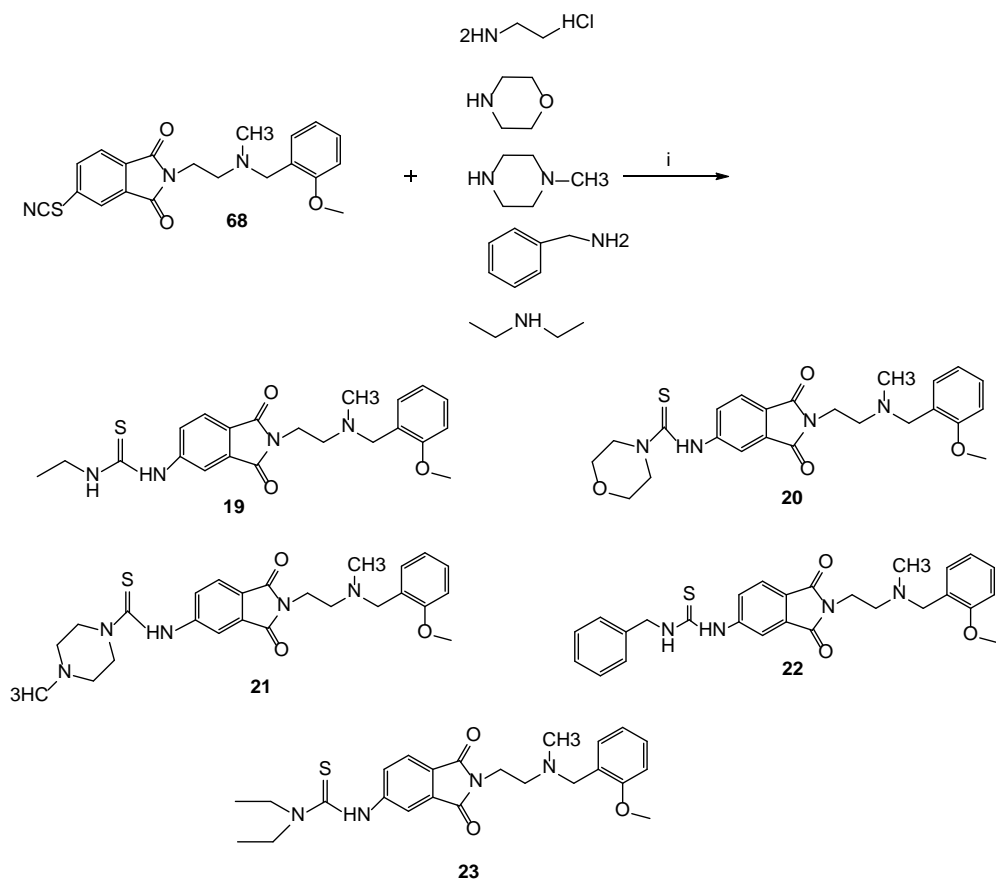
Condition: (i) Toluene, reflux, (ii) methanol, EtOCOCF₃ (iii) formic acid 85%, form aldehyde 40% (iv) NHOH, Ethanol (v) Ethanol, reflux, 3 hours

Scheme 9:



Condition: (i) Ethanol, reflux, 5 h (ii) SnCl₂, ethanol, reflux, 1h (iii) DCM, tiocarbonyl di pyridine, RT 16 hours.

Scheme 10:



Condition: DMF, Et₃N, RT

2.7.2 Biology:

To determine the potential interest of compounds **1-23**, their inhibitory potency against GSK-3 β was evaluated by luminescence assay.

For the characterization of the mechanism of action of the lead compound **13**, the application of the ESI-QTOF methodology developed by Andrisano and coworkers was applied (Annalisa D'Urzo 2016).

To estimate the toxicity and the bioavailability in vivo for the lead compound **13**, we used zebrafish model.

2.8 Results and Discussion

2.8.1 The evaluation of GSK-3 β inhibition:

Target compounds have been evaluated for their ability to inhibit GSK-3 β by using a luminescence assay. The method of Baki (A. Baki, 2007) was followed to analyze the inhibition of GSK-3 β . Assays were performed in 50 mM HEPES, 1 mM EDTA, 1 mM EGTA, and 15 mM magnesium acetate pH 7.5 assay buffer using white 96-well plates. In a typical assay, 10 μ L of test compound (dissolved in DMSO at 1 mM concentration and diluted in advance in assay buffer to the desired concentration) and 10 μ L (20 ng) of enzyme were added to each well followed by 20 μ L of assay buffer containing 25 μ M substrate and 1 μ M ATP. The final DMSO concentration in the reaction mixture did not exceed 1%. After 30 min incubation at 30 °C, the enzymatic reaction was stopped with 40 μ L of Kinase-Glo reagent. After 10 min, luminescence in the entire visible range was recorded using a Victor™ X3 Perkin Elmer multimode reader. The activity is proportional to the difference of the total and consumed ATP. The inhibitory activities were calculated on the basis of maximal kinase and luciferase activities measured in the absence of inhibitor and in the presence of reference compound inhibitor SB-415826 (M.P. Coghlan, 2000) at total inhibition concentration, respectively. The linear regression parameters were determined and the IC₅₀ extrapolated (Graph Pad Prism 4.0, GraphPad Software Inc.).

2.8.2 Results and Discussion for the compounds (1-13):

As could be observed in table 1, increasing the length of the spacer between the naphthalendiimide and the methoxybenzyl moiety led to a decrease in the inhibition activity (**1** vs **2-4**) as well as the elimination of the methoxy substituent (**5**) or its replacement with group characterized by different chemical-physical properties, such as methyl (**6**) or nitro group (**7**). Elimination of the chain in compound (**9**) led to a decrease in the activity, as well as the concomitant elimination of both the chain and an aromatic ring (**10**).

The elimination of one of carbonyl group (**11**) led to reduce the activity toward the enzyme. Replacement of the methoxybenzylamino group with dimethylamino amino group in the naphthalimide group in compound (**12**) led to a drop of the activity.

The phthalimide with dimethylamino amino group in compound (**13**) do not induces a similar reduction of the activity.

Table 1: Inhibitory activity towards GSK-3 β for compounds **1-13**.

Compound	% inhibition	IC ₅₀ (μ M)
1		1.56 \pm 0.05
2		2.10 \pm 0.14
3		2.38 \pm 0.54
4		3.01 \pm 0.74
5	69.15 at 10 μ M	
6	33.64 at 10 μ M	
7	31.62 at 10 μ M	
8	46.75 at 10 μ M	
9		9.50 \pm 1.43
10		20.22 \pm 0.40
11		45.00 \pm 10.90
12		21.72 \pm 2.68
13		9.51 \pm 0.13

The compounds (**1-4**) and the compound **9** showed good levels of activity toward GSK-3 β , but since the structures are characterized by a naphthalimide moiety, and it was reported in the literature it is able to interact with DNA (Czerwinska I 2014) that may lead to additional deleterious interaction which could result to serious side effects.

The compound **13** characterized by an IC₅₀ (9.51 \pm 0.13), it exhibited good level of activity toward GSK-3 β , so that we decided to investigate its mechanism of action.

2.8.3 Mechanism of action for the compound **13**:

The application of the ESI-QTOF methodology developed by Andrisano and coworkers (Annalisa D'Urzo 2016) was applied for the characterization of the mechanism of action of compound **13**. The Lineweaver-Burk plot was first obtained for Tideglusib as reference compound, and then following the same procedure the mechanism of **13** was investigated. The analysis of Lineweaver-Burk reciprocal plots for this compound reported in Figure (35) reveals a non ATP-competitive mechanism of action. Reciprocal plot obtained by

monitoring enzymatic velocity of **13** (0-10 μ M) at increasing ATP concentration (15-125 μ M) shows a decreasing v_{\max} value while the K_M value resulted not affected by inhibitor concentration (Figure. 35 A). Conversely, the graph obtained by plotting the inverse of velocity, expressed as P-GSM intensity, versus reciprocal GSM concentrations showed a change in v_{\max} only at higher inhibitor concentrations, while the x-intercept value ($1/K_M$) increases proportionally with the concentration of compound **13**. The detailed analysis of these plots compared to that obtained for tideglusib (data not shown) reveals that **13** is a non ATP- competitive inhibitor. Moreover, it was also possible to determine the K_i value for this novel compound and promising compound by plotting the slope values versus the concentration of compound **13**, A K_i value of 3.49 μ M was determined.

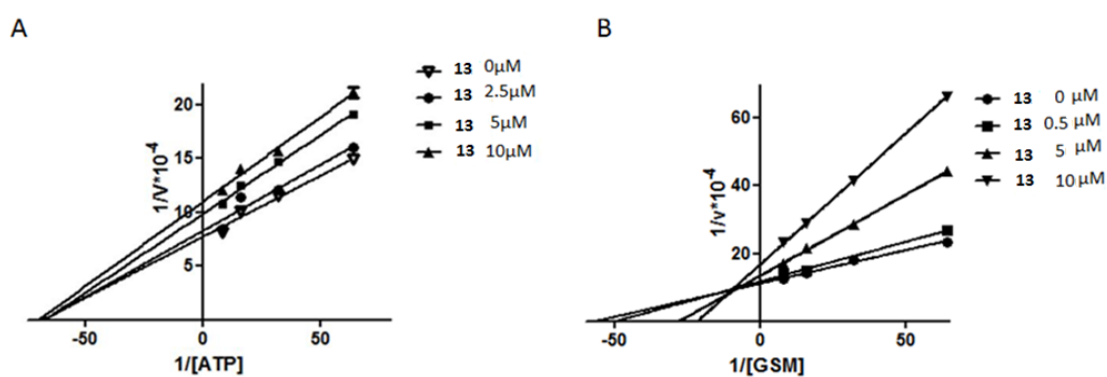


Figure 35: Kinetic study of compound **13** mechanism on GSK-3 β inhibition. Overlaid Lineweaver–Burk reciprocal plots of GSK-3 β initial velocity at increasing ATP (A) or substrate (B) concentration (0.015–0.125 mM) in the absence and in the presence of compound **13** are shown.

2.8.4 In vivo Evaluation for the compound **13** by using zebrafish model:

The compound **13** was tested for their in vivo activity on wild-type zebrafish embryos. In literature it is reported that Wnt pathways is activated with sequential alteration of the normal embryogenic development. The final effect of the treatment of zebrafish embryo with GSK3- β inhibitors in 5 hours post fertilization (hpf), determines the appearance of eyeless phenotype with crooked tail after 48 hpf (Funke, A 1958, Hormann, R. E. 2004, Kimmel, C. B 1995).

We exposed the embryos to these compounds at early stages of development. The embryos were collected and maintained in E2 into 40-well plates, 10 embryos per well

and maintained in E2 medium at 28 °C. Compounds were added 5 hpf (50% epiboly) with three concentrations 25 µM, 40 µM and 50 µM, the embryos allowed to grow in chemical compound solution up to 2 days. The phenotypes were compared using the Axio Scope.A1 microscope system at 44–48 hpf, compound **13** causes the eyeless phenotype and crooked tail at 40 µM figure (36).

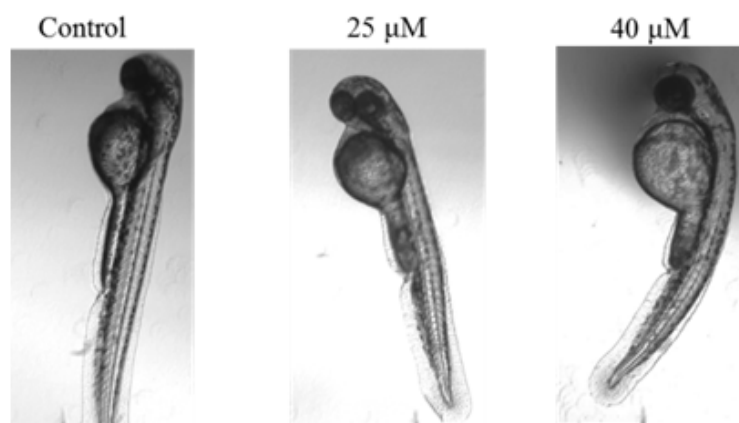


Figura 36: Effects on wild-type zebrafish embryos by compounds **13**. The embryos were collected and maintained in E2 medium at 28 °C, compounds were added 5 hpf, and the phenotypes were compared at 44–48 hpf. This compound causes the eyeless phenotype and crooked tail at 40 µM.

2.8.5 Results and Discussion for the compounds (14-23):

The compound **13** considered as a lead compound for developing new non-ATP competitive GSK-3β inhibitors, and it was subjected for further modifications in order in order to obtain a novel agent characterized with better activity and to increase the lipophilicity for better pharmacokinetic properties.

Modifying compound **13** led to the compounds (**14-18**), the compounds (**14-17**) characterized by a different substitution pattern in the phthalimide series, using different basic functions (**14,15**) and even without any basic function (**16,17**), resulted in reducing the activity levels of GSK-3β inhibition as it is observed in table 2.

Interestingly compound **18** is defined by *o*-methoxyethylendiamino chain and a phthalimide, and its value of IC₅₀ 7.5± 0.18.

Table 2: Inhibitory activity towards GSK-3 β for the compounds **14-18**

Compound	% inhibition	IC ₅₀ (μ M)
14	< 40% at 100 μ M	
15	< 40% at 100 μ M	
16	45.51% at 100 μ M	
17	< 40% at 100 μ M	
18		7.5 \pm 0.18

Compound **18** subjected for further modifications through adding a chain linked to the benzyle ring, ethyleamine **19**, morpholin **20**, methyl pyrazine **21**, benzyle **22**, and N-butylamine **23**, the synthesised compounds **19- 23** are currently under the evaluation for their activity as GSK-3 β inhibitions.

2.9 Conclusion

In this work it has been developed a hit compound **13** exhibited good level of activity toward GSK-3 β , characterized by micromolar range, studying the the mechanisms of action indicated that it acts as non-ATP competitive GSK-3 β inhibitors. Applying the compounds on zebrafish model caused eyeless phenotype at 25 μ M and a crooked tail at 50 μ M. In order to obtain more potent derivatives compound **13** was subjected for further optimization which led to have an interesting deritive **18** charchtrized with lower IC₅₀ value. More modifications were applied on the compound **18** by adding a chain with different sustituent linked to the benzyle ring by the aim to enhance the potency and increase the lipophilicity for better pharmacokinetic properties, and the synthesized compound currently are under the biological evaluation against GSK-3 β .

2.10 Experimental Section

Chemistry:

Melting points were measured in glass capillary tubes on a Buchi SMP-20 apparatus and are uncorrected. ESI-MS spectra were recorded on Perkin-Elmer 297 and Waters ZQ 4000. ^1H NMR and ^{13}C NMR were recorded on Varian VRX 200 and 300 instruments. Chemical shifts are reported in parts per million (ppm), and are relative to peak of tetramethylsilane (TMS). Spin multiplicities are given as s (singlet), br s (broad singlet), d (doublet), t (triplet), q (quartet) or m (multiplet). Although IR spectral data are not included (because of the lack of unusual features), they were obtained for all compounds reported, and they were consistent with the assigned structures. Chromatographic separations were performed on silica gel columns by flash (Kieselgel 40, 0.040-0.063 mm, Merck) or gravity (Kieselgel 60, 0.063-0.200 mm, Merck) column chromatography. Reactions were followed by thin layer chromatography (TLC) on Merck (0.25 mm) glass-packed precoated silica gel plates (60 F254) and then visualized in an iodine chamber or with a UV lamp. The term “dried” refers to the use of anhydrous sodium sulfate.

General procedure for the synthesis of 41-44: compounds **41-44** have been synthesized following the procedure reported in literature (Andrea Milelli 2012).

General procedure for the synthesis of derivatives 1-4: a mixture of **41-44** and 2-methoxy benzaldehyde (in a ratio 1:1.2) in toluene was refluxed in a Dean Stark apparatus for 3h. Following solvent removal, the residue was taken up in EtOH, NaBH_4 (in a 1:2.5 molar ratio) was added, and the stirring was continued at room temperature for 12h. The mixture was made acidic with 6 N HCl and the solvent removed. Then, the residue was dissolved in water and the resulting solution was washed with ether, made basic with K_2CO_3 and extracted with DCM (3x30ml). Removal of the dried solvent gave the desired products **1-4** which were purified by flash chromatography. **1-4** were finally converted into the para-toluen sulfonate salt.

2- (2- (2-Methoxybenzylamino) ethyl)-1H- benzo [de] isoquinoline -1,3 (2H)- dione (1): Compound **1** was synthesized from compound **41**; eluting solvent petroleum ether / CHCl_3 / MeOH / aqueous 33% ammonia (6:3.5:0.5/0.1); yellow oil ; 24% yield; ^1H -NMR (400 MHz, CDCl_3) δ 1.92 (s, H1), 2.97 (t, $J = 6.6$ Hz, 2H), 3.77 (s, 3H), 3.84 (s, 2H), 4.32

(t, $J=8.0$ Hz, 2H), 6.76-6.88 (m, 2H), 7.12-7.24 (m, 2H), 7.62-7.70 (m, 2H), 8.08- 8.13 (m, 2H), 4.48-8.52 (m, 2H); MS (ESI⁺) $m/z = 361$ (M+H)⁺.

2- (3- (2-Methoxybenzylamino) propyl)- 1H- benzo [de] isoquinoline- 1,3 (2H)- dione

(2): Compound **2** was synthesized from **42**; eluting solvent petroleum ether /CHCl₃/ MeOH /aqueous 33% ammonia (6:3.5:0.5/0.1); yellow oil; 24% yield; ¹H-NMR (400 MHz, CDCl₃) δ 1.91-2.05 (m, 2H), 2.36 (s, 1H), 2.73 (t, $J = 7.0$ Hz, 2H), 3.81 (s, 3H), 3.84 (s, 2H), 4.25 (t, $J = 7.0$ Hz, 2H), 6.82-6.90 (m, 2H), 7.15-7.25 (m, 2H), 7.65-7.74 (m, 2H), 8.13-8.17 (m, 2H), 8.52-8.55 (m, 2H); MS (ESI⁺) $m/z = 375$ (M+H)⁺.

2-(4- (2- Methoxybenzylamino) butyl) -1H- benzo [de] isoquinoline- 1,3 (2H)-dione

(3): Compound **3** was synthesized from **43**; eluting solvent petroleum ether/ CHCl₃/ MeOH/ aqueous 33% ammonia (6:3.5:0.5/0.1); yellow oil; 29% yield; ¹H-NMR (400 MHz, CDCl₃) δ 1.60-1.82 (m, 4H), 2.45 (s, 1H), 2.67 (t, $J = 7.0$ Hz, 2H), 3.79 (s, 3H), 3.83 (s, 2H), 4.17 (t, $J = 7.4$ Hz, 2H), 6.81-6.92 (m, 2H), 7.16-7.25 (m, 2H), 7.69 (t, $J = 8.0$ Hz, 2H), 8.12-8.17 (m, 2H), 8.51-8.55 (m, 2H); MS (ESI⁺) $m/z = 389$ (M+H)⁺.

2- (5- (2-Methoxybenzylamino) pentyl)- 1H- benzo[de] isoquinoline-1,3 (2H)-dione

(4): Compound **4** was synthesized from **44**; eluting solvent petroleum ether /CHCl₃/ MeOH/ aqueous 33% ammonia (6:3.5:0.5/0.1); yellow oil; 34% yield; ¹H-NMR (400 MHz, CDCl₃) δ 1.27-1.80 (m, 7H), 2.65 (t, $J = 7.4$ Hz, 2H), 3.81 (s, 2H) ,3.84 (s, 3H), 4.17 (t, $J = 7.8$ Hz, 2H), 6.84-6.94 (m, 2H), 7.19-7.30 (m, 2H), 7.72 (t, $J = 8.2$ Hz, 2H), 8.15-8.19 (m, 2H), 8.53-8.57 (m, 2H); ¹³CNMR (101, CDCl₃) δ 24.76, 27.91, 29.18, 40.19, 48.57, 48.76, 55.15, 110.11, 120.32, 122.57, 126.58, 127.18, 127.98, 128.35, 130.02, 131.02, 131.45, 133.72, 157.55, 164.02; MS (ESI⁺) $m/z = 403$ (M+H)⁺.

General procedure for the synthesis of compounds 45- 46: To a solution of Ethylendiamin and other solution of n-methylethylenediamine in DCM (1eq) we added Boc (1eq), the resulting mixture was stirred for 12 h in room temperature, concentrated under reduced pressure. The crude residue was used for the synthesis of **47**, **48**, **49**, **50** without any further purification.

General procedure for the synthesis of compounds 47-50: A mixture of **45-46** with the corresponding aldehyde (in ratio 1:1.2) into luene was reflux Edina Dean –Stark apparatus for 3h. Following solvent removal, the residue was taken up in EtOH, NaBH₄ (in a 1:2.5 molar ratio) was added, and the stirring was continued at room temperature

for 12h. Following solvent removal; then dissolving in DCM. The organic layer was washed with saturated solution of sodium chloride, The combined organic extracts were dried (MgSO_4) and concentrated under reduced pressure, The crude residue was then subjected to flash silica gel column chromatography with DCM / MeOH / aq NH_3 33% (9:1:0.1).

Tert-butyl (2-(benzylamino) ethyl) carbamate (47): 77% yield; $^1\text{H-NMR}$ (400 MHz, CDCl_3) δ 1.42 (s, 9H), 2.67 (t, 2H), 3.24 (t, 2H), 3.77 (s, 2H), 7.12-7.26 (m, 4H).

Tert-butyl (2-((2-methylbenzyl) amino) ethyl) carbamate (48): 65% yield, $^1\text{H-NMR}$ (400 MHz, CDCl_3) δ 1.22 (s, 9H), 2.21 (s, 3H), 2.70 (t, 2H), 3.27 (t, 2H), 3.84 (s, 2H), 7.10-7.27 (m, 4H).

Tert-butyl (2-((2-nitrobenzyl) amino) ethyl) carbamate (49): 71% yield; $^1\text{H-NMR}$ (400 MHz, CDCl_3) δ 1.19 (s, 9H), 2.75 (t, 2H), 3.33 (t, 2H), 3.72 (s, 2H), 6.99-7.17 (m, 4H).

Tert-butyl (2-((2-methoxybenzyl) (methyl) amino) ethyl) carbamate (50): 41% yield; $^1\text{H-NMR}$ (400 MHz, CDCl_3) δ 1.28 (s, 9H), 2.27 (s, 3H), 2.52 (t, 2H), 3.27 (t, 2H), 3.75 (s, 2H), 3.89 (s, 3H), 7.02-7.20 (m, 4H).

General procedure for the synthesis of compounds 51-54: The solution of **47-50** in MeOH was acidified with 6 NHCl and the solvent removed. Then, the residue was dissolved in water and the resulting solution was washed with ether, made basic with K_2CO_3 and extracted with DCM (3x30mL). The combined organic extracts were dried (MgSO_4) and concentrated under reduced pressure, the crude residue was then subjected to flash silica gel column chromatography with DCM / MeOH / aq NH_3 33% (9:1:0.1).

General procedure for the synthesis of compounds 5-8: To a solution of 1 eq of the compound (20-23) in toluin, we added 1 q of 1,8 naftalinamide, then the resulting mixture was stirred under reflux for 5 hours, concentrated under reduced pressure, the crude residue was then subjected to flash silica gel column chromatography with DCM / MeOH / aq NH_3 -33% (9:1:0.1).

2-(2-(Benzylamino) ethyl)-1H-benzo[de]isoquinoline-1,3(2H)-dione (5): 55% yield' $^1\text{H-NMR}$ (400 MHz, CDCl_3) δ 1.32 (s, 9H), 2.97 (t, 2H), 3.66 (t, 2H), 3.79 (s, 2H), 7.09-7.26 (m, 4H), 7.98-8.11 (m, 4H). MS (ESI^+) $m/z = 331$ ($\text{M}+\text{H}$) $^+$.

2-(2-((3-Methylbenzyl)amino)ethyl)-1H-benzo[de]isoquinoline-1,3(2H)-dione(6): 49% yield, $^1\text{H-NMR}$ (400 MHz, CDCl_3); δ 1.29 (s, 9H), 2.25 (s, 3H), 2.98 (t, 2H), 3.45 (t, 2H), 3.79 (s, 2H), 7.03-7.21 (m, 6H), 8.02-8.33 (m, 4H); MS (ESI^+) $m/z = 345$ ($\text{M}+\text{H}$) $^+$.

2-(2-((3-Nitrobenzyl)amino)ethyl)-1H-benzo[de]isoquinoline-1,3(2H)-dione (7): 60% yield; $^1\text{H-NMR}$ (400 MHz, CDCl_3) δ 1.19 (s, 9H), 2.88 (t, 2H), 3.57 (t, 2H), 3.99 (s, 2H), 6.91-7.15 (m, 6H), 8.11-8.27 (m, 4H); MS (ESI^+) $m/z = 367$ ($\text{M}+\text{H}$) $^+$.

2-(2-((3-Methoxybenzyl) (methyl)amino) ethyl)- 1H- benzo [de] isoquinoline-1, 3(2H)- dione (8): 47% yield, $^1\text{H-NMR}$ (400 MHz, CDCl_3) δ 1.19 (s, 9H), 2.25 (s, 3H), 2.72 (t, 2H), 3.44 (t, 3H), 3.89 (s, 3H), 3.99 (s, 3H), 6.99-7.15 (m, 6H), 7.99-8.15 (m, 4H); MS (ESI^+) $m/z = 375$ ($\text{M}+\text{H}$) $^+$.

Tert- butyl (2-chloroethyl) carbamate (56): to a solution of 2-chloroethylamine hydrochloride (18 mmol, 1 eq) in 4 ml of water we added triethylamine dropwise (23 mmol, 1.3 eq), the resulting mixture was stirred at room temperature for 30 minutes. Then we added a dissolved Boc₂O (20 mmol, 1.1 eq) in 20 ml of THF, resulting mixture was stirred at room temperature for 12 h. Then it was extracted with EtOAc, concentrated under reduced pressure. The crude residue was used for the synthesis of **60** without further purification.

General procedure for the synthesis of (9-10): Compounds **9-10** have been synthesized following the procedure reported in literature (Braña MF, 2002).

N-(2-(dimethylamino) ethyl) benzamide (11): To a solution of benzoic acid in dichloromethane, we added EDCI, HOBT and triethylamine; the resulting mixture was stirred for 30 minutes. Then we added Dimethylethylenediamine, the resulting mixture was stirred at RT for 12h, concentrated under reduced pressure. The crude residue was then subjected to flash silica gel column chromatography with DCM/MeOH, (9: 1), yellow oil, 47% yield; $^1\text{H-NMR}$ (400 MHz, CDCl_3) δ 2.45b (s, 6H), 2.77 (t, 2H), 3.65 (m, 2H), 7.30-7.44 (m, 4H), 7.66 (s, 1H), 7.81-7.83 (m, 1H); MS (ESI^+) $m/z = 178$ ($\text{M}+\text{H}$) $^+$.

General procedure for the synthesis of compounds 12-13: The corresponding anhydride was dissolved in ethanol and we added Dimethylethylenediamine and DMAP, the resulting mixture was stirred at reflux for 4 h then concentrated under reduced pressure, the crude residue was then subjected to flash silica gel column chromatography with DCM/MeOH, (9: 1).

2-(2-(Dimethylamino) ethyl)- 1H- benzo [de] isoquinoline-1,3 (2H)- dione (12): 61% yield; yellow oil; $^1\text{H-NMR}$ (400 MHz, CDCl_3) δ 2.01 (s, 6H), 2.72 (t, 2H), 3.54 (t, 2H), 7.31 (d, 2H), 7.89 (d, 2H), 8.11 (d, 2H); MS (ESI^+) $m/z = 269$ ($\text{M}+\text{H}$) $^+$.

2-(2-(Dimethylamino) ethyl) isoindoline-1, 3-dione (13): 72% yield; Yellow oil; ¹H-NMR (400 MHz, CDCl₃) δ 2.28 (s, 6H), 2.58 (t, 2H), 3.79 (t, 2H), 7.67-7.70 (m, 2H), 7.78-7.83 (m, 2H). MS (ESI+) m/z = 219 (M+H)⁺.

Tert-butyl (2-(piperazin-1-yl)ethyl)carbamate (58): Compound **55** (9 mmol, 1 eq) was dissolved in DMF, we added triethylamine (1.2 ml, 1 eq) and piperazine (36mmol, 4 eq). The resulting mixture was stirred under reflux for 12h, concentrated under reduced pressure. The crude residue was then subjected to flash silica gel column chromatography with DCM / MeOH / aq NH₃ 33% in the ratio (9.5: 0.5: 0.05); 43% yield; yellow oil; ¹H-NMR (400 MHz, CDCl₃) δ 1.36 (s, 9H), 2.33-2.40 (m, 6H), 3.13-3.14 (m, 2H), 3.30-3.36 (m, 2H), 3.51-3.54 (m, 2H), 5.03 (s, 1H).

Tert-butyl (2-morpholinoethyl) carbamate (59): Compound **55** (6 mmol, 1 eq) was dissolved in DMF, we added DIPEA (1.19 ml, 6 mmol, 1 eq) and morpholine (0:55 ml, 6 mmol, 1 eq). The resulting mixture was stirred under reflux for 12h, concentrated under reduced pressure. The crude residue was then subjected to flash silica gel column chromatography with DCM / MeOH / aq NH₃ 33% (9.5: 0.5: 0:02);); yellow oil 55% yield, ¹H-NMR (400 MHz, CDCl₃) δ 1.31 (s, 9H), 2.31-2.45 (m, 6H), 3.21 (t, 2H), 3.61-3.68 (m, 4H).

2-(Piperazin-1-yl) ethan-1-amine (60): We dissolved compound **58** (3.21 mmol) in dioxane, the solution was cooled to 0°C, and then we added 20 ml of HCl 3N. The resulting stirred overnight at room temperature. Then the solution was basified with potassium carbonate, extracted with DCM (3 x 30 ml). The organic layer was washed with saturated solution of sodium chloride, the combined organic extracts were dried (MgSO₄) and concentrated under reduced pressure; ¹H-NMR (400 MHz, CDCl₃) δ 2.81 (t, 2H), 2.95 (t, 2H), 3.10 (m, 4H), 3.53-3.65 (m, 2H).

2-Morpholinoethan-1-amine (61): We dissolved compound **59** (3.21 mmol) in dioxane, the solution was cooled to 0 ° C; we added 20 ml of HCl 3N. The resulting stirred overnight at room temperature. Then the solution was basified with potassium carbonate, extracted with DCM (3 x 30 ml). The organic layer was washed with saturated solution of sodium chloride, The combined organic extracts were dried (MgSO₄) and concentrated under reduced pressure; 80% yield, yellow oil; ¹H-NMR (400 MHz, CDCl₃) δ 2.29-2.36 (m, 4H), 2.97 (t, 2H), 3.15 (m, 2H), 3.52-3.63 (m, 4H).

General procedure for the synthesis of compounds 14-17: To a suspension of Phthalic anhydride (6 mmol, 1 eq) in water (20 ml) we added 5 ml of acetic acid and the

corresponding amine (6 mmol, 1 eq); the resulting mixture stirred under reflux for 4 hours. The purification procedure differs based on the nature of the side chain.

Work-up for the compounds 14-15: The resulting solution was basified (PH=9) with sodium bicarbonate and extracted with DCM (3 x 20 ml). The combined organic extracts were dried (MgSO₄) and concentrated under reduced pressure. The crude residue was then subjected to flash silica gel column chromatography with, DCM / MeOH / aq NH₃ 33% (9: 1: 0:02).

2-(2-Morpholinoethyl) isoindoline-1,3-dione (14): 65% yield; yellow oil; ¹H-NMR (400 MHz, CDCl₃) δ 2.49-2.51 (m, 4H), 2.60-2.64 (m, 2H), 3.61-3.63, (m, 4H), 3.79-3.82 (t, 2H), 7.69-7.72 (m, 2H), 7.82-7.84 (m, 2H); ESI-MS (m/z): 261 (M+H)⁺.

2-(2-(Piperazin-1-yl)ethyl)isoindoline-1,3-dione (15): 43% yield; yellow oil; ¹H-NMR (400 MHz, CDCl₃) δ 1.91 (s, 1H), 2.12-2.24 (m, 4H), 2.61-2.72 (m, 4H), 2.89-2.95 (m, 2H), 3.76 (t, 2H), 7.63-7.77 (m, 2H), 7.86-7.91 (m, 2H); ESI-MS (m/z): 260 (M+H)⁺.

Work-up for the compounds 16-17: After the resulting solution cooled to room temperature we added, the precipitated solid was filtered and crystallized in ethanol.

2-(2-Hydroxyethyl) isoindoline-1, 3-dione (16): 66% yield; yellow oil; ¹H-NMR (400 MHz, CDCl₃) δ 2.57 (s, 1H), 3.84-3.90 (m, 4H), 7.69-7.73 (m, 2H), 7.80-7.84 (m, 2H). ESI-MS (m/z): 192 [M +H].⁺

2-Phenethylisoindoline-1, 3-dione (17): 71% yield; yellow oil; ¹H-NMR (400 MHz, CDCl₃) δ 4.84 (s, 2H), 7.25-7.30 (m, 3H), 7.42-7.44 (m, 2H), 7.76-7.78 (m, 2H), 7.80-7.83 (m, 2H). ESI-MS (m/z): 238 (M+H)⁺.

N1-(2-methoxybenzyl) ethane-1, 2-diamine (62): A mixture of the appropriate diamine and aldehyde (in a 5:1 molar ratio) in toluene was refluxed in a Deane Stark apparatus for 5 h. Following solvent removal, the residue was taken up in EtOH, NaBH₄ (1:2.5 molar ratio) was added at 0 ° C, and the stirring was continued at room temperature for 4 h. The solvent was then removed and the residue was dissolved in dichloromethane and washed with brine. Removal of the dried solvent gave a residue that was purified by flash chromatography using as eluent a mixture of Dichloromethane /methanol/33% aqueous ammonia (9:1:0.1), providing the desired products.

2-(2-((2-Methoxybenzyl) amino) ethyl) isoindoline-1, 3-dione (18): Phthalic anhydride was dissolved in ethanol and we added the compound (62) and DMAP, the resulting mixture was stirred at reflux for 4 h then concentrated under reduced pressure. The crude residue was then subjected to flash silica gel column chromatography with DCM/MeOH, (9: 1); ¹H-NMR (400 MHz, CDCl₃) δ 7.9 (s, 1H), 7.25 (d, 1H), 6.76-6.83 (m, 3H), 3.77 (s,

2H), 3.70 (s, 3H), 3.59-3.63 (m, 2H), 2.74 (t, 2H); ¹³CNMR (101, CDCl₃) δ 170, 169.1, 157.2, 132.5, 127.9, 123.8, 122.4, 119.7, 112.6, 57.2, 51.9, 48.9, 45.3.

Hoxybenzyl) amino)ethyl) acetamide (63): We dissolved **63** in Methanol, then we cooled the flask till -78 under the Nitrogen, we added the ETOOCF₃ dropwise, and we left the reaction stirring at 0 ° C for 1 hour, then the result mixture was extracted with DCM . The organic layer was washed with saturated solution of sodium chloride, the combined organic extracts were dried (MgSO₄) and concentrated under reduced pressure. The crude residue was then subjected to flash silica gel column chromatography with DCM / MeOH / aq NH₃ 33% (9: 1: 0:01).

2,2,2- Trifluoro-N-(2-((2-methoxybenzyl) (methyl) amino)ethyl) acetamide (64): We dissolved **64** in Formic acid, then we added form aldehyde dropwise, the result mixture was stirred under reflux for 12 hours. The resulting solution was cooled to room temperature then basified (PH=8) with sodium bicarbonate and extracted with DCM. The combined organic extracts were dried (MgSO₄) and concentrated under reduced pressure. The crude residue was then subjected to flash silica gel column chromatography with, DCM / MeOH / aq NH₃ 33% (9.9: 0.1:0:1).

N1- (2-methoxybenzyl)- N1-methylethane-1,2- diamine (65): We dissolved **65** in Ethanol then we added 2 eq of NHOH dissolved in water dropwise, the resulting mixture was stirred overnight in room temperature, then the result mixture was extracted with DCM. The organic layer was washed with water. The combined organic extracts were dried (MgSO₄) and concentrated under reduced pressure. The crude residue was then subjected to flash silica gel column chromatography with, DCM / MeOH / aq NH₃ 33% (9.5:0.5:0:1).

2-(2-((2-Methoxybenzyl)(methyl)amino) ethyl)-5-nitroisindoline-1,3-dione (66): We dissolved **66** in Ethanol, then we left the reaction stirring in room temperature for 15 minutes, then we added 1 eq of 4 Nitro phthalic anhydride, the result mixture stirred under reflux for 5 hours, then concentrated under reduced pressure. The crude residue was then subjected to flash silica gel column chromatography with, DCM / MeOH / aq NH₃ 33% (9.5:0.5:0:1).

5-Amino-2-(2-((2-methoxybenzyl) (methyl) amino) ethyl) isoindoline -1, 3-dione (67): We dissolved **67** in Ethanol, and then we added SnCl₂, the reaction stirred under reflux for 1 hour. Then concentrated under reduced pressure, and washed with water then extracted with DCM, the combined organic extracts were dried (MgSO₄) and

concentrated under reduced pressure. The crude residue was then subjected to flash silica gel column chromatography with, DCM / MeOH / aq NH₃ 33% (9.5: 0.5: 0:1).

2-(2-((2-Methoxybenzyl)(methyl)amino)ethyl)-5-thiocyanatoisoindoline-1,3-dione

(68): In a flask, provided with an inert atmosphere, we placed compound **68** dissolved in DCM anhydrous. The resulting solution was treated drop wise with a solution of Thiocarbonyl dipyridine in DCM anhydrous, The resulting mixture was left stirring overnight in room temperature, then it was concentrated under reduced pressure. The crude residue was then subjected to flash silica gel column chromatography with, DCM / MeOH / aq NH₃ 33% (9.5: 0.5: 0:1).

General procedure for the synthesis of (19-23): We dissolved the amine in DMF then we added TE₃N, and we left the result mixture stirring in room temperature for 5 minutes, before adding the compound **68** (dissolved in DMF), The resulting mixture was left stirring for 3 hours in room temperature, then it was concentrated under reduced pressure. The crude residue was then subjected to flash silica gel column chromatography with, DCM / MeOH / aq NH₃ 33% (9.5: 0.5: 0:1).

1-Ethyl-3-(2-(2-((2-methoxybenzyl)(methyl)amino)ethyl)-1,3-dioxisoindolin-5-yl)

thiourea (19): ¹H-NMR (400 MHz, CDCl₃) δ 8.01 (s, 2H), 7.82 (d, 1H), 7.47 (d, 2H), 6.83-6.79 (m, 3H), 5.28 (s, 2H), 3.87-3.8 (m, 7H), 3.76 (d, 2H), 2.83 (t, 3H), 2.39 (s, 3H); ¹³CNMR (101, CDCl₃) δ 168.25, 167.9, 164.65, 157.82, 145.10, 142.14, 134.53, 132.90, 131.28, 129.19, 123.88, 120.46, 120.29, 110.6, 107.36, 55.40, 55.059, 54.50, 53.43, 46.89, 41.65, 35.26; MS (ESI+) m/z = 426.53 (M+H)⁺.

N-(2-(2-((2-methoxybenzyl)(methyl)amino)ethyl)-1,3-dioxisoindolin-5-yl)

morpholine - 4- carbothioamide (20): ¹H-NMR (400 MHz, CDCl₃) δ 7.69 (t, 2H), 7.53 (d, 1H), 7.26-7.19 (m, 2H), 6.84 (t, 3H), 3.91-3.755 (m, 15H), 2.84 (s, 1H), 2.41 (s, 3H); ¹³CNMR (101, CDCl₃) δ 182.1, 167.83, 167.77, 157.83, 145.69, 133.164, 131.18, 128.1, 127.24, 123.6, 120.41, 117.57, 110.55, 77.31, 77, 76.68, 66.19, 55.38, 55.29, 54.86, 54.27, 49.43, 48.66, 41.6, 35.32; MS (ESI+) m/z = 468.6 (M+H)⁺.

N-(2-(2-((2-methoxybenzyl)(methyl)amino)ethyl)-1,3-dioxisoindolin-5-yl)-4 methyl

piperazine -1- carbothioamide (21): ¹H-NMR (400 MHz, CDCl₃) δ 8.25 (d, 2H), 7.98 (t, 1H), 7.3 (d, 1H), 6.9 (m, 3H), 3.75 (m, 11H), 2.64 (t, 2H), 2.3- 2.17 (m, 10H); ¹³CNMR (101, CDCl₃) δ 181.1, 167.98, 167.7, 158.7, 140.6, 132.7, 130, 129.8, 128.9, 128.6, 127.8, 126.5, 122.5, 120.7, 112.8, 59.7, 56.9, 56.6, 56.1, 51.9, 51.6, 49.3, 46.7, 43.8; MS (ESI+) m/z = 481.6 (M+H)⁺.

1-Benzyl-3-(2-(2-((2-methoxybenzyl)(methyl)amino)ethyl)-1,3-dioxoisindolin-5-yl)thiourea (22): $^1\text{H-NMR}$ (400 MHz, CDCl_3) δ 7.86 (s, 3H), 7.74 (d, 2H), 7.62 (d, 6H), 7.31-7.26 (m, 3H), 4.79 (d, 2H), 3.79-3.66 (m, 7H), 2.92-2.77 (m, 2H), 2.33 (s, 3H); $^{13}\text{C-NMR}$ (101, CDCl_3) δ 180.64, 180.62, 167.78, 167.61, 157.69, 157.7, 144.02, 133.30, 130.88, 128.75, 127.87, 127.76, 124.13, 120.32, 110.47, 77.31, 77, 76.68, 55.32, 55.11, 54.45, 48.78, 41.81, 35.48; MS (ESI+) $m/z = 488.6$ ($\text{M}+\text{H}$) $^+$.

1,1-Diethyl-3-(2-(2-((2-methoxybenzyl)(methyl)amino)ethyl)-1,3-dioxoisindolin-5-yl)thiourea (23): $^1\text{H-NMR}$ (400 MHz, CDCl_3) δ 8.19 (t, 2H), 7.9 (d, 1H), 7.29 (t, 1H), 6.79-6.9 (m, 3H), 3.71-3.59 (m, 11H), 2.61 (t, 2H), 2.27 (s, 3H), 1.2 (t, 6H); $^{13}\text{C-NMR}$ (101, CDCl_3) δ 180.6, 168.6, 168.4, 158.56, 140.76, 132.58, 130.9, 129.78, 128.63, 127.98, 127.52, 122.84, 120.21, 113.1, 58.9, 56.83, 55.87, 49.72, 35.7, 13.3, 13.12; MS (ESI+) $m/z = 454.6$ ($\text{M}+\text{H}$) $^+$.

Chapter 3. Multi Target Directed Ligand approach in AD

The only used drugs for the treatment of Alzheimer's disease (AD), with the exception of memantine, are cholinesterase (ChE) inhibitors, which derived from the classical drug design strategy based on the "one-molecule-one-target" paradigm. This strategy enforced many effective drugs able to hit a single target of a given disease, but such drugs that modulate a single target may not be clinically effective when dealing with multifactorial diseases, such as AD. Molecules developed through this strategy are usually highly selective for a given target but it should be noted that a highly selective ligand for a given target does not always result in a clinically efficacious drug. This may happen because (1) the ligand does not recognize the target *in vivo*, (2) the ligand does not reach the site of action, or (3) the interaction with the respective target does not have enough impact on the diseased system to restore it effectively.

Among several drug discovery methods, a very promising modern strategy consists of designing multi-target-directed ligands (MTDLs) able to modulate simultaneously multiple targets. This methodology has been specifically developed for the treatment of disorders with complex pathological mechanisms (multifactorial) such as AD.

Several strategies can be used to develop drugs able to modulate simultaneously different targets (Morphy, R 2005). The first approach is called multiple-medication therapy (MMT), which consists of the administration of a cocktail of two or three different drugs, characterized by different mechanisms of action and in two or more individual dosage forms. This approach has some disadvantages including patient compliance issues. In another strategy called multiple-compound medication (MCM) (single-pill drug combination), two or more drugs are comprised in a single dosage form, which implies the incorporation of several drugs into the same formulation in order to simplify dosing regimens and enhance patient compliance. Finally, a third strategy is now emerging on the basis of the assumption that a single compound may be able to hit multiple targets simultaneously. These compounds are called Multi-Target-Directed Ligands (MTDL). This approach has been widely used as design strategy by a lot of scientists as evidenced by the increased number of publications in the field in recent years. MTDLs may have some advantages or disadvantages compared to the two other approaches (Schmitt, B, 2004). For instance, MTDLs can show a less complex ADMET profile in contrast to MMT/MCM, in which the different drugs can suffer of several troubles related to their bioavailability, pharmacokinetic properties, and metabolism. Not last, by this approach

the risk of possible problems arising from drug-drug interactions would be avoided and the therapeutic regimen greatly simplified in relation to MMT (Kola, I 2004).

There is, therefore, a strong indication that the development of compounds able to hit multiple targets might disclose new avenues for the treatment of, for instance, major neurodegenerative diseases, for which an effective cure is an urgent need and a principal goal (Cavalli, A 2008, Morphy, R 2005).

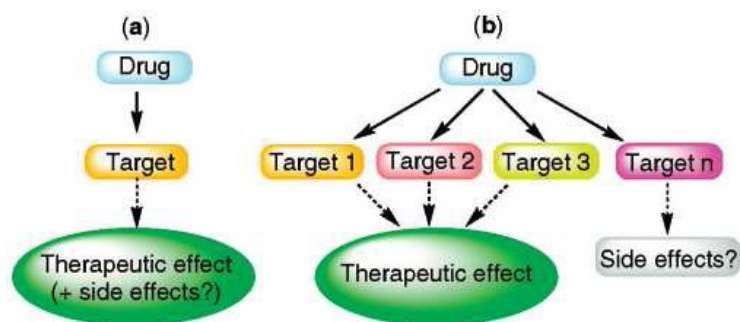


Figure 37: Pathways leading to the discovery of new medications (a) Target driven drug discovery approach; (b) MTDLs approach to drug discovery (Cavalli, A. 2008).

The methods for generating novel MTDLs are based on the combination of distinct pharmacophores of different drugs in the same structure by cleavable or non cleavable metabolically stable linker groups (termed as conjugates) or the pharmacophores can be overlapped (fused or merged) by taking advantage of structure commonalities to afford hybrid molecules. Important in the design of new MTDLs is that each pharmacophore of these new drugs should retain the ability to interact with its specific site (s) on the target and, consequently, to generate specific pharmacological responses that, taken together could enable the modulation of multiple targets.

The multifactorial nature of AD and the lack of therapeutic effectiveness of the current FDA-approved drugs, which are based on the single-target paradigm, has inexorably fueled the rational design and development of novel MTDLs able to directly interact with multiple targets associated with AD by the molecular hybridization of different pharmacophoric subunits from known bioactive molecules. The main challenges in designing and synthesizing multitarget anti-Alzheimer agents are the choice of the targets to be hit and the potency of the compounds at the different targets, since a multitarget action will be only effective when balanced activities are achieved at the different targets.

One of the most widely adopted approaches in the field of anti-AD MTDLs has been to modify the molecular structure of an AChEI in order to provide it with additional biological properties useful for treating AD. Well known drugs such as tacrine, donepezil, rivastigmine, berberine, have been used as structural scaffold for the design and development of new compounds as MTDLs for the treatment of AD.

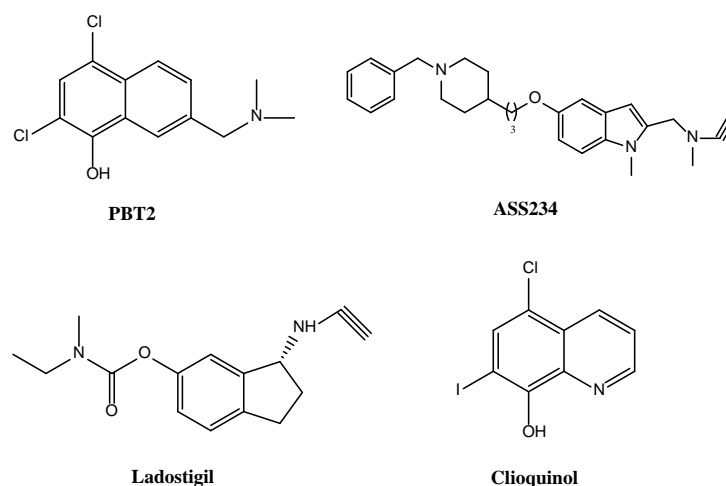


Figure 38: Structure of some developed MTDLs for AD disease

In spite of the fact that MTDLs are not true network medicines yet, they may be considered as lead drugs possessing a great value as a real alternative to the current unsuccessful pharmacological therapies for effectively fighting against AD and other complex diseases. The researchers exploit the strategy of MTDL in designing “dual binding site” AChEIs able to simultaneously interact with AChE catalytic (CAS) and peripheral sites (PAS) which may lead to advantages in reducing A β aggregation (Recanatini, M 2004). Indeed, Inestrosa et al discovered that AChE is endowed with interesting noncholinergic activities: it exerts A β pro-aggregating action by promoting the formation of A β fibrils through the PAS of the enzyme (Alvarez, A 1995) and therefore, AChEIs able to bind at PAS can block the proaggregating action of the enzyme (DeFerrari, G.V 2001, Inestrosa, N.C 1996). Pang and coworkers developed dimers of tacrine with the aim of enhancing its affinity towards AChE (Pang, Y.P 1996). Interestingly, the lead compound, **XV**, also acts as NMDAR antagonist (Li, W 2007), as inhibitor of the nitric oxide synthase and is able to reduce *in vitro* A β formation by inhibition of BACE-1 (Fu, H 2008). This compound resulted 500-fold more potent than

tacrine in inhibiting *hAChE* (Pang, Y.P 1996). The structure-activity relationships around this class of compounds are summarized in Figure 39.

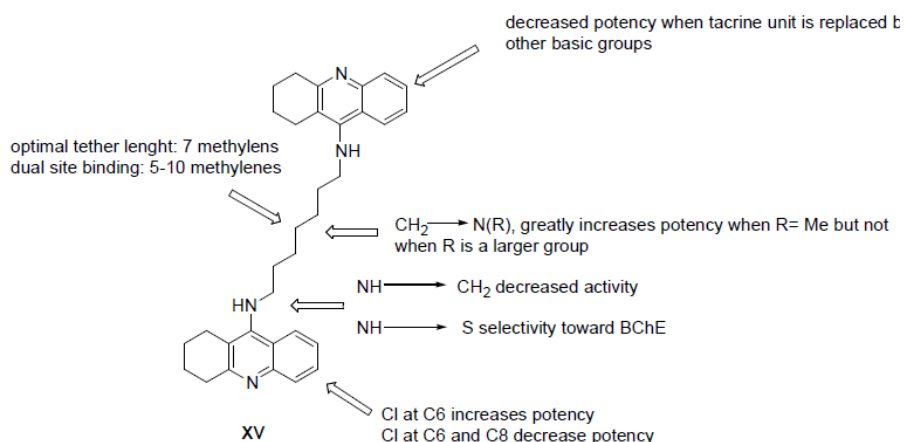


Figure 39: structure-activity relationships studies on bis-tacrine derivatives as MTDLs (Muñoz-Torrero, D 2008).

In 2003, Sharpless and coworkers developed new dual-binding AChEIs (Lewis, W.G 2002), using tacrine as catalytic-site inhibitor and phenylphenanthridium and other molecules as PAS-inhibitors; these compounds contain alkyl-azide and alkyl-acetylene side chains with varying length to allow to undergo a Huisgen 1,3-dipolar cycloaddition leading to the formation of a 1,2,3-triazole ring within the enzyme AChE (click chemistry *in situ*). The compound **XVI** (figure 40) is one of the most potent AChE inhibitors, having K_D values between 77 fM (*Torpedo californica* AChE) and 410 fM (mouse AChE), clearly lower than those of tacrine and propidium (18 and 1100 nM on mouse AChE, respectively). It is important to point out that the **XVI** *anti* isomer was not obtained using this approach and was chemically synthesized and found to be less active by two-orders of magnitude than its *syn* isomer. X-Ray structure of the complexes of both *syn* and *anti* isomers of **XVI** with mouse AChE confirmed that **XVI** is a dual-binding inhibitor and the triazole ring is not just a passive linker but it establishes hydrogen-bonding and stacking interactions with amino acids located in the AChE mid gorge (Manetsch, R. 2004, Krasinski, A 2005).

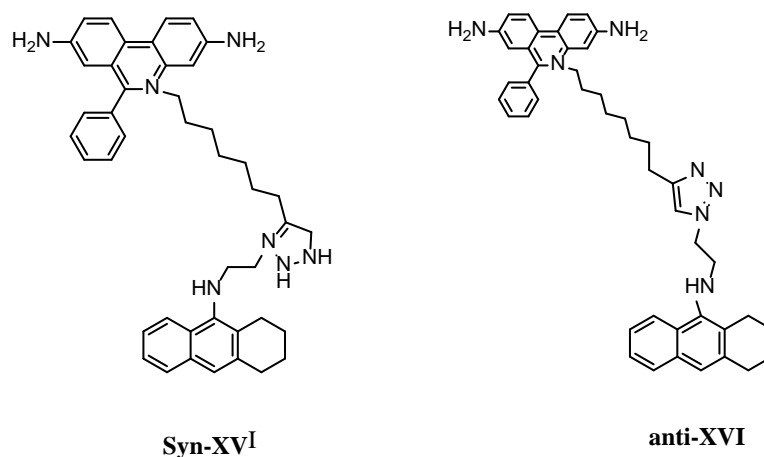


Figure 40: Chemical structure of **XVI** (Lewis, W.G 2002, Manetsch, R 2004, Krasinski, A 2005).

Ladostigil (TV3326), one of the most promising MTDLs, described as ChEI and neuroprotective against oxidative stress, is structurally constituted by a carbamate moiety derived from rivastigmine, introduced into the position 6 of a unit of rasagiline. This modification resulted in a drop of approximately 5-fold of *in vitro* MAO B inhibitory activity compared to that of rasagiline. *In vitro* ladostigil was found to selectively inhibit 100-fold more potently BuChE than AChE (Youdim, M.B 2006), which could be advantageous as, in contrast to AChE, the central levels of BuChE are not reduced as AD progresses, so that BuChE inhibition may contribute to the maintenance of ACh levels in the synaptic cleft (Giacobini E. 2001).

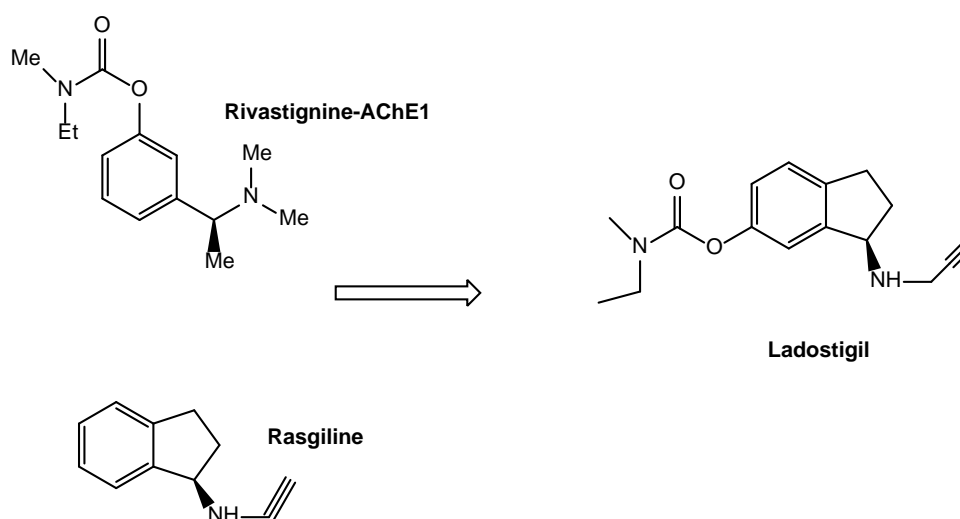


Figure 41: Drug design leading to Ladostigil

It was reported that cortical ChE activity of rats was inhibited by 20-80% after oral administration of 9-200 mg/kg of ladostigil. Furthermore, ladostigil increased dose-dependently brain ACh levels in scopolamine-induced spatial memory deficits in rats (Weinstock M 2000). Moreover, the ability of ladostigil to inhibit both MAO isoforms provides it with effective antidepressant capacity. In an *in vivo* experiment using rats it was observed that a single dose of 120 mg/kg of ladostigil was necessary to inhibit brain MAO isoforms activity by at least 50%. Ladostigil does not inhibit MAO A and MAO B *in vitro* at concentrations below 250 μ M and 1 mM, respectively, but it does in the brain *in vivo* probably due to the formation of an active metabolite. One of these is produced by the hydrolysis of the carbamate moiety by ChE to yield the 6-OH derivative, a molecule able to inhibit MAO A and MAO B with IC₅₀ values of 0.46 μ M and 0.35 μ M, respectively. On July 2014, Avraham Pharmaceuticals Ltd (www.avphar.com) announced successful interim results in a Phase IIb clinical trial for the evaluation of the safety and efficacy of ladostigil in patients diagnosed with MCI. These findings suggest that ladostigil may have a therapeutic value for the treatment of extrapyramidal symptoms in AD and dementia with Lewy bodies (DLB).

PBT2 is another example of MTDL, it is a second-generation 8-hydroxyquinoline derivative of clioquinol developed to resolve the toxicity problems, as well as to improve its solubility and ability to cross the BBB (Crouch PJ 2012). It was observed that PBT2 selectively chelates copper and zinc while forming soluble complexes able to pass through cellular membranes, leading to bioavailable delivery of these two metals into the cells (Adlard PA 2008, Crouch PJ 2011, Adlard PA 2011). PBT2 also showed significant therapeutic effects on both AD mouse model (Adlard PA 2008) and phase II clinical trials (Lannfelt L 2008; Faux NG 2010). This compound also exhibited neuroprotective activity as a copper-zinc ionophore able to enhance the inhibition of the phosphorylation of the GSK-3 α and β isoforms and subsequently lower A β levels (Crouch PJ 2011).

ASS234 is another MTDL designed and conceived for use in AD therapy. Structurally, ASS234 is based on the hybridization of the benzylpiperidine moiety from donepezil, responsible for the ChE inhibition, and the indolyl propargylamine of FA65, a potent MAO inhibitor and derivative of PF9601N. Previous studies reported ASS234 as a potent dual inhibitor of both ChE and MAO isoforms (Bolea I 2011). More recently, new findings with this brain-permeable molecule have revealed neuroprotective properties of ASS234 against A β ₁₋₄₂-induced toxicity in SH-SY5Y cells. By potently reducing A β self-aggregation *in vitro*, ASS234 was able to prevent the formation of

fibrillary and oligomeric species. This activity might be due to the direct interaction of ASS234 with the amyloid peptides during the oligomerization process, by stabilizing the less extended forms of A β , hence preventing further assembly towards toxic species. Moreover, ASS234 was also able to block the AChE-dependent aggregation of both A β ₁₋₄₀ and A β ₁₋₄₂, revealing its capacity to bind to the PAS (Bolea I 2013).

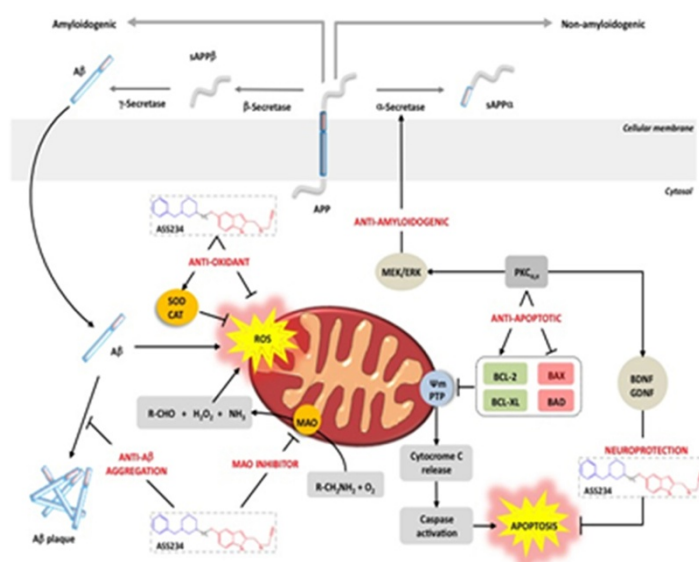


Figure 42: The multiple targets and activities reported for ASS234 for use in AD pathology (Bolea I 2013).

Besides the anti-amyloid properties of ASS234, this multi-target molecule was also reported to have significant antioxidant activity, by capturing free radical species *in vitro* (ORAC-FL) as well as by increasing the expression of the antioxidant enzymes catalase and superoxide dismutase-1 (SOD-1) in A β ₁₋₄₂-treated SH-SY5Y cells. It was reported that ASS234 is able to inhibit MAO and ChE activities after subcutaneous administration in rats (Stasiak A 2014). To date, the different properties that have been reported for ASS234 provide strong evidence to consider this molecule a promising compound for use in AD therapy, which has prompted new studies currently under investigation.

A very promising MTDL is memoquin, which has been developed in the Melchiorre's group. It was generated through incorporation of the benzoquinone fragment of coenzyme Q10 into the flexible chain of caproctamine. The design of this compound was based on the finding that coenzyme Q10 has been reported to have two different beneficial actions against AD: ROS scavenger and inhibitor of the deposition of A β in the brain. The

antioxidant activity of memoquin was confirmed by its *in vitro* ability to neutralize radicals and to act as a substrate for the NADPH quinone oxidoreductase 1 (NQO1), an enzyme responsible for the *in vivo* transformation of memoquin into the more antioxidant hydroquinone form (Melchiorre, C. 2007).

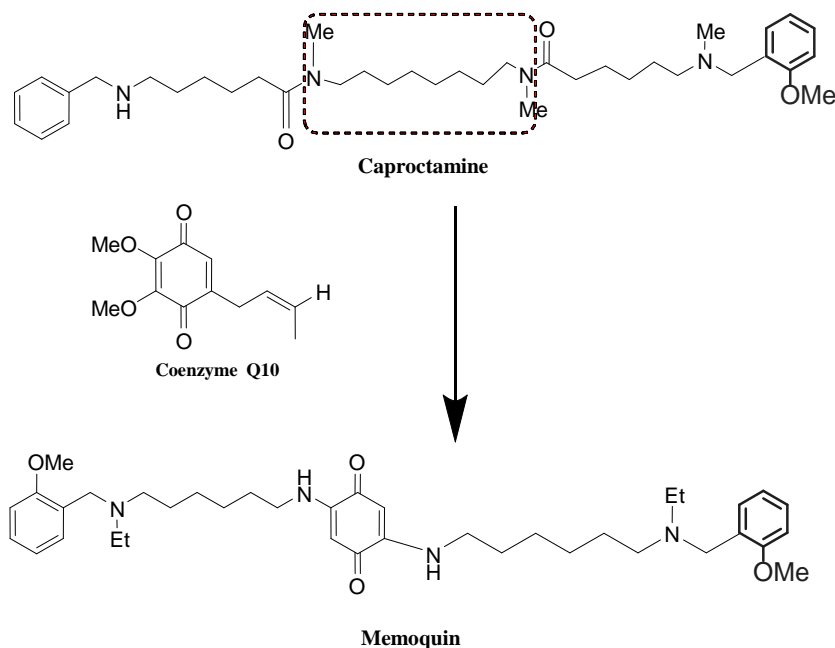


Figure 43: Drug design for memoquin

Memoquin displayed a nanomolar inhibitory potency against human AChE, and was able to inhibit the AChE-induced A β aggregation and to inhibit the self-assembly of A β . Moreover, the anti-amyloidogenic profile of memoquin was also evaluated by testing its ability to act as an inhibitor of BACE-1. The compound was found to have an IC₅₀ value of 108 nM against this enzyme. In addition, memoquin has been tested *in vivo* in an AD transgenic mouse model: it showed the ability to ameliorate the cholinergic and cognitive impairment, and to reduce A β deposition and τ hyperphosphorylation at three different stages of neurodegeneration (2, 6, and 15 months of age). Further studies on memoquin showed other promising properties, such as good oral bioavailability, efficacy in crossing the blood-brain barrier, and a favorable safety profile in preclinical non-regulatory acute and chronic toxicology studies (Cavalli, A 2007, Bolognesi, M.L 2009).

3.1 Multi-target-directed ligands developed in Diego Muñoz-Torrero group

As previously mentioned, the design of inhibitors able to simultaneously reach both sites of AChE, dual binding site AChE inhibitors (AChEIs), emerged some years ago as a promising source of multitarget anti-Alzheimer compounds, inasmuch as they should be endowed at least with potent anticholinesterase and A β antiaggregating effects.

In the recent years Drs. Pelayo Camps and Diego Muñoz-Torrero have developed new agents with strong affinity and inhibitory potency towards AChE and able to inhibit A β aggregation. They developed a series of dual binding site AChE inhibitors named huprine-tacrine hybrids (Galdeano, C 2012), which consist of a unit of racemic or enantiopure hupine Y, 14, as the active site interacting unit, and a moiety of tacrine or 6 chlorotacrine, as the peripheral site interacting unit, and oligomethylene linkers—of different lengths, or, for compounds XII and XIV, a linker incorporating a protonatable methylamino group in order to enable cation- π interactions with midgorge aromatic residues (Figure 44).

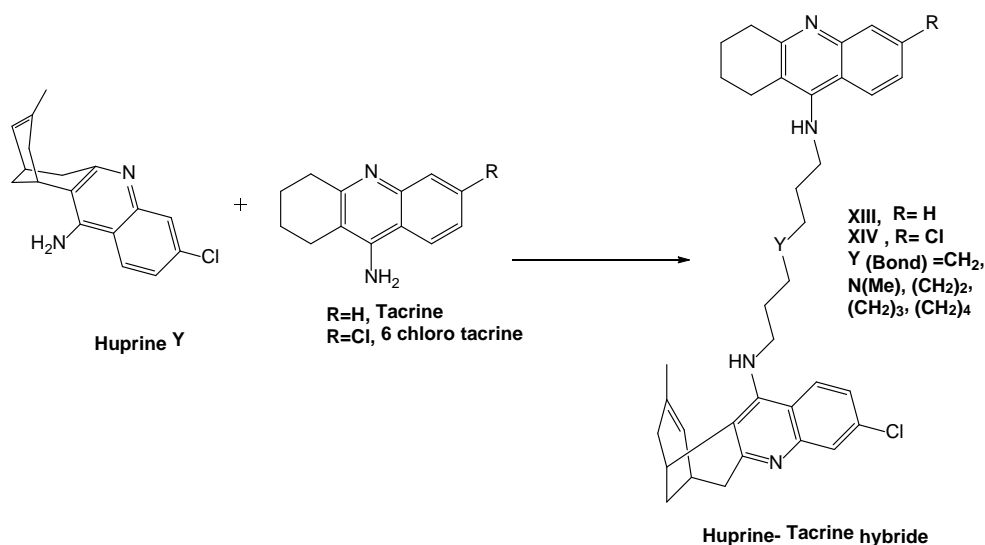


Figure 44: Design of huprine-tacrine hybrids **XII**, **XIV**

The dual site binding huprine-tacrine hybrids within AChE was further confirmed by kinetic and molecular modelling studies—(Galdeano, C 2012). The inhibition of the catalytic activity of hAChE was potent with IC₅₀ values in the range 0.31–11.5 nM, and the experiments to assess their *in vitro* neutralization of the pathological chaperoning effect of AChE toward the A β aggregation showed a 23–67% of inhibition at 100 μ M concentration of inhibitor. Moreover, these compounds also demonstrated a potent inhibitory activity

towards hBChE (IC_{50} = 24.6–139 nM), a significant inhibitory activity of the self-induced A β aggregation (28–61% of inhibition at 10 μ M concentration of inhibitor) and BACE-1 (IC_{50} = 4.9–7.3 μ M).

In 2008, Drs. Camps and Muñoz-Torrero, developed novel series of donepezil–tacrine hybrids designed to simultaneously interact with the active, peripheral and midgorge binding sites of AChE. These compounds contained a unit of tacrine or 6-chlorotacrine, to occupy the same position as tacrine at the AChE active site, and the 5,6-dimethoxy-2-[4-piperidiny]methyl]-1-indanone moiety of donepezil or the corresponding indane moiety, (Figure 45), (Galdeano, C 2012, Scarpellini, M 2006, Camps, P 2008).

All donepezil–tacrine hybrids (XV, XVI, XVII, XVIII) turned out to be highly potent inhibitors of hAChE (IC_{50} = 0.27–5.13 nM) and hBChE (IC_{50} = 7.25–88.7 nM). Moreover, six out of the eight hybrids of the series, particularly those bearing an indane moiety, exhibited a significant AChE-induced A β aggregation inhibitory activity (38–66% of inhibition at 100 μ M concentration of inhibitor) (Camps, P 2008).

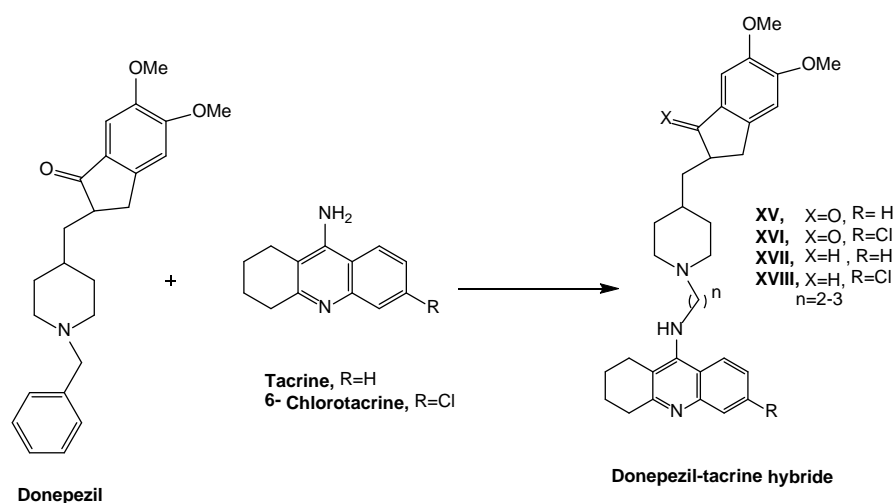


Figure 45: Design of donepezil–tacrine hybrids XV, XVI, XVII, and XVIII

In 2009, Drs. Camps and Muñoz-Torrero established a collaboration with Dr. Rodolfo Lavilla of the Universitat de Barcelona in Spain, to develop two series of dual binding site AChE inhibitors which consisted of a unit of 6-chlorotacrine, as the active site interacting unit and a Povarov-type multi component reaction-derived pyrano[3,2-c] quinoline scaffold, reminiscent of the peripheral site inhibitor propidium, to block the peripheral site (Figure 46) (Formosa X 2006, Galdeano C 2012, Galdeano C 2009).

The novel compounds were endowed with the AChE inhibitory activity of the parent 6-chlorotacrine ($IC_{50} = 7.03\text{--}50.0\text{ nM}$), while exhibiting a significant *in vitro* inhibitory activity toward the AChE-induced (23–46% inhibition at 100 μM concentration of inhibitor) and self-induced $A\beta$ aggregation (12–49% inhibition at 50 μM concentration of inhibitor) and toward BACE-1 (14–78% inhibition at 2.5 μM concentration of inhibitor), which makes them promising anti-Alzheimer lead compounds (Galdeano, C 2009).

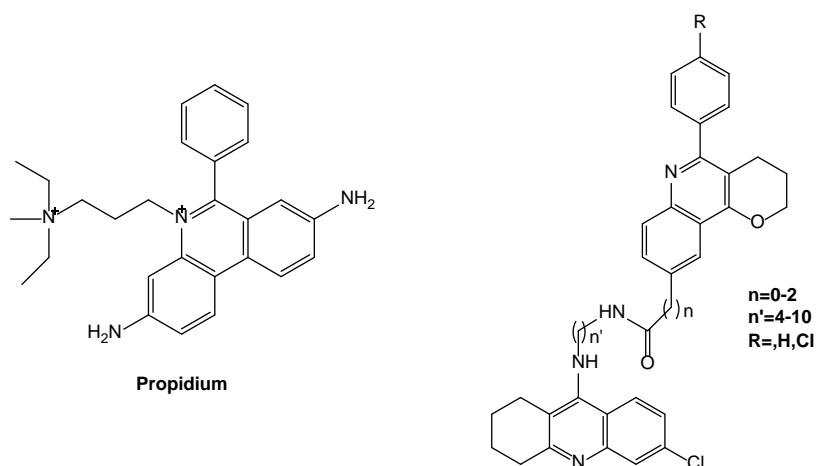


Figure 46: Structure of propidium, and pyrano[3,2-*c*] quinoline–6-chlorotacrine hybrids

In 2014 the group of Muñoz-Torrero developed a novel family of multitarget hybrid compounds (Figure 47), which consisted of a unit of the natural product rhein attached, through different linkers, to a unit of huprine Y, 4. The linkages between the huprine and rhein moieties involved an N–C bond from the exocyclic amino group of huprine Y and an amide bond from the carboxylic acid of rhein. Chains from 5 to 11 methylene groups were considered for the linkers to afford suitable distances between huprine and rhein moieties to achieve a dual site binding to AChE and to explore the effect of the length of the linker in a target with a large binding site such as BACE-1.

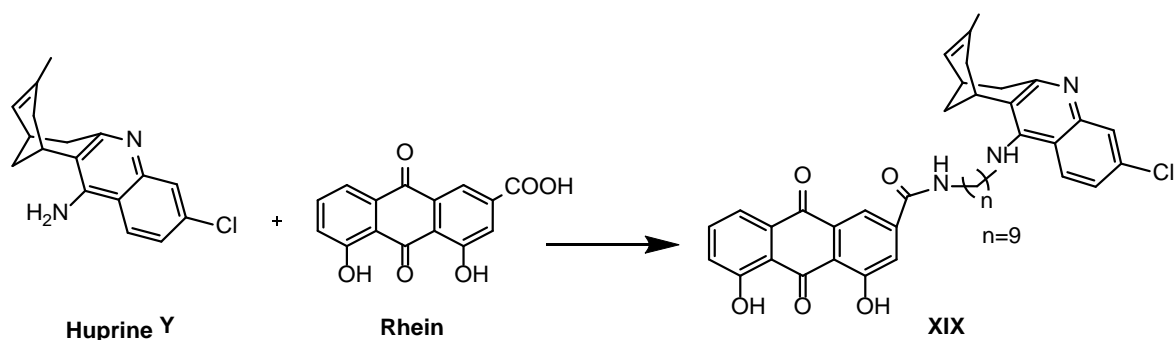


Figure 47: Design of the novel nonamethylene-linked rhein–huprine **XIX**

The lead rhein–huprine hybrid, the nonamethylene-linked compound–**XIX** (Figure 48) exhibits potent inhibitory activities against human hAChE ($IC_{50} = 2.39$ nM)–and hBChE ($IC_{50} = 513$ nM), and strikingly against human BACE-1 ($IC_{50} = 80$ nM), and it showed 43% of A β antiaggregating activity at 10 μ M concentration *in vitro* and ability to cross the blood-brain barrier. In *in vivo* studies in *Escherichia coli* cells, this rhein–huprine hybrid showed 47% of A β antiaggregating activity and 34% of tau antiaggregating activity at 10 μ M concentration (Muñoz-Torrero, D, 2014).

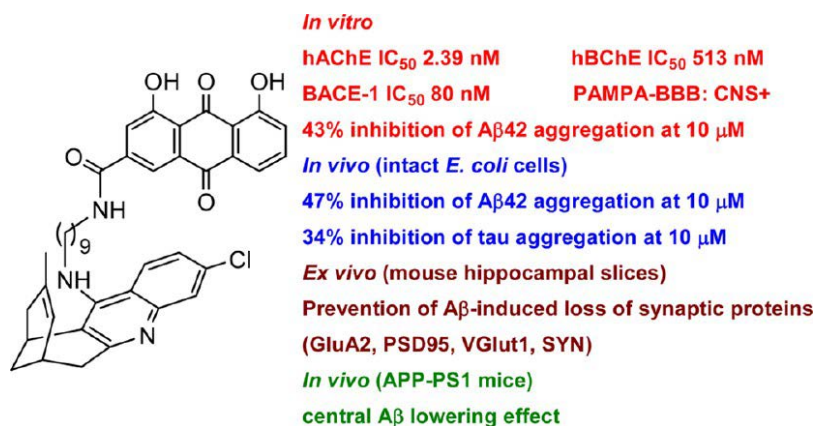


Figure 48: The biological profile of the novel rhein–huprine hybrid **XIX** (Muñoz-Torrero, D, 2014)

Ex vivo studies with this compound in brain slices of C57bl6 mice have revealed that they efficiently protect against the A β -induced synaptic dysfunction, preventing the loss of synaptic proteins and/or have a positive effect on the induction of long-term potentiation. *In vivo* experiments with transgenic APP/PS1 mice have shown that intraperitoneal administration of this compound for 4 weeks leads to lower hippocampal levels of total soluble A β and increased levels of its precursor APP both in initial and advanced stages of

this AD model, thus suggesting a reduction of APP processing by BACE-1 inhibition. Therefore, the novel nonamethylene-linked rhein–huprine hybrid has emerged as very promising disease-modifying anti-Alzheimer drug candidate (Muñoz-Torrero, D, 2014).

3.2 Drug design

The aspartic protease BACE-1 (β -secretase) is recognized as one of the most promising targets in the treatment of AD. The accumulation of β -amyloid peptide ($A\beta$) in the brain is a major factor in the pathogenesis of AD. $A\beta$ is formed by initial cleavage of β amyloid precursor protein (APP) by BACE-1; therefore its inhibition represents one of the therapeutic approaches to control progression of AD, by preventing the abnormal generation of $A\beta$. For this reason, in the last decade, many research efforts have focused on the identification of new BACE-1 inhibitors as anti-Alzheimer drug candidates.

As previously mentioned, the compound **XIX**, which was designed and synthesized by the group of Muñoz-Torrero in 2014 as a MTDL, showed a potent BACE-1 inhibitory activity; ($IC_{50} = 80$ nM) among other activities of interest. Due to its interesting profile, we investigated new scaffold modifications on the huprine moiety of this compound in order to further expand the structure-activity relationships in this structural class and to obtain novel useful chemical entities as potent BACE-1 inhibitors.

In particular, we wanted to synthesize novel huprine-rhein hybrids which might be endowed with better cell membrane permeabilities, including brain permeability, while retaining BACE-1 inhibitory activity. Indeed, Lercher group (Andreas Lerchner 2010) designed a series of macrocyclic BACE-1 inhibitors with different basicity in order to increase the potency of the compounds and to enhance the brain permeation. This group reported that there was a strong correlation between pK_a values of their basic amino group and permeability properties.

In this context, we designed novel analogues of the compound **XIX** by replacing its huprine Y moiety by other huprines in order to obtain different pK_a values of the pyridine nitrogen atom of the huprine moiety with the aim of retaining or increasing the potency towards BACE-1 and improving brain permeability. In this project, we envisaged the synthesis of one analogue, **28**, with lower basicity, and one analogue, **29**, with higher basicity than the parent **XIX** (Figure 49).

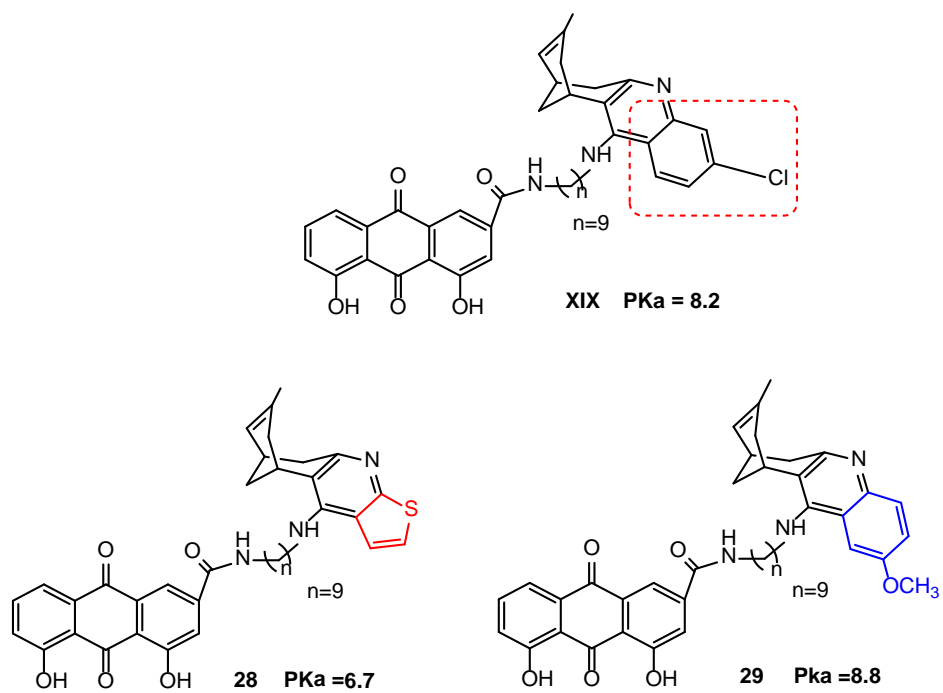


Figure 49: Design of the novel rhein–huprine hybrids with different basicity

3.3 Methods

3.3.1 Synthesis:

The synthetic route to the target compounds is depicted in Scheme 1. It started with an initial acidic hydrolysis of the diacetal protected form of malonaldehyde (1,1,3,3-tetramethoxypropane) in the presence of aqueous HCl followed by reaction with two equivalents of dimethyl acetonedicarboxylate, in the presence of NaOH in MeOH, to give tetraester **70**. Acidic hydrolysis followed by decarboxylation of tetraester **70** with HCl and AcOH, afforded diketone **71**. Addition of MeLi to diketone **71** gave oxaadamantanol **72**, which was transformed into the corresponding mesylate **73**, by treatment with MsCl in the presence of Et₃N. Silica gel-induced fragmentation of mesylate **73** gave the enone **74**.

The synthesis of the rhein–huprine hybrid **28** is depicted in Scheme 2. It started with a Friedländer condensation of enone **74** with 2-aminothiophene-3-carbonitrile, in the presence of AlCl₃, followed by a tedious silica gel column chromatography purification, which gave the novel thienohuprine **75**.

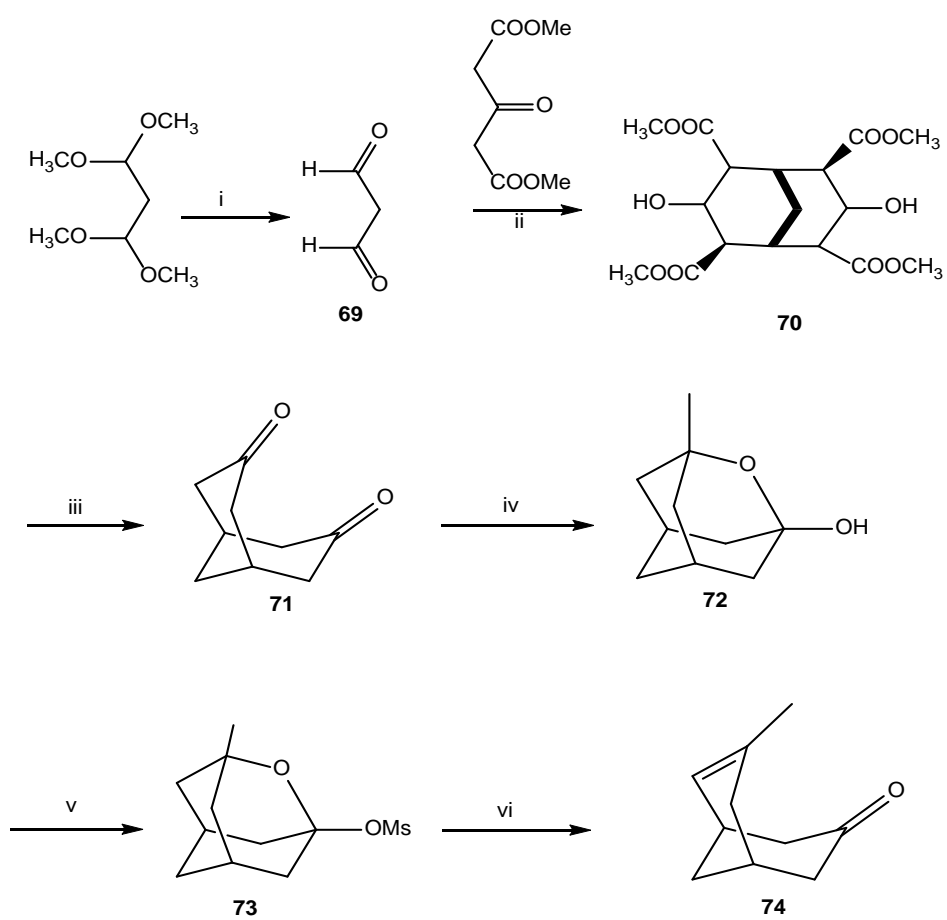
The subsequent alkylation of racemic huprine **75** with 9-bromononanenitrile in the presence of NaOH in DMSO at r. t. overnight gave cyanoalkylhuprine **76**, after silica gel column chromatography purification.

Cyanoalkylhuprine **76** was reduced with LiAlH₄ in Et₂O at r. t. overnight to afford the corresponding aminoalkylhuprine **77**, which was used for the next step without any further purification.

A suspension of rhein in EtOAc and DMF was treated with EDC·HCl, Et₃N and HOBT, it was allowed to stir for 1 h and then it was treated with the aminoalkylhuprine **77**, the novel rhein–huprine hybrid **28** after silica gel column chromatography purification of the crude product.

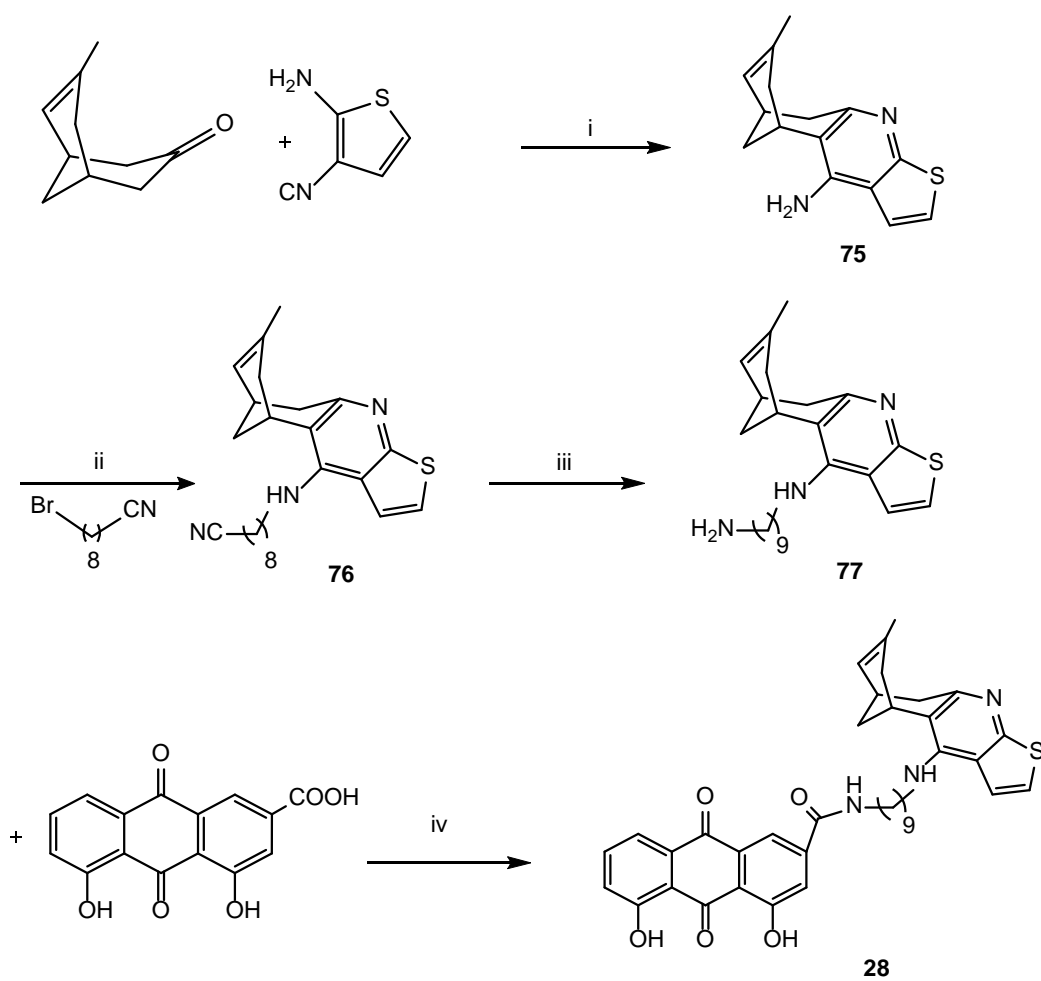
The synthesis of the novel rhein–huprine hybrid **29** is depicted in Scheme 3. It was carried out following the same methodology used for the synthesis of hybrid **28**, i.e. by an initial Friedländer condensation of enone **74** with 2-amino-5-methoxybenzonitrile to afford the novel methoxyhuprine **78**, followed by alkylation with 9-bromononanenitrile, LiAlH₄ reduction of the resulting nitrile **79**, and final amide coupling of the primary amine **80** with rhein.

Scheme 1:



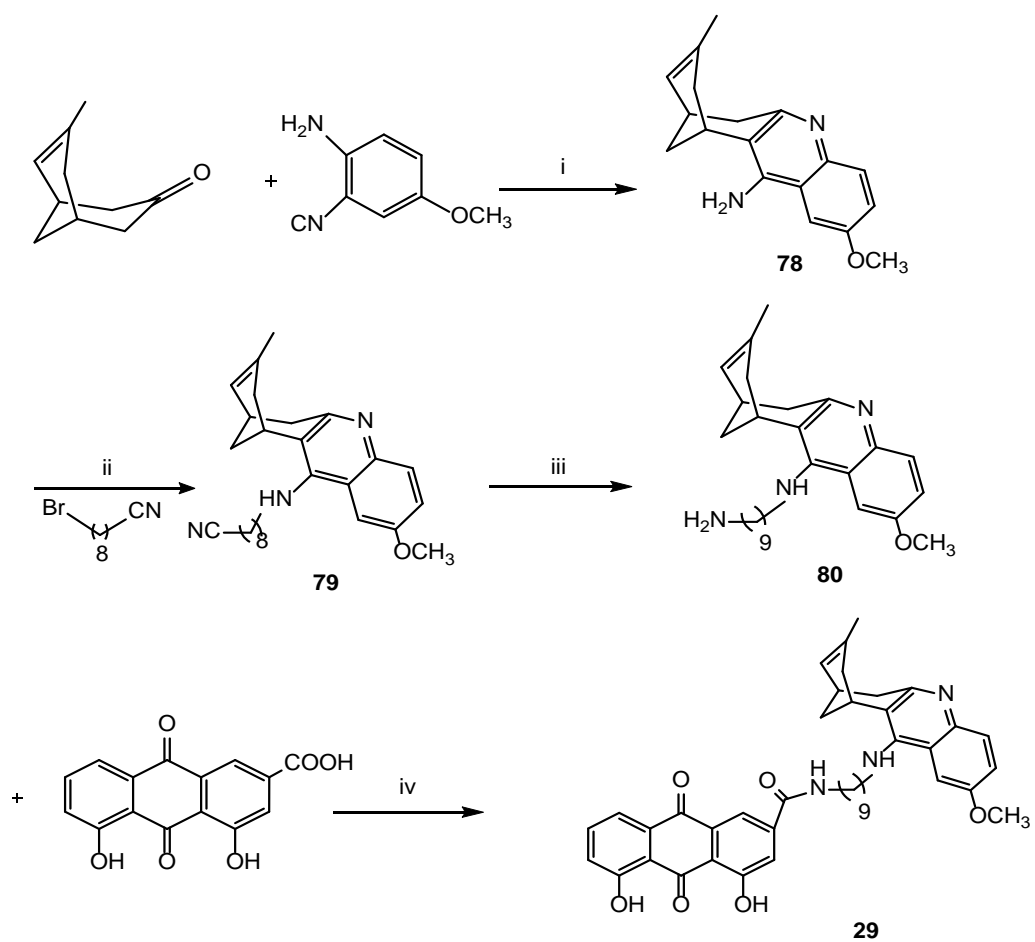
Conditions: (i) HCl, H₂O, (ii) NaOH, MeOH, (iii) HCl, AcOH, H₂O, (iv) MeLi, THF, (v) MsCl, Et₃N, CH₂Cl₂, (vi) SiO₂, CH₂Cl₂

Scheme 2:



Conditions: (i) AlCl₃, 1,2-dichloroethane, (ii) KOH, DMSO, 9-bromononanenitrile, (iii) LiAlH₄, Et₂O, (iv) EDC, Et₃N, HOBT, EtOAc, DMF.

Scheme 3:



Conditions: (i) AlCl_3 , 1,2-dichloroethane, (ii) KOH, DMSO, 9-bromononanenitrile, (iii) LiAlH_4 , Et_2O , (iv) EDC, Et_3N , HOBT, EtOAc , DMF.

3.3.2 Biology:

To determine the potential interest of compounds **28-29** for the treatment of AD, their inhibitory potency against recombinant human AChE and BChE was evaluated by studying the hydrolysis of acetylthiocholine (ATCh) following the method of Ellman et al (Ellman, G. L. 1961). The inhibitory potency was expressed as IC₅₀ values, which represent the concentration of inhibitor required to decrease enzyme activity by 50%.

The evaluation of the inhibition of A β 42 and tau aggregation in intact *Escherichia coli* cells was carried out through a methodology that is based on the *in vivo* staining with thioflavin S of inclusion bodies (IBs) of aggregated proteins in intact *E. coli* cells that overexpress a given amyloidogenic protein, in the presence and absence of the inhibitors and monitoring of the corresponding changes in the fluorescence of thioflavin S (Pouplana, S. 2014).

The novel racemic rhein-huprine hybrids were tested *in vitro* against human recombinant BACE-1 using a FRET assay (Ballatore, C. 2010), and their antioxidant activity was evaluated by total polyphenols, ABTS⁺ and DPPH assays.

The brain penetration of the synthesized hybrids was assessed using the parallel artificial membrane permeation assay for blood-brain barrier described by Di et al (Di, L. 2003).

3.4 Results and discussion

3.4.1 Activity toward cholinesterases:

Human recombinant AChE (Sigma, Milan, Italy) inhibitory activity was evaluated spectrophotometrically by the method of Ellman et al. Initial rate assays were performed at 37 °C with a Jasco V-530 double beam spectrophotometer. Stock solutions of the tested compounds (1 mM) were prepared in MeOH and diluted in MeOH. The assay solution consisted of a 0.1 M potassium phosphate buffer, pH 8.0, with the addition of 340 μ M 5,5'-dithiobis (2-nitrobenzoic acid) (DTNB, used to produce the yellow anion of 5-thio-2-nitrobenzoic acid), 0.02 unit/mL hAChE, and 550 μ M substrate (acetylthiocholine iodide). Assay solutions with and without inhibitor were preincubated at 37 °C for 20 min, followed by the addition of substrate. Blank solutions containing all components except hAChE were prepared in parallel to account for the nonenzymatic hydrolysis of the substrate. Five increasing concentrations of the inhibitor were used, able to give an inhibition of the enzymatic activity in the range of 20–80%. The results were plotted by placing the percentage of inhibition in function of the decimal log of the final inhibitor concentration. Linear regression and IC₅₀ values were calculated using Microcal Origin 3.5 software (Microcal Software, Inc.).

Human serum BChE inhibitory activities were also evaluated spectrophotometrically by the method of Ellman et al. The reactions took place in a final volume of 300 μ L of 0.1 M phosphate-buffered solution pH 8.0, containing hBChE (0.02 u/mL) and 333 μ M DTNB solution. Inhibition curves were performed in duplicates using at least 10 increasing concentrations of inhibitor and preincubated for 20 min at 37 °C. One duplicate sample without inhibitor was always present to yield 100% of BChE activity. Then substrate butyrylthiocholine iodide (300 μ M, Sigma-Aldrich) was added and the reaction was developed for 5 min at 37 °C. The color production was measured at 414 nm using a labsystems Multiskan spectrophotometer. Data from concentration–inhibition experiments of the inhibitors were calculated by nonlinear regression analysis, using the GraphPad Prism program package (GraphPad Software; San Diego, USA), which gave estimates of the IC₅₀ values. Results are expressed as mean \pm SEM of at least four experiments performed in duplicate.

The table 3 shows that monomeric thienohuprine **75** and methoxyhuprine **78** turned out to be moderate inhibitors toward hAChE and hBChE, exhibiting IC₅₀ values in the micromolar range. The novel rhein–huprine hybrid **29** exhibited higher inhibitory activity toward hAChE than for hBChE exhibiting IC₅₀ values in the micromolar range, while the compound **28** was found essentially inactive against hAChE, but exhibited moderate inhibitory activity toward hBChE comparing with **Rac-HUPY** and the compound **XIX**.

Table 3: hAChE and hBChE inhibitory activities of the novel huprines and rhein–huprine hybrids.

Compound	IC ₅₀ hAChE (μM) ± SEM	IC ₅₀ hBChE (μM) ± SEM
Rac-HUPY	0.00126 ± 0.00004	0.181 ± 0.015
75	2.61 ± 0.17	0.531 ± 0.047
78	5.16 ± 0.44	2.90 ± 0.02
28	>>10 ^a	40.8 ± 8.9
29	1.40 ± 0.24	100 ± 9

^a% inhibition at 15 μM = 15.2 ± 2.5%

3.4.2 Aβ42 aggregation inhibition assay in intact *Escherichia coli* cells overexpressing Aβ 42 and tau

- **Cloning and overexpression of Aβ42 peptide:**

Escherichia coli competent cells BL21 (DE3) were transformed with the pET28a vector (Novagen, Inc., Madison, WI, USA) carrying the DNA sequence of Aβ42. Because of the addition of the initiation codon ATG in front of both genes, the overexpressed peptide contains an additional methionine residue at its N terminus. For overnight culture preparation, 10 mL of lysogeny broth (LB) medium containing 50 μg·mL⁻¹ of kanamycin were inoculated with a colony of BL21 (DE3) bearing the plasmid to be expressed at 37 °C. After overnight growth, the OD₆₀₀ was usually 2–2.5. For expression of Aβ42 peptide, 20 μL of overnight culture were transferred into Eppendorf tubes of 1.5 mL containing 980 μL of LB medium with 50 μg·mL⁻¹ of kanamycin, 1 mM of isopropyl 1-thio-β-D-galactopyranoside (IPTG) and 10 μM of each hybrid or reference compound to be tested in DMSO. The samples were grown for 24 h at 37

°C and 1400 rpm using a Thermomixer (Eppendorf, Hamburg, Germany). In the negative control (without drug), the same amount of DMSO was added in the sample.

- **Cloning and overexpression of tau protein:**

E. coli BL21 (DE3) competent cells were transformed with pTARA containing the RNA-polymerase gen of T7 phage (T7RP) under the control of the promoter pBAD. *E. coli* BL21 (DE3) with pTARA competent cells were transformed with pRKT42 vector encoding four repeats of tau protein in two inserts. For overnight culture preparation, 10 mL of M9 medium containing 0.5% of glucose, 50 $\mu\text{g}\cdot\text{mL}^{-1}$ of ampicillin, and 12.5 $\mu\text{g}\cdot\text{mL}^{-1}$ of chloramphenicol were inoculated with a colony of BL21 (DE3) bearing the plasmids to be expressed at 37 °C. For expression of tau protein, the required volume of overnight culture to obtain 1:500 dilution was added into fresh M9 minimal medium containing 0.5% of glucose, 50 $\mu\text{g}\cdot\text{mL}^{-1}$ of ampicillin, 12.5 $\mu\text{g}\cdot\text{mL}^{-1}$ of chloramphenicol, and 250 μM of Th-S. The bacterial culture was grown at 37 °C and 250 rpm. When the cell density reached $\text{OD}_{600} = 0.6$, 980 μL of culture were transferred into eppendorf tubes of 1.5 mL with 10 μL of each compound to be tested in DMSO and 10 μL of arabinose at 25%. The final concentration of drug was fixed at 10 μM . The samples were grown overnight at 37 °C and 1400 rpm using a Thermomixer (Eppendorf, Hamburg, Germany). As negative control (maximal presence of tau) the same amount of DMSO without drug was added in the sample. In parallel, non-induced samples (in absence of arabinose) were also prepared and used as positive controls (absence of tau). In addition, these samples were used to assess the potential intrinsic toxicity of the compounds and to confirm the correct bacterial growth.

3.4.2.1 Activity toward A β 42 aggregation:

The A β 42 antiaggregating activity has been evaluated by using an assay based on the direct thioflavin S staining of IBs in intact *E. coli* cells that were genetically altered to overexpress A β 42 protein.

The table 4 shows that the novel rhein-huprine hybrids exhibited a moderately potent A β 42 antiaggregating activity in *E. coli* cells, with percentages of inhibition at 10 Mm slightly lower than that of compound XIX (47% inhibition).

Table 4: Inhibitory activities of the novel rhein–huprine hybrids toward A β 42 in intact *E. coli* cells.

Compound	A β 42 aggregation (% inhibition)
A β 42 Non Induced (C+)	100.0 \pm 0.7
A β 42 Induced (C-)	0.0 \pm 1.0
75	-3.7 \pm 0.9
28	23.9 \pm 1.1
78	-5.4 \pm 2.1
29	40.0 \pm 2.7

*Using 10 μ M as a concentration of drug.

3.4.2.2 Activity toward tau protein aggregation:

The anthraquinone–derived rhein moiety of the novel hybrids allows these compounds to have the ability to inhibit tau-protein aggregation. Their expected tau antiaggregating activity has been evaluated by using an assay based on the direct thioflavin S staining of IBs in intact *E. coli* cells that were genetically altered to overexpress tau protein.

The results showed that the novel rhein–huprine hybrids significantly inhibit tau protein aggregation at 10 μ M concentration of inhibitor with percentages of inhibition higher than that of the parent hybrid **XIX**–(34% of inhibition). The most active compound is the methoxyhuprine-based hybrid **29**, which exhibited 52% inhibition of tau aggregation at 10 μ M, while the thienohuprine-based hybrid **28** exhibited 41% inhibition and the novel monomeric huprines were either inactive or only weakly active.

Table 5: Inhibitory activities of the novel rhein–huprine hybrids toward tau aggregation in intact *E. coli* cells.

Compound	tau aggregation (% inhibition)
tau Non Induced (C+)	100.0 \pm 1.5
tau Induced (C-)	0.0 \pm 1.1
75	2.6 \pm 3.6
28	40.7 \pm 2.2
78	12.8 \pm 4.5
29	52.4 \pm 1.9

*Using 10 μ M as a concentration of drug.

3.4.3 Activity toward BACE-1:

β -Secretase (BACE-1, Sigma) inhibition studies were performed by employing a peptide mimicking APP sequence as substrate (Methoxycoumarin-Ser-Glu-Val-Asn-Leu-Asp-Ala-Glu-Phe-Lys-dinitrophenyl, M-2420, Bachem, Germany). The following procedure was employed: 5 μ L of test compounds (or DMSO, if preparing a control well) were pre-incubated with 175 μ L of enzyme (in 20 mM sodium acetate pH 4.5 containing CHAPS 0.1% w/v) for 1 h at room temperature. The substrate (3 μ M, final concentration) was then added and left to react for 15 min. The fluorescence signal was read at $\lambda_{em}=405$ nm ($\lambda_{exc}=320$ nm). The DMSO concentration in the final mixture was maintained below 5% (v/v) to guarantee no significant loss of enzyme activity, the fluorescence intensities with and without inhibitor were compared and the percent inhibition due to the presence of the test compounds were calculated. The background signal was measured in control wells containing all the reagents, except BACE-1 and subtracted. The % inhibition due to the presence of increasing test compound concentration was calculated by the following expression: $100 - (IF_i/IF_o \times 100)$ where IF_i and IF_o are the fluorescence intensities obtained for BACE-1 in the presence and in the absence of inhibitor, respectively.

Unfortunately, it was not possible to determine IC_{50} values due to interferences in fluorescence emission of compounds at higher concentrations, the IC_{50} value for the novel thienohuprine-based hybrid **28** has been extrapolated taking into account some percentages of inhibition obtained in the range from 4 nM until 80 nM. The maximum percentage of inhibition detected was of 34% at 80 nM.

Table 6: Inhibitory Activities of the novel Rhein–Huprine Hybrids and Reference Compounds toward BACE-1

Compound	Inhibition at <5 μ M
28	0.49 μ M \pm 0.08
29	n.d.

n.d.: not detectable

3.4.4 Antioxidant activity:

The antioxidant activity of the tested compounds was determined by three different analytical methods: total polyphenols, the 1,1-diphenyl-2-picryl-hydrazyl (DPPH) and, 2,20-azino-bis-(3-ethylbenzothiazoline-6-sulfonic acid (ABTS⁺).

- *Sample pre treatment:*

Samples (1 mg) were weighed and homogenized with EtOH (1 mL). The homogenate was sonicated for 5 min and filtered through a 0.45 µm polytetrafluoroethylene (PTFE) filter from Waters (Milford, USA) into a vial.

- *Antioxidant capacity- ABTS⁺ assay:*

The antioxidant capacity (AC) was first measured using an ABTS⁺ radical decolorization assay. 1 mM Trolox (standard antioxidant) was prepared in MeOH. Working standards were obtained by diluting 1 mM Trolox with MeOH. Solutions of known Trolox concentration were used for calibration. An ABTS⁺ radical cation was prepared by passing 5 mM aqueous stock solution of ABTS (in MeOH) through manganese dioxide powder. Excess manganese dioxide was filtered through a 0.45 µm PTFE filter. Then, 245 µL of ABTS⁺ solution were added to 5 µL of Trolox or to samples and the solutions were stirred for 30 s. The homogenate was shaken vigorously and kept in darkness for 1 h. Absorption of the samples was measured on a UV/VIS ThermoMultiskan Spectrum spectrophotometer at 734 nm and MeOH blanks were run in each assay. Results were expressed as Trolox equivalents (µmol Trolox / µmol tested compound). Analyses were carried out in triplicate.

- *Antioxidant capacity- DPPH assay:*

The antioxidant capacity (AC) was also determined through the evaluation of the free radical-scavenging effect on the DPPH radical. Solutions of known Trolox concentration were used for calibration. Five µL of samples or Trolox were mixed with 250 µL of methanolic DPPH (0.025 g L⁻¹). The homogenate was shaken vigorously and kept in darkness for 30 min. Absorption of the samples was measured on the spectrophotometer at 515 nm. Results were expressed as Trolox equivalents (µmol Trolox / µmol tested compound). Analyses were carried out in triplicate.

• *Analysis of total polyphenols:*

For the TP assay, each sample was analyzed three times; 20 μL of the samples were mixed with 188 μL of Milli-Q water in a thermo microtiter 96-well plate (nuncTM, Roskilde, Denmark), and 12 μL of F-C reagent and 30 μL of sodium carbonate (200 g/L) were added following a described procedure. The mixtures were incubated for 1 h at room temperature in the dark. After the reaction period, 50 μL of Milli-Q water was added and the absorbance was measured at 765 nm in a UV/Vis Thermo Multiskan Spectrum spectrophotometer (Vantaa, Finland). Results were expressed as mg of gallic acid equivalents (GAE)/g sample. The total polyphenols content was expressed in mg of gallic acid, the value is assigned by comparing the scavenging capacity of an antioxidant to that of gallic acid; high total polyphenols value indicates a high level of antioxidant activity. Table 7 shows that both monomeric huprines **75** and **78** showed higher antioxidant activity than rhein, and to our surprise, higher than the corresponding hybrids. DPPH and ABTS⁺ assays are based on the trolox equivalent antioxidant capacity (TEAC), to assess the amount of radicals that can be scavenged by an antioxidant. The TEAC value is assigned by comparing the scavenging capacity of an antioxidant to that of trolox. A high TEAC value indicates a high level of antioxidant activity. Values listed in table 7 show an outstanding antioxidant activity for the novel rhein–huprine hybrids **28** and **29** when measured through the DPPH and ABTS⁺ assays, more potent than that of the known antioxidant gallic acid and of monomeric huprines **75** and **78** and rhein, which still display a significant antioxidant activity.

Table 7: Antioxidant activity by total polyphenols, ABTS⁺ and DPPH assays.

Compound	Total Phenolics (mg gallic acid.g ⁻¹)	ABTS ⁺ μmol Trolox.μmol ⁻¹	DPPH μmol Trolox.μmol ⁻¹
Rhein	29.50 ± 2.04	4.019 ± 0.180	5.756 ± 0.273
Gallic acid	1004 ± 3.08	12.51 ± 0.409	9.723 ± 0.409
75	151.6 ± 5.70	4.770 ± 0.408	3.941 ± 0.313
28	99.93 ± 5.01	20.68 ± 2.521	12.41 ± 0.360
78	90.12 ± 6.19	5.010 ± 0.206	2.635 ± 0.129
29	10.69 ± 1.16	21.57 ± 1.242	12.40 ± 1.01

Mean ± SD. Results for total phenolics assay in mg of gallic acid. μmol⁻¹ compound. Results for ABTS⁺ and DPPH assays expressed in μmol Trolox. μmol⁻¹ compound

3.4.5 In vitro BBB permeation assay:

To evaluate the brain penetration of the different compounds, a parallel artificial membrane permeation assay for blood-brain barrier was used, following the method described by Di et al (2003). The *in vitro* permeability (P_e) of fourteen commercial drugs through lipid extract of porcine brain membrane together with the test compounds was determined. Commercial drugs and target compounds were tested using a mixture of PBS:EtOH 70:30. Assay validation was made by comparing the experimental permeability with the reported values of the commercial drugs by bibliography and lineal correlation between experimental and reported permeability of the fourteen commercial drugs using the parallel artificial membrane permeation assay was evaluated (P_e (exp) = 1.6315 P_e (lit) - 1.3308; $R^2=0.9341$). From this equation and taking into account the limits established by Di et al. for BBB permeation, we established the ranges of permeability as compounds of high BBB permeation (CNS+): P_e (10^{-6} cm s⁻¹) > 5.196; compounds of low BBB permeation (CNS-): P_e (10^{-6} cm s⁻¹) < 1.933 and compounds of uncertain BBB permeation (CNS+/-): 5.196 > P_e (10^{-6} cm s⁻¹) > 1.933.

Table 8 shows permeability results from the different commercial and target compounds (three different experiments in triplicate) and predictive penetration in the CNS. The novel monomeric huprines, the methoxyhuprine based hybrid **29** and the thienohuprine-based hybrid **28** were predicted to be able to cross the BBB, with their measured P_e values being far above the threshold for high BBB permeation (Table 8).

Table 8: Permeability ($P_e 10^{-6} \text{ cm s}^{-1}$) in the PAMPA-BBB assay of 14 commercial drugs, the target compounds and predictive penetration in the CNS.

Compound	Bibliography value^(a)	Experimental value (n=3) \pm S.D.	CNS Prediction
Verapamil	16.0	28.6 \pm 0.3	
Testosterone	17.0	26.4 \pm 0.3	
Costicosterone	5.1	6.7 \pm 0.1	
Clonidine	5.3	6.5 \pm 0.05	
Ofloxacin	0.8	0.99 \pm 0.06	
Lomefloxacin	0.0	0.8 \pm 0.05	
Progesterone	9.3	16.8 \pm 0.03	
Promazine	8.8	13.8 \pm 0.3	
Imipramine	13.0	12.3 \pm 0.1	
Hidrocortisone	1.9	1.4 \pm 0.05	
Piroxicam	2.5	2.1 \pm 0.03	
Desipramine	12.0	17.8 \pm 0.1	
Cimetidine	0.0	0.7 \pm 0.03	
Norfloxacin	0.1	0.9 \pm 0.02	
75		18.6 \pm 1.4	CNS+
*28		8.4 \pm 0.8	CNS+
78		16.8 \pm 1.3	CNS+
*29		10.4 \pm 0.8	CNS+

Taken from Di et al. (2003); *Poor dissolution

3.5 Conclusion

The new hybrids endowed with a very interesting multipotent pharmacological profile, as they should be able to block the neurodegenerative cascade associated to AD at different levels. These new rhein-huprine hybrids display lower hAChE and hBACE-1 inhibitory activities than the lead **XIX**, even though they retain or display increased potencies as A β 42 and tau antiaggregating agents. Also, we have demonstrated that they are endowed with a potent antioxidant activity. PAMPA-BBB studies suggest that the novel rhein-huprine hybrids should be able to readily penetrate into the CNS.

3.6 Experimental Section

Chemistry:

Tetramethyl 3,7- dihydroxy bicyclo [3.3.1] nona-2,6- diene- 2,4,6,8-t etracarboxylate (70): In a 2L round bottomed flask equipped with a magnetic stirrer, a solution of 1,1,3,3-tetramethoxypropane (113 mL; 113 g; 0.69mol) and 2NHCl(345 mL; 0.69mol) was prepared and stirred at r. t. for 1.5 h. Then, the solution was alkalized dropwise with 5N NaOH (240 mL; 1.2mol), and diluted with MeOH (337 mL). The resulting solution was treated with dimethyl 1,3-acetonedicarboxylate (199 mL; 236 g, 1.36mol) and MeOH (231 mL). The reaction mixture was stirred at r. t. for 72 h, treated with concentrated HCl (21 mL). The resulting precipitate was separated by filtration in vacuum, washed with H₂O (2 × 25 mL), and dried under reduced pressure to give the tetraester **70** (78.8 g, 30% yield) as a beige solid.

Bicyclo[3.3.1]nonane-3,7-dione (71): In a 3 neck 2 L round bottomed flask equipped with a magnetic stirrer, a suspension of tetraester **70** (78.8 g; 205mmol) in H₂O (205 ml) was prepared and successively treated with concentrated HCl (205 mL) and AcOH (420mL). The reaction mixture was stirred under reflux for 24 h. The resulting mixture was allowed to cool to r. t., then it was extracted with CH₂Cl₂ (5 × 212 mL) and the combined organic layers were washed with 5N NaOH (2 × 345 mL), dried with anhydrous Na₂SO₄, filtered, and evaporated under reduced pressure to give diketone **87** (19.0 g, 61% yield) as a yellowish solid.

¹H NMR (200 MHz, CDCl₃) δ 2.23 (s, 2H), 2.38 (d, *J* = 15.4 Hz, 4H), 2.62 (dd, *J* = 15.4 Hz, *J'* = 5.4 Hz, 4H), 2.88 (s, 2H); ¹³C NMR (50.4 MHz, CDCl₃) δ 31.0, 32.3, 47.5, 208.9.

3-Methyl-2-oxadamantan-1-ol (72): In a 3 neck 1L round bottomed flask equipped with an inert atmosphere, magnetic stirrer, and pressure equalizing dropping funnel, -MeLi (1.6 N solution in Et₂O; 93.5 mL; 150mmol) was cooled to 0 °C in an ice bath and treated dropwise with a solution of diketone **71** (19.0 g; 125mmol) in anhydrous THF (250 mL). The reaction mixture was stirred at 0°C for 35 min. Then, the mixture was treated dropwise with saturated aqueous NH₄Cl (250 mL) and extracted with Et₂O (3 × 200 mL). The combined organic layers were dried with anhydrous Na₂SO₄, filtered, and evaporated under reduced pressure to afford **72** (18.8 g, 90% yield) as a yellow solid. The ¹H and ¹³C NMR data coincided with those previously reported (Camps, P.; El Achab, R.; Font-Bardia, M.; Görbig, D.; Morral, J.; Muñoz-Torrero, D.; Solans, X.; Simon, M. Easy

synthesis of 7-alkylbicyclo[3.3.1]non-6-en-3-ones by silica gel-promoted fragmentation of 3-alkyl-2-oxadamant-1-yl mesylates. *Tetrahedron* **1996**, *52*, 5867–5880).

3-Methyl-2-oxadamantan-1-yl methanesulfonate (73): In 3 neck 1 L round bottomed flask, provided with an inert atmosphere and magnetic stirrer, a solution of oxadamantanol (18.8 g, 112mmol) and freshly distilled Et₃N (23.2 mL, 16.8 g, 166mmol) in anhydrous CH₂Cl₂ (525 ml) was prepared, cooled to -10°C with an ice/NaCl bath, and treated dropwise with MsCl (13.8 mL, 20.4 g, 178 mmol). Then the reaction mixture was stirred at -10 °C for 30 mins. The resulting solution was poured onto a mixture 10% aq.HCl (228 mL) and crushed ice (58 mL) and extracted with CH₂Cl₂ (2×110mL). The combined organic layers were washed with saturated aq. NaHCO₃ (178 mL) and H₂O (178 mL), dried with anhydrous Na₂SO₄, filtered, and evaporated under reduced pressure to give mesylate **73** (23.6 g, 86% yield) as a brown solid. The ¹H and ¹³C NMR data coincided with those previously reported (Camps, P.; **1996**).

7-Methylbicyclo[3.3.1]non-6-en-3-one (74): In 1 L round bottomed flask provided with magnetic stirrer, a suspension of mesylate **73** (11.8 g, 48.0mmol) and SiO₂ (12 g) in CH₂Cl₂ (125 mL) was prepared, and then stirred at r. t. for 3 h. The resulting suspension was evaporated under reduced pressure and the residue purified through silica gel column chromatography (hexane:EtOAc 50:50), to give the enone **74** (5.75g, 80% yield) as a colorless oil. The ¹H and ¹³C NMR data coincided with those previously reported (Camps, P.; **1996**).

5,6,9,10- Tetrahydro-7-methyl-5,9- methanocycloocta[b] thieno[3,2-e] pyridin-4-amine (75): In a triple neck 250 mL round bottomed flask equipped with an inert atmosphere, magnetic stirrer, a pressure equalizing dropping funnel and condenser, a suspension of 2-aminothiophene-3-carbonitrile (1.00 g; 8.05mmol) and AlCl₃ (1.34 g; 10.0 mmol) in 1,2-dichloroethane (15 mL) was prepared and treated with a solution of enone **74** (1.01 g; 6.72mmol) in anhydrous 1,2-dichloroethane (61 mL). The reaction mixture was stirred under reflux overnight. Then, it was allowed to cool to room temperature, diluted with water (35 mL), and THF (35 mL), then basified with 5N NaOH (15 mL), stirred for 30 min at room temperature, and extracted with CH₂Cl₂ (6 × 50 mL). The combined organic layers were dried with anhydrous Na₂SO₄, filtered, and evaporated under reduced pressure, to give a solid residue (1.92 g), which was purified by silica gel column chromatography, to afford the novel huprine **75** (1.37 g, 80% yield) as a yellow solid.

75·HCl: mp 227–228 °C; ¹H NMR (400 MHz, CD₃OD) δ 1.58 (s, 3H, 7-CH₃), superimposed in part 1.92 (dm, *J*=12.4 Hz, 1H, 12-H_{syn}), 1.95 (br d, *J*=18.0 Hz, 1H, 6-H_{endo}), 2.05 (dm, *J*=12.4 Hz, 1H, 12-H_{anti}), 2.50 (dd, *J*=17.6 Hz, *J'*= 4.4 Hz, 1H, 6-H_{exo}), 2.76 (m, 1H, 9-H), 2.80 (br d, *J*=17.6 Hz, 1H, 10-H_{endo}), 3.17 (dd, *J*=17.6 Hz, *J'*=5.6 Hz, 1H, 10-H_{exo}), 3.34 (m, 1H, 5-H), 4.86 (s, NH, ⁺NH), 5.56 (br d, *J*=4.8 Hz, 1H, 8-H), 7.53 (d, *J*=6.0 Hz, 1H, 3-H), 7.68 (d, *J*=6.0 Hz, 1H, 2-H); ¹³C NMR (100.6 MHz, CD₃OD)δ 23.5 (CH₃, 7-CH₃), 27.4 (CH, C5), 28.3 (CH, C9), 29.2 (CH₂, C12), 35.5 (CH₂, C10), 35.9 (CH₂, C6), 116.2 (C, C4a), 120.8 (CH, C3), 121.7 (C, C3a), 123.8 (CH, C2), 125.0 (CH, C8), 134.7 (C, C7), 149.1 (C, C10a), 149.8 (C, C11a), 154.2 (C, C4); HRMS (ESI) calcd for (C₁₅H₁₆N₂S + H⁺): 257.1107, found 257.1107.

9-[(5,6,9,10-Tetrahydro-7-methyl-5,9-methanocycloocta[*b*]thieno[3,2-*e*]pyridin-4-yl)amino]nonanenitrile (76): In a tripleneck 50 mL round bottomed flask, provided with an inert atmosphere, magnetic stirrer, and 4Å molecular sieves, a suspension of the thienohuprine**75** (1.00 g, 3.90 mmol) and powdered KOH (85% purity; 849mg; 12.9mmol) in anhydrous DMSO (16.6 mL) was prepared—and stirred, heating with a heatgun each 10 min during 1 h. Then it was stirred for another 1 h at r. t., and treated with 9-bromononanenitrile (935 mg; 4.29mmol). The reaction mixture was stirred at r. t. overnight. The resulting mixture was diluted with 2N NaOH (120 mL) and extracted with CH₂Cl₂ (4 × 100 mL). The combined organic layers were washed with H₂O (5 × 100 mL), dried with anhydrous Na₂SO₄, filtered, and evaporated under reduced pressure to give a dark brown oil, which was purified by column chromatography (hexane: EtOAc: Et₃N50: 50:0.2), to give nitrile **76** (760mg, 50% yield) as a yellow oil.

76·HCl: mp 92–93 °C; ¹H NMR (400 MHz, CD₃OD) δ 1.36–1.54 (complex signal, 8H, 4-H₂, 5-H₂, 6-H₂, 7-H₂), 1.59 (s, 3H, 7'-CH₃), 1.64 (tt, *J*=*J'*=7.2 Hz, 2H, 3-H₂), 1.81 (tt, *J*=*J'*=7.2 Hz, 2H, 8-H₂), 1.89 (br d, *J*=17.2 Hz, 1H, 6'-H_{endo}), superimposed in part 1.91 (dm, *J*=12.4 Hz, 1H, 12'-H_{syn}), 2.07 (dm, *J*=12.4 Hz, 1H, 12'-H_{anti}), 2.43 (t, *J*=7.2 Hz, 2H, 2-H₂), 2.52 (dd, *J*=17.2 Hz, *J'*=4.8 Hz, 1H, 6'-H_{exo}), superimposed in part 2.75 (m, 1H, 9'-H), 2.76 (br d, *J*=17.6 Hz, 1H, 10'-H_{endo}), 3.16 (dd, *J*=17.6 Hz, *J'*=5.6 Hz, 1H, 10'-H_{exo}), 3.33 (m, 1H, 5'-H), 3.86 (tm, *J*= 7.2 Hz, 2H, 9-H₂), 4.85 (s, NH, ⁺NH), 5.57 (br d, *J*=4.8 Hz, 1H, 8'-H), 7.54 (d, *J*=5.6 Hz, 1H, 3'-H), 7.72 (d, *J*=5.6 Hz, 1H, 2'-H); ¹³C NMR (100.6 MHz, CD₃OD)δ 17.4 (CH₂, C2), 23.6 (CH₃, 7'-CH₃), 26.4 (CH₂, C3), 27.1 (CH, C5'), 27.7 (CH₂, C7), 27.9 (CH, C9'), 29.5 (CH₂, C12'), 29.6 (CH₂), 29.7 (CH₂), 30.1 (CH₂) (C4, C5, C6), 30.9 (CH₂, C8), 35.5 (CH₂, C10'), 35.9 (CH₂, C6'), 46.7 (CH₂,

C9), 117.3 (C, C4a'), 119.1 (C, C3a'), 121.3 (C, C1), 122.7 (CH, C3'), 123.5 (CH, C2'), 125.0 (CH, C8'), 134.5 (C, C7'), 147.0 (C, C10a'), 152.4 (C, C11a'), 153.2 (C, C4'); HRMS (ESI) calcd for (C₂₄H₃₁N₃S + H⁺): 394.2311, found 394.2313.

N-(5,6,9,10-Tetrahydro-7-methyl-5,9-methanocycloocta[*b*]thieno[3,2-*e*]pyridin-4-yl)nonane- 1,9-diamine (77): In a 2 neck 50 mL round bottomed flask equipped with an inert atmosphere and magnetic stirrer, a suspension of nitrile **76** (585 mg; 1.49 mmol) in anhydrous Et₂O (25 mL) was cooled to 0 °C with an ice bath and treated dropwise with a solution of LiAlH₄ in Et₂O (4M solution; 1.2 mL; 4.80 mmol). The reaction mixture was stirred at room temperature overnight. Then it was cooled at 0 °C with an ice bath, diluted dropwise with 1N NaOH (40 mL) and water (90 mL) and extracted with CH₂Cl₂ (3 × 100 mL). The combined organic layers were dried with anhydrous Na₂SO₄, filtered, and concentrated under reduced pressure to give amine **77** (599 mg, quantitative yield) as a yellow oil, which was used for the next step without any further purification.

77·2HCl: mp 86–87 °C; ¹H NMR (400 MHz, CD₃OD) δ 1.36–1.54 (complex signal, 10H, 3-H₂, 4-H₂, 5-H₂, 6-H₂, 7-H₂), 1.58 (s, 3H, 7'-CH₃), 1.66 (tt, *J*=*J*'=7.6 Hz, 2H, 8-H₂), 1.81 (tt, *J*=*J*'=7.6 Hz, 2H, 2-H₂), 1.89 (br d, *J*=18.0 Hz, 1H, 6'-H_{endo}), superimposed in part 1.91 (dm, *J*=12.8 Hz, 1H, 12'-H_{syn}), 2.07 (dm, *J*=12.8 Hz, 1H, 12'-H_{anti}), 2.52 (dd, *J*=18.0 Hz, *J*'=4.8 Hz, 1H, 6'-H_{exo}), superimposed in part 2.76 (m, 1H, 9'-H), 2.77 (br d, *J*=17.6 Hz, 1H, 10'-H_{endo}), 2.91 (t, *J*=7.6 Hz, 2H, 9-H₂), 3.16 (dd, *J*=17.6 Hz, *J*'=5.6 Hz, 1H, 10'-H_{exo}), 3.34 (m, 1H, 5'-H), 3.86 (tm, *J*=7.6 Hz, 2H, 1-H₂), 4.85 (s, NH, ⁺NH), 5.57 (br d, *J*=4.8 Hz, 1H, 8'-H), 7.54 (d, *J*=6.0 Hz, 1H, 3'-H), 7.72 (d, *J*=6.0 Hz, 1H, 2'-H); ¹³C NMR (100.6 MHz, CD₃OD) δ 23.5 (CH₃, 7'-CH₃), 27.2 (CH, C5'), 27.5 (CH₂, C3), 27.8 (CH₂, C4), 28.0 (CH, C9'), 28.6 (CH₂, C5), 29.4 (CH₂, C12'), 30.1 (CH₂), 30.3 (CH₂), 30.4 (CH₂)(C6, C7, C8), 31.0 (CH₂, C2), 35.5 (CH₂, C10'), 35.9 (CH₂, C6'), 40.8 (CH₂, C9), 46.6 (CH₂, C1), 117.3 (C, C4a'), 119.2 (C, C3a'), 122.6 (CH, C3'), 123.5 (CH, C2'), 125.0 (CH, C8'), 134.6 (C, C7'), 147.1 (C, C10a'), 152.5 (C, C11a'), 153.3 (C, C4'); HRMS (ESI) calcd for (C₂₄H₃₅N₃S + H⁺) 398.2624, found 398.2629.

9,10-Dihydro-4,5-dihydroxy-9,10-dioxo-N-{9-[(5,6,9,10-tetrahydro-7-methyl-5,9-methanocycloocta[*b*]thieno[3,2-*e*]pyridin-4-yl)amino]nonyl}anthracene-2-carboxamide (28): In a 50 mL round bottomed flask provided with a magnetic stirrer, a suspension of rhin (387 mg; 1.36 mmol) in EtOAc (17.2 mL) and DMF (1.7 mL) was treated with EDC·HCl (356 mg; 1.86 mmol), Et₃N (0.43 mL; 312 mg; 3.09 mmol) and HOBT (253 mg; 1.87 mmol). The mixture was stirred for 1 h and treated with a solution

ofamine **77** (493 mg; 1.24mmol) in EtOAc (20 mL) and DMF (2 mL). The reaction mixture was stirred for 24h at r. t.-and evaporated under reduced pressure to give a brown solid residue(1.53 g),which was purified by silica gel column chromatography (CH₂Cl₂:MeOH:50% aq. NH₄OH 95:5:1) to give the novel hybrid **28** (581 mg, 71% yield) as a brown solid .

28·HCl: mp 174–175 °C; ¹H NMR (400 MHz, CD₃OD) δ 1.37–1.50 (complex signal, 10H, 3'-H₂, 4'-H₂, 5'-H₂, 6'-H₂, 7'-H₂), 1.57 (s, 3H, 7''-CH₃), 1.66 (tt, *J*=*J*'=6.8 Hz, 2H, 2''-H₂), 1.76 (tt, *J*=*J*'=7.2 Hz, 2H, 8''-H₂), 1.86 (br d, *J*=17.2 Hz, 1H, 6''-H_{endo}), superimposed in part 1.87 (dm, *J*=11.6 Hz, 1H, 12''-H_{syn}), 2.03 (dm, *J*=11.6 Hz, 1H, 12''-H_{anti}), 2.49 (dm, *J*=17.2 Hz, 1H, 6''-H_{exo}), superimposed in part 2.71 (br d, *J*=17.6 Hz, 1H, 10''-H_{endo}), 2.73 (m, 1H, 9''-H), 3.08 (dd, *J*=17.6 Hz, *J*'=5.6 Hz, 1H, 10''-H_{exo}), 3.26 (m, 1H, 5''-H), 3.41 (t, *J*=6.8 Hz, 2H, 1'-H₂), 3.72 (tm, *J*=7.2 Hz, 2H, 9'-H₂), 4.85 (s, OH, NH, ⁺NH), 5.54 (br d, *J*=4.8 Hz, 1H, 8''-H), 7.25 (d, *J*=8.0 Hz, 1H, 6-H), 7.40 (d, *J*=6.0 Hz, 1H, 3''-H), 7.52 (d, *J*=6.0 Hz, 1H, 2''-H), 7.59 (br s, 1H, 3-H), superimposed in part 7.60 (d, *J*=8.0 Hz, 1H, 8-H), 7.68 (dd, *J*=*J*'=8.0 Hz, 1H, 7-H), 7.99 (br s, 1-H); ¹³C NMR (100.6 MHz, CD₃OD) δ 23.5 (CH₃, 7''-CH₃), 27.1 (CH, C5''), 27.7 (CH + CH₂), 28.0 (CH₂) (C9'', C6', C7'), 29.3 (CH₂, C12''), 29.9 (CH₂), 30.0 (CH₂), 30.1 (CH₂), 30.3 (CH₂) (C2', C3', C4', C5'), 30.9 (CH₂, C8'), 35.4 (CH₂, C10''), 35.8 (CH₂, C6''), 41.1 (CH₂, C1'), 46.7 (CH₂, C9'), 116.8 (C, C10a), 117.2 (C, C4a''), 118.3 (C, C4a), 118.9 (CH, C1), 119.0 (C, C3a''), 120.9 (CH, C8), 122.5 (CH, C3''), 123.3 (CH, C2''), 123.7 (CH, C3), 125.0 (CH, C8''), 125.8 (CH, C6), 134.5 (C, C8a), 134.6 (C, C7''), 135.0 (C, C9a), 138.7 (CH, C7), 143.6 (C, C2), 147.0 (C, C10a''), 152.4 (C, C11a''), 153.2 (C, C4''), 163.3 (C, C4), 163.5 (C, C5), 167.1 (C, CONH), 181.8 (C, C9), 193.4 (C, C10); HRMS (ESI) calcd for (C₃₉H₄₁N₃O₅S + H⁺) 664.2840, found 664.2838.

6,7,10,11-Tetrahydro-2-methoxy-9-methyl-7,11-methanocycloocta[*b*]quinolin-12-amine (78): The methoxyhuprine**78** was prepared as described for **75**. From 2-amino-5-methoxybenzotrile (223 mg, 1.51 mmol), enone**74**(188 mg, 1.25 mmol), and AlCl₃ (250 mg, 1.87 mmol), and stirring the reaction mixture under reflux for 3 days, a yellow solid residue (300 mg) was obtained and purified by silica gel column chromatography (CH₂Cl₂:MeOH:50% aq. NH₄OH 99.8:0.2:0.4), to afford the novel methoxyhuprine **78** (150 mg, 43% yield) as a yellow solid.

78·HCl: mp 285–286 °C; ¹H NMR (400 MHz, CD₃OD) δ 1.58 (s, 3H, 9-CH₃), superimposed in part 1.95 (dm, *J*=12.4 Hz, 1H, 13-H_{syn}), 1.99 (br d, *J*=17.6 Hz, 1H, 10-

H_{endo}), 2.07 (dm, $J=12.4$ Hz, 1H, 13-H_{anti}), 2.51 (dd, $J=17.6$ Hz, $J'=4.0$ Hz, 1H, 10-H_{exo}), 2.77 (m, 1H, 7-H), 2.87 (br d, $J=17.6$ Hz, 1H, 6-H_{endo}), 3.18 (dd, $J=17.6$ Hz, $J'=5.6$ Hz, 1H, 6-H_{exo}), 3.40 (m, 1H, 11-H), 3.97 (s, 3H, 2-OCH₃), 4.87 (s, NH, ⁺NH), 5.57 (br d, $J=4.8$ Hz, 1H, 8-H), 7.47 (dd, $J=9.2$ Hz, $J'=2.4$ Hz, 1H, 3-H), 7.67 (d, $J=9.2$ Hz, 1H, 4-H), 7.70 (d, $J=2.4$ Hz, 1H, 1-H); ¹³C NMR (100.6 MHz, CD₃OD) δ 23.5 (CH₃, 9-CH₃), 27.6 (CH, C11), 28.3 (CH, C7), 29.4 (CH₂, C13), 35.7 (CH₂), 36.0 (CH₂) (C6, C10), 56.7 (CH₃, 2-OCH₃), 102.8 (CH, C1), 114.7 (C, C12a), 117.9 (C, C11a), 121.7 (CH), 126.1 (CH) (C3, C4), 125.0 (CH, C8), 134.2 (C), 134.9 (C) (C4a, C9), 150.4 (C, C5a), 155.4 (C, C12), 159.3 (C, C2); HRMS (ESI) calcd for (C₁₈H₂₀N₂O + H⁺): 281.1648, found 281.1650.

9-[(6,7,10,11-Tetrahydro-2-methoxy-9-methyl-7,11-methanocycloocta[*b*]quinolin-12-yl)amino]nonanenitrile (79): Nitrile **79** was prepared as described for **76**. From huprine **78** (260 mg, 0.93 mmol) and 9-bromononanenitrile (222 mg, 1.02 mmol), a brown oily residue (450 mg) was obtained and purified by silica gel column chromatography (CH₂Cl₂:MeOH:50% aq. NH₄OH 99.8:0.2:0.2), to afford nitrile **79** (114 mg, 29% yield) as a yellow oil.

79·HCl: mp 162–163 °C; ¹H NMR (400 MHz, CD₃OD) δ 1.32–1.50 (complex signal, 8H, 4-H₂, 5-H₂, 6-H₂, 7-H₂), 1.58 (s, 3H, 9'-CH₃), 1.62 (tt, $J=J'=6.8$ Hz, 2H, 3-H₂), superimposed in part 1.88 (m, 2H, 8-H₂), 1.94 (br d, $J=17.6$ Hz, 1H, 10'-H_{endo}), superimposed in part 1.96 (dm, $J=12.8$ Hz, 1H, 13'-H_{syn}), 2.09 (dm, $J=12.8$ Hz, 1H, 13'-H_{anti}), 2.43 (m, 2H, 2-H₂), 2.56 (dm, $J=17.6$ Hz, 1H, 10'-H_{exo}), 2.77 (m, 1H, 7'-H), 2.88 (br d, $J=17.6$ Hz, 1H, 6'-H_{endo}), 3.20 (dd, $J=17.6$ Hz, $J'=5.6$ Hz, 1H, 6'-H_{exo}), 3.48 (m, 1H, 11'-H), 3.96 (s, 3H, 2'-OCH₃), superimposed in part 3.98 (m, 2H, 9-H₂), 4.85 (s, NH, ⁺NH), 5.59 (br d, $J=4.4$ Hz, 1H, 8'-H), 7.53 (dd, $J=9.2$ Hz, $J'=2.4$ Hz, 1H, 3'-H), 7.66 (d, $J=2.4$ Hz, 1H, 1'-H), 7.72 (d, $J=9.2$ Hz, 1H, 4'-H); ¹³C NMR (100.6 MHz, CD₃OD) δ 17.1 (CH₂, C2), 23.3 (CH₃, 9'-CH₃), 26.2 (CH₂, C3), 27.3 (CH, C11'), 27.6 (CH₂, C7), 27.8 (CH, C7'), 29.3 (CH₂, C13'), 29.4 (CH₂), 29.6 (CH₂), 29.9 (CH₂) (C4, C5, C6), 31.7 (CH₂, C8), 35.8 (CH₂, C6'), 36.4 (CH₂, C10'), 48.9 (CH₂, C9), 56.3 (CH₃, 2'-OCH₃), 105.9 (CH, C1'), 117.2 (C), 118.6 (C) (C11a', C12a'), 121.1 (C, C1), 121.6 (CH), 125.4 (CH) (C3', C4'), 125.0 (CH, C8'), 134.4 (C), 135.1 (C) (C4a', C9'), 149.4 (C, C5a'), 156.1 (C, C12'), 158.1 (C, C2'); HRMS (ESI) calcd for (C₂₇H₃₅N₃O + H⁺): 418.2853, found 418.2862.

N-(6,7,10,11-Tetrahydro-2-methoxy-9-methyl-7,11-methanocycloocta[b]quinolin-12-yl) nonane-1,9-diamine (80): Amine **80** was prepared as described for **77**. From nitrile **79** (60 mg, 0.14 mmol), amine **80** (34 mg, 58% yield) was obtained as a yellow oil, and directly used in the next step without further purification.

80·2HCl: ^1H NMR (400 MHz, CD_3OD) δ 1.28–1.48 (complex signal, 10H, 3- H_2 , 4- H_2 , 5- H_2 , 6- H_2 , 7- H_2), 1.58 (s, 3H, 9'- CH_3), 1.66 (m, 2H, 8- H_2), 1.88 (m, 2H, 2- H_2), 1.93 (br d, $J=17.6$ Hz, 1H, 10'- H_{endo}), superimposed in part 1.96 (dm, $J=12.8$ Hz, 1H, 13'- H_{syn}), 2.09 (dm, $J=12.8$ Hz, 1H, 13'- H_{anti}), 2.56 (dd, $J=17.6$ Hz, $J'=4.0$ Hz, 1H, 10'- H_{exo}), 2.77 (m, 1H, 7'-H), superimposed in part 2.89 (d, $J=18.0$ Hz, 1H, 6'- H_{endo}), 2.91 (m, 2H, 9- H_2), 3.20 (dd, $J=18.0$ Hz, $J'=5.6$ Hz, 1H, 6'- H_{exo}), 3.49 (m, 1H, 11'-H), 3.96 (s, 3H, 2'- OCH_3), 3.97 (m, 2H, 1- H_2), 4.86 (s, NH, ^+NH), 5.59 (br d, $J=4.4$ Hz, 1H, 8'-H), 7.53 (dd, $J=9.2$ Hz, $J'=2.4$ Hz, 1H, 3'-H), 7.66 (d, $J=2.4$ Hz, 1H, 1'-H), 7.73 (d, $J=9.2$ Hz, 1H, 4'-H); ^{13}C NMR (100.6 MHz, DMSO-d_6) δ 23.1 (9'- CH_3), 25.4, 25.8, 26.0, 26.1, 26.9, 27.9, 28.4, 28.5, 28.7 (C3, C4, C5, C6, C7, C8, C7', C11', C13'), 30.1 (C2), 34.5, 35.6 (C6', C10'), 38.7 (C9), 47.0 (C1), 55.8 (2'- OCH_3), 104.7 (C1'), 115.4, 117.0 (C11a', C12a'), 120.9, 123.9, 124.2 (C3', C4', C8'), 132.6, 133.4 (C4a', C9'), 148.1 (C5a'), 153.7 (C, C12'), 156.0 (C, C2'); HRMS (ESI) calcd for ($\text{C}_{27}\text{H}_{39}\text{N}_3\text{O} + \text{H}^+$) 422.3166, found 422.3181.

9,10-Dihydro-4,5-dihydroxy-9,10-dioxo-N-{9-[(6,7,10,11-tetrahydro-2-methoxy-9-methyl-7,11-methanocycloocta[b]quinolin-12-yl)amino]nonyl}anthracene-2-carboxamide (29): Hybrid **29** was prepared as described for **28**. From rhein (74 mg, 0.26 mmol) and amine **80** (100 mg, 0.24 mmol), a brown solid residue (425 mg) was obtained and purified by silica gel column chromatography (CH_2Cl_2 : MeOH: 50% aq. NH_4OH 95:5:1), to afford the novel hybrid **29** (73 mg, 45% yield) as an orange solid.

29·HCl: mp 137–138 °C; ^1H NMR (400 MHz, CD_3OD) δ 1.38–1.46 (complex signal, 10H, 3'- H_2 , 4'- H_2 , 5'- H_2 , 6'- H_2 , 7'- H_2), 1.60 (s, 3H, 9''- CH_3), 1.67 (tt, $J=J'=6.4$ Hz, 2H, 2'- H_2), 1.85 (tt, $J=J'=6.8$ Hz, 2H, 8''- H_2), 1.93 (br d, $J=18.0$ Hz, 1H, 10''- H_{endo}), superimposed in part 1.94 (dm, $J=13.2$ Hz, 1H, 13''- H_{syn}), 2.07 (dm, $J=13.2$ Hz, 1H, 13''- H_{anti}), 2.53 (dd, $J=18.0$ Hz, $J'=5.2$ Hz, 1H, 10''- H_{exo}), 2.75 (m, 1H, 7''-H), 2.80 (br d, $J=17.6$ Hz, 1H, 6''- H_{endo}), 3.14 (dd, $J=17.6$ Hz, $J'=5.6$ Hz, 1H, 6''- H_{exo}), 3.39 (m, 1H, 11''-H), 3.43 (dt, $J=J'=6.4$ Hz, 2H, 1'- H_2), 3.83 (s, 3H, 2''- OCH_3), superimposed in part 3.84 (m, 2H, 9''- H_2), 4.85 (s, OH, NH, ^+NH), 5.59 (br d, $J=5.2$ Hz, 1H, 8''-H), 7.33 (dd, $J=8.0$ Hz, $J'=1.2$ Hz, 1H, 6-H), 7.37 (dd, $J=9.2$ Hz, $J'=2.4$ Hz, 1H, 3''-H), 7.41 (d, $J=2.4$

Hz, 1H, 1''-H), 7.50 (d, $J=9.2$ Hz, 1H, 4''-H), 7.65 (dd, $J=7.6$ Hz, $J'=1.2$ Hz, 1H, 8-H), 7.69 (d, $J=1.6$ Hz, 1H, 3-H), 7.73 (dd, $J=8.0$ Hz, $J'=7.6$ Hz, 1H, 7-H), 8.12 (d, $J=1.6$ Hz, 1H, 1-H); ^{13}C NMR (100.6 MHz, CD_3OD) δ 23.5 (CH_3 , 9''- CH_3), 27.4 (CH, C11''), 27.5 (CH_2), 27.7 (CH_2) (C6', C7'), 27.9 (CH, C7''), 29.4 (CH_2 , C13''), 29.7 (CH_2), 29.9 (CH_2), 30.0 (CH_2), 30.1 (CH_2) (C2', C3', C4', C5'), 32.0 (CH_2 , C8'), 35.8 (CH_2 , C6''), 36.3 (CH_2 , C10''), 41.0 (CH_2 , C1'), 49.1 (CH_2 , C9'), 56.3 (CH_3 , 2''- OCH_3), 105.8 (CH, C1''), 116.7 (C, C10a), 117.1 (C), 118.2 (C), 118.3 (C) (C4a, C11a'', C12a''), 118.8 (CH, C1), 120.7 (CH, C8), 121.6 (CH), 125.2 (2CH) (C3'', C4'', C8''), 123.7 (CH, C3), 125.8 (CH, C6), 134.4 (C), 134.9 (2C) (C9a, C4a'', C9'') C8''), 134.6 (C, C8a), 138.7 (CH, C7), 143.6 (C, C2), 149.3 (C, C5a''), 155.7 (C, C12''), 157.9 (C, C2''), 163.3 (C, C4), 163.5 (C, C5), 167.1 (C, CONH), 181.8 (C, C9), 193.3 (C, C10); HRMS (ESI) calcd for ($\text{C}_{42}\text{H}_{45}\text{N}_3\text{O}_6 + \text{H}^+$) 688.3381, found 688.3378.

Chapter 4. Epigenetic modifications and AD diseases

Epigenetic processes, the changes in gene expression independent of any variation in the DNA coding sequence, are critical physiological mechanisms in the normal development and differentiation of the cells (Abel 2008, Portela 2010). Dysregulation of epigenetic processes are involved in different disorders of signal transduction pathways including cell differentiation, cell apoptosis, vascular remodeling, inflammation reaction and immune responses, (Portela 2010; Mihaylova 2013), synaptic plasticity and cognition (Abel 2008). Eukaryotic DNA is compressed through its unity histone octamers, each octamer is composed of two recognizable copies of the four core histones (H2A, H2B, H3, and H4), which form nucleosomes that interconnected by sections of a linker DNA strands formed by 147 base pairs (Allis, 2007); these structures are compressed together to form chromatin (Kouzarides 2007, Stein 1980).

The main types of epigenetic modifications which can alter the chromatin structure and genome transcription include histone modifications (acetylation, phosphorylation, SUMOylation, methylation, ADP ribosylation, and ubiquitination), DNA methylation, nucleosome remodeling and RNA mediated pathways (Peterson 2004, Goldberg 2007, Portela 2010).

- *DNA methylation:* DNA methylation emerges in high levels in the brain of mammals especially at CpG dinucleotide sites (Ehrlich, 1982); this process occurs by covalent addition of a methyl group from S-adenosyl methionine (SAM), to the 5-carbon of the cytosine residue to form 5-methylcytosine (5-mC) (Miranda 2007). This modification has important role in heterochromatin organization and long-term transcription silencing (Rottach 2009).

- *Histone modifications:* Histone modifications includes acetylation, phosphorylation, SUMOylation, methylation, ADP ribosylation, and ubiquitination, affect chromatin structure by changing the level of attraction between the negatively-charged DNA and the positively-charged histone tails (Herranz 2007).

Epigenetic studies have shown that histone acetylation is involved in the etiology of AD. It was suggested that abnormal histone acetylation can contribute to the development of AD. Dysregulation of gene transcription has shown to be associated with impairments in

learning and memory. Studies reported that changes in histone gene transcription related to aging in rodent models have shown downregulation of genes which are linked to synaptic function, as well as with mitochondrial function and DNA damage responses (Jiang 2001, Blalock 2003).

The cellular and molecular processes that underlie learning and memory leading to transient changes in histone acetylation have become well established in the hippocampus, as well as in other brain regions (Levenson 2004, Fontan 2008). Studies showed that mice exposed to enriched environments exhibit increased acetylation of histones H3 and H4 in the hippocampus and cortex (Fischer 2007, Koseki 2012). Interestingly, aged mice show impairments in learning-promoted increases in histone acetylation levels.

In basal conditions, it has not seen any difference in acetylation levels between 3-month old mice when compared to 16-month old mice. But after undergoing contextual fear conditioning, acetylation levels specifically at H4K12 in the brain were elevated in 3-month old mice, but not in the 16-month old mice (Peleg 2010). The loss of acetylation at H4K12 for the 16-month old mice was correlated with hippocampus- dependent memory impairment. Other studies have shown that changes in certain histone acetylation marks are connected with the activity of specific HDAC proteins in the hippocampus. An increase in acetylation levels at H4K5 and H4K12 is correlated with loss of HDAC2 protein function (Guan 2009) and rises in H4K8 acetylation levels associated with the loss of HDAC3 protein function (McQuown 2011). These studies suggest that learning and memory impairments may be due to the dysregulated expression of genes through epigenetic mechanisms. Dynamic regulation of gene transcription through acetylation of histone proteins has provided a therapeutic path, and with the development of HDAC inhibitors pharmacological modification of gene transcription can be achieved through this pathway.

4.1 The biological role of Histone Acetylases and Histone Deacetylases

Histone acetylation is regulated by the activities of two antagonistic enzymes: Histone Acetylases (HATs) and Histone Deacetylase (HDACs).

4.1.1 Histone Acetylases (HATs)

HATs add acetyl groups on to ϵ -amino groups of lysine residues within the *N*-terminal tail of histones resulting in neutralization of the Histones positive charge (Yang 2007), which prevents interaction with the phosphate groups of the DNA leading to relaxed chromatin structure, and increase the ctivation of gene transcription (Herranz 2007). Acetylation is also implicated in remodelling and replication of chromatin, regulating microtubule dynamics and intracellular transport (Kouzarides 2007; Kazantsev 2007).

4.1.2 Histone deacetylases (HDACs)

Removing the acetyl groups from of lysine residues within the *N*-terminal tail of histones, results in transcription repression through leading to enhance the chromatin condensation and transcription silencing (Hanan 2008).

In physiological conditions, the balance between HATs and HDACs is preserved to obtain normal cellular function. This equilibrium can be deranged in pathological circumstances. In neurodegenerative diseases HAT activity is greatly reduced (Saha 2006), conversely the activity of HDAC is increased (Saha 2006) which leads to histone hypoacetylation, transcriptionally inactive (Herranz 2007), decrease appearance of cell survival genes and enhances the appearance of apoptotic genes (Saha 2006).

Therefore, dysregulation of the balance of HDACs is supposed to play important role in the progression of neurodegenerative diseases, and inhibiting of the HDACs activity would be a therapeutic approach through enhancing transcriptional activation of disease modifying genes to retrieve the damaged neurons during neurodegeneration diseases (Lu 2006; Feinberg 2007; Hanen2008). These functions show that these classical HDACs have specific and extensive roles in memory formation, synaptic plasticity, neuronal growth and differentiation, which are essential for neuronal survival.

HDACs are classified into four groups according to their yeast counter parts, including structure and cellular localization. Class I, II and IV are called classical HDACs which contain 11 enzymes sharing Zn^{2+} as a catalytic domain (Ruijter 2003, Chuang 2009). Class III HDACs are called sirtuins and have 7 members whose catalytic mechanism is Zn^{2+} independent and require nicotinamide adenine dinucleotide (NAD^+) (Michishita. 2005).

- **Class I HDACs:** It Contains HDAC1, 2, 3, and 8, and these enzymes share the same homology to yeast transcriptional regulator RPD3 (Chuang 2009, Delcuve 2012), with

molecular weights range from 22 to 55 kDa (de Ruijter *et al.*, 2003). The members of this class are primarily nuclear-localized and ubiquitously expressed, except HDAC3 which migrates between the nucleus and cytoplasm (Longworth 2006).

Class I HDACs play distinct role in cell proliferation and have specific and important roles in neuronal survival, growth and differentiation, memory formation and synaptic plasticity.

- **Class II HDACs:** Which are homologous to the yeast Hda1, is sub divided into Class IIa (HDAC 4, 5, 7 and 9) and Class IIb (HDAC6 and 10) (Chuang 2009, Delcuve 2012). Their molecular weights/protein are in the range of 120 -135 kDa (Witt 2008).

Class IIa HDACs: (4, 5, 7, and 9) localize to the nucleus and cytoplasm (Grozing 2000) and their localization is regulated by the phosphorylation of key residues within the 14-3-3 proteins which bind to conserved *N*-terminal sites of HDACs (Grozing 2000-Kao, H.Y. 2001). This class is highly expressed in the heart, skeletal muscle and brain and plays important role in tissue-specific expression (Lucio2008).

Class IIb HDACs: Contains HDAC 6 and 10, HDAC6 is a distinct enzyme within the classical HDACs because it contains two catalytic domains and this enzyme was identified as a microtubule-associated deacetylase as it regulates the microtubule dependent cell motility, (B. P. VAN 2003, Guardiola 2002). HDAC 4 and 6 are involved in neurotoxic activity and their inhibition can lead to neurodegenerative therapeutics (Bolger 2005, Dompierre 2007, Bardai 2011). HDAC10 has a catalytic domain on its *N*-terminus, and a second catalytic domain on the C-terminus (Tong, J.J 2002). Its function is still not well known but it has been shown that it has the ability to associate with other HDACs such as HDAC3 and to act as a recruiter not as a deacetylase (Andrea B. P. VAN 2003).

- **Class III HDACs:** This class is known as *Sirtuins* consist of 7 enzymes depending on their amino acid sequence (Dryden S 2003) and has the same homology to yeast Sir2 (Michan 2007). The members of this class differ in their localization: SIRT 1, 6 and 7 localize to the nucleus, SIRT 2 to the cytoplasm, while SIRT 3, 4 and 5 to the mitochondria (Michishita. 2005).

- **Class IV HDACs:** This class contains only HDAC 11, is structurally related to class I and class II, it is highly expressed in kidney, heart, brain and skeletal muscle (Gao 2002), but its function is not largely known (Villagra. A 2009, Gao. L 2002).

4.2 The role of HDAC in the development of AD

Histone acetylation is implicated in gene expression through chromatin modification, and the acetylation was mainly in the *N*-terminal of histone H3 and H4. It was suggested that the cognitive deficit is one of key characteristics of AD patients. After the obtained results of an experiment performed on mice, it revealed that the deregulation of histone acetylation associated with age-dependent memory impairment. The aged mice display a deregulation of histone H4 lysine12 (H4K12) acetylation and fail to start a hippocampal gene expression which is implicate in memory consolidation, while the vorinostat-treated mice showed an increase of H4K12 acetylation and restore learning-induced gene expression (S. Peleg, 2010). Other studies showed that Histone acetylation H4 also is implicated in the pathology of AD, and applying HDAC inhibitors led to alteration in some important gene expression through regulating the histone acetylation. Another experiment includes applying class I HDAC inhibitors in a mouse model of AD such as sodium valproate, resulted in restore contextual memory (M. Kilgore 2010). The level of histone acetylation is affected by HDACs, and it was reported that using HDAC inhibitors led to alter the levels of the proteins like A β , GSK-3 β , and tau hyperphosphorylation which have advantages in treating AD (J. Huang, 2010).

HDAC2 is a negative regulator in learning and memory, it was reported that mice overexpressing HDAC2 showed decrease in synaptic plasticity and synapse number and memory formation, and the treatment of these mice with vorinostat resulted inrescue of synaptic number and learning impairments.

Also HDAC6 protein level is significantly increased in cortex and hippocampus in AD brains compared with the normal brains, and application of Tubacin (a selective inhibitor of HDAC6) attenuates site-specific phosphorylation of tau, which indicated that HDAC6 has a key rolein the AD.

Another report by Gao et al. indicated that there is significant reduction of SirT1 in the parietal cortex of AD patients compared with the control, and the accumulation of A β and

tau in AD patients may be associated with the loss of SirT, which suggests the involvement of Sir2 in the pathology of AD.

All of these studies led the researchers to suggest that HDAC proteins may be implicated in AD development, and regulate the level of histone acetylation which may alter the expression of some important genes involved in memory and cognition processes and in AD pathology. HDAC inhibitors could ameliorate cognitive deficits and memory impairment in AD, through the inhibition of A β -induced hyperphosphorylation of tau protein; and through the regulation of the expression of important genes participating in the learning and memory.

4.3 HDAC inhibitors in therapy

During the last years, both academic and industrial laboratories have reported about new natural and synthetic compounds as HDAC inhibitors (HDACIs). In fact, HDAC are emerging as important target to treat different diseases such as immune disorders, cancer, diabetes, sickle-cell anemia and neurodegenerative disorders (Kazantsev 2008).

Two HDACIs are currently in therapy for the treatment of cutaneous cell T lymphoma (CTCL) and they are SAHA and FK228. In particular, SAHA is a classic hydroxamate-based HDACI and its structure, like most of the other HDACIs such as TSA, could be divided in three parts: hydrophobic cap region, and aliphatic linker and a Zinc-binding group. Both SAHA and TSA are highly potent HDACIs with an IC₅₀ in the nanomolar range of concentration. This high activity could be explained analyzing the crystal structure between TSA, or SAHA, and the enzyme. Indeed, it could be observed that the aromatic moiety of TSA interacts with critical amino acids located at the entrance of a tunnel through hydrophobic interactions, and the aliphatic chain located between the cap group and the zinc-binding group establishes van der Waals interactions with amino acids located in the tunnel. At the bottom, the Zinc atom interacts with the two oxygen atoms of the hydroxamate function; this moiety interacts also with two His and Tyr (Figure 50).

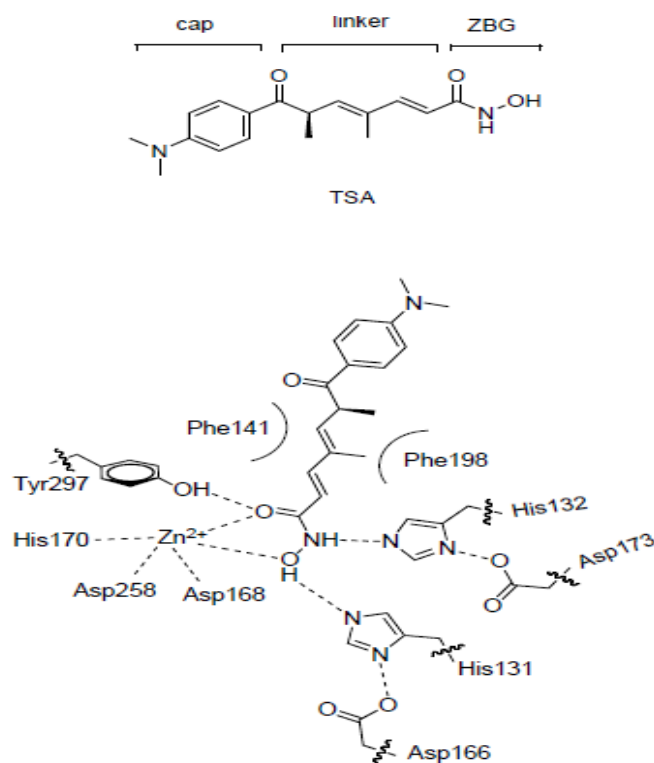


Figure 50: General structure of TSA and its binding with HDAC (E. Costa 2006)

Based on the chemical structure and on the nature of the zinc-binding group, HDACIs could be divided in different chemical groups: hydroxamates, benzamide, aliphatic acids, electrophilic ketones and cyclic peptides.

- *Hydroxamates:*

Compounds belonging to this class have been the first to be developed and are highly active thanks to the hydroxamic acid able to interact with the zinc-binding group located, at the bottom of the tunnel of the active site. The importance of this group has been confirmed by SAR studies reporting that its replacement or its modification, such as methylation, induces a dramatic loss of the activity. The first discovered compound of this class was TSA in 1990: this is a natural product extracted from *Streptomyces hygroscopicus* strain and displaying a K_i value of 3.4 nM towards HDAC. As already reported, closely related to TSA is SAHA, which was the first HDAC I approved by the FDA and it showed an IC_{50} of about 1 nM towards HDAC (Wagner 2010). Structure-activity relationships studies performed on SAHA reveal that the distance between the Cap and the zinc-binding group is optimal when is of six methylenes. At the opposite, the

capping group could be greatly modified by introducing different aryl substituent without any loss in activity.

An example is compound **XX** in which the benzyl group was replaced by an indole, without loss in activity ($IC_{50} = 14$ nM).

Among the hydroxamate based compounds CBHA and its derivatives are very important since they demonstrated the possibility to replace the aliphatic linker with an aromatic moiety without losing the activity.

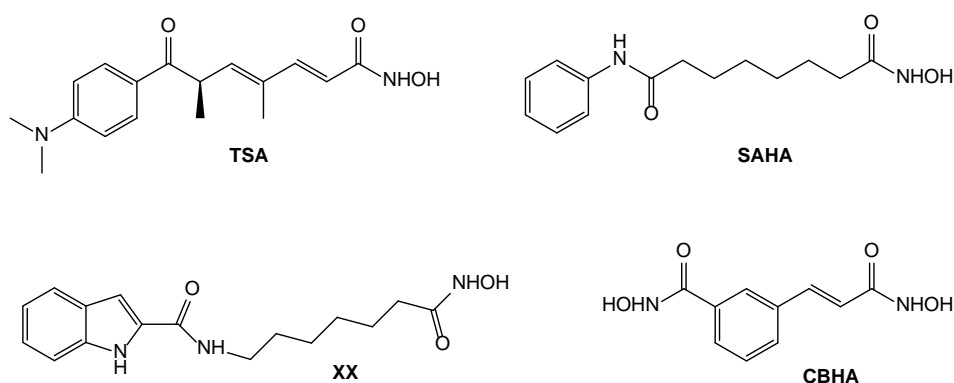


Figure 51: Structure of TSA and SAHA, XX, CBHA

Over the years hundreds of interesting and promising hydroxamate-based HDACIs have been reported either in patent or in scientific papers and many of them are currently evaluated in pre-clinical or clinical studies (Wagner 2010, Chuang 2009).

- *Benzamide:*

This class of compounds is characterized by the presence of a benzamide group in place of the hydroxamic acid for example butyric acid, valproic acid, MS-275 and XXI in (figure 52). It is hypothesized that the aniline group is able to establish critical interactions with amino acids located in the active site. Indeed, its acetylation as well as its replacement with other group induced a decrease in the inhibitory activity. In general, benzamides are less active than hydroxamic acids. Example of benzamides is MS-275 which is a specific inhibitor of HDAC1 and HDAC3 ($IC_{50} = 0.5$ and 1.7 μ M) and currently it is in clinical trials for the treatment of various cancers (Grayson 2010). From SAR performed on this compound emerged that the substitution on position 3, 4 and 5 on the benzamide ring induced drop in the activity probably due to steric hindrance.

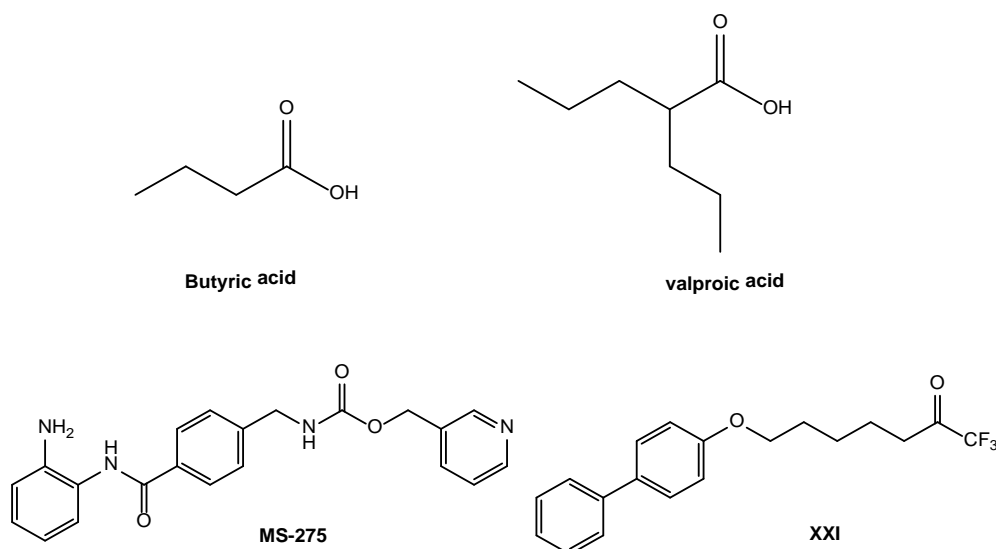


Figure 52: Structure of butyric acid, valproic acid, MS-275 and XXI

- *Aliphatic acids:*

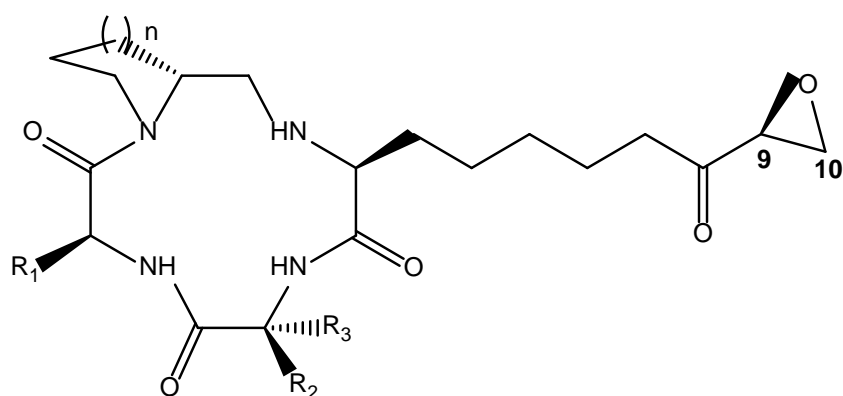
The carboxylic acids group is a well-known metal binding group and carboxylic acid characterized by a simple aliphatic chain possesses HDAC inhibitory activity. Examples of this class are butyric acid and valproic acid (Khan 2008, Grayson 2010).

- *Electrophilic ketones:*

Electrophilic ketones, such as trifluoromethyl ketones or α -keto amides, have been recently reported as weak HDAC inhibitors. The inhibitory activity seems to be due to the hydrated form of the ketones, which is able to coordinate the metal ion. SAR studies conducted on this class of derivatives showed that the linker could be replaced with other groups, even if the best activity is obtained with an aliphatic chain constituted by five or six methylenes, and the replacement of the trifluoromethyl group led to a drop of the activity.

- *Cyclic peptides:*

Compounds belonging to this class possess a macrocycle containing hydrophobic amino acids as a capping group. The first inhibitors belonging to this group were discovered through screening of natural products and examples are Trapoxin A and Chlamydocin and Cyl-2 (Grayson 2010, Furumai 2002, Grayson 2010).



Trapoxin A ($R_1=R_2=\text{benzyle}$, $R_3=\text{H}$, $n=2$)
Trapoxin B ($R_1=R_2=\text{benzyle}$, $R_3=\text{H}$, $n=1$)
Chlamydocin ($R_1=\text{benzyle}$, $R_2=R_3=\text{Me}$, $n=1$)
HC-Toxin ($R_1=R_2=\text{Me}$, $R_3=\text{H}$, $n=1$)
Cyl-2 ($R_1=\text{Bu}$, $R_2=\text{H}$, $R_3=4\text{-MeObenzyle}$, $n=2$)
WF-3161 ($R_1=\text{Bu}$, $R_2=\text{H}$, $R_3=\text{Benzyle}$, $n=2$)

Figure 53: Structure of chlamydocin and trapoxin A and B

These compounds showed an epoxyketone moiety, which is essential to obtain an irreversible inhibition; indeed, the replacement of this group led to a reduction of the activity. These compounds are very interesting because they displayed great activity and selectivity: for instance, Trapoxin A, Chlamydocin and Cyl-2 are 640 to 57000-fold selective for HDAC1 versus HDAC6 (Khan2008). Among cyclic peptides, the only one under clinical investigation is FK228, called Romidepsin, which is a natural compound isolated from *Chromobacterium violaceum*.

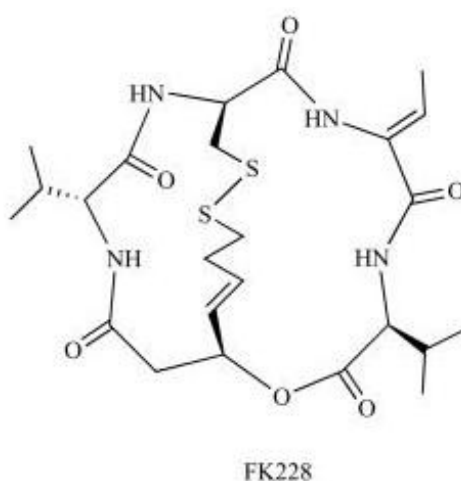


Figure 54: Structure of FK 228

The mechanism of action of this compound has been deeply investigated and seems that the disulphide bridge is reduced in vivo by the glutathione reductase and the obtained thiol group is able to chelate the zinc atom present in the enzyme.

4.4 Drug Design

As discussed in the introduction, the development of new MTDLs potentially useful in the treatment of multifactorial diseases represents an exciting research field. In particular, MTDLs are particularly useful to treat diseases such as cancer and AD. Indeed, today one of the most used drugs in the anticancer therapy is Imatinib: this compound, used for the treatment of acute myeloid leukemia, exerts its antiproliferative action by interacting with different biological targets, in this case kinases, involved in the development of the disease.

Similarly, also in the field of anti-AD drug discovery, one of the most promising agents currently in clinical trial exerts its therapeutic potential interacting with different targets; Ladostigil is, indeed, able to simultaneously inhibit two targets responsible for the development of AD, the enzymes AChE and mono amino oxidase.

One of the most useful design strategy for MTDLs consists of identifying two molecules that simultaneously administered are able to act synergistically in order to potentiate the biological activity of both compounds. Then, fragments of these molecules responsible for the biological actions are selected and combined in a unique chemical entity to provide hybrid.

The aim of this work has been the development of new MTDLs able to simultaneously target two proteins responsible for the development of AD, namely GSK3 β and HDAC, as neuroprotective agents.

Indeed, it was recently reported that combination of lithium, a GSK-3 β inhibitor, and valproic acid, a HDAC inhibitor, results in a synergistic neuroprotective effect against glutamate excitotoxicity. In particular, when the two drugs were administered singularly did not show any protective effects against glutamate-induced neurotoxicity in Cerebellar granule cells. From the analysis of the mechanism of action, it appears that responsible of this effect is the potentiation of GSK-3 β inhibition induced by the combination of lithium and valproic acid. Importantly, the potentiation of lithium-induced neuroprotection is achieved also combining lithium with other HDAC inhibitor such as TSA (Leng Y 2008). Moreover, Sharma et al reported that sub-effective dose combination of lithium chloride and Valproic acid produced a synergistic neuroprotection against streptozotocin-induced cognitive deficits in rats (Leng Y 2008).

Furthermore, it is reported that HDAC3 is directly phosphorylated by GSK3 β and inhibition of GSK-3 β protects against HDAC3-induced neurotoxicity (F. H. Bardai 2011). These studies provide a strong rationale for the design of MTDLs able to simultaneously interact with GSK-3 β and HDAC. On these bases, we have designed and synthesized a series of MTDLs by coupling the two pharmacophoric fragments responsible for GSK-3 β and HDAC inhibition, namely the imide and the hydroxamic acid functions, respectively. In order to evaluate the best distance between these two fragments, four derivatives have been synthesized endowed with an aliphatic linker characterized by a different length (Figure 55).

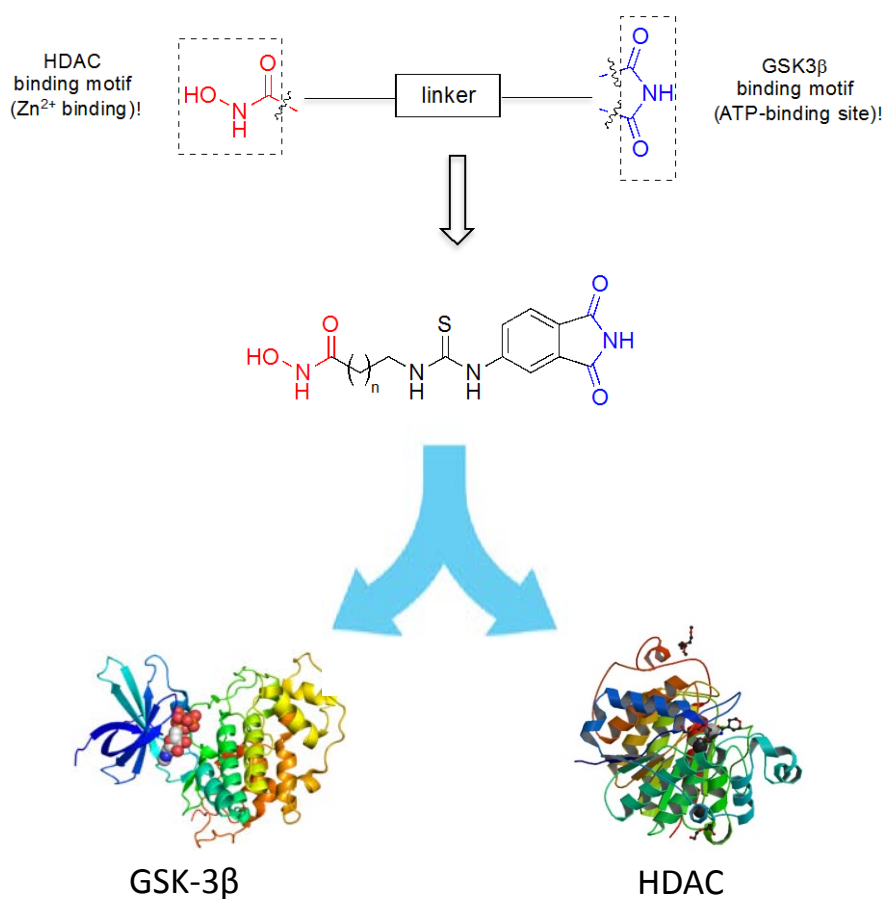


Figure 55: Drug design for GSK-3 β – HDAC as MTDLs for AD

4.5 Methods

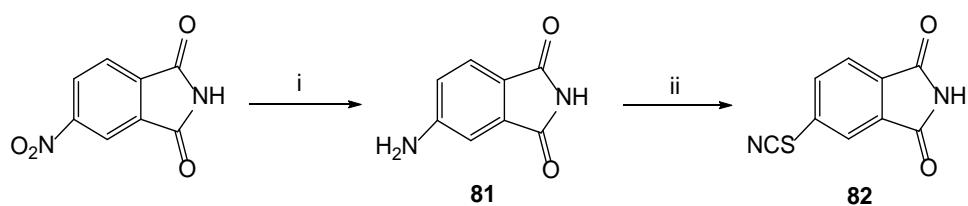
Synthesis:

The compounds (**24-27**) were synthesized by following the procedure in (Scheme 3). Compound **82** was synthesized starting from 4-Nitroptalimide which was reduced in acidic condition and using ultra sonic for 2 hours, to give compound **81**. Amine function was then transformed into isothiocyanate group using thiocarbonyl dipyridine, to give the compound **82**.

The hydroxamic acid chains were synthesized through reaction of the corresponding bromo carboxylic acid with sodium azide, to give through nucleophilic substitution the corresponding azido acids **83-86**. The carboxylic function was transformed in a protected hydroxamic acid one. Then the azide group was reduced to amine group through Staudinger reaction to give the compounds **91-94**.

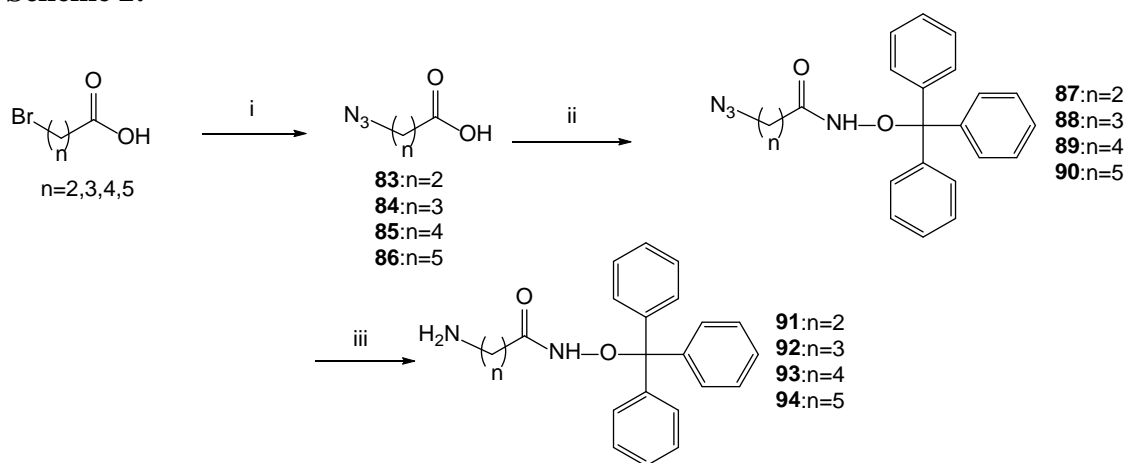
Reaction of compound **82** with the amine (**91-94**) gave, respectively, compounds **95-98**. The final acid hydrolysis allowed the removal of all protecting groups, leading to the formation of the final products **24-27**.

Scheme 1:



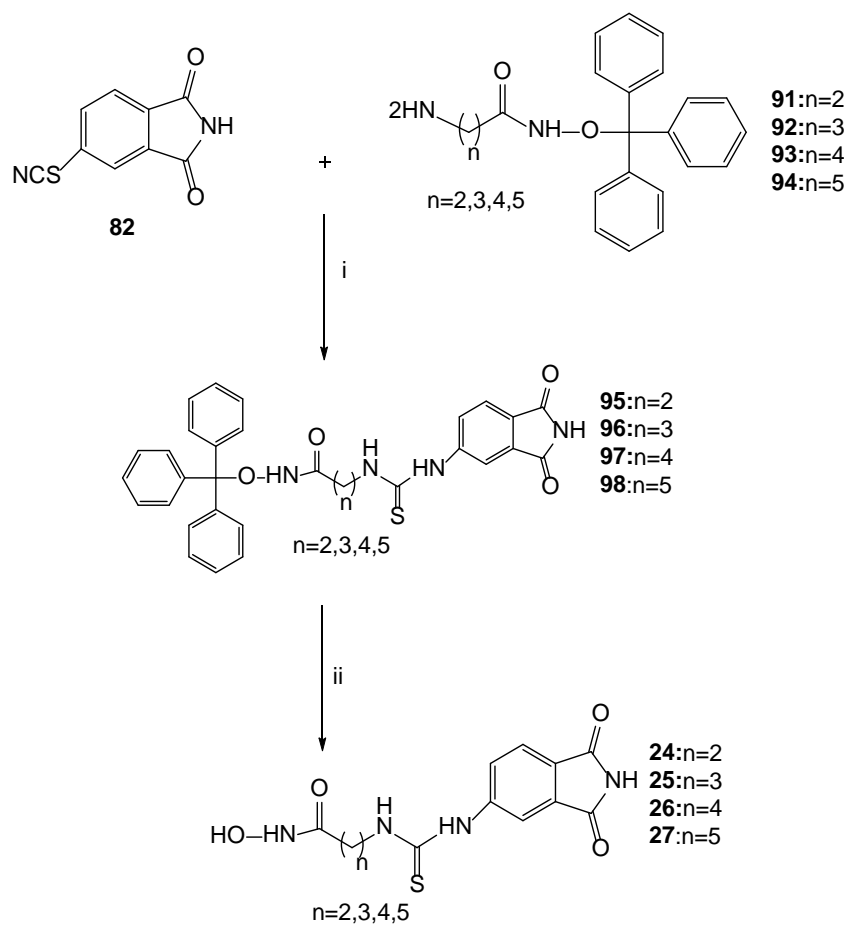
Conditions: (i) Reduction, (ii) TCP, DCM anhydrous, room temperature

Scheme 2:



Conditions: (i) NaN_3 , DMF, Reflex, 16 h; (ii) *o*-tritylhydroxylamine, IBCF, NMM, THF, 2h, room temperature (iii) PPh_3 , DCM, overnight, room temperature

Scheme 3:



Conditions: (i) DMF, Et_3N , 2h, room temperature (ii) TFA, Et_3SiH , room temperature, 30 min.

4.6 Results and discussion

Target compounds have been evaluated for their ability to inhibit GSK-3 β , by using a luminescence assay, and HDAC1, by using fluorimetric assay (Table 9).

As reported in Table 9, all the synthesized compounds turned out to be good GSK-3 β inhibitors with an IC₅₀ in the micromolar range of concentration. In particular, the inhibitory activity is strictly related to the length of the spacer. The best compound of the serie was **27**, characterized by a five methylene spacer, with an IC₅₀ of 2.69 \pm 0.01 μ M. Interesting, reducing the length of the spacer we observed a parallel decrease of the inhibitory activity, in particular compound **24**, characterized by the shorter linker, was the least active of the series (IC₅₀ = 19.96 \pm 1.76 μ M). Considering HDAC1 inhibitory activity, the most interesting compound of the series is again **27**, which induced, at 5 μ M, an almost completely abolishing of the enzymatic activity. Compounds characterized by shorter linkers, such as **24-26**, were less potent than compound **27**. It is worth to note that compound **27** is slightly more active than SAHA (residual activity at 5 μ M, 13.49 vs 27.74).

Table 9: Inhibitory activity of compounds **24-27** against GSK-3 β and HDAC1

Compound	GSK-3 β IC ₅₀ (μ M)	HDAC1 % residual activity at 5 μ M
24	19.96 \pm 1.76	54.96
25	n.d.	55.80
26	4.11 \pm 0.01	53.37
27	2.69 \pm 0.01	13.49
SAHA	n.a. ^a	27.74
10	20.22 \pm 0.40	n.d. ^b

^a not active up to 50 μ M;

^b n.d. not determined.

Compound **27** turned out to be the best of the series in terms of inhibition of both targets. For this reason, it was selected for further biological evaluations. In particular, to investigate its HDAC inhibitory potential in cell, Western blotting analyses were performed in neuroblastoma (SH-SY5Y) cell lines. Cells were treated with compound **27** and its parent compound, SAHA and **10**, for 30 h at three different concentrations (0.1, 1 and 5 μM). From (Figure 56), it could be observed that compound **27** was able to induce hyperacetylation of both histone H3 in lysine residues 9 and 14 (H3K9K14ac) and α -tubulin (Tub-ac), compared to control, although in a less extent compared to the well-known HDAC inhibitor, SAHA. It is worth to note that such effects are already visible at the concentration of 0.1 μM .

By a closer look to (Figure 56), it appears that compound **27** induces a more significant increase of α -tubulin acetylation level compared to H3K9–14ac signal. Since α -tubulin is a substrate of HDAC6 and acetylated α -tubulin levels function as a biochemical marker for HDAC6 cellular activity, the increase in the level of acetyl- α -tubulin compared to H3K9K14ac could be ascribed to an intrinsic selectivity of compound **27** for HDAC6.

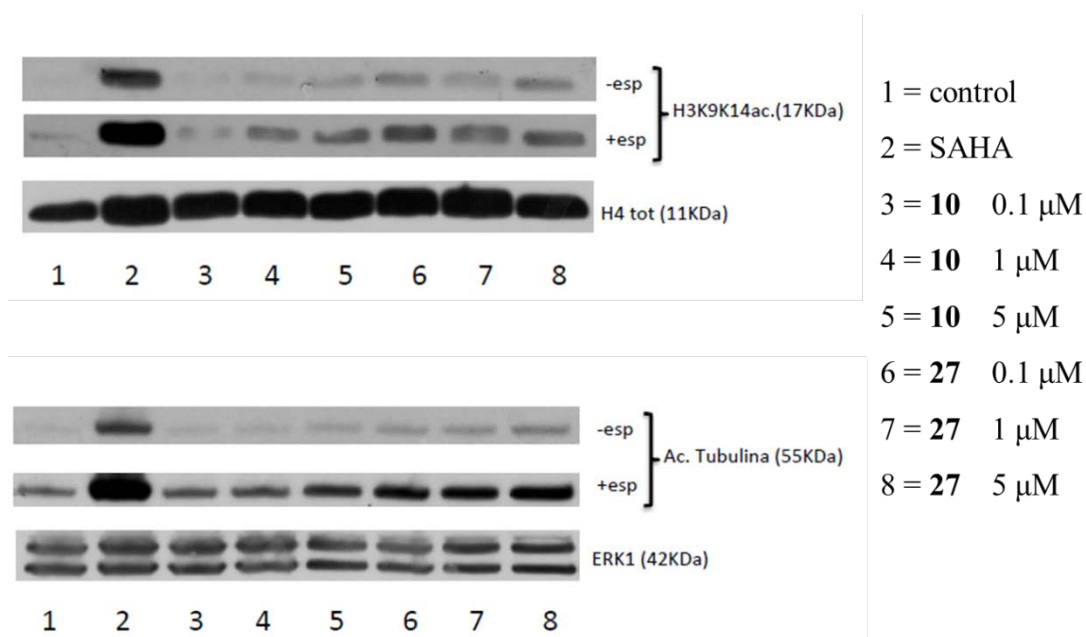


Figure 56: Western blot analyses carried out for the indicated target compounds in SHSY-5Y cells after 30 h of treatment.

Studies are currently ongoing in order to evaluate the potential toxicity of compound **27**, its neuroprotective active against different toxic stress (such as ROS and β -amyloid) and its effect on neurite outgrowth and synaptic activity in SH-SY5Y neuronal cells.

4.7 Conclusion

This study allowed us to discover of new GSK-3 β -HDAC inhibitor as MTDLs endowed with different biological activities as anti Alzheimer agents. All the synthesized compounds indicated to be good GSK-3 β inhibitors with an IC₅₀ in the micromolar range of concentration. In particular, the inhibitory activity is strictly related to the length of the spacer. The best compound of the serie was **27**, characterized by a five methylene spacer, with an IC₅₀ of 2.69 ± 0.01 μ M. Considering HDAC1 inhibitory activity, the most interesting compound of the series is compound **27**, which induced, at 5 μ M, an almost completely abolishing of the enzymatic activity. The activity of compound **27** HDAC inhibitor is slightly more active than SAHA (residual activity at 5 μ M, 13.49 vs 27.74).

The compound **27** was subjected for further biological evaluations. In particular, to investigate its HDAC inhibitory potential in neuroblastoma (SH-SY5Y) cell lines and the results showed that the compound **27** could be ascribed to an intrinsic selectivity of compound **27** for HDAC6.

The compound **27** Studies are currently ongoing in order to evaluate the potential toxicity of compound **27**, its neuroprotective active against different toxic stress (such as ROS and β -amyloid) and its effect on neurite outgrowth and synaptic activity in SH-SY5Y neuronal cells.

The promising results in this study may represent a new GSK-3 β -HDAC inhibitor as MTDLs hopefully useful for the Alzheimer treatment, therefore more biological investigations for the compound **27** are currently ongoing to evaluate its potential toxicity, its neuroprotective active against different toxic stress and its effect on neurite outgrowth and synaptic activity in SH-SY5Y neuronal cells.

4.8 Experimental Section

Chemistry:

Melting points were taken in glass capillary tubes on a Buchi SMP-20 apparatus and are uncorrected. ESI-MS spectra were recorded on Perkin-Elmer 297 and WatersZQ 4000. ¹H NMR and ¹³C NMR were recorded on Varian VRX 200 and 300 instruments. Chemical shift are reported in parts per millions (ppm) relative to peak of tetramethylsilane (TMS) and spin multiplicities are given as s (singlet), br s (broad singlet), d (doublet), t (triplet), q (quartet) or m (multiplet) Although IR spectral data are not included (because of the lack of unusual features), they were obtained for all compounds reported, and they were consistent with the assigned structures. Chromatographic purifications were performed on silica gel columns by flash (Kieselgel 40, 0.040-0.063 mm, Merck) or gravity (Kieselgel 60, 0.063-0.200 mm, Merck) column chromatography. Reactions were followed by thin layer chromatography (TLC) on Merck (0.25 mm) glass-packed precoated silica gel plates (60 F254) and then visualized in an iodine chamber or with a UV lamp. The term “dried” refers to the use of anhydrous sodium sulfate.

5-Aminoisoindoline-1, 3-dione (81): To a suspension of 4 Nitroptalimide (5g, 0.026 mol) in a mixture of glacial acetic acid (20 mL), ethanol (20 mL) and water (10 mL) was added reduced iron powder (7.28 g, 0.13 mol). The resulting suspension was exposed to ultrasonic irradiation for 2 h at 30 °C monitoring with TLC analysis the progress of reaction. The reaction mixture was filtered to remove the iron residue, which was washed with ethyl acetate (30 mL). The filtrate was partitioned with 2M KOH and the basic layer was further extracted with ethyl acetate (3 x 200 mL). The combined organic extracts were washed with brine (2 x 200 mL) and water (3 x 200 mL), dried (MgSO₄) and concentrated under reduced pressure. The crude residue was finally purified by flash silica gel column chromatography, using DCM: MeOH: Ammonium hydroxide (90:10:1) as mobile phase. ¹H NMR (400 MHz, DMSO-d₆, ppm): δ 6.35 (s, 2H), 6.75 (d, J= 8 Hz, 1H), 6.82 (s, 1H), 7.38 (d, J = 8 Hz, 1H).

5-Thiocyanatoisoindoline-1, 3-dione (82): In a flask, provided with an inert atmosphere, we placed compound **70** (3g; 0.018 mol) dissolved in DCM anhydrous. The resulting solution was treated dropwise with a solution of thiocarbonyl dipyridine (4.29 g, 0.018 mol) in DCM anhydrous. The resulting mixture was left stirring overnight at room

temperature, after that it was concentrated under reduced pressure. The crude residue was purified by flash silica gel column chromatography using petroleum ether : ethyl acetate (70:30) as mobile phase. ^1H NMR (400 MHz, CDCl_3) δ : 7.600 (d, $J = 8.4$ Hz, 1H), 7.410 (d, $J = 2.4$ Hz, 1H), 7.281 (q, $J = 10$ Hz, 1H); ^{13}C NMR (101 MHz, CDCl_3) δ 168.121, 167.865, 136.289, 135.509, 134.395, 131.712, 130.011, 124.614, 120.460. MS (ESI^+) $m/z = 205$ ($\text{M}+\text{H}$) $^+$.

General procedure for the synthesis of compounds 83-86: To a suspension of appropriate carboxylic acid (3-bromopropanoic acid, 4-bromobutanoic acid, 5-bromopentanoic acid) 1 eq in dimethylformamide, sodium azide (4eq) was added and the reaction mixture was stirred at 60 °C for 16 hours, the mixture was diluted with water and acidified with 2N HCl. The acidic layer was further extracted with dichloromethane (3 x 200 mL). The organic phase was washed with saturated solution of sodium chloride, the combined organic extracts were dried (MgSO_4) and concentrated under reduced pressure to give a yellow oil crude residue.

General procedure for the synthesis of compounds 87-90: Methylmorpholine was added to the appropriate amount of compounds **83-86** dissolved in THF anhydrous. The resulting mixture was cooled to -5 °C for 5 minutes before adding isobutyl chloroformate. The resulting mixture was left at 0 °C for 10 minutes, then *o*-tritylhydroxylamine and *N*-methylmorpholine were added. The resulting mixture was stirred at room temperature for 2 hours. After this time the mixture was poured into 2N HCl. The organic layer was washed with water, solution of sodium bicarbonate 5%, saturated solution of sodium chloride. The combined organic extracts were dried (MgSO_4) and concentrated under reduced pressure. The crude residue was then purified by flash silica gel column chromatography using ethyl acetate, hexane (2.5 : 7.5) as mobile phase.

3-Azido-*N*-(trityloxy) propanamide (87): ^1H NMR (400 MHz, DMSO-d_6) δ 7.31 (s, 15H), 2.41 (t, 2H), 1.81 (m, 2H).

4-Azido-*N*-(trityloxy) propanamide (88): ^1H NMR (400 MHz, DMSO-d_6) δ 7.30 (s, 15H), 2.32 (t, 2H), 1.6 (m, 2H), 1.43 (m, 2H).

5-Azido-*N*-(trityloxy) pentanamide (89): ^1H NMR (400 MHz, DMSO-d_6) δ 7.29 (s, 15H), 2.53 (t, 2H), 1.61 (m, 4H), 1.51 (m, 2H).

6-Azido-*N*-(trityloxy) hexanamide (90): ^1H NMR (400 MHz, DMSO-d_6) δ 7.33 (s, 15H), 2.71 (t, 2H), 1.51 (m, 6H), 1.34 (m, 2H).

General procedure for the synthesis of compounds 91-94: The appropriate azide **87-90** was dissolved in methanol then some drops of water and triphenylphosphine were added. The resulting mixture was stirred at room temperature for 16 hours, then concentrated under reduced pressure. The crude residue was then purified by flash silica gel column chromatography, using DCM : MeOH : ammonia aq (90: 10: 1) as mobile phase.

3-Amino-N-(trityloxy) propanamide (91): ^1H NMR (400 MHz, DMSO- d_6) δ 7.28 (dd, $J = 10.3, 3.6$ Hz, 15H), 2.35 (t, $J = 7.0$ Hz, 2H), 1.74 (t, $J = 7.3$ Hz, 2H), 1.26-1.15 (m, 2H), 1.09-1.00 (m, 2H); ^{13}C NMR (101 MHz, CDCl $_3$) δ : 141.8, 140.8, 129.0, 128.2, 127.8, 93.2, 38.9, 31.5, 30.2, 26.3.

4-Amino-N-(trityloxy) propanamide (92): ^1H NMR (400 MHz, DMSO- d_6) δ 7.29 (s, 15H), 2.67 (t, 2H), 2.31 (t, 2H), 1.9 (m, 2H); ^{13}C NMR (101 MHz, CDCl $_3$) δ 168.09, 147.92, 147.52, 146.99, 129.2, 127.98, 126.03, 99.34, 43.87, 31.15, 29.94.

5-Amino-N-(trityloxy) pentanamide (93): ^1H NMR (400 MHz, DMSO- d_6) δ 7.30 (s, 15H), 2.43 (t, $J = 6.8$ Hz, 2H), 1.75 (t, $J = 7.0$ Hz, 2H), 1.27-1.02 (m, 6H), 0.98-0.87 (m, 2H); ^{13}C NMR (101 MHz, DMSO- d_6) δ 170.7, 142.9, 129.4, 127.9, 127.8, 92.1, 41.9, 33.3, 32.4, 28.7, 26.5, 25.3.

6-Amino-N-(trityloxy)hexanamide (94): ^1H NMR (400 MHz, DMSO- d_6) δ 7.38-7.15 (m, 15H), 2.46 (t, $J = 5.3$ Hz, 2H), 1.75 (t, $J = 7.2$ Hz, 2H), 1.32-1.21 (m, 2H), 1.20-1.01 (m, 6H), 0.99-0.88 (m, 2H); ^{13}C NMR (101 MHz, DMSO- d_6) δ : 170.6, 143.0, 129.4, 128, 127.8, 92.1, 55.4, 42.0, 33.6, 29.1, 28.8, 26.7, 25.2.

General procedure for the synthesis of compounds 95-98: To a solution of compound **82** (150 mg, 0.734 mmol) in dichloromethane 0.734 mmol of appropriate amine (**91-94**) were added, and 0.734 mmol of triethylamine. The resulting mixture was stirred at room temperature for 16 hours, then concentrated under reduced pressure. The crude residue was purified by flash silica gel column chromatography using ethyl acetate: petroleum ether (8: 2), as mobile phase.

3-(3-(1,3-Dioxoisindolin-5-yl) thioureido)-N-(trityloxy) propanamide (95): ^1H -NMR (400 MHz, DMSO- d_6) δ 11.43 (s, 1H), 10.32 (d, 1H), 8.19 (d, 2H), 7.95 (t, 1H), 7.29 (s, 15H), 6.97 (s, 1H), 3.57 (t, 2H), 2.61 (t, 2H).

4-(3-(1,3-Dioxoisindolin-5-yl) thioureido)-N-(trityloxy) butanamide (96): ^1H -NMR (400 MHz, DMSO- d_6) δ 11.54 (s, 1H), 10.6 (s, 1H), 8.38 (d, 2H), 7.78 (t, 1H), 7.34 (s, 15H), 7.56 (s, 1H), 3.8 (d, 2H), 2.54 (t, 2H), 1.87-1.93 (m, 2H).

5-(3-(1,3-Dioxoisindolin-5-yl)thioureido)-N-(trityloxy) pentanamide (97): ¹H-NMR (400 MHz, DMSO-d₆) δ 12.01 (s, 1H), 11.1 (s, 1H), 8.26 (d, 2H), 7.69(t, 1H), 7.27 (s, 15H), 7.49 (s, 1H), 3.68 (d, 2H), 2.48 (t, 2H), 1.57-1.54 (m, 4H).

6-(3-(1,3-Dioxoisindolin-5-yl)thioureido)-N-(trityloxy) hexanamide (98): ¹H-NMR (400 MHz, DMSO-d₆) δ 11.19 (s, 1H), 10.10 (d, 1H), 8.16 (t, 2H), 7.72 (t, 1H), 7.26 (s, 15H), 3.36 (d, 2H), 1.80(d,2H), 1.42(m, 4H), 1.1(m,2H).

General procedure for the synthesis of compounds 24-27: The appropriate compound (95-98) was dissolved in dichloromethane then trifluoroacetic acid was added; the mixture was stirred at room temperature for few minutes then triethylsilan dropwise was added. The resulting mixture was stirred at room temperature for 12 hours, then concentrated under reduced pressure. The crude residue was purified by flash silica gel column chromatography, using DCM:MeOH (9.5:0.5) as mobile phase.

3-(3-(1,3-Dioxoisindolin-5-yl)thioureido)-N-hydroxypropanamide (24): ¹H-NMR (400 MHz, DMSO-d₆) δ 11.45 (s, 1H), 10.77 (s, 1H), 9.08 (s, 1H), 8.12 (s, 2H), 7.65 (t, 1H), 7.23 (s, 1H), 7.03 (s, 1H), 3.86 (t, 2H), 2.13 (t, 2H); ¹³C NMR (101 MHz, DMSO-d₆) δ 178.32, 171.21, 167.19, 167.03, 140.72, 131.9, 130.65, 127.45, 126.92, 123.29, 43.87, 34.8; MS (ESI⁺) m/z = 308.3 (M+H)⁺.

4-(3-(1,3-Dioxoisindolin-5-yl)thioureido)-N-hydroxybutanamide (25): ¹H-NMR (400 MHz, DMSO-d₆) δ 11.43 (s, 1H), 10.57 (s, 1H), 10.1 (s, 1H), 8.23 (s, 2H), 7.76 (t, 1H), 7.19 (s, 1H), 7.0 (s, 1H), 3.59 (t, 2H), 3.25 (t, 2H), 1.86- 1.76 (m, 2H); ¹³C NMR (101 MHz, DMSO-d₆) δ 179.42, 170.31, 167.24, 167.17, 139.82, 133.64, 131.35, 127.35, 127.02, 122.52, 45.19, 31.48, 26.71; MS (ESI⁺) m/z = 322.34 (M+H)⁺.

5-(3-(1,3-Dioxoisindolin-5-yl)thioureido)-N-hydroxypentanamide (26): ¹H-NMR (400 MHz, DMSO-d₆) δ 11.76 (s, 1H), 10.32 (s, 1H), 9.98 (s, 1H), 8.27 (s, 2H), 7.9 (t, 1H), 7.25 (s, 1H), 7.13(s, 1H), 3.74 (t, 2H), 2.65-2.54 (m, 2H), 1.61- 1.59 (m, 4H); ¹³C NMR (101 MHz, DMSO-d₆) δ 178.92, 169.48, 166.28, 166.08, 140.19, 132.94, 130.95, 127.85, 126.92, 121.92, 43.17,32.98, 29.71, 23.8; MS (ESI⁺) m/z = 336.37 (M+H)⁺.

6-(3-(1,3-Dioxoisindolin-5-yl)thioureido)-N-hydroxyhexanamide (27): ¹H-NMR (400 MHz, DMSO-d₆) δ 12.06 (s, 1H), 11.12 (s, 1H), 10.65 (s, 1H), 8.37 (s, 2H), 7.53 (t, 1H), 7.47 (s, 1H), 7.24(s, 1H), 3.64 (t, 2H), 2.75-2.64 (m, 2H), 1.53- 1.39 (m, 6H); ¹³C NMR (101 MHz, DMSO-d₆) δ 179.32, 168.51, 167.47, 166.17, 141.67, 134.83, 131.18, 127.37, 127.1, 121.92, 45.96,33.04, 29.83, 27.8, 23.84; MS (ESI⁺) m/z = 350.38 (M+H)⁺.

Chapter 5. DNA as target: Topoisomerases structures

5.1 Introduction to cancer therapy

Cancer is the name given to a collection of related diseases when some of the body's cells begin to divide without stopping and spread rapidly into surrounding tissues. These abnormal cells able to grow beyond their usual boundaries pervade adjoining parts of the body and spreading to other tissues. Cancer developed in different tissues of the body and has many distinct types which differ substantially in their behavior and response to treatments.

Cancer is one of the central causes of death worldwide, besides infectious diseases, malnutrition and cardiac diseases; the global cancer burden is continuously rising, mainly due to the permanent growth of the world's population and the proceeding ageing, especially in more developed countries. Another reason is the increasing adoption of cancer associated behaviors particularly smoking, physical inactivity, and unhealthy diets. In 2008, about 12.7 million cancer cases and 7.6 million cancer deaths were estimated to have occurred worldwide, there of 3.4 million incidences and 1.8 million deaths in Europe, it is expected that cancer related deaths will at least double by 2030 (World Cancer Report 2008).

Cancer developments associated with multiple genetic changes, losing the control over a number of processes and mutations which may be produced in any cell division event due to faulty DNA replication or repair. Cells become abnormal and lose its monitoring on growth, old or damaged cells survive when they should die, and new cells form when they are not needed. These extra cells can divide uncontrollably forming growths called tumors. There are two different types of tumor: benign and malignant.

Benign tumors: This type can form in different part of the body but remain confined in the initial location, unlike malignant ones, do not spread into or invade nearby tissues, they can form in different part of the body and grow slowly When removed, they usually do not grow back, (Cooper M.G 2000).

Malignant tumors: These tumors are able to spread into and invade nearby tissues. These tumors grow in different body sites from the primary tumor, they can pass more easily to distant places in the body through bloodstream or lymphatic channels and form new

tumors far from the original tumor, these secondary tumors may grow, invade and damage nearby tissues, and spread again, forming the so called “metastasis”.

Due to the abundance of diverse cancer types, there are different treatment options, based on the location, stage of the cancer, the presence of metastases, and also the patient’s general health state. Among the most common methods currently in use are: surgery, radiation therapy, chemotherapy, bone-marrow transplantation, immune and hormonal therapy.

Chemotherapy is the most common form of cancer treatment and includes the use of chemical entities able to alter the cell division process, through the infliction of serious damages to DNA or proteins triggering the apoptosis process or stopping their proliferation. Chemotherapeutics are classified into four different categories based on their target or the nature of their composition. These groups include: cytotoxics, biological, targeted therapeutics, and hormonal therapeutics. Cytotoxics were discovered primarily due to their abilities to kill cells. The cytotoxic targets include: DNA (intercalating, alkylating and cross-linking agents); DNA synthesis pathway enzymes (antimetabolites); tubulin (antimicrotubule and tubulin polymerizing agents); and topoisomerases (topoisomerases I and II).

Topoisomerases are the major enzymes that maintain the topology and the integrity of DNA. Inhibition of topoisomerase interferes with all central DNA processing steps such as replication, transcription, translation and recombination.

5.2 DNA-Topoisomerases

DNA topoisomerases are crucial enzymes found in all living organisms. The first topoisomerase was discovered in 1971 (Wang 1971), and it was described by its ability in eliminating the negative superhelical coils from DNA. The functions of topoisomerase enzymes are related with DNA processing and are common in all living cells. Topoisomerases control the steady-state level of DNA supercoiling, which in role facilitate DNA-protein interaction and block the damaging excess of supercoils. These DNA associated enzymes have fundamental role in replication, transcription, recombination and other various cellular processes (Wang 2002, Gellert 1981, Nitiss, 1994, Postow 1999). Topoisomerase enzymes are able to modify the conformation of DNA by a complex catalytic action includes DNA strand cleavage, strand passage and

relegation of the DNA strands. Topoisomerases are classified mainly in two distinct classes, characterized by their mechanistic and physical properties (Champoux 2001). Type I topoisomerase makes transient single strand breaks in DNA, facilitating regulated rotation about the nick before rejoining; this action does not need an energy cofactor, instead this energy can be obtained from that stored in the supercoiled DNA.

Depending on the type of DNA adduct these topoisomerases can be classified in type I and type II. The type I enzymes are further subdivided into type IA and type IB.

Type IA topoisomerases (containing eukaryotic topoisomerase IIIa and IIIb) establish a transient covalent phosphotyrosine attach to the 5' end of DNA; this type has the ability to relax only negatively supercoiled DNA and for this reaction needs magnesium and a single stranded stretch of DNA. Type IB topoisomerases (including eukaryotic topoisomerase I and mitochondrial topoisomerase I) linkage to the 3' DNA terminus and this type is able to relax both positively and negatively supercoiled DNA with the same effectiveness and the reaction does not demand a single-stranded region of DNA or metal (Wang 1996, Champoux 1998).

The type II enzymes modify the topology by causing an intact helix pass through a transient double-stranded break in the DNA backbone (Berger 1998). It requires ATP for the catalytic function. During cleavage, two tyrosines attack opposite stands of the DNA duplex establishing covalent 5'-phosphotyrosine linkages to DNA in a four base pair stagger.

Topoisomerases I and II have become main targets for cancer therapy and they have been extensively studied over the past three decades for the rational drug design of novel anti-cancer drugs. In this introduction, we will describe briefly the role of the different types of these enzymes and their pharmacological significance.

5.2.1 DNA topoisomerases I

Topoisomerases I are enzymes that involve DNA topology by transiently cleaving one DNA strand at a time. The gene for human topoisomerase I has been mapped to chromosome 20q12-13.2 (Juanet al 1988). The topoisomerase I gene is 100 kD a monomeric protein, it needs phosphorylation for full activity. This protein is abundant in the nucleus and also exists in nucleoplasm and mitochondria (Fleischmann 1984, Zhang 2001m Christensen 2002).

Stewart has revealed by proteolysis studies that the enzyme consists of four main domains: a highly charged 24kDa NH₂-terminal domain, a positively charged 56 kDa core

domain, 7kDa linker domain, and 6 kDa COOH-terminal domain which includes the catalytic Tyr-723. Recently, the determination of X-ray crystal structure of human topoisomerase I explained the mechanism of action of this enzyme on DNA (Stewart 1998, Redinbo 1998), and helped in understanding the structure-activity relationships for several topoisomerases inhibitors (Staker2002).

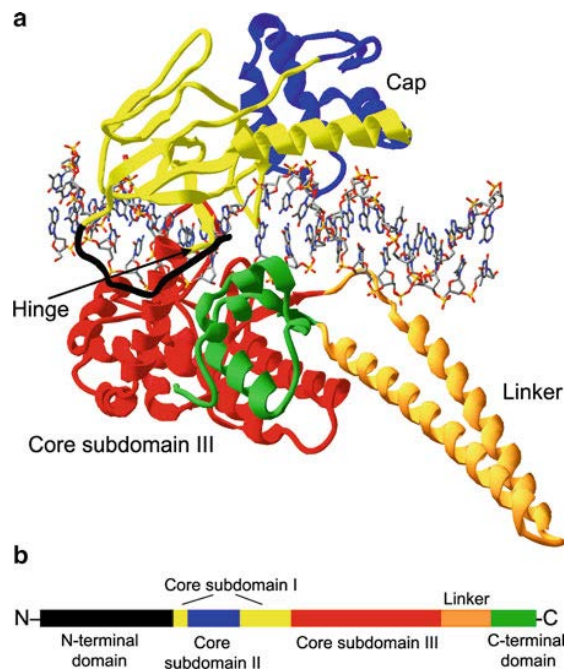


Figure 57: The domain structure of human TopI (a) Ribbon diagram of the co-crystal structure of humanTop1 containing a 22 base pair duplex oligonucleotide (pdb entry 1K4T) (b) The domain structure of human Top1 is depicted on a linear representation of the protein (Staker 2002).

Based on the polarity of the strand cleavage, topoisomerase I is divided into topoisomerase IA and IB (Wang 2002). Topoisomerase IA composes a transient 5-phospho-tyrosine covalent intermediate, results a free 3-OH strand and enhances passage of the intact strand through the broken strand; topoisomerase IB gives a 3-phospho-tyrosine covalent intermediate, forms a free 5-OH strand and leaves the broken strand free to rotate around the intact strand. The two types have the same chemistry function in breaking the phosphodiester bond, the enzyme attacks a phosphodiester bond of the DNA with a tyrosyl group building a covalent bond on one side of the break and forming a free hydroxylated strand on the other side. And the reverse reaction through attacking the phosphotyrosine by the free hydroxylated strand retrieves the phosphodiester bond and releases the enzyme for next catalytic cycle.

Topoisomerase I exists throughout the cell cycle and its function differs less than topoisomerase II during the cell cycle (Heck 1988, Romig 1990), therefore, topoisomerase I emerged as an attractive target for drug design in anticancer therapy.

5.2.2 DNA topoisomerases II

Topoisomerase II has main role in DNA replication and transcription. Topoisomerase II also plays a major role in chromosome condensation and separation during mitosis. Studies have revealed that topoisomerase II partly involves in forming chromosome scaffold and nuclear matrix. (Adolphs 1977). Topoisomerases II insert double-strand breaks in a DNA duplex and impose the passing of another duplex through this break before resealing it. The cleavage-religation reaction is similar to those carried out by type I topoisomerases with the formation of a covalent bond between a tyrosine from the enzyme and the DNA phosphate, but the transient link is exclusively formed with the 5'-end of the DNA breaks. These enzymes have different function in cell cycle regulation and nuclear isolation (Austin 1995).

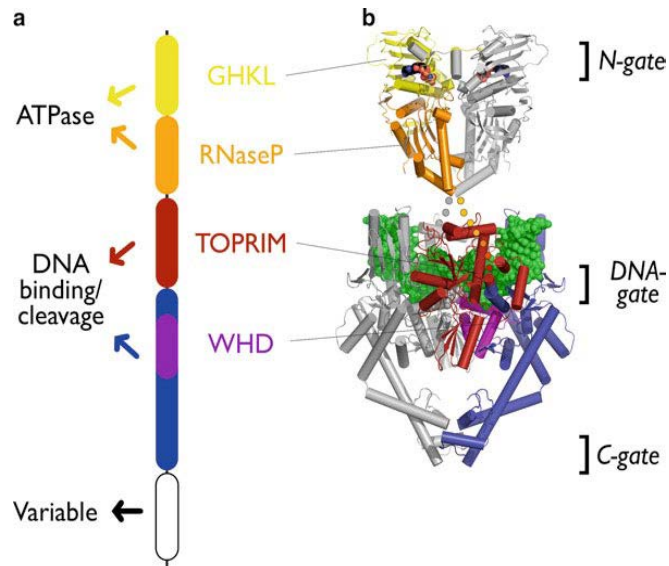


Figure 58: Topoisomerase II organization and structure (a) Linear domain map, from N- to C-terminus (top to bottom), highlighting the relative position of conserved functional elements (b) Top2 ATP as a domain and DNA binding and cleavage (Classen 2003, Schmidt 2010).

Topoisomerase II α is expressed in the proliferating compartments of all tissues and is detectable in both the cell nucleus and cytoplasm, whereas topoisomerase II β is a 180 kDa protein localized ubiquitously and is centralize in the nucleoli and nucleoplasm (Turley 1997). During mitosis, topoisomerase II α links completely to the mitotic chromatin, while topoisomerase II β distributes into the cytosol (Meyer 1997). The levels of topoisomerase II β are stable over the cell cycle and topoisomerase II α levels are closely associated to the proliferation state of the cell, being increased 2-3 fold during G2/M phases and in rapidly proliferating cells (Turley 1997). All types of topoisomerases II are ATP-dependent multimeric enzymes with a dyad symmetry. Each unit of the enzyme is consisted of an ATP-binding domain and a catalytic breakage- religation domain including covalent bond-forming tyrosine residue.

5.3 Topoisomerases as Targets for Cancer Chemotherapy

Several anticancer agents currently in clinical use are known to exert their cytotoxic function partly by targeting DNA topoisomerase enzymes. Since cancer cells in several cases are highly proliferative cells, and topoisomerases are implicated in replication and proliferation processes, the levels of these enzymes are higher in growing cancer cells comparing to normal cells, making these enzymes an important target for potential selective anticancer drugs.

Topoisomerase levels are increased in several haematological malignancies and solid tumours comparing to normal cells. Studies revealed that the levels of topoisomerase I are 14-16 folds higher in cancerous colon tissue than in normal tissue (Giovanella 1989). Overexpression of topoisomerase isoforms has been found in human cervix, lung and colon cancers; furthermore, it was reported a content of 10-fold more elevate in topoisomerase I and topoisomerase II in ovarian tumors tissues compared to the corresponding normal tissues (McLeod 1994, Vander Zee 1991). The inhibition of topoisomerases in tumour cells will result in unwinding, strand separation and inhibition of the reproduction of DNA. Concerning drugs which selectively interact with the topoisomerase enzymes, the increased levels of these enzymes were found in many tumors and this finding could provide a higher level of tumor cell selectivity that would reduce the DNA damage to normal tissue and minimize side effects.

The interaction of topoisomerases with DNA can be broken down into several key steps:

1. Enzyme-DNA-binding;
2. Cleavage of DNA by transesterification from the phosphodiester DNA backbone to an enzyme catalytic tyrosine resulting in a covalent bond between the protein and one terminus of the DNA nick (3' terminus in the case of topo I and 5' terminus of a double-strand break in the case of topoisomerase II);
3. DNA strand passage;
4. Resealing of the DNA break concerted with the release of the topoisomerase enzyme;
5. ATP hydrolysis (topoisomerase II only).

Topoisomerase targeting agents can function at any of the above steps resulting in inhibition or poisoning of the enzyme leading to cell death. Topoisomerase inhibitors are classified based on the mechanism of action into two classes: catalytic inhibitors and topoisomerase poisons.

Topoisomerase poisons stabilize the drug-DNA-enzyme ternary complex, inhibiting religation of the cleaved strand(s). Subsequent with a cut in the replication complexes, transient topoisomerase mediated breaks become permanent double-stranded breaks, triggering apoptosis cascade (cell death syndrome) (Fortune 2000).

Catalytic inhibitors act by binding directly to topoisomerases, binding to DNA modifying its structure so that it can no longer be recognized by the topoisomerases or by trapping topoisomerase II in a closed clamp form prohibiting the enzyme turnover (Roca 1994).

5.3.1 Anticancer topoisomerase I-targeted drugs

The potent anticancer activity of Camptothecin was known before the discovery of Topoisomerase I as its molecular target. It was studied extensively in the Cancer Chemotherapy National Service Center of the National Cancer Institute during the 1960s (DeWys 1968). Camptothecin sodium salt proved remarkable activity and enhances the survival time in mice bearing several lymphocytic leukemias (Gallo 1971). Camptothecin sodium salt was demonstrated to be efficient in patients with advanced disseminated melanoma or gastrointestinal malignancies (Gottlieb 1970, Moertel 1972). Unfortunately, its use was discontinued in the 1970s because of severe side effects (Wall 1995), included myelo-suppression, vomiting, diarrhea, and hemorrhagic cystitis, and currently it is used as reference for clinical investigation for Topoisomerase I-targeted agents.

Camptothecin derivatives such as topotecan (Hycamtin®) and irinotecan (Camptosar®, Campto®) are water-soluble and endowed with fewer side effects. All the camptothecin derivatives are potent topoisomerase I poisons by stabilizing the transient covalent DNA-

topoisomerase I cleavage complex and prohibition religation of the cleaved DNA strand. Although camptothecins proved to be potent anticancer, all of them suffer from clear limitation (Pommier 2009) in addition to their dose-limiting toxicity, which prohibits the use of curative doses (Giovannella BC 1989). Camptothecins are rapidly inactivated due to the instability of the six-membered lactone ring; indeed, at physiological pH camptothecins are in equilibrium with their inactive (carboxylate) form.

Topotecan (Hycamtin) received FDA approval in 1996 for the treatment of advanced metastatic ovarian carcinoma and since then it has been approved for the use in the treatment of small cell lung cancer. This drug has the shortest plasma half-life of any camptothecin reported to date and requires repeated daily administration or continuous infusion over several days or even weeks (Takimoto 1998). Irinotecan, (CPT-11, Camptosar), was approved by FDA for the treatment of colorectal and gastro esophageal malignancies (Makeyev 2012).

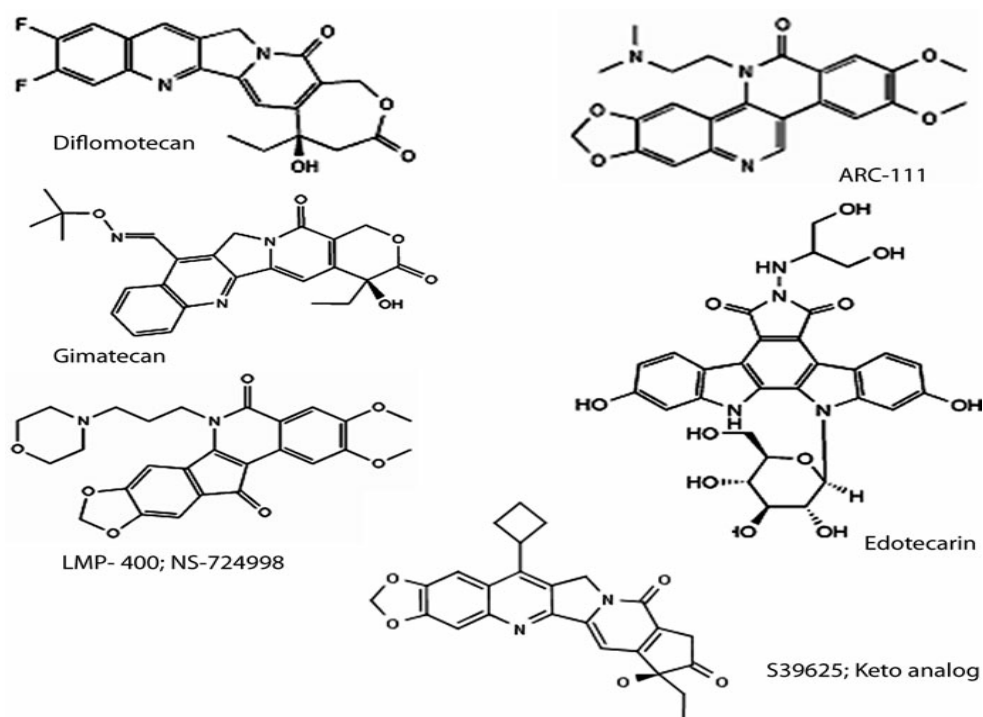


Figure 59: Chemical structures of Topoisomerase I inhibitors

Homocamptothecin family resulted from modulating the metabolically liable camptothecin lactone ring from a six-membered α -hydroxylactone to a seven-membered α -hydroxylactone ring (Troconiz 2006). Diflomotecan BN80915 is the

difluorohomocamptothecin derivative, which is one of the most potent topoisomerase inhibitors (Lansiaux 2001). In preclinical safety studies, the dose-limiting toxicity of diflomotecan was myelosuppression (Troconiz2006). Currently diflomotecan is under Phase II clinical trial for advanced metastatic cancer, SCLC malignancy.

Gimatecan (ST1481) is a seven-position modified lipophilic camptothecin derivative developed to provide rapid uptake and increase accumulation and stabilize the Topoisomerase I-DNA-drug ternary complex compared with conventional camptothecins (Perego 2006), Gimatecan showed good tolerability in Phase I clinical trial. Gimatecan has undergone Phase II clinical study in advanced epithelial ovarian, fallopian tube, and peritoneal cancers, advanced breast cancer, malignant glioma, and metastatic colorectal cancer (Mariani 2006, Hu 2009); these studies have demonstrated that gimatecan is active as a single agent with bone marrow suppression as serious side effect.

Edotecarin from Indolocarbazolesgroup, is a derivative of NB-506 that as a Topoisomerase Iinhibitor enhances single-strand DNA cleavage more efficiently than NB-506 or camptothecin (Long 2002, Yamada 2006, Hurwitz 2007).

The indenoquinoline NSC314622 was found as a potential Topoisomerase inhibitor by COMPARE analysis from 48-h cytotoxicity screening of the NCI 60-cell line panel (Long 2000).

Other indenoisoquinoline derivatives, such as LMP400 (NSC 743400) and LMP776 (NSC 725776), have been developed (Pommier 2009) and are currently in Phase 1 of clinical trial for Lymphomas Malignancy.

Nitidine and fagaronine are benzo- phenanthridine alkaloids, they are active as Topoisomerase I inhibitors (Zee 1975, Janin 1993). An extensive structure-activity relationship was proceeded around the dibenzo[c,h][1,6]naphthyridin-6-one family of compounds, which displayed a potent Top1-targeting activity and suitable pharmaceutical properties (Zhu 2006, Satyanarayana 2008), Many of these compounds that had unique DNA cleavage site selectivity were potent cytotoxic agents in cancer cell lines.

5.3.2 Anticancer topoisomerase II-targeted drugs

Topoisomerase II catalyzes the transient breaking and rejoining of two strands of double helix allowing the strands to pass through one to another. With this mechanism topoisomerase II monitors and changes the topologic state of DNA in nucleus. Topoisomerase II inhibitors act by inhibiting the catalytic activity of the enzyme, thus blocking its action. Such ligands can inhibit religation of broken DNA by stabilizing

topoisomerase II DNA cleavage complex while others can act by accelerating the enzyme rate to produce more DNA cleavage and inhibition of ligation. (Baldwin 2005) These mechanisms of topoisomerase II inhibitors lead to permanent double strand cuts in DNA and promote apoptotic signals resulting in efficient death of cancer cells. The mechanism of action of topoisomerase II is summarized in Figure 61.

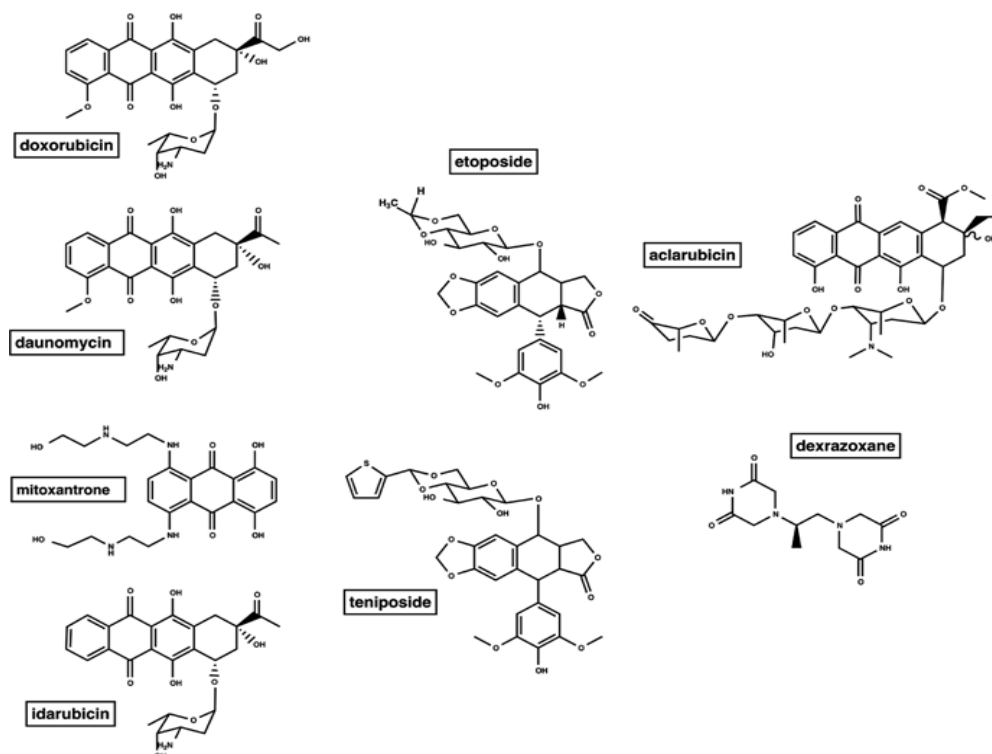


Figure 60: Chemical structures of FDA-approved drugs targeting topoisomerase II.

Anthracyclines (Figure 60) is the largest group of approved topoisomerase II targeting agents including doxorubicin (approved in 1974), daunomycin (approved in 1979), idarubicin, aclarubicin and Mitoxantrone. Several earlier clinical studies with anthracyclines revealed that anthracyclines target topoisomerase II and produce free radicals that damage DNA and other cellular structures, as well as acting as DNA intercalating agents. Some anthracyclines have substantial antitumor activity, but they also have significant toxicity, including cardiotoxicity. Aclarubicin is distinct among approved anthracyclines because it is topoisomerase II catalytic inhibitor. Mitoxantrone, is a potent intercalating agent that has been approved for leukemia and advanced hormone refractory prostate cancer, and it is the only topoisomerase II poison that has been approved for a non-cancer indication, such as multiple sclerosis (Giovannoni 2011).

Similar to the other anthracyclines, mitoxantrone can lead to substantial cardiotoxicity, albeit to a lesser extent than anthracyclines (Hamzehloo 2006).

Etoposide is an effective antimitotic and antineoplastic agent which has been in clinical use for over two decades; it was derived from Podophyllotoxins. After preclinical studies and clinical trials for over 20 years, Food and Drug Administration (FDA) approved its use in clinics for cancer chemotherapy (Baldwin 2005).

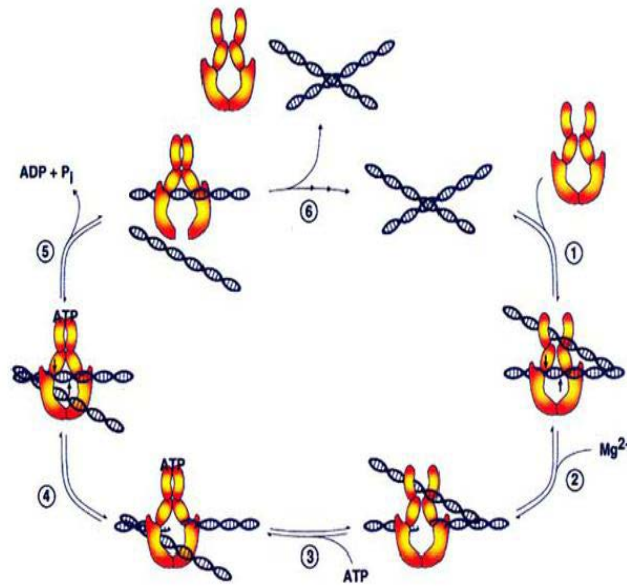


Figure 61: Mechanism of action of topoisomerase II: (1) Topoisomerase II-DNA binding (2) pre-strand passage DNA cleavage-religation equilibrium (3) ATP binding and DNA strand passage (4) post-strand passage DNA cleavage-religation equilibrium (5) ATP hydrolysis and gate opening (6) DNA release and enzyme turnover (Baldwin 2005).

Studies revealed that the main mechanism of action of etoposide is as topoisomerase II inhibitors and it is considered a DNA poison. The binding of etoposide to topoisomerase II is reversible; hence the longevity of the efficiency of etoposide is due to the exposure time (Hainsworth 1995). Beside topoisomerase II inhibition action, some metabolic products of etoposide bind directly to DNA leading to single strand cuts (Baldwin 2005).

Teniposide is another topoisomerase II inhibitor, which is almost 10-fold more cytotoxic than etoposide. It is used in the treatment of refractory childhood acute lymphoblastic leukaemia, even if its use is limited, due to a higher incidence of hypersensitivity reactions. The appearance of myelosuppression represents the dose limiting toxicity for

this compound and some studies reported of acute non-lymphocytic leukaemia with 11q23 chromosomal abnormalities in patients treated with teniposide (Stine 1997).

Doxorubicin (Adriamycine®) is isolated from *Streptomyces peucetius* var. *caesius*, (Arcamone 1969), it acts with three direct mechanisms: the first mechanism of action is intercalation between base pairs interfering with DNA and RNA synthesis. Doxorubicin also acts as a topoisomerase II inhibitor. Similar to Etoposide, through stabilizing the enzyme DNA cleavage complex, leading to the accumulation of double strand breaks which are signals for programmed cell death (Swift 2006), another mechanism for doxorubicin is the interaction with cell membrane, by binding to negatively charged phospholipids, result in modification of the membrane dynamics and fluidity (Speelmans 1994). Doxorubicin is a widely used chemotherapeutic in clinic in various cancers, such as breast, ovarian, bladder, lung, thyroid and gastric cancers, as well as neuroblastoma, lymphoma, leukemia, Kaposi's sarcoma and in the treatment of breast cancer.

5.4 Drug design

Tryptanthrin (indolo-[2, 1-b]-quinazoline-6, 12-Dione) is a weakly basic alkaloid which consists of a quinazoline ring fused to an indole moiety with carbonyl groups in the 6- and 12-positions. Tryptanthrin has been isolated from numerous natural sources; in particular, it was first isolated from *Isatistinctoria* and it also produced by culture of the yeast *Candida lipolytica*, fungi such as *Schizophyllum commune* and *Leucopaxillus cerealis* and from various plants such as *Polygonum tinctorium*. A number of biological actions have been associated to tryptanthrin and its derivatives. For instance, tryptanthrin is reported to have antifungal, antimicrobial (Honda, G 2010), tuberculostatic and antimalaria activity (Bhattacharjee, A. K 2002). Furthermore, it is able to inhibit enzymes such as COX-2, 5-lipoxygenase (5-LOX) and nitric oxide (NO) synthase. It is worth to note that tryptanthrin shows antiproliferative effects in leukemia cell lines and *in vivo* in intestinal and lung cancers. Indeed, tryptanthrin targets indoleamine 2,3-dioxygenase (IDO-1) and suppresses angiogenesis by reducing the expression of angiogenic factors.

Recently, Liang and coworkers reported about a tryptanthrin derivative, benzo[b]tryptanthrin, as Topoisomerase inhibitor. In particular, this compound is able to inhibit both topoisomerase I and II and shows cytotoxic activity in colon cancer cell lines (Liang JL 2012). Further studies on this compound revealed that it behaves as topoisomerase II inhibitor by binding to the ATP-binding pocket in competition with ATP (Kyu 2015). Moreover, benzo[b]tryptanthrin is able to induce a down-regulation of multidrug resistance protein 1 (MDR1) in adriamycin resistant breast cancer cell line (MCF7) and induces apoptosis through activation of caspase-3 and PARP.

Aim of the present work was the development of 7- and 9-substituted Tryptanthrin derivatives with the aim of increasing the affinity towards topoisomerase II and the cytotoxic activity.

In particular, we chose to introduce different substituents characterized by different chemical physical properties, such as:

- morpholine: compounds **30** and **36**;
- N,N-dimethylethylendiamine: compound **31** and **37**;
- diethylenamine: compounds **32** and **38**;
- N-methylpiperazine: compounds **33** and **39**;
- aminoethanol: compounds **34** and **40**;

- piperidine: compounds **35** and **41**.

In particular, all these substituents are characterized by a basic function which can contribute to improve the water solubility of tryptanthrin derivatives as well as their ability to interact with the targets reported above through ionic bonds of the protonated amine functions with ionized acidic residues, located in target structures.

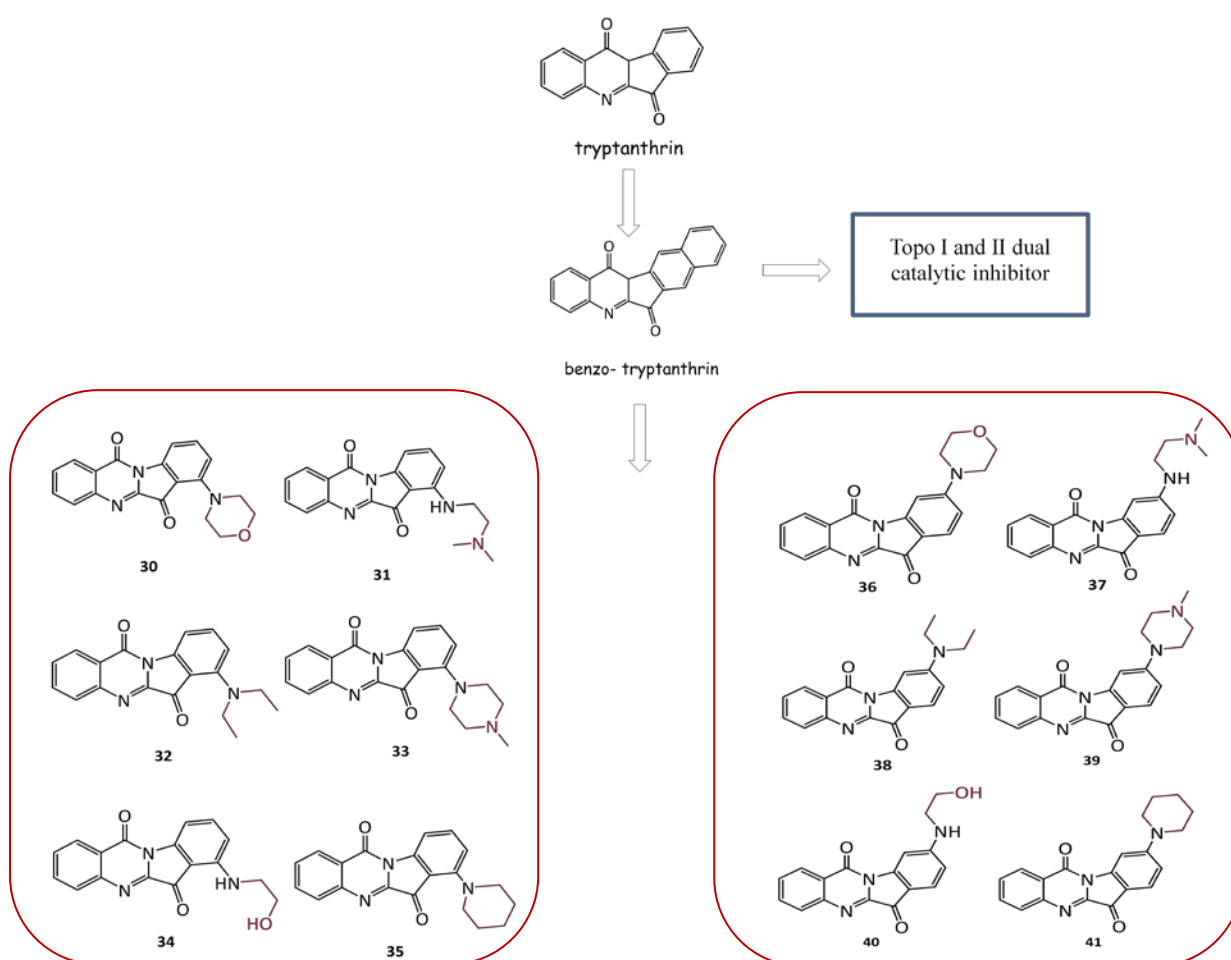


Figure 62: Drugs design leading to compounds **30-41**.

5.5 Methods

5.5.1 Synthesis:

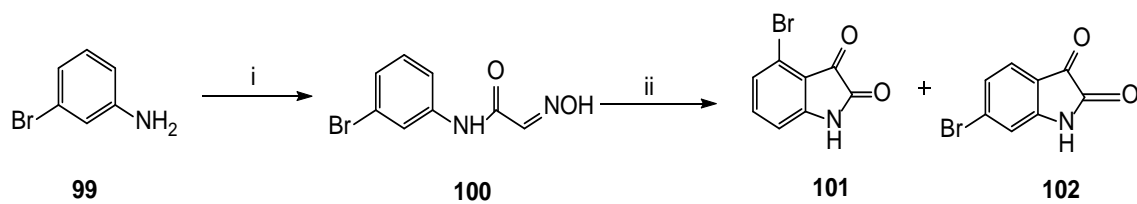
Bromoisatin 101 and 102 were synthesized following the procedure reported in literature (Panagiotis 2004). (Scheme 1) The Bromotryptanthrin **103 and 104** were synthesized by reaction of **101** and **102** with isatoicanhydride in toluene followed by addition of Et₃N and stirring under reflux for 5 hours (Scheme 2 and 3).

The compound **30-41** were obtained by the reaction of the two isomers of Bromoisatine (**101-102**) (Scheme 1) with isatoic anhydride, to provide the tryptanthrine derivatives **103** and **104** (Scheme 2). These bromo derivatives were reacted with different amines (scheme 4 and 5). By dissolving **103** and **104** in DMF then adding the corresponding amine, and leave the reaction stirring under reflux for 3 hours.

5.5.2 Biology:

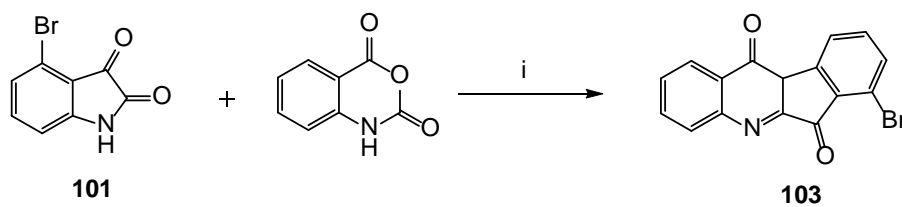
The synthesized compounds are currently under biological evaluation towards topoisomerases I and II.

Scheme 1:



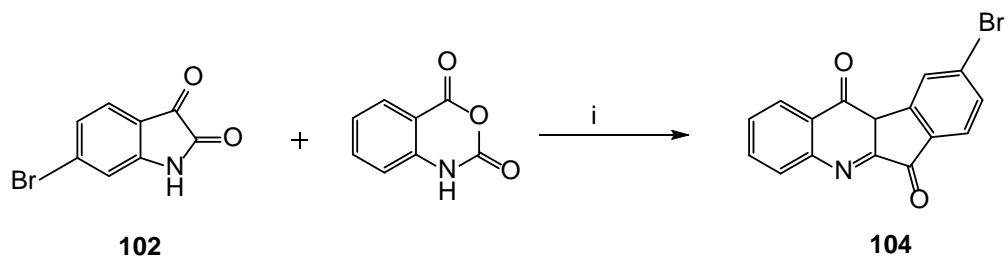
Conditions: (i) chloral hydrate, Na_2SO_4 , $\text{H}_2\text{NOH.HCl}$, H_2O , HCOOH ; (ii) H_2SO_4

Scheme 2:



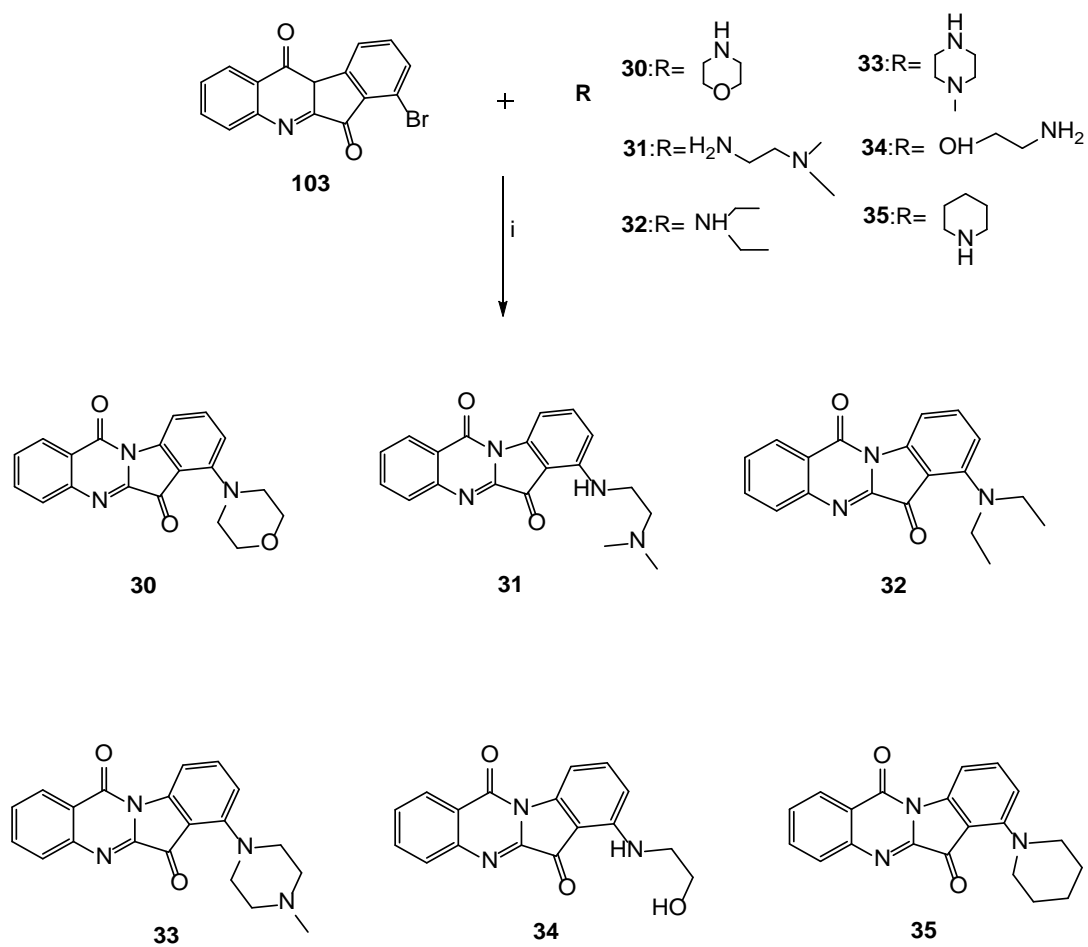
Conditions: (i) Toluene, Et_3N , reflux, 5 h

Scheme 3:



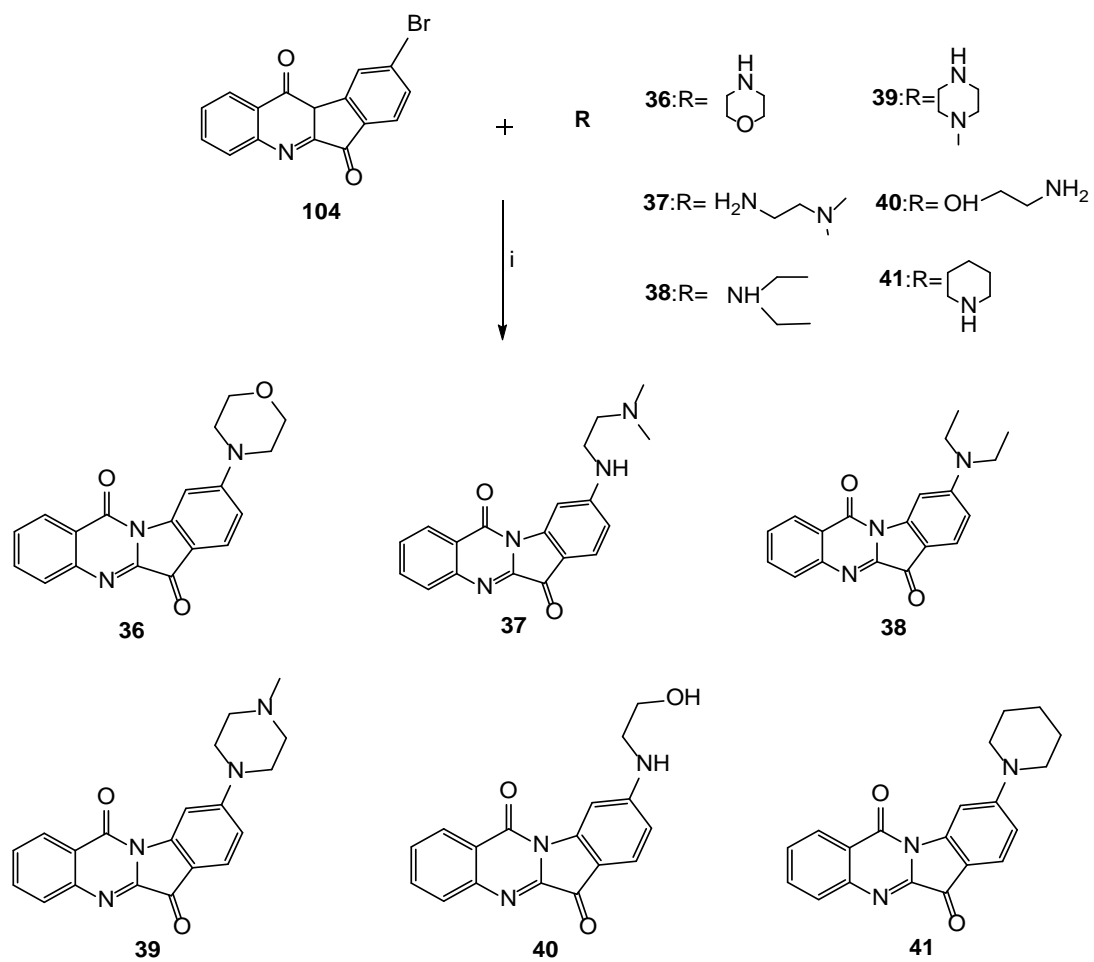
Conditions: (i) Toluene, Et_3N , reflux, 5 h

Scheme 4:



Conditions: (i) DMF, reflux, 3h

Scheme 5:



Conditions: (i) DMF, reflux, 3h

5.6 Conclusion

In this work we designed and synthesised 12 new compounds as potential topoisomerases inhibitors for cancer treatment. The new compounds were achieved by linking several different positively charged chains on tryptanthrin, with the aim of increasing the affinity towards topoisomerases. The synthesized compounds are currently under biological evaluation towards topoisomerases I and II.

5.7 Experimental Section

Chemistry:

Melting points were taken in glass capillary tubes on a Buchi SMP-20 apparatus and are uncorrected. ESI-MS spectra were recorded on Perkin-Elmer 297 and WatersZQ 4000. ¹H NMR and ¹³C NMR were recorded on Varian VRX 200 and 300 instruments. Chemical shift are reported in parts per million (ppm) relative to peak of tetramethylsilane (TMS) and spin multiplicities are given as s (singlet), br s (broad singlet), d (doublet), t (triplet), q (quartet) or m (multiplet) Although IR spectral data are not included (because of the lack of unusual features), they were obtained for all compounds reported, and they were consistent with the assigned structures. Chromatographic separations were performed on silica gel columns by flash (Kieselgel 40, 0.040-0.063 mm, Merck) or gravity (Kieselgel 60, 0.063-0.200 mm, Merck) column chromatography. Reactions were followed by thin layer chromatography (TLC) on Merck (0.25 mm) glass-packed precoated silica gel plates (60 F254), and then visualized in an iodine chamber or with a UV lamp. The term “dried” refers to the use of anhydrous sodium sulfate.

General procedure for the synthesis of (101-102): compounds **101-102** have been synthesized following the procedure reported in literature (Panagiotis 2004).

4-Bromoindoline-2,3-dione (100): Solid orange, ¹H NMR (400 MHz, CDCl₃) δ 11.17 (s, 1 H), 7.46 (dd, 1 H), 7.22 (dd, 1 H), 6.89 (dd, 1 H).

6-Bromoindoline-2,3-dione (101): Red solid, ¹H NMR (400 MHz, CDCl₃) δ 11.10 (s, 1H), 7.47 (d, 1 H), 7.26 (dd, 1 H), 7.08 (d, 1 H).

General procedure for the synthesis of (103-104): A solution of Bromoisatin **101-102** (1 mmol), isatoic anhydride (1 mmol), and Et₃N (5mmol) in toluene (5 mL) was refluxed for 5 hand concentrated under reduced pressure. The crude residue was then purified by flash silica gel column chromatography with DCM/ MeOH, (97:3), as mobile phase.

8-Bromo-6H-indeno[2,1-b]quinoline-6,11(10bH)-dione (103): yellow solid, ¹H NMR (400 MHz, CDCl₃) δ 7.84 (d, 1H), 7.56- 7.49 (m, 2H), 7.32- 7.26 (m, 4H), 4.21 (s, 1H).

9-Bromo-6H-indeno[2,1-b]quinoline-6,11(10bH)-dione (104): Dark yellow solid, ¹H NMR (400 MHz, CDCl₃) δ 7.76 (t, 1H), 7.89- 7.69 (m, 4H), 7.43- 7.32 (m, 2H), 4.27 (s, 1H).

General procedure for the synthesis of (30-35): To a solution of appropriate **103-104** (0.611 mmol) in DMF, the appropriate amine (0.611 mmol) was added, The resulting mixture was stirred at room temperature for 3 hours, then concentrated under reduced pressure The crude residue was then purified by flash silica gel column chromatography using DCM:MeOH,(98:2) as mobile phase.

7-Morpholinoindolo[2,1-b]quinazoline-6,12-dione (30): ^1H NMR (400 MHz,DMSO), δ 8.39 (d, J = 8 Hz, 1H), 7.96 (d, J = 8 Hz, 1H), 7.97(d, J = 8 Hz, 1H), 7.80 (t, J = 8 Hz, 1H), 7.62 (t, J = 8 Hz, 1H), 7.54 (t, J = 8 Hz, 1H), 6.81 (d, J = 8 Hz, 1H), 3.98-3.95 (m, 4H), 3.48-3.42 (m, 4H); ^{13}C NMR (101 MHz, DMSO) δ 178.33, 158.08, 151.53, 147.18 ,146.81, 145.05, 139.08, 134.85, 130.22, 129.46, 127.38, 123.34, 115.28, 110.51, 108.73, 66.69, 51.07. ESI-MS (m/z): 334 [M +H].⁺

7-((2-(Dimethylamino)ethyl)amino)indolo[2,1-b]quinazoline-6,12-dione (31): ^1H NMR (400 MHz, DMSO), δ 8.277 (d, J = 7.6 Hz, 1H), 7.911(d, J = 6 Hz, 1H), 7.69 (t, J = 7.6 Hz, 1H), 7.623 (t, J = 9.6 Hz, 2H), 7.545 (t, J = 6.8 Hz, 1H), 6.769 (d, J = 8.8 Hz, 1H), 3.497-3.467 (m, 2H), 2.611-2.504 (m, 2H), 2.301 (s, 6H); ^{13}C NMR (101 MHz, DMSO) δ 178.4, 152.9, 144.47, 142.8, 140.7, 107.04, 138.57, 129.04, 127.12, 121.76, 120.57, 115.05, 113.39, 104.5, 57.83, 44.49, 44.39, 43.87; ESI-MS (m/z): 335.15 [M +H].⁺

7-(Diethylamino)indolo[2,1-b]quinazoline-6,12-dione (32): ^1H NMR (400 MHz, DMSO), δ 8.337 (d, J =8 Hz, 1H), 7.93 (d, J = 8.4 Hz, 1H),7.732 (t, J = 9.6 Hz, 1H), 7.595 (d, J = 7.6 Hz, 1H), 7.533 (t, J = 8 Hz, 1H), 7.386 (t, J = 8.8 Hz, 1H), 6.512 (d, J = 8.4 Hz, 1H), 3.383- 3.329 (m , 4H), 1.318- 1.237 (m, 6H); ^{13}C NMR (101 MHz, DMSO) δ 181.3, 147.31, 146.97, 146.14 , 145.77, 144.56, 141.73, 132.45, 131.69, 123.12, 123.009, 116.09, 115.31, 113.45, 109.62,45.87, 43.76, 11.6, 10.9, ESI-MS (m/z): 320 [M +H].⁺

7-(4-Methylpiperazin-1-yl) indolo[2,1-b]quinazoline-6,12-dione (33): ^1H NMR (400 MHz, DMSO), δ 8.42 (d, J = 8 Hz, 1H), 8.14 (d, J = 8 Hz, 1H), 7.99 (d, J = 8 Hz, 1H), 7.98 (t, J = 8 Hz, 1H), 7.64-7.60 (m, 2H), 6.81 (d, J = 8 Hz, 1H), 3.66-3.49 (m, 4H), 3.06 (s, 4H), 2.64 (s, 3H); ^{13}C NMR (101 MHz, DMSO) δ 179.87, 153.84, 145.32, 145.19, 141.34, 139.41, 129.87, 127.97, 127.12, 122.35, 121.05, 115.23, 114.36, 108.62, 108.13, 54.89, 53.92, 50.12, 49.75, 44.32, ESI-MS (m/z): 347 [M +H].⁺

7-((2-Hydroxyethyl)amino)indolo[2,1-b]quinazoline-6,12-dione (34): ^1H NMR (400 MHz, DMSO), δ 8.244 (d, J = 7.6 Hz, 1H), 8.88 (d, J= 6.4 Hz, 2H), 7.786 (t, J = 8 Hz, 1H), 7.588 (t, J = 6 Hz, 1H), 7.507 (t, J = 7.6 Hz, 1H), 7.51 (d, J = 7.6 Hz, 1H), 4.981 (t, J = 8 Hz, 1H), 3.648-3.609 (m, 2H), 3.449-3.329 (m, 2H); ^{13}C NMR (101 MHz, DMSO) δ 180.729, 158 .086 ,149.509 ,146.936 ,146.453 ,144.847 ,139.943 ,135.274 ,129.974

,129.644 ,127.218 ,123.282 ,110.850 ,105.579 ,103.878 ,59.853 ,44.826; ESI-MS (m/z): 308 [M +H].⁺

7-(Piperidin-1-yl)indolo[2,1-b]quinazoline-6,12-dione (35): ¹H NMR (400 MHz, DMSO) δ 8.24 (d, 1H), 7.91-7.76 (m, 2H), 7.63- 7.53 (m, 3H), 6.9 (t, 1H), 4.13 (t, 2H), 2.98 (s, 3H), 1.64- 1.53 (m, 2H), 1.12 (t, 3H); ¹³C NMR (101 MHz, DMSO) δ 181.86, 161.47, 152.6, 152, 148.53, 146.7, 136.87, 133.62, 128.12, 127.9, 126.43, 121.33, 119.86, 114.65, 113.96, 59.54, 43.94, 20.86, 12.74; ESI-MS (m/z): 319.14 [M +H]⁺

9-Morpholinoindolo[2,1-b] quinazoline-6,12-dione (36): ¹H NMR (400 MHz, DMSO) δ 8.409 (d, J = 8.4 Hz, 1H), 8.03 (d, J = 8 Hz, 1H), 7.89-7.82 (m, 2H), 7.69 (t, J = 8.4 Hz, 1H), 7.73 (d, J = 8 Hz, 1H), 3.94-3.88 (m, 4 H), 3.59- 3.50 (m , 4H); ¹³C NMR (101 MHz, DMSO) δ 179.45, 154.56, 148.84, 145.36, 142.93, 140.15, 133.88, 127.53, 126,44, 122,63, 121.63, 120.73, 115.93, 102.42, 103.14, 63.88, 62.74, 51.20, 50.96; ESI-MS (m/z): 334 [M +H].⁺

9-((2-(Dimethylamino)ethyl)amino)indolo[2,1-b]quinazoline-6,12-dione (37): ¹H NMR (400 MHz, DMSO) δ 8.32 (t, 1H), 7.96- 7.65 (m, 2H), 7.65 (d, 1H), 7.43 (s, 1H), 6.85 (s, 1H), 6.74 (d, 1H), 6.12 (s, 1H), 3.61 (t, 2H), 2.78 (t, 2H), 2.31 (s, 6H); ¹³C NMR (101 MHz, DMSO) δ 187.5, 162.55, 155.86, 152.09, 148.75, 146.7, 135.8, 133.65, 128.98, 128.21, 120, 108.76, 106.87, 105.98, 62.9, 48.12, 47.97, 47.64; ESI-MS (m/z): 334.38 [M +H].⁺

9-(Diethylamino)indolo[2,1-b]quinazoline-6,12-dione (38): ¹H NMR (400 MHz, DMSO) δ 8.309 (d, J = 7.6 Hz, 1H), 7.937 (d, J = 7.6 Hz, 1H), 7.734 (t, J = 8 Hz, 1H), 7.66 (t, J = 9.2 Hz, 2H),7.53 (t, J = 7.2 Hz, 1H), 6.485 (d, J = 11.2 Hz, 1H), 3.526-3.472 (m, 4H), 1.270-1.222 (m , 6H); ¹³C NMR (101 MHz, DMSO) δ: 181.65, 155.46, 151.32, 145.42, 1441.68, 143.21, 129.72, 127.31, 122.08, 124.32, 121.03, 115.90, 103.37, 101.46, 102.66, 44.37, 43.96, 12.98, 12.01; ESI-MS (m/z): 320 [M +H].⁺

9-(4-Methylpiperazin-1-yl)indolo[2,1-b]quinazoline-6,12-dione (39): Red solid, ¹H NMR (400 MHz, DMSO) δ 8.39 (d, J = 7.6 Hz, 1H), 8.051 (t, J = 8.4 Hz, 1H), 7.84 (d, J = 7.6 Hz, 1H), 7.744 (d, J = 8.8 Hz, 1H), 7.651 (t, J = 14.8 Hz, 1H), 7.00 (t, J = 8 Hz,1H), 6.702 (d, J = 8.4 Hz, 1H), 3.641- 3.541 (m, 4H), 2.60- 2.55 (m, 4H), 2.38 (s, 3H); ¹³C NMR (101 MHz, DMSO) δ: 179.85, 155.32, 151.43, 147.79, 142.13, 141.35, 129.89, 127.45, 122.97, 122.76, 121.28, 115.50, 103.65, 102.66, 102.17, 52.11, 51.90, 47.44, 46.53, 42.59; ESI-MS (m/z): 347 [M +H].⁺

9-((2-Hydroxyethyl)amino)indolo[2,1-b]quinazoline-6,12-dione (40): Red solid; ¹H NMR (400 MHz, CDCl₃) δ 10.01 (s, 1H), 8.23 (d, 1H), 7.75-7.87 (d, 2H), 7.71 (d, 1H),

7.43 (t, 1H), 6.87 (s, 1H), 5.73 (t, 1H), 4.8 (s, 1H), 3.51- 3.65 (m, 4H); ¹³C NMR (101 MHz, CDCl₃) δ: 188.01, 161.86, 153.97, 150.76, 146.96, 145.92, 133.52, 129.94, 127, 126.86, 126.21, 121, 109.87, 107,12, 105.67, 62.03, 43.90; ESI-MS (m/z): 307.31 [M +H].⁺

9-(Piperidin-1-yl)indolo[2,1-b]quinazoline-6,12-dione (41): Red solid (71%);¹H NMR (400 MHz, CDCl₃) δ 8.34 (d, J = 7.8 Hz, 1H), 7.99 (d, J = 7.8 Hz, 2H), 7.79 (d, J = 7.4 Hz, 1H), 7.67 (d, J = 8.7 Hz, 1H), 7.59 (t, J = 7.4 Hz, 1H), 6.62 (d, J = 8.6 Hz, 1H), 3.57 (s, 4H), 1.71 (s, 6H); ¹³C NMR (101 MHz, CDCl₃) δ 177.7; 158.6, 156.8, 149.1, 146.9, 134.8, 130.1, 129.2, 127.7, 127.1, 123.3, 110.8, 110.2, 100.5, 48.6, 25.5, 24.2; ESI-MS (m/z): 331.1321[M +H].⁺

Biography

- Abel, T & Zukin, RS. (2008). Epigenetic targets of HDAC inhibition in neurodegenerative and psychiatric disorders. *Current Opinion in Pharmacology*, 5, 57-64.
- Adlard, P.A., Cherny, R.A., Finkelstein, D.I., Gautier, E., Robb, E., Cortes, M., Volitakis, I., Bush, A.I., 2008, "Rapid Restoration of Cognition in Alzheimer's Transgenic Mice with 8-Hydroxy Quinoline Analogs Is Associated with Decreased Interstitial A β ", *Neuron*, vol. 59, no. 1, pp. 43.
- Adem A, 1993. 'The next generation of cholinesterase inhibitors.' *Acta Neurol Scand Suppl.*, 149: 10-12.
- Adem A, Jossan SS, Oreland L. 1989. 'Tetrahydroaminoacridine inhibits human and rat brain monoamine oxidase.', *Neurosci Lett.*, 107: 313-17.
- Adnan Ali , Klaus P. Hoeflich , and James R. Woodgett , Glycogen Synthase Kinase-3: Properties, Functions, and Regulation *Chem. Rev.*, 2001, 101 (8), pp 2527–2540.
- Adolphs KW, Cheng SM, Paulson JR, Laemmli UK, Isolation of a protein scaffold from mitotic HeLa cell chromosomes. *Proc. Natl. Acad. Sci. USA*, (1977), 74, 4937-4941.
- Aghdam, S.Y., and Barger, S.W. (2007). Glycogen synthase kinase-3 in neurodegeneration and neuroprotection: lessons from lithium. *Curr Alzheimer Res* 4, 21-31.
- Akk G, Steinbach JH (2005) Galantamine activates muscle- type nicotinic acetylcholine receptors without binding to the acetylcholine- binding site. *J Neurosci* 25: 1992- 2001.
- Alper, G.; Girgin, F. K.; Ozgonul, M.; Menten, G.; Ersoz, B. *Eur. Neuropsychopharmacol.* 1999, 9, 247–252.
- Alessi D.R., Caudwell F.B., Andjelkovic M., Hemmings B.A., Cohen P. (1996). Molecular basis for the substrate specificity of protein kinase B; comparison with MAPKAP kinase-1 and p70 S6 kinase. *FEBS Lett.*, 399, 333–338.
- Alvarez, A.; Bronfman, F.; Pérez, C.A.; Vicente, M.; Garrido, J.; Inestrosa, N.C. *Neurosci. Lett.* 1995, 201, 49-52.
- Alzheimer, A. 1907, "Über eine eigenartige Erkrankung der Hirnrinde", *Allgem Z Psychiatr-Gerich Med*, vol. 64, pp. 146-148 Lage, J.M.M. 2006, "100 Years of Alzheimer's disease (1906-2006)", *JAlzheimers Dis*, vol. 9, no. 3, pp. 15.
- Altman, R., & Rutledge, J.,C. 2010, "The vascular contribution to Alzheimer's disease", *Clin Sci (Lond)*, vol. 119, no. 10, pp. 407.
- Aliev G, Li Y, Palacios HH, and Obrenovich ME. 2011. Oxidative stress induced mitochondrial DNA deletion as a hallmark for the drug development in the context of the cerebrovascular diseases. *Recent Pat Cardiovasc. Drug Discov.* 6 (3): 222-241.
- Ali A, Hoeflich KP, Woodgett JR. Glycogen synthase kinase-3: properties, unctions, and regulation. *Chem Rev.* 2001;101:2527-40.
- Alabed, Y.Z., Pool, M., OngTone, S., Sutherland, C., and Fournier, A.E. (2011). GSK3 β regulates myelin-dependent axon outgrowth inhibition through CRMP4. *J. Neurosci.* 30, 5635–5643.

- Allis CD, Jenuwein T, Reinberg D, Caparros M-L (2007) Epigenetics. New York: Cold Spring Harbor Laboratory Press.
- Amit, S., Hatzubai, A., Birman, Y., Andersen, J.S., Ben-Shushan, E., Mann, M., Ben-Neriah, Y., and Alkalay, I. (2002). Axin-mediated CKI phosphorylation of beta-catenin at Ser 45: a molecular switch for the Wnt pathway. *Genes Dev* 16, 1066-1076.
- Andreas Lerchner, Rainer Machauer, Claudia Betschart, Siem Veenstra, Heinrich Rueeger, Clive McCarthy, Marina Tintelnot-Blomley, Anne-Lise Jatou, Sabine Rabe, Sandrine Desrayaud, Albert Enz, Matthias Staufenbiel, Paolo Paganetti, Jean-Michel Rondeau, Ulf Neumann. Macrocyclic BACE-1 inhibitors acutely reduce A β in brain after po application. *Bioorganic & Medicinal Chemistry Letters* Volume 20, Issue 2, 15 January 2010, Pages 603–607.
- Andres, A., Brown, W.M. & Kosik, K.S. 1992, "Structure and novel exons of the human tau gene", *Biochemistry*, vol. 31, no. 43, pp. 10626.
- Andrea Milelli et al, Structure activity relationships of novel substituted naphthalene diimides as anticancer agents, *European Journal of Medicinal Chemistry* 57 (2012) 417-428.
- Aplin, A.E., Gibb, G.M., Jacobsen, J.S., Gallo, J.M., and Anderton, B.H. (1996). In vitro phosphorylation of the cytoplasmic domain of the amyloid precursor protein by glycogen synthase kinase-3beta. *J Neurochem* 67, 699-707.
- Austin CA, Patel S, Ono K, Nakane H, Fisher LM. Site-specific DNA cleavage by mammalian DNA topoisomerase II induced by novel flavone and catechin derivatives. *Biochem. J.* (1992), 282, 883-889.
- Azoulay-Alfaguter, I., Yaffe, Y., Licht-Murava, A., Urbanska, M., Jaworski, J., Pietrokovski, S., Hirschberg, K., and Eldar-Finkelman, H. (2011). Distinct molecular regulation of glycogen synthase kinase-3alpha isozyme controlled by its N-terminal region: functional role in calcium/calpain signaling. *J Biol Chem* 286, 13470-13480.
- Asojo OA, Asojo OA, Ngamelue MN, Homma K, and Lockridge O (2011) Cocrystallization studies of full-length recombinant butyrylcholinesterase (BChE) with cocaine. *Acta Crystallographica Section F: Structural Biology and Crystallization Communications* 67:434-437.
- Baas P.W., Qiang L. (2005). Neuronal microtubules: when the MAP is the roadblock. *Trends Cell Biol.*, 15, 183–187.
- Baki, A. Bielik, L. Molnár, G. Szendrei, G.M. Keserü, A high throughput luminescent assay for glycogen synthase kinase-3beta inhibitors, *Assay Drug Dev. Technol.* 5 (2007) 75-83.
- Baum, L., Hansen, L., Masliah, E., and Saitoh, T. (1996). Glycogen synthase kinase 3 alteration in Alzheimer disease is related to neurofibrillary tangle formation. *Mol Chem Neuropathol* 29, 253- 261.
- Bachovchin DA and Cravatt BF (2012) The pharmacological landscape and therapeutic potential of serine hydrolases. *Nature Reviews Drug Discovery* 11:52-68.
- Bayer TA, Jäkälä P, Hartmann T, Havas L, McLean C, Culvenor JG, Li QX, Masters CL, Falkai P, Beyreuther K., 1999. 'Alpha-synuclein accumulates in Lewy bodies in Parkinson's disease and dementia with Lewy bodies but not in Alzheimer's disease beta-amyloid plaque cores.', *Neurosci Lett.*, 266: 213-16.
- Bandekar, P. P.; Roopnarine, K. A.; Parekh, V. J.; Mitchell, T. R.; Novak, M. J.; Sinden, R. R. *J. Med. Chem.* 2010, 53, 3558.

- Bartus RT, Dean RL, Beer B, Lippa AS. 1982. 'The cholinergic hypothesis of geriatric memory dysfunction.', *Science*: 408-14.
- Bartus RT. 2000. 'On neurodegenerative diseases, models, and treatment strategies: lessons learned and lessons forgotten a generation following the cholinergic hypothesis, *Exp Neurol.*: 495-529.
- Bax, B., Carter, P.S., Lewis, C., Guy, A.R., Bridges, A., Tanner, R., Pettman, G., Mannix, C., Culbert, A.A., Brown, M.J., et al. (2001). The structure of phosphorylated GSK-3beta complexed with a peptide, FRATtide, that inhibits beta-catenin phosphorylation. *Structure* 9, 1143-1152.
- Bardai, FH & D'Mello, SR. (2011). Selective toxicity by HDAC3 in neurons: regulation by Akt and GSK3beta. *J Neurosci*, 31, 1746-1751.
- Ballatore, C.; Brunden, K. R.; Piscitelli, F.; James, M. J.; Crowe, A. Yao, Y.; Hyde, E.; Trojanowski, J. Q.; Lee, V. M.-Y.; Smith, A. B., III Discovery of brain-penetrant, orally bioavailable aminothienopyridazine inhibitors of Tau aggregation. *J. Med. Chem.* 2010, 53, 3739–3747.
- Beurel, E., and Jope, R.S. (2008). Differential regulation of STAT family members by glycogen synthase kinase-3. *J Biol Chem* 283, 21934-21944.
- Beurel, E., and Jope, R.S. (2008). Differential regulation of STAT family members by glycogen synthase kinase-3. *J Biol Chem* 283, 21934-21944.
- Berger J.M. (1998) Structure of DNA topoisomerases. *Biochim. Biophys. Acta.*1400: 3-18.
- Bhattacharjee, A. K.; Hartell, M. G.; Nichols, D. A.; Hicks, R. P.; Stanton, B.; Van Hamont, J. E.; Milhous, W. K. *Eur. J. Med. Chem.* 2004, 39, 59.
- Bhattacharjee, A. K.; Skanchy, D. J.; Jennings, B.; Hudson, T. H.; Brendle, J. J.; Werbovetz, K. A. *Bioorg. Med. Chem.* 2002, 10, 1979.
- Bhat,R.,Xue,Y.,Berg,S., Hellberg, S., Ormo, M., Nilsson,Y., Radesater, A.C., Jerning, E., Markgren,P.O.,Borgegard,T., Nylöf, M., Giménez- Cassina, A., Hernández, F.,Lucas, J.J.,Díaz-Nido, J., and Avila,J.(2003).Structural insights and biological effects of glycogen synthase kinase3-specific inhibitor AR-A014418. *J. Biol.Chem.* 278, 45937–45945.
- Billard, W.; Binch, H.; Bratzler, K.; Chen, L.Y.; Crosby, G.; Duffy, R.A.; Dugar, S; Lachowicz, J.; McQuade, R.;Pushpavaman, P., Ruperto, V.B.; Taylor, L.A.; Clader, J.W. *Bioorg. Med. Chem. Lett.* 2000, 10, 2209-2211.
- Bijur, G.N., and Jope, R.S. (2003). Glycogen synthase kinase-3 beta is highly activated in nuclei and mitochondria. *Neuroreport* 14, 2415-2419.
- Bijur, G.N., and Jope, R.S. (2001). Proapoptotic stimuli induce nuclear accumulation of glycogen synthase kinase-3 beta. *J Biol Chem* 276, 37436-37442.
- Bidon-Chanal A, Fuertes A, Alonso D, Perez DI, Martinez A, Luque FJ, et al. Evidence for a new binding mode to GSK-3: allosteric regulation by the marine compound palinurin. *Eur J Med Chem.* 2013; 60: 479-89.
- Blennow, K., DeLeon, M. J. & Zetterberg, H. (2006) Alzheimer's disease. *Lancet*, 368, 387-403.
- Blessed, G., Tomlinson, B.E. & Roth, M. 1968, "The association between quantitative measures of dementia and of senile changes in the cerebral matter of elderly subjects", *Brit J Psychiat*, vol. 114, pp. 797-811.
- Blennow K, de Leon MJ, Zetterberg H., 2006. 'Alzheimer's Disease', *Lancet*, 368: 387-403.

- Brunden KR, Trojanowski JQ, and Lee VM. 2009. Advances in tau-focused drug discovery for Alzheimer's disease and related tauopathies. *Nat. Rev. Drug Discov.* 8 (10): 783-793.
- Blalock EM, Chen KC, Sharrow K, Herman JP, Porter NM, Foster TC, Landfield PW (2003) Gene microarrays in hippocampal aging: statistical profiling identifies novel processes correlated with cognitive impairment. *J Neurosci* 23:3807-3819.
- Blaney SM, Takimoto C, Murry DJ, Kuttesch N, McCully C, Cole DE, Godwin K, Balis FM (1998) Plasma and cerebrospinal fluid pharmacokinetics of 9-aminocamptothecin (9-AC), irinotecan (CPT-11), and SN-38 in nonhuman primates. *Cancer Chemother Pharmacol* 41(6): 464–468
- Bonda DJ, Wang X, Perry G, Smith MA, Zhu X,. 2010. 'Mitochondrial dynamics in Alzheimer disease: opportunities for future treatment strategies, *Drugs and Aging*, 27: 1-12.
- Bowen, D.M.; Benton, J.S.; Spillane, J.A. *J. Neurol. Sci.* 1982, 57, 191-202.
- Bolger, TA & Yao, TP. (2005). Intracellular Trafficking of Histone Deacetylase 4 Regulates Neuronal Cell Death. *J Neurosci*, 25, 9544-9553.
- Bolognesi, M.L.; Cavalli, A.; Melchiorre, C. *Neurotherapeutics* 2009, 6, 152-162.
- Braña, M.F.; Domínguez, G.; Sáez, B.; Romerdahl, C.; Robinson, S.; Barlozzari, T. *Eur. J. Med. Chem.* 2002, 37, 541-551.
- Brown KL, Cosseau C, Gardy JL, Hancock RE. 'Complexities of targeting innate immunity to treat infection. ', *Trends Immunol*, 28: 260-66.
- Buller, C.L., Loberg, R.D., Fan, M.H., Zhu, Q., Park, J.L., Vesely, E., Inoki, K., Guan, K.L., and Brosius, F.C., 3rd (2008). A GSK-3/TSC2/mTOR pathway regulates glucose uptake and GLUT1 glucose transporter expression. *Am J Physiol Cell Physiol* 295, C836-843.
- Casadesus, G., Smith, M.,A., Basu, S., Hua, J., Capobianco, D.,E., Siedlak, S.,L., Zhu, X., & Perry, G., 2007, "Increased isoprostane and prostaglandin are prominent in neurons in Alzheimer disease", *Mol Neurodegener*, vol. 2, pp. 2.
- Cavalli, A.; Bolognesi, M.L.; Minarini, A.; Rosini, M.; Tumiatto, V.; Recanatini, M.; Melchiorre, C. *J. Med. Chem* 2008, 51, 347-372.
- Cavalli, A.; Bolognesi, M.L.; Capsoni, S.; Andrisano, V.; Bartolini, M.; Margotti, E.; Cattaneo, A.; Recanatini, M.; Melchiorre, C. *Angew. Chem. Int. Ed.* 2007, 46, 3689-3692.
- Carolan CG, Dillon GP, Khan D, Ryder SA, Gaynor JM, Reidy S, Marquez JF, Jones M, Holland V, and Gilmer JF (2010) Isosorbide-2-benzyl carbamate-5-salicylate, a peripheral anionic site binding subnanomolar selective butyrylcholinesterase inhibitor. *Journal of Medicinal Chemistry* 53:1190-1199.
- Carmichael, J. et al. (2002) GSK-3b inhibitors prevent cellular polyglutamine toxicity caused by the Huntington's disease mutation. *J. Biol. Chem.* 277, 33791–33798.
- Cagnin A., Brooks D. J., Kennedy A. M., Gunn R. N., Myers R., Turkheimer F. E., Jones T., Banati R. B. (2001). In-vivo measurement of activated microglia in dementia. *Lancet* 358, 461.
- Camps, P.; El Achab, R.; Font-Bardia, M.; Görbig, D.; Morral, J.; Muñoz-Torrero, D.; Solans, X.; Simon, M. Easy synthesis of 7-alkylbicyclo[3.3.1]non-6-en-3-ones by silica gel-promoted fragmentation of 3-alkyl-2-oxadamant-1-yl mesylates. *Tetrahedron* **1996**, 52, 5867–5880).

- Camps, P.; Formosa, X.; Galdeano, C.; Gómez, T.; Muñoz-Torrero, D.; Scarpellini, M.; Viayna, E.; Badia A.; Clos, M.V.; Camins, A.; Pallàs, M.; Bartolini, M.; Mancini, F.; Andrisano, V.; Estelrich, J.; Lizondo, M.; Bidon-Chanal, A.; Luque, F.J.J. *Med. Chem.* 2008, 51, 3558.
- Chuang, DM, Leng, Y, Marinova, Z, Kim, HJ & Chiu, CT. (2009). Multiple roles of HDAC inhibition in neurodegenerative conditions. *Trends Neurosci*, 32, 591-601.
- Christensen M.a., Barthelmes H.U., Feineis S., Knudsen B.R, Andersen A H., Boege F. and Meilke C. (2002) Changes in mobility account for camptothecin-induced subnuclear relocation of topoisomerase I. *J. Bioi. Chem.* 277: 15661-15665.
- Cheng, A., Hou, Y., & Mattson, M.,P. 2010, "Mitochondria and neuroplasticity", *ASN Neuro*, vol. 2, no. 5. Gibson, G.E., Sheu, K.F. & Blass, J.P. 1998, "Abnormalities of mitochondrial enzymes in Alzheimer disease", *J Neural Transm*, vol. 105, no. 8-9, pp. 855.
- Champoux, J. J. (2001). "DNA topoisomerases: structure, function, and mechanism." *Annu. Rev. Biochem.*70: 369-413.
- Chuang, DM, Leng, Y, Marinova, Z, Kim, HJ & Chiu, CT. (2009). Multiple roles of HDAC inhibition in neurodegenerative conditions. *Trends Neurosci*, 32, 591-601.
- Chen Y, Sun J, Fang L, Liu M, Peng S, Liao H, Lehmann J, and Zhang Y (2012) Tacrine–Ferulic Acid–Nitric Oxide (NO) Donor Trihybrids as Potent, Multifunctional Acetyl- and Butyrylcholinesterase Inhibitors. *Journal of Medicinal Chemistry* 55:4309-4321.
- Citron, M. *Nature Rev. Neurosci.* 2004, 5, 677-685.
- Classen, S., Olland, S., and Berger, J.M. (2003). Structure of the topoisomerase II ATPase region and its mechanism of inhibition by the chemotherapeutic agent ICRF-187. *Proc Natl Acad Sci USA* 100, 10629–10634.
- Coulson EJ, Paliga K, Beyreuther K, Masters CL,. 2000. 'What the evolution of the amyloid protein precursor supergene family tells us about its function.', *Neurochem.*, 36: 175-84.
- Czerwinska I, Sato S, Juskowiak B, Takenaka S. Interactions of cyclic and non-cyclic naphthalene diimide derivatives with different nucleic acids. *Bioorg Med Chem.* 2014 May 1;22(9):2593-601
- Conde,S.,Perez,D.I.,Martinez, A., Perez, C., and Moreno, F.J. (2003). Thienyl and phenyl alpha-halomethylketones: new inhibitors of glycogen synthase kinase (GSK- 3beta) from a library of compound searching. *J. Med.Chem.* 46, 4631–4633.
- Covey, J. M., C. Jaxel, et al. (1989). "Protein-linked DNA strand breaks induced in mammalian cells by camptothecin, an inhibitor of topoisomerase I." *Cancer Res* 49(18): 5016–22.
- Conde S., Perez D.I., Martinez A., Perez C., Moreno F.J. (2003). Thienyl and phenyl - halomethylketones: New inhibitors of GSK-3β from a library of compound searching. *J. Med. Chem.*, 46, 4631–4633.
- Contestabile, A., 2010, "The history of the cholinergic hypothesis", *Behav Brain Res.*
- Crouch, P.J. 2007, "Mitochondria in aging and Alzheimer's disease" ,*Rejuvenation Res*, vol. 10, no. 3, pp. 349-57.
- Curtain, C.C., Ali, F., Volitakis, I., Cherny, R.A., Norton, R.S., Beyreuther, K., Barrow, C.J., Masters, C.L., Bush, A.I. & Barnham, K.J. 2001, "Alzheimer's disease amyloid-beta binds copper and zinc to

generate an allosterically ordered membrane-penetrating structure containing superoxide dismutase-like subunits", *J Biol Chem*, vol. 276, no. 23, pp. 20466.

- Darvesh S, Grantham DL, and Hopkins DA (1998) Distribution of butyrylcholinesterase in the human amygdala and hippocampal formation. *The Journal of Comparative Neurology* 393:374-390.
- Darvesh S, Hopkins D, and Geula C (2003) Neurobiology of butyrylcholinesterase. *Nature Reviews Neuroscience* 4:131-138.
- Darvesh S, McDonald R, Darvesh K, Mataija D, Conrad S, Gomez G, Walsh R, and Martin E (2007) Selective reversible inhibition of human butyrylcholinesterase by aryl amide derivatives of phenothiazine. *Bioorganic & Medicinal Chemistry* 15:6367-6378.
- Dajas- Bailador FA, Heimala K, Wonnacott S 'The allosteric potentiation of nicotinic acetylcholine receptors by galantamine is transduced into cellular responses in neurons: Ca²⁺ signals and neurotransmitter release.', *Mol Pharmacol.*,1217-26.
- Dajani, R., Fraser, E., Roe, S.M., Young, N., Good, V., Dale, T.C., and Pearl, L.H. (2001). Crystal structure of glycogen synthase kinase 3 beta: structural basis for phosphate-primed substrate specificity and autoinhibition. *Cell* 105, 721-732.
- Dann CE, Hsieh JC, Rattner A, Sharma D, Nathans J, Leahy DJ. Insights into Wnt binding and signalling from the structures of two Frizzled cysteine-rich domains. *Nature*. 2001;412:86-90.
- Delcuve GP, Khan DH, Davie JR (2012) Roles of histone deacetylases in epigenetic regulation: emerging paradigms from studies with inhibitors. *Clin Epigenetics* 4:5.
- De Ruijter, AJM, van Gennip, AH, Caron, HN, Kemp, S & Van Kuilenburg, ABP. (2003). Histone deacetylases (HDACs): characterization of the classical HDAC family. *Biochemical Journal*, 370, 737-749.
- De Ferrari, G.V.; Canales, M.A.; Shin, I.; Weiner, L.M.; Silman, I.; Inestrosa, N.C. *Biochemistry*. 2001, 40, 10447-10457.
- De Strooper, B. (2003). Aph-1, Pen-2, and Nicastrin with Presenilin generate an active gamma-Secretase complex. *Neuron* 38, 9-12.
- Dehmelt L., Halpain S. (2004). Actin and microtubules in neurite initiation: are MAPs the missing link? *J. Neurobiol.*, 58, 18–33.
- De Ruijter AJ, van Gennip AH, Caron HN, Kemp S, van Kuilenburg AB (2003) Histone deacetylases (HDACs): characterization of the classical HDAC family. *Biochem J* 370:737-749.
- DeWys WD, Humphreys SR, Goldin A (1968) Studies on the therapeutic effectiveness of drugs with tumor weight and survival time indices of Walker 256 carcinosarcoma. *Cancer Chemo Rep* 52:229–242.
- Decker M, Kraus B, and Heilmann J (2008) Design, synthesis and pharmacological evaluation of hybrid molecules out of quinazolinimines and lipoic acid lead to highly potent and selective butyrylcholinesterase inhibitors with antioxidant properties. *Bioorganic & Medicinal Chemistry* 16:4252-4261.
- Di, L.; Kerns, E. H.; Fan, K.; McConnell, O. J.; CarTer, G. T. High throughput artificial membrane permeability assay for blood-brain barrier. *Eur. J. Med.Chem.* 2003, 38, 223-232.
- Dominguez, D.I.; De Strooper, B. *Trends Pharmacol. Sci.* 2002, 23, 324-330.
- Doble, B.W., and Woodgett, J.R. (2003). GSK-3: tricks of the trade for a multi-tasking kinase. *J Cell Sci* 116, 1175-1186.

- Duyckaerts, C., Delatour, B. & Potier, M. 2009, "Classification and basic pathology of Alzheimer disease", *Acta Neuropathol*, vol. 118, no. 1, pp. 5-36.
- Dryden S., Nahhas F., Nowak J., Goustin A., Tainsky M. (2003). Role for human SIRT2 NAD-dependent deacetylase activity in control of mitotic exit in the cell cycle. *Mol. Cell. Biol.* 23, 3173–3185. 10.1128/MCB.23.9.3173-3185.2003.
- Eastman Q, Grosschedl R. Regulation of LEF-1/TCF transcription factors by Wnt and other signals. *Curr Opin Cell Biol.* 1999;11:233-40.
- E. Costa, E. Dong, D.R. Grayson, W.B. Ruzicka, M.V. Simonini, M. Veldic, A. Guidotti Epigenetic Targets in GABAergic Neurons to Treat Schizophrenia *Advances in Pharmacology*, Vol 54, 2006, Pages 95–117.
- Ehrlich, M, Gama-Sosa, MA, Huang, LH, Midgett, RM, Kuo, KC, McCune, RA & Gehrke, C. (1982). Amount and distribution of 5-methylcytosine in human DNA from different types of tissues of cells. *Nucleic Acids Res*, 10, 2709-2721.
- Eglen, R.M., and Reisine, T. (2009). The current status of drug discovery against the human kinome. *Assay Drug Dev. Technol.* 7, 22–43.
- Elisabet Viayna, Irene Sola, Manuela Bartolini, Angela De Simone, Cheril Tapia-Rojas, Felipe G. Serrano, Raimon Sabaté, Jordi Juárez -Jiménez, Belén Pérez, F. Javier Luque, Vincenza Andrisano, M. Victòria Clos, Nibaldo C. Inestrosa, and Diego Muñoz -Torrero. Synthesis and Multitarget Biological Profiling of a Novel Family of Rhein Derivatives As Disease-Modifying Anti-Alzheimer Agents. *J. Med. Chem.* 2014, 57, 2549–2567.
- Embi, N., Rylatt, D.B., and Cohen, P. (1980). Glycogen synthase kinase-3 from rabbit skeletal muscle. Separation from cyclic-AMP-dependent protein kinase and phosphorylase kinase. *Eur J Biochem* 107, 519-527.
- Ferri, C. P., et al, (2005) Global prevalence of dementia: a Delphi consensus study. *Lancet*, 366, 2112-7.
- Feinberg, AP. (2007). Phenotypic plasticity and the epigenetics of human disease. *Nature*, 447, 433-440.
- F. H. Bardai and S. R. d’Mello, “Selective toxicity by HDAC3 in neurons: regulation by Akt and GSK3 β ,” *Journal of Neuroscience*, vol. 31, no. 5, pp. 1746–1751, 2011.
- Fischer A, Sananbenesi F, Wang X, Dobbin M, Tsai LH (2007) Recovery of learning and memory is associated with chromatin remodelling. *Nature* 447:178-182.
- Finch & Morgan, T.E. 2007, "Systemic inflammation, infection, ApoE alleles, and Alzheimer disease: a position paper", *Curr Alzheimer Res*, vol. 4, no. 2, pp. 185-9.
- Fleming M, Melzig MF. Serine-proteases as plasminogen activators in terms of fibrinolysis. *J. Pharm. Pharmacol.* 2012;64(8):1025-39.
- Fleischmann G., Pflugfelder G., Steiner E.K., Javaherian K., Howard G.C., Wang J.C. and Elgin S.C.R. (1984) *Drosophila* DNA topoisomerase I is associated with transcriptionally active regions of the genome. *Proc. Natl. Acad. Sci. USA.* 81: 6958-6962.
- Fontan-Lozano A, Romero-Granados R, Troncoso J, Munera A, Delgado-Garcia JM, Carrion AM (2008) Histone deacetylase inhibitors improve learning consolidation in young and in KA-induced neurodegeneration and SAMP-8-mutant mice. *Mol Cell Neurosci* 39:193-201.

- Fortune JM, Osheroff N. Topoisomerase II as a target for anticancer drugs: when enzymes stop being nice. *Prog. Nucleic Acid Res. Mol. Biol.*, (2000), 64, 221-253.
- Folkesson A, Honoré PH, Andersen LM, Kristensen P, and Bjerrum OJ (2010) Low dose of donepezil improves gabapentin analgesia in the rat spared nerve injury model of neuropathic pain: single and multiple dosing studies. *Journal of Neural Transmission* 117:1377-1385.
- Forman MS, Trojanowski JQ, Lee VM., 2004. 'Neurodegenerative diseases: a decade of discoveries paves the way for therapeutic breakthroughs.', *Nat Med.*, 10: 1055-63.
- Formosa X. PhD thesis. Unitat de Química Farmacèutica, Departament de Farmacologia i Química Terapèutica. Universitat de Barcelona, 2006.
- Froelich-Ammon SJ, Osheroff N. Topoisomerase poisons: harnessing the dark side of enzyme mechanisms. *J. Biol. Chem.*, (1995), 270, 21429-21432.
- Franca-Koh, J., Yeo, M., Fraser, E., Young, N., and Dale, T.C. (2002). The regulation of glycogen synthase kinase-3 nuclear export by Frat/GBP. *J Biol Chem* 277, 43844-43848.
- Francis PT, Ramírez MJ, and Lai MK (2010) Neurochemical basis for symptomatic treatment of Alzheimer's disease. *Neuropharmacology* 59:221-229.
- Francis P, Palmer A, Snape M, and Wilcock G (1999) The cholinergic hypothesis of Alzheimer's disease: a review of progress. *The Journal of Neurology, Neurosurgery & Psychiatry* 66:137-147.
- Frame S., Cohen P. (2001). GSK3 takes centre stage more than 20 years after its discovery. *Biochem. J.*, 359, 1–16.
- Funke, A.; Paulsen, A.; Cibrario, N. Chloromethyl- and aminomethyl(acetyl)benzodioxan isomers and derivatives resulting from oxidation of the acetyl group. *Bull. Soc. Chim. Fr.* 1958, 470–473.
- Furumai et al., 2002 R. Furumai, A. Matsuyama, N. Kobashi, K.H. Lee, M. Nishiyama, H. Nakajima, A. Tanaka, Y. Komatsu, N. Nishino, M. Yoshida, S. Horinouchi FK228 (depsipeptide) as a natural prodrug that inhibits class I histone deacetylases *Cancer Res.*, 62 (2002), pp. 4916–4921.
- Fu, H.; Li, W.; Luo, J.; Lee, N.T.; Li, M.; Tsim, K.W.; Pang, Y.; Youdim, M.B.; Han, Y. *Biochem. Biophys. Res. Commun.* 2008, 366, 631-636.
- Garcia-Alloza M, Gil-Bea FJ, Diez-Ariza M, Chen CPLH, Francis PT, Lasheras B, and Ramirez MJ (2005) Cholinergic-serotonergic imbalance contributes to cognitive and behavioral symptoms in Alzheimer's disease. *Neuropsychologia* 43:442-449.
- Gaughan G, Park H, Priddle J, Craig I, and Craig S (1991) Refinement of the localization of human butyrylcholinesterase to chromosome 3q26.1-q26.2 using a PCR-derived probe. *Genomics* 11:455-458.
- Galasko DR, Peskind E, Clark CM, Quinn JF, Ringman JM, Jicha GA, Cotman C, Cottrell B, Montine TJ, Thomas RG, Aisen P., 2012. 'Antioxidants for Alzheimer disease: a randomized clinical trial with cerebrospinal fluid biomarker measures.', *Arch Neurol.*, 69: 836-41.
- Gao, L, Cueto, MA, Asselbergs, F & Atadja, P. (2002). Cloning and Functional Characterization of HDAC11, a Novel Member of the Human Histone Deacetylase Family. *J Biol Chem*, 277, 25748- 25755.
- Gallo RC, Whang-Peng J, Adamson RH (1971) Studies on the antitumor activity, mechanism of action, and cell cycle effects of camptothecin. *J Natl Cancer Inst* 46:789–795.
- Gauthier S (2002) Advances in the pharmacotherapy of Alzheimer's disease. *Canadian Medical Association Journal* 166:616-623.

- Galdeano, C.; Viayna, E.; Sola I.; Formosa, X.; Camps, P.; Badia, A.; Clos, M.V.; Relat, J.; Ratia, M.; Bartolini, M.; Mancini, F.; Andrisano, V.; Salmona, M.; Minguillón C.; González-Muñoz, G.C.; Rodríguez-Franco, M.I.; Bidon-Chanal, A.; Luque, F.J.; Muñoz-Torrero, D. *J. Med. Chem.* 2012, 55, 661.
- Galdeano C. PhD thesis. Unitat de Química Farmacèutica, Departament de Farmacologia i Química Terapèutica. Universitat de Barcelona, 2012.
- Galdeano, C. Experimental Master. Unitat de Química Farmacèutica, Departament de Farmacologia i Química Terapèutica. Universitat de Barcelona, 2006.
- Gayle, DA, Ling, Z, Tong, C, Landers, T, Lipton, JW & Carvey, PM. (2002). Lipopolysaccharide (LPS)-induced dopamine cell loss in culture: roles of tumor necrosis factor- α , interleukin-1 α , and nitric oxide. *Developmental Brain Research*, 133, 27-35.
- Getman DK, Eubanks JH, Camp S, Evans GA, and Taylor P (1992) The human gene encoding acetylcholinesterase is located on the long arm of chromosome 7. *American Journal of Human Genetics* 51:170-177.
- Gebhardt R, Lerche KS, Gotschel F, Gunther R, Kolander J, Teich L, et al. 4-Aminoethylamino-emodin-a novel potent inhibitor of GSK-3 β acts as an insulin-sensitizer avoiding downstream effects of activated beta-catenin. *J Cell Mol Med.* 2010; 14: 1276-93.
- Ghoshal, A., Das, S., Ghosh, S., Mishra, Manoj, Kumar, Sharma, V., Koli, P., Sen, E., & Basu, A., 2007, "Proinflammatory mediators released by activated microglia induces neuronal death in Japanese encephalitis", *Glia*, vol. 55, no. 5, pp. 483.
- Giacobini E (2004) Cholinesterase inhibitors: new roles and therapeutic alternatives. *Pharmacological Research* 50:433-440.
- Giovanella BC, Stehlin JS, Wall ME, Wani MC, Nicholas AW, Liu LF et al (1989) DNA topoisomerase I-targeted chemotherapy of human colon cancer xenografts. *Science* 246:1046–1048.
- Giunta, B. 2008, "Inflammaging as a prodrome to Alzheimer's disease", *J Neuroinflammation*, vol. 5, pp. 51.
- Gottlieb JA, Guarino AM, Call JB, Oliverio VT, Block JB (1970) Preliminary pharmacologic and clinical evaluation of camptothecin sodium (NSC 100880). *Cancer Chemo Rep* 54:461–470
- Greig N, Utsuki T, Ingram D, Wang Y, Pepeu G, Scali C, Yu Q, Mamczarz J, Holloway H, Giordano T, Chen D, Furukawa K, Sambamurti K, Brossi A, and Lahiri D (2005) Selective butyrylcholinesterase inhibition elevates brain acetylcholine, augments learning and lowers Alzheimer beta-amyloid peptide in rodent. *Proceedings of the National Academy of Sciences of the United States of America* 102:17213-17218.
- Grozinger, CM & Schreiber, SL. (2000). Regulation of histone deacetylase 4 and 5 and transcriptional activity by 14-3-3-dependent cellular localization. *Proceedings of the National Academy of Sciences of the United States of America*, 97, 7835-7840.
- Guardiola, AR & Yao, TP. (2002). Molecular cloning and characterization of a novel histone deacetylase HDAC10. *The Journal of Biological Chemistry*, 277, 3350-3356.
- Grant WB, Campbell A, Itzhaki RF, Savory J., 2002. 'The significance of environmental factors in the etiology of Alzheimer's disease.', *J Alzheimers Dis*, 4: 179-89.

- Greenblatt HM, Kryger G, Lewis T, Silman I, Sussman JL. 1999. 'Structure of acetylcholinesterase complexed with (-)-galanthamine at 2.3 Å resolution.', *FEBS Lett.*321-26.
- Grimes CA, Jope RS. The multifaceted roles of glycogen synthase kinase 3β in cellular signaling. *Prog Neurobiol.* 2001;65:391-426.
- Grayson, DR, Kundakovic, M & Sharma, RP. (2010). Is there a future for histone deacetylase inhibitors in the pharmacotherapy of psychiatric disorders? *Mol Pharmacol*, 77, 126-135.
- Gellert, M. (1981). "DNA Topoisomerases." *Annu. Rev. Biochem.*50(1): 879-910.
- Graeber, M.,B. & Streit, W.,J. 2010, "Microglia: biology and pathology", *Acta Neuropathol*, vol. 119, no. 1, pp. 89.
- Guo, Z., Cupples, L.A., Kurz, A., Auerbach, S.H., Volicer, L., Chui, H., Green, R.C., Sadovnick, A.D., Duara, R., DeCarli, C., Johnson, K., Go, R.C., Growdon, J.H., Haines, J.L., Kukull, W.A. & Farrer, L.A. 2000, "Head injury and the risk of AD in the MIRAGE study", *Neurology*, vol. 54, no. 6, pp. 1316.
- Guan JS, Haggarty SJ, Giacometti E, Dannenberg JH, Joseph N, Gao J, et al (2009). HDAC2 negatively regulates memory formation and synaptic plasticity. *Nature* 459(7243): 55-60.
- Guglielmotto M, Giliberto L, Tamagno E, Tabaton M 2010. 'Oxidative stress mediates the pathogenic effect of different Alzheimer's disease risk factors.', *Front Aging Neurosci*, 2, 3.
- HP, Zhu X, Casadesus G, Castellani RJ, Nunomura A, Smith MA, Lee H-g, Perry G 2010. 'Antioxidant approaches for the treatment of Alzheimer's disease. *Expert Rev Neurother*: 1201-08.
- Haass C, Selkoe DJ (2007). Soluble protein oligomers in neurodegeneration: lessons from the Alzheimer's amyloid beta-peptide. *Nat Rev Mol Cell Biol* 8(2): 101-112.
- Hamulakova S, Janovec L, Hrabínova M, Kristian P, Kuca K, Banasova M, and Imrich J (2012) Synthesis, design and biological evaluation of novel highly potent tacrine congeners for the treatment of Alzheimer's disease. *European Journal of Medicinal Chemistry* 55:23-31.
- Hart, M.J., de los Santos, R., Albert, I.N., Rubinfeld, B., and Polakis, P. (1998). Downregulation of beta-catenin by human Axin and its association with the APC tumor suppressor, beta-catenin and GSK3β. *Curr Biol* 8, 573-581.
- Hansen, L., Arden, K.C., Rasmussen, S.B., Viars, C.S., Vestergaard, H., Hansen, T., Moller, A.M., Woodgett, J.R., and Pedersen, O. (1997). Chromosomal mapping and mutational analysis of the coding region of the glycogen synthase kinase-3α and β isoforms in patients with NIDDM. *Diabetologia* 40, 940-946.
- Hagen, T., and Vidal-Puig, A. (2002). Characterisation of the phosphorylation of beta-catenin at the GSK-3 priming site Ser45. *Biochem Biophys Res Commun* 294, 324-328.
- Hanger, D.P., Betts, J.C., Loviny, T.L., Blackstock, W.P., and Anderton, B.H. (1998). New phosphorylation sites identified in hyperphosphorylated tau (paired helical filament-tau) from Alzheimer's disease brain using nanoelectrospray mass spectrometry. *J Neurochem* 71, 2465-2476.
- Hanen, E, Hauke, J, Trankle, C, Eyupoglu, IY, Wirth, B & Blumcke, I. (2008). Histone deacetylase inhibitors: possible implications for neurodegenerative disorders. *EXPERT OPINION ON INVESTIGATIONAL DRUGS*, 17, 169-184.
- Hamilton G, Proitsi P, Jehu L, Morgan A, Williams J, O'Donovan MC, Owen MJ, Powell JF, Lovestone S. Candidate gene association study of insulin signaling genes and Alzheimer's disease: evidence for SOS2,

PCK1, and PPARgamma as susceptibility loci. *Am. J Med Genet B Neuropsychiatr. Genet.* 2007;144:508–516.

- Herranz M, Esteller M (2007) DNA methylation and histone modifications in patients with cancer: potential prognostic and therapeutic targets. *Methods Mol Biol* 361:25-62.
- Heck MM, Hittelman WN, Earnshaw WC, Differential expression of DNA topoisomerases I and II during the eukaryotic cell cycle, *Proc. Natl. Acad. Sci. USA*, (1988), 85, 1086-1090.
- Hemmings, B.A., Yellowlees, D., Kernohan, J.C., and Cohen, P. (1981). Purification of glycogen synthase kinase 3 from rabbit skeletal muscle. Copurification with the activating factor (FA) of the (Mg-ATP) dependent protein phosphatase. *Eur J Biochem* 119, 443-451.
- Hicks, R. P.; Nichols, D. A.; DiTusa, C. A.; Sullivan, D. J.; Hartell, M. G.; Koser, B. W.; Bhattacharjee, A. K. *Internet Electronic J Mol. Des.* 2005, 4, 751.
- Hooper C, Killick R, Lovestone S. The GSK3 hypothesis of Alzheimer's disease. *J Neurochem.* 2008 Mar;104(6):1433-9.
- Hoshi M, Takashima A, Noguchi K, Murayama M, Sato M, Kondo S, Saitoh Y, Ishiguro K, Hoshino T, Imahori K. Regulation of mitochondrial pyruvate dehydrogenase activity by tau protein kinase I/glycogen synthase kinase 3beta in brain. *Proc. Natl. Acad. Sci USA.* 1996;93:2719–2723.
- Honda, G.; Tabata, M.; Tsuda, M. *Planta Med.* 1979, 37, 172.
- Ho SM Tang WYBelmonte de FJPrinsGS. 2006 Developmental exposure to estradiol and bisphenol A increases susceptibility to prostate carcinogenesis and epigenetically regulates phosphodiesterase type 4 variant 4. *Cancer Res* 66:5624–5632.
- Hoeflich, K.P., Luo, J., Rubie, E.A., Tsao, M.S., Jin, O., and Woodgett, J.R. (2000). Requirement for glycogen synthase kinase-3beta in cell survival and NF-kappaB activation. *Nature* 406, 86-90.
- Hormann, R. E.; Tice, C. M.; Chortyk, O.; Smith, H.; Meteyer, T. Diacylhydrazine ligands for modulating the expression of exogenous genes in mammalian systems via an ecdysone receptor complex. *PCTWO 2004/072254* 2004, pp 1–120.
- Hu,S., Begum, A.N., Jones, M.R., Oh, M.S., Beech, W.K., Beech, B. H., Yang, F.,Chen, P.,Ubeda, O.J., Kim,P.C., Davies,P.,Ma, Q.,Cole, G. M., and Frautschy, S.A.(2009). GSK3 inhibitors show benefits in an Alzheimer's disease(AD)model of neurodegeneration but adverse effects in controlanimals. *Neurobiol. Dis.* 33, 193–206.
- Ibach B and Haen E (2004) Acetylcholinesterase inhibition in Alzheimer's Disease. *Current Pharmaceutical Design* 10:231-251.
- Inestrosa, N.C.; Alvarez, A, Perez, C.A.; Moreno, R.D.; Vicente, M.; Linker, C.; Casanueva, O.I.; Soto, C.; Garrido,J. *Neuron* 1996, 16, 881-891.
- Iqbal, K. & Grundke-Iqbal, I. 2010, "Alzheimer's disease, a multifactorial disorder seeking multitherapies", *Alzheimers Dem*, vol. 6, no. 5, pp. 420.
- Iqbal, K. 2009, "Mechanisms of tau-induced neurodegeneration", *Acta Neuropathol*, vol. 118, no. 1, pp. 53-69.
- Ishiguro, K., Shiratsuchi, A., Sato, S., Omori, A., Arioka, M., Kobayashi, S., Uchida, T., and Imahori, K. (1993). Glycogen synthase kinase 3 beta is identical to tau protein kinase I generating several epitopes of paired helical filaments. *FEBS Lett* 325, 167-172.

- Itzhaki, R.F. & Wozniak, M.A. 2004, "Alzheimer's disease, the neuroimmune axis, and viral infection", *J Neuroimmunol*, vol. 156, no.1-2, pp. 1-2.
- Jaworski, T., Dewachter, I., Lechat, B., Gees, M., Kremer, A., Demedts, D., Borghgraef, P., Devijver, H., Kugler, S., Patel, S., et al. (2011). GSK-3 α /beta kinases and amyloid production in vivo. *Nature* 480, E4-5; discussion E6.
- Jackson, G.R., Wiedau-Pazos, M., Sang, T.K., Wagle, N., Brown, C.A., Massachi, S., and Geschwind, D.H. (2002). Human wild-type tau interacts with wingless pathway components and produces neurofibrillary pathology in *Drosophila*. *Neuron* 34, 509-519.
- Jho E, Lomvardas S, Costantini F. A GSK3 β phosphorylation site in axin modulates interaction with beta-catenin and Tcf-mediated gene expression. *Biochem Biophys Res Commun*. 1999;266:28-35.
- J. Huang, Y. J. Chen, W. H. Bian, J. Yu, Y. W. Zhao, and X. Y. Liu, "Unilateral amyloid- β 25-35 injection into the rat amygdala increases the expressions of aberrant τ phosphorylation kinases," *Chinese Medical Journal*, vol. 123, no. 10, pp. 1311–1314, 2010.
- Jia, J., Amanai, K., Wang, G., Tang, J., Wang, B., and Jiang, J. (2002). Shaggy/GSK3 antagonizes Hedgehog signalling by regulating Cubitus interruptus. *Nature* 416, 548-552.
- Jiang CH, Tsien JZ, Schultz PG, Hu Y (2001) The effects of aging on gene expression in the hypothalamus and cortex of mice. *Proc Natl Acad Sci U S A* 98:1930-1934.
- Jick, H., ZORNBERG, G. L., JICK, S. S., SESHADRI, S. & DRACHMAN, D. A. (2000) Statins and the risk of dementia. *Lancet*, 356, 1627-31.
- Jones R. W., et al., 2008. The Atorvastatin/Donepezil in Alzheimer's Disease Study (LEADe): design and baseline characteristics. *Alzheimers Dement*, 4, 145-53.
- Jope RS, Yuskaitis CJ, Beurel E. Glycogen synthase kinase-3 (GSK3): inflammation, diseases, and therapeutics. *Neurochem Res*. 2007;32:577-95.
- Jope, R.S., Yuskaitis, C.J., and Beurel, E. (2007). Glycogen synthase kinase-3 (GSK3): inflammation, diseases, and therapeutics. *Neurochem Res* 32, 577-595.
- Kaidanovich-Beilin, O., Lipina, T.V., Takao, K., van Eede, M., Hattori, S., Laliberte, C., Khan, M., Okamoto, K., Chambers, J.W., Fletcher, P.J., et al. (2009). Abnormalities in brain structure and behavior in GSK-3 α mutant mice. *Mol Brain* 2, 35.
- Kaufman SE, Donnell RW, Aiken DC, and Magee C (2011) Prolonged Neuromuscular Paralysis Following Rapid-Sequence Intubation with Succinylcholine. *The Annals of Pharmacotherapy* 45:e21.
- Kamal MA, Tan Y, Seale JP, and Qu X (2009) Targeting BuChE-inflammatory pathway by SK0506 to manage type 2 diabetes and Alzheimer disease. *Neurochemical Research* 34:2163-2169.
- Kataoka, M.; Hirata, K.; Kunikata, T.; Ushio, S.; Iwaki, K.; Ohashi, K.; Ikeda, M.; Kurimoto, M. *J. Gastroenterol.* 2001, 36, 5.
- Kang JH, Irwin DJ, Chen-Plotkin AS, Siderowf A, Caspell C, Coffey CS, Waligorska T, Taylor P, Pan S, Frasier M, Marek K, Kiebertz K, Jennings D, Simuni T, Tanner CM, Singleton A, Toga AW, Chowdhury S, Mollenhauer B, Trojanowski JQ, Shaw LM (2013) Association of cerebrospinal fluid beta-amyloid 1-42, T-tau, P-tau181, and alphasynuclein levels with clinical features of drug-naive patients with early Parkinson disease. *JAMA Neurol* 70:1277-1287.

- Kay, D.W., Beamish, P. & Roth, M. 1964, "Old age mental disorders in Newcastle Upon Tyne. Part I A study of prevalence", *Br J Psychiatry*, vol. 110, pp. 146.
- Kazantsev, AG. (2007). Developing a neuroprotective therapy for Parkinson's and Huntington's diseases. *Expert Opinion on Therapeutic Patents*, 17, 159-172.
- Kazantsev, AG & Thompson, LM. (2008). Therapeutic application of histone deacetylase inhibitors for central nervous system disorders. *Nature Reviews Drug Discovery*, 7, 854-868.
- Khan, N, Jeffers, M, Kumar, S, Hackett, C, Boldog, F, Khramtsov, N, Qian, X, Mills, E, Berghs, SC, Carey, N, Finn, PW, Collins, LS, Tumber, A, Ritchie, JW, Jensen, PB, Lichenstein, HS & Sehested, H. (2008). Determination of the class and isoform selectivity of small-molecule histone deacetylase inhibitors. *Biochemical Journal*, 409, 581-589.
- Khalil M, Teunissen C, and Langkammer C. 2011. Iron and neurodegeneration in multiple sclerosis. *Mult. Scler. Int.* 2011: 606807.
- Kitazawa M, Yamasaki TR, and LaFerla FM. 2004. Microglia as a potential bridge between the amyloid beta-peptide and tau. *Ann. N. Y. Acad. Sci.* 1035: 85-103.
- King, T.D., Bijur, G.N., and Jope, R.S. (2001). Caspase-3 activation induced by inhibition of mitochondrial complex I is facilitated by glycogen synthase kinase-3beta and attenuated by lithium. *Brain Res* 919, 106-114.
- Kimmel, C. B.; Ballard, W. W.; Kimmel, S. R.; Ullmann, B.; Schilling, T. F. Stages of Embryonic Development of the Zebrafish. *Dev. Dyn.* 1995, 203, 253–310.
- Kouzarides, T. (2007). Chromatin Modifications and Their Function. *Cell*, 128, 693-705.
- Kotova, O., Al-Khalili, L., Talia, S., Hooke, C., Fedorova, O.V., Bagrov, A.Y., and Chibalin, A.V. (2006). Cardiotonic steroids stimulate glycogen synthesis in human skeletal muscle cells via a Src and ERK1/2-dependent mechanism. *J Biol Chem* 281, 20085-20094.
- Krivogorsky, B.; Grundt, P.; Yolken, R.; Jones-Brando, L. *Antimicrob. Agents Chemother.* 2008, 52, 4466.
- Kockeritz L, Doble B, Patel S, Woodgett JR. Glycogen synthase kinase-3—an overview of an over-achieving protein kinase. *Curr Drug Targets.* 2006;7:1377-88.
- Koseki T, Mouri A, Mamiya T, Aoyama Y, Toriumi K, Suzuki S, Nakajima A, Yamada T, Nagai T, Nabeshima T (2012) Exposure to enriched environments during adolescence prevents abnormal behaviours associated with histone deacetylation in phencyclidine-treated mice. *Int J Neuropsychopharmacol* 15:1489-1501
- Krasinski, A.; Radić, Z.; Manetsch, R.; Raushel, J.; Taylor, P.; Sharpless, K.B.; Kolb, H.C. *J. Am. Chem. Soc.* 2005, 127, 6686-6692.
- Kola, I.; Landis, J. Can the pharmaceutical industry reduce attrition rates? *Nat. Rev. Drug Discovery* 2004, 3,711–715.
- Lane R, Potkin S, and Enz A (2006) Targeting acetylcholinesterase and butyrylcholinesterase in dementia. *International Journal of Neuropsychopharmacology* 9:101-124.
- Lagna G, Carnevali F, Marchioni M, Hemmati-Brivanlou A. Negative regulation of axis formation and Wnt signaling in *Xenopus* embryos by the Fbox/ WD40 protein beta TrCP. *Mech Dev.* 1999;80:101-6.

- Lace, G.L., Wharton, S.B. & Ince, P.G. 2007, "A brief history of tau: the evolving view of the microtubule-associated protein tau in neurodegenerative diseases", *Clin Neuropathol*, vol. 26, no. 2, pp. 43.
- Lewis, W.G.; Green, L.G.; Grynszpan, F.; Radić, Z.; Carlier, P.R.; Taylor, P.; Finn, M.G.; Sharpless, K.B. *Angew. Chem. Int. Ed.*, 2002, 41, 1053-1057.
- Leroy, K., and Brion, J.P. (1999). Developmental expression and localization of glycogen synthase kinase-3beta in rat brain. *J Chem Neuroanat* 16, 279-293.
- Leroy, K., Boutajangout, A., Authelat, M., Woodgett, J.R., Anderton, B.H., and Brion, J.P. (2002). The active form of glycogen synthase kinase-3beta is associated with granulovacuolar degeneration in neurons in Alzheimer's disease. *Acta Neuropathol* 103, 91-99.
- Leclerc S., Garnier M., Hoessel R., Marko D., Bibb J. A., Snyder G. L., Greengard P., Biernat J., Wu Y. Z., Mandelkow E. M., Eisenbrand G., Meijer L. (2001). Indirubins inhibit glycogen synthase kinase-3 beta and CDK5/p25, two protein kinases involved in abnormal tau phosphorylation in Alzheimer's disease. A property common to most cyclin-dependent kinase inhibitors? *J. Biol. Chem.* 276, 251.
- Levenson JM, O'Riordan KJ, Brown KD, Trinh MA, Molfese DL, Sweatt JD (2004) Regulation of histone acetylation during memory formation in the hippocampus. *J Biol Chem* 279:40545-40559.
- Leng Y¹, Liang MH, Ren M, Marinova Z, Leeds P, Chuang DM. Synergistic neuroprotective effects of lithium and valproic acid or other histone deacetylase inhibitors in neurons: roles of glycogen synthase kinase-3 inhibition *J Neurosci.* 2008 Mar 5;28(10):2576-88.
- Lee, J., and Kim, M.S. (2007). The role of GSK3 in glucose homeostasis and the development of insulin resistance. *Diabetes Res Clin Pract* 77 Suppl 1, S49-57.
- Liston D, Nielsen J, Villalobos A, Chapin D, Jones S, Hubbard S, Shalaby I, Ramirez A, Nason D, and White W (2004) Pharmacology of selective acetylcholinesterase inhibitors: implications for use in Alzheimer's disease. *European Journal of Pharmacology* 486:9-17.
- Liu, C., Li, Y., Semenov, M., Han, C., Baeg, G.H., Tan, Y., Zhang, Z., Lin, X., and He, X. (2002). Control of beta-catenin phosphorylation/degradation by a dual-kinase mechanism. *Cell* 108, 837-847.
- Luo, Y.; Bolon, B.; Kahn, S.; Bennett, B.D.; Babu-Khan, S.; Denis, P.; Fan, W.; Kha, H.; Zhang, J.; Gong, Y. Martin, L.; Louis, J.C.; Yan, Q.; Richards, W.G.; Citron, M.; Vassar, R. *Nat. Neurosci.* 2001, 4, 231-232.
- Lu, Q, Qiu, X, Hu, N, Wen, H, Su, Y & Richardson, BC. (2006). Epigenetics, disease, and therapeutic interventions. *Ageing Research Reviews*, 5, 449-467.
- Lucas F.R., Salinas P.C. (1997). WNT-7a induces axonal remodeling and increases synapsin I levels in cerebellar neurons. *Dev. Biol.*, 192, 31-44.
- Lucio-Eterovic, A, Cortez, M, Valera, E, Motta, F, Queiroz, R, Machado, H, Carlotti, C, Neder, L, Scrideli, C & Tone, L. (2008). Differential expression of 12 histone deacetylase (HDAC) genes in astrocytomas and normal brain tissue: class II and IV are hypoexpressed in glioblastomas. *BMC Cancer*, 8, 243.
- Lucas, J.J., Hernandez, F., Gomez-Ramos, P., Moran, M.A., Hen, R., and Avila, J. (2001). Decreased nuclear beta-catenin, tau hyperphosphorylation and neurodegeneration in GSK-3beta conditional transgenic mice. *EMBO J* 20, 27-39.

- Luo J. Glycogen synthase kinase 3beta (GSK3beta) in tumorigenesis and cancer chemotherapy. *Cancer Lett.* 2009;273:194-200.
- M.; Tsim, K.W.; Jiang, H.; Chen, K.; Li, X.; Han, Y. *Mol. Pharmacol.* 2007, 71, 1258-1267.
- Manetsch, R.; Krasiński, A.; Radić, Z.; Raushel, J.; Taylor, P.; Sharpless, K.B.; Kolb, H.C. *J. Am. Chem. Soc.* 2004, 126, 12809-12818.
- Mahley RW, Weisgraber KH, Huang Y., 2006. 'Apolipoprotein E4: a causative factor and therapeutic target in neuropathology, including Alzheimer's disease.', *Proc Natl Acad Sci USA*, 103: 5644-51
- Mattson MP. 2004. Pathways towards and away from Alzheimer's disease. *Nature* 430 (7000): 631-639.
- Matsubayashi H., Sese S., Lee J.S., Shirakawa T., Iwatsubo T., Tomita T., Yanagawa S. (2004). Biochemical characterization of the Drosophila Wingless signaling pathway based on RNA interference. *Mol. Cell. Biol.*, 24, 2012–2024.
- Martorana, A., Esposito, Z., & Koch, G., 2010, "Beyond the cholinergic hypothesis: do current drugs work in Alzheimer's disease?", *CNS Neurosci Ther*, vol. 16, no. 4, pp. 235.
- Mayeux, R., Ottman, R., Maestre, G., Ngai, C., Tang, M.X., Ginsberg, H., Chun, M., Tycko, B. & Shelanski, M. 1995, "Synergistic effects of traumatic head injury and apolipoprotein-epsilon 4 in patients with Alzheimer's disease", *Neurology*, vol. 45, no. 3, pp. 555.
- Martin, M., Rehani, K., Jope, R.S., and Michalek, S.M. (2005). Toll-like receptor-mediated cytokine production is differentially regulated by glycogen synthase kinase 3. *Nat Immunol* 6, 777-784.
- Mateo, I., Infante, J., Llorca, J., Rodriguez, E., Berciano, J., and Combarros, O. (2006). Association between glycogen synthase kinase-3beta genetic polymorphism and late-onset Alzheimer's disease. *Dement Geriatr Cogn Disord* 21, 228-232.
- Masson P, Froment M-T, Fortier P-L, Visicchio J-E, Bartels CF, and Lockridge O (1998) Butyrylcholinesterase-catalysed hydrolysis of aspirin, a negatively charged ester, and aspirin-related neutral esters. *Biochimica et Biophysica Acta (BBA) - Protein Structure and Molecular Enzymology* 1387:41-52.
- McGeer, P.,L. & McGeer, E.,G. 2007, "NSAIDs and Alzheimer disease: epidemiological, animal model and clinical studies", *Neurobiol Aging*, vol. 28, no. 5, pp. 639.
- McCombie, S.W.; Lin, S.I.; Tagat, J.R.; Nazareno, D.; Vice, S.; Ford, J.; Asberom, T.; Leone, D.; Kozlowski, J.A.;
- McQuown SC, Barrett RM, Matheos DP, Post RJ, Rogge GA, Alenghat T, Mullican SE, Jones S, Rusche JR, Lazar MA, Wood MA (2011) HDAC3 is a critical negative regulator of long-term memory formation. *J Neurosci* 31:764-774.
- Mesulam M, Guillozet A, Shaw P, Levey A, Duysen E, and Lockridge O (2002) Acetylcholinesterase knockouts establish central cholinergic pathways and can use butyrylcholinesterase to hydrolyze acetylcholine. *Neuroscience* 110:627-639.
- Meijer, L., Skaltsounis, A.L., Magiatis, P., Polychronopoulos, P., Knockaert, M., Leost, M., Ryan, X.P., Vonica, C.A., Brivanlou, A., Dajani, R., et al. (2003). GSK-3-selective inhibitors derived from Tyrian purple indirubins. *Chem Biol* 10, 1255-1266.
- Meijer, L., Flajolet, M., and Greengard, P. (2004). Pharmacological inhibitors of glycogen synthase kinase 3. *Trends Pharmacol Sci* 25, 471-480.

- Meraz-Rios MA, Toral-Rios D, Franco-Bocanegra D, Villeda-Hernandez J, and Campos- Pena V. 2013. Inflammatory process in Alzheimer's Disease. *Front Integr. Neurosci.*7: 59. Meares, G.P., and Jope, R.S. (2007). Resolution of the nuclear localization mechanism of glycogen synthase kinase-3: functional effects in apoptosis. *J Biol Chem* 282, 16989-17001.
 - Miller JR. The Wnts. *Genome Biol.* 2002;3:REVIEWS3001.
 - Meyer KN, Kjeldsen E, Straub T, Knudsen BR, Hickson ID, Kikuchi A, Kreipe H, Boege F. Cell cycle-coupled relocation of types I and II topoisomerases and modulation of catalytic enzyme activities. *J. Cell Biol.*, (1997), 136, 775-788.
- McLeod HL, Douglas F, Oates M, Symonds RP, Prakash D, Van der Zee GJ, Kaye SB, Brown R, Keith WN. Topoisomerase I and II activity in human breast, cervix, lung and colon cancer. *Int. J. Cancer*, (1994), 59, 607-611.
- Miranda, TB & Jones, PA. (2007). DNA methylation: the nuts and bolts of repression. *J Cell Physiol*, 213, 384-390.
 - Mitscher, L. A.; Baker, W. *Med. Res. Rev.* 1998, 18, 363.
 - Miklossy, J. 2008, "Chronic inflammation and amyloidogenesis in Alzheimer's disease - Role of spirochetes", *J Alzheimers Dis*, vol. 13, no. 4, pp. 381-391.
 - Miyoshi, K. 2009, "What is 'early onset dementia'?", *Psychogeriatrics*, vol.9, no. 2, pp. 67. Levy-Lahad E, Lahad A, Wijsman EM, Bird TD, Schellenberg GD., 1995. 'Apolipoprotein E genotypes and age of onset in early-onset familial Alzheimer's disease.', *Ann Neurol.*, 38: 678-80.
 - Michishita, E, Park, JY, Burneskis, JM, Barrett, JC & Horikawa, I. (2005). Evolutionarily Conserved and Nonconserved Cellular Localizations and Functions of Human SIRT Proteins. *Mol Biol Cell*, 16, 4623-4635.
 - Michan, S & Sinclair, D. (2007). Sirtuins in mammals: insights into their biological function. *Biochemical Journal*, 404, 1-13.
 - Michishita, E, Park, JY, Burneskis, JM, Barrett, JC & Horikawa, I. (2005). Evolutionarily Conserved and Nonconserved Cellular Localizations and Functions of Human SIRT Proteins. *Mol Biol Cell*, 16, 4623-4635.
 - M. Kilgore, C. A. Miller, D. M. Fass et al., "Inhibitors of class I histone deacetylases reverse contextual memory deficits in a mouse model of alzheimer's disease," *Neuropsychopharmacology*, vol. 35, no. 4, pp. 870-880, 2010.
 - Morphy, R.; Rankovic, Z. *J. Med. Chem.* 2005, 48, 6523-6543.
 - Morishima-Kawashima, M., Hasegawa, M., Takio, K., Suzuki, M., Yoshida, H., Titani, K., and Ihara, Y. (1995). Proline-directed and non-proline-directed phosphorylation of PHF-tau. *J Biol Chem* 270, 823-829.
 - Morales I, Guzman-Martinez L, Cerda-Troncoso C, Farias GA, and Maccioni RB. 2014.
 - Morphy, R.; Rankovic, Z. Designed multiple ligands. An emerging drug discovery paradigm. *J. Med. Chem* 2005, 48, 6523-6543.
 - Moertel CG, Schutt AJ, Reitemeier RJ, Hahn RG (1972) Phase II study of camptothecin (NSC 100880) in the treatment of advanced gastrointestinal cancer. *Cancer Chemo Rep* 56:95-101.

- Morales I, Guzman-Martinez L, Cerda-Troncoso C, Farias GA, and Maccioni RB. 2014. Neuroinflammation in the pathogenesis of Alzheimer's disease. A rational framework for the search of novel therapeutic approaches. *Front Cell Neurosci*.8: 112.
- M.P. Coghlan, A.A. Culbert, D.A. Cross, S.L. Corcoran, J.W. Yates, N.J. Pearce, O.L. Rausch, G.J. Murphy, P.S. Carter, L. Roxbee Cox, D. Mills, M.J. Brown, D. Haigh, R.W. Ward, D.G. Smith, K.J. Murray, A.D. Reith, J.C. Holder, Selective small molecule inhibitors of glycogen synthase kinase-3 modulate glycogen metabolism and gene transcription, *Chem. Biol.* 7 (2000) 793-803.
- Mudher, A. & Lovestone, S. (2002) Alzheimer's disease-do taoists and baptists finally shake hands? *Trends Neurosci*, 25, 22-6. MATTSON, M. P. (2004) Pathways towards and away from Alzheimer's disease. *Nature*, 430, 631-9.
- Muñoz-Torrero, D. *Curr. Med. Chem.* 2008, 15, 2433-2455.
- Nunomura, A. 2001, "Oxidative damage is the earliest event in Alzheimer disease", *J Neuropathol Exp Neurol*, vol. 60, no. 8, pp. 759-67.
- ODDO, S., CACCAMO, A., KITAZAWA, M., TSENG, B. P. & LAFERLA, F. M. (2003) Amyloid deposition precedes tangle formation in a triple transgenic model of Alzheimer's disease. *Neurobiol Aging*, 24, 1063-70.
- Onyango, I.G., Lu, J., Rodova, M., Lezi, E., Crafter, A.B. & Swerdlow, R.H., 2010, "Regulation of neuron mitochondrial biogenesis and relevance to brain health", *Biochim Biophys Acta*, vol. 1802, pp. 228.
- Paling NR, Wheadon H, Bone HK, Welham MJ. Regulation of embryonic stem cell self-renewal by phosphoinositide 3-kinase-dependent signaling. *J Biol Chem.* 2004;279:48063-70.
- Palomo V, Soteras I, Perez DI, Perez C, Gil C, Campillo NE, et al. Exploring the binding sites of glycogen synthase kinase 3. Identification and characterization of allosteric modulation cavities. *J Med Chem.* 2011; 54: 8461-70.
- Pang, Y.P.; Quiram, P.; Jelacic, T.; Hong, F.; Brimijoin, S. *J. Biol. Chem.* 1996, 271, 23646-23649
- Perez, M. et al. (2003) Prion peptide induces neuronal cell death through a pathway involving glycogen synthase kinase 3. *Biochem. J.* 372, 129–136.
- Pei, J.J., Braak, E., Braak, H., Grundke-Iqbal, I., Iqbal, K., Winblad, B., and Cowburn, R.F. (1999). Distribution of active glycogen synthase kinase 3beta (GSK-3beta) in brains staged for Alzheimer disease neurofibrillary changes. *J Neuropathol Exp Neurol* 58, 1010-1019.
- Perez, D.I., Conde, S., Perez, C., Gil, C., Simon, D., Wandosell, F., Moreno, F.J., Gelpi, J.L., Luque, F.J., and Martinez, A. (2009). Thienyl halomethyl ketones: irreversible glycogen synthase kinase 3 inhibitors usefull pharmacological tools. *Bioorg. Med. Chem.* 17, 6914–6925.
- Peterson, CL & Laniel, MA. (2004). Histones and histone modifications. *Current Biology*, 14, R546-R551.
- Peleg S, Sananbenesi F, Zovoilis A, Burkhardt S, Bahari-Javan S, Agis-Balboa RC, Cota P, Wittnam JL, Gogol-Doering A, Opitz L, Salinas-Riester G, Dettenhofer M, Kang H, Farinelli L, Chen W, Fischer A (2010) Altered histone acetylation is associated with age-dependent memory impairment in mice. *Science* 328:753-756.
- Perl, D. & Brody, A. 1980, "Alzheimer's disease: X-ray spectrometric evidence of aluminum accumulation in neurofibrillary tangle-bearing neurons", *Science*, vol. 208, no. 4441, pp. 297-299.

- Periodontal diseases", *Alzheimers Dem*, vol. 4, no. 4, pp. 242-250.
- Perl DP. 2010. 'Neuropathology of Alzheimer's disease. ', *Mt Sinai J. Med. (New York)*, 77: 32-42.
- Pitzer, K. K.; Scovill, J. P.; Kyle, D. E.; Gerena, L. *PCT Int. Appl. WO0018769A2*, 2000.
- Potter, A.; Corwin, J.; Lang, J.; Piasecki, M.; Lenox, R.; Newhouse, P.A. *Psychopharmacology* 1999, 142, 334-342.
- Polakis, P. (2000). Wnt signaling and cancer. *Genes Dev* 14, 1837-1851.
- Poupiana, S.; Espargaró, A.; Galdeano, C.; Viayna, E.; Sola, I.; Ventura, S.; Muñoz-Torrero, D.; Sabate, R. Thioflavin-S staining of bacterial inclusion bodies for the fast, simple, and inexpensive screening of amyloid aggregation inhibitors. *Curr. Med. Chem.* 2014, 21, 1152–1159.
- Portela, A & Esteller, M. (2010). Epigenetic modifications and human disease. *Nat Biotechnol*, 28, 1057-1068.
- Postow L., Peter B.J. and Cozzarelli N.R (1999) Knot what we thought before: the twisted story of replication. *BioEssays*. 21: 805-808.
- Pommier Y, Cushman M (2009) The indenoisoquinoline noncamptothecin topoisomerase I inhibitors: update and perspectives. *Mol Cancer Therapy*.
- P. J. Hajduk, J. Dinges, J. M. Schkeryantz, D. Janowick, M. Kaminski, M. Tufano, D. J. Augeri, A. Petros, V. Nienaber, P. Zhong, R. Hammond, M. Coen, B. Beutel, L. Katz and S. W. Fesik, *J. Med. Chem.*, 1999, 42, 3852-3859.
- Praticò D. 2008. 'Evidence of oxidative stress in Alzheimer's disease brain and antioxidant therapy: lights and shadows.', *Ann N Y Acad Sci.*, 1147: 70-78.
- Pohanka M, Sobotka J, Stetina R. Sulfur mustard induced oxidative stress and its alteration by epigallocatechin gallate. *Toxicol Lett.* 2011a;201:105–109.
- Qing, H., He, G., Ly, P.T., Fox, C.J., Staufienbiel, M., Cai, F., Zhang, Z., Wei, S., Sun, X., Chen, C.H., et al. (2008). Valproic acid inhibits Abeta production, neuritic plaque formation, and behavioral deficits in Alzheimer's disease mouse models. *J Exp Med* 205, 2781-2789.
- Qizilbash N, Whitehead A, Higgins J, et al. 1998. 'Cholinesterase inhibition for Alzheimer's disease: a meta-analysis of the tacrine trials', *Journal of the American Medical Association* , 280: 1777-82.
- Quirion, R.; Wilson, A.; Rowe, W. J. *Neurosci.* 1995, 15, 1455-1462.
- Reiman EM, Webster JA, Myers AJ, et al. GAB2 alleles modify Alzheimer's risk in APOE epsilon4 carriers. *Neuron.* 2007;54:713–720.
- Rogaeva, E.,etal . (2007) The neuronal sortilinrelated receptor SORL1 is genetically associated with Alzheimer disease. *Nat Genet.*
- Romig H, Richter A. Expression of the topoisomerase I gene in serum stimulated human fibroblasts. *Biochim. Biophys. Acta.*, (1990), 1048, 274-280.
- Roca J, Ishida R, Berger JM, Andoh T, Wang JC. Antitumour bisdioxopiperazines inhibit yeast DNA topoisomerase II by trapping the enzyme in the form of a closed protein clamp. *Proc. Natl. Acad. Sci. USA*, (1994), 91, 1781-1785.
- Rylatt, D.B., Aitken, A., Bilham, T., Condon, G.D., Embi, N., and Cohen, P. (1980). Glycogen synthase from rabbit skeletal muscle. Amino acid sequence at the sites phosphorylated by glycogen synthase kinase-

3, and extension of the N-terminal sequence containing the site phosphorylated by phosphorylase kinase. *Eur J Biochem* 107, 529-537.

- Scovill, J.; Blank, E.; Konnick, M.; Nenortas, E.; Shapiro, T. *Antimicrob. Agents Chemother.* 2002, 46, 882.
- Schmidt, B.H., Burgin, A.B., Deweese, J.E., Osheroff, N., and Berger, J.M. (2010). A novel and unified two-metal mechanism for DNA cleavage by type II and IA topoisomerases. *Nature* 465, 641–644.
- Scarpellini, M. *Experimental Master*. Unitat de Química Farmacèutica, Departament de Farmacologia i Química Terapèutica. Universitat de Barcelona, 2006.
- S. D. Hanton, *Chem. Rev.*, 2001, 101, 527-570.
- Selenica M. L., Jensen H. S., Larsen A. K., Pedersen M. L., Helboe L., Leist M., Lotharius J. (2007). Efficacy of small-molecule glycogen synthase kinase-3 inhibitors in the postnatal rat model of tau hyperphosphorylation. *Br. J. Pharmacol.* 152, 959–979. doi:10.1038/sj.bjp.0707471.
- Sieiman RJ., Catchpoole D.R and Stewart B.W. (1998) Drug-induced death of leukaemic cells after G2/M arrest: higher order DNA fragmentation as an indicator of mechanism. *Br. J. Cancer.* 77: 40-50
- S. L. Cole and R. Vassar, *J. Biol. Chem.*, 2008, 283, 29621-29625.
- Smith, P.D. et al. (2003) Cyclin-dependent kinase 5 is a mediator of dopaminergic neuron loss in a mouse model of Parkinson's disease. *Proc. Natl. Acad. Sci. U. S. A.* 100, 13650–13655.
- Smith AG. Embryo-derived stem cells: of mice and men. *Annu Rev Cell Dev Biol.* 2001;17:435-62.
- Schmitt, B.; Bernhardt, T.; Moeller, H.J.; Heuser, I.; Frolich, L. Combination therapy in Alzheimer's disease: a review of current evidence. *CNS Drugs* 2004, 18, 827-844.
- Summers WK (2006) Tacrine, and Alzheimer's treatments. *Journal of Alzheimer's Disease* 9:439-445.
- Spittaels, K., Van den Haute, C., Van Dorpe, J., Geerts, H., Mercken, M., Bruynseels, K., Lasrado, R., Vandezande, K., Laenen, I., Boon, T., et al. (2000). Glycogen synthase kinase-3beta phosphorylates protein tau and rescues the axonopathy in the central nervous system of human four-repeat tau transgenic mice. *J Biol Chem* 275, 41340-41349.
- S. Peleg, F. Sananbenesi, A. Zovoilis et al., "Altered histone acetylation is associated with age-dependent memory impairment in mice," *Science*, vol. 328, no. 5979, pp. 753–756, 2010.
- S. Sankaranarayanan, E. A. Price, G. Wu, M.-C. Crouthamel, X.-P. Shi, K. Tugusheva, K. X. Tyler, J. Kahana, J. Ellis, L. Jin, T. Steele, S. Stachel, C. Coburn and A. J. Simon, *J. Pharmacol. Exp. Ther.*, 2008, 324, 957-969.
- Stewart L., Redinbo M.R, Qiu X., Hoi W.G.J. and Champoux J.J. (1998) A model for the mechanism of human topoisomerase I. *Science.* 279: 1534-1540.
- Staker, B. L., K. Hjerrild, et al. (2002). "The mechanism of topoisomerase I poisoning by a camptothecin analog." *Proc. Natl. Acad. Sci. U. S. A.* 99(24): 15387-15392.
- Stein, A. (1980). DNA wrapping in nucleosomes. The linking number problem re-examined. *Nucleic Acids Res*, 8, 4803-4820.
- Stewart L., Redinbo M.R, Qiu X., Hoi W.G.J. and Champoux J.J. (1998) A model for the mechanism of human topoisomerase I. *Science.* 279: 1534-1540.

- Sun, X., Sato, S., Murayama, O., Murayama, M., Park, J.M., Yamaguchi, H., and Takashima, A. (2002). Lithium inhibits amyloid secretion in COS7 cells transfected with amyloid precursor protein C100. *Neurosci Lett* 321, 61-64.
- Swerdlow, R.H. & Khan, S.M., 2009, "The Alzheimer's disease mitochondrial cascade hypothesis: An update", *Exp Neurol*, vol. 218, no. 2, pp. 308.
- Taipale, J., and Beachy, P.A. (2001). The Hedgehog and Wnt signalling pathways in cancer. *Nature* 411, 349-354.
- Tanzi, R., Kovacs, D., Kim, T., Moir, K., Guenette, S. & Wasco, W. 1996, "The gene defects responsible for familial Alzheimer's disease", *Neurobiol Dis*, vol. 3, no. 3, pp. 159-168.
- Terry, R. & Pena, C. 1965, "Experimental production of neurofibrillary degeneration 2. Electron microscopy, phosphatase histochemistry and electron probe analysis", *J Neuropathol Exp Neurol*, vol. 24, pp. 200.
- Ter Haar E., Coll J.T., Austen D.A., Hsiao H.M., Swenson L., Jain J. (2001). Structure of GSK3beta reveals a primed phosphorylation mechanism. *Nat. Struct. Biol.*, 8, 593–596.
- Terry, A. V., JR. & BUCCAFUSCO, J. J. (2003) The cholinergic hypothesis of age and Alzheimer's disease-related cognitive deficits: recent challenges and their implications for novel drug development. *J Pharmacol Exp Ther*, 306, 821-7.
- Thanmbisetty, M., 2010. Association of plasma clusterin concentration with severity, pathology, and progression in Alzheimer disease. *Arch Gen Psychiatry*, 67, 739-48.
- Tucker RP. 1990. The roles of microtubule-associated proteins in brain morphogenesis: a review. *Brain Res. Brain Res. Rev.*15 (2): 101-120.
- Tuppo, E.,E. & Arias, H.,R. 2005, "The role of inflammation in Alzheimer's disease", *Int J Biochem Cell Biol*, vol. 37, no. 2, pp. 289.
- Turner PR, O'Connor K, Tate WP, and Abraham WC (2003) Roles of amyloid precursor protein and its fragments in regulating neural activity, plasticity and memory. *Progress in Neurobiology* 70:1-32.
- Turley H, Comley M, Houlbrook S, Nozaki N, Kikuchi A, Hickson ID, Gatter K, Harris AL, The distribution and expression of the two isoforms of DNA topoisomerase II in normal and neoplastic human tissues, *B. J. Cancer*, (1997), 75(9).
- Twig, G., Hyde, B., & Shirihai, O.S. 2008, "Mitochondrial fusion, fission and autophagy as a quality control axis: The bioenergetic view", *Biochim Biophys Acta*, vol. 1777, pp. 1092.
- Van der Flier, W.M., Pijnenburg, Y.A.L., Fox, N.C. & Scheltens, P. 2011, "Early-onset versus late-onset Alzheimer's disease: the case of the missing APOE epsilon 4 allele", *Lancet Neurol*, vol. 10, no. 3, pp. 280-288.
- Van Gool W. A., Weinstein H. C., Scheltens P., Walstra G. J., Scheltens P. K. (2001). Effect of hydroxychloroquine on progression of dementia in early Alzheimer's disease: an 18 month randomised, double-blind, placebo-controlled study. *Lancet* 358, 455–460.1016/S0140-6736(01)05623-9.
- Van Marum R (2008) Current and future therapy in Alzheimer's disease. *Fundamental & Clinical Pharmacology* 22:265-274.
- Van der Zee AG, Hollerman H, De Jong S, Boonstra H, Gouw A, Willems PH, Zijlstra JG, Devries EJ. P-glycoprotein expression and DNA topoisomerase I and II activity in benign tumours of the ovary and in

malignant tumours of the ovary before and after platinum/cyclophosphamide chemotherapy, *Cancer Research*, (1991), 51(1),5915-5920.

- Verdel A, Curtet S, Brocard MP, Rousseaux S, Lemercier C, Yoshida M, Khochbin S (2000) Active maintenance of mHDA2/mHDAC6 histone-deacetylase in the cytoplasm. *Curr Biol* 10:747-749.
- Vernier, J.M.; El-Abdellaoui, H.; Holsenback, H.; Cosford, N.D.; Bleicher, L.; Barker, G.; Bontempi, B.; Chavez- Noriega, L.; Menzaghi, F.; Rao, T.S.; Reid, R.; Saccaan, A.I.; Suto, C.; Washburn, M.; Lloyd, G.K.; McDonald, I.A. *J.Med. Chem.* 1999, 42, 1684-1686.
- Verdile. G.; Fuller, S.; Atwood, C.S.; Laws, S.M.; Gandy, S.E.; Martins, R.N. *Pharmacol. Res.* 2004, 50, 397-409.
- Villagra, A, Cheng, F, Wang, HW, Suarez, I, Glozak, M, Maurin, M, Nguyen, D, Wright, KL, Atadja, PW, Bhalla, K, Pinilla-Ibarz, J, Seto, E & Sotomayor, EM. (2009). The histone deacetylase HDAC11 regulates the expression of interleukin 10 and immune tolerance. *Nat Immunol*, 10, 92-100.
- Von Bernhardt R, Eugenín J. 2012. 'Alzheimer's disease: redox dysregulation as a common denominator for diverse pathogenic mechanisms.', *Antioxid Redox Signal.*, 16: 974-1031.
- Wani MC, Wall ME (1969) Plant antitumor agents. II. The structure of two new alkaloids from *Camptotheca acuminata*. *J Org Chem* 34:1364–1367.
- Wagner, JM, Hackanson, B, Lubbert, M & Jung, M. (2010). Histone deacetylase (HDAC) inhibitors in recent clinical trials for cancer therapy. *Clin Epigenetics*, 1, 117-136.
- Wang J.C. (1996) DNA topoisomerases. *Annu. Rev. Biochem.* 65: 635-692
- Wang, J. C. (1971). "Interaction between DNA and an *Escherichia coli* protein omega." *J. Mol. Biol.*55(3): 523-533.
- Wang, J. C. (2002). "Cellular roles of DNA topoisomerases: a molecular perspective." *Nat. Rev. Mol. Cell Biol.*3(6): 430-440.
- Wagman, A.S., Johnson, K.W., and Bussiere, D.E. (2004). Discovery and development of GSK3 inhibitors for the treatment of type 2 diabetes. *Curr Pharm Des* 10, 1105-1137.
- Watkins P, Zimmerman H, Knapp M, Gracon S, and Lewis K (1994) Hepatotoxic effects of tacrine administration in patients with Alzheimer's disease. *JAMA* 271:992-998.
- Wang Y, Wang F, Yu J-P, Jiang F-C, Guan X-L, Wang C-M, Li L, Cao H, Li M-X, and Chen J-G (2012) Novel multipotent phenylthiazole–tacrine hybrids for the inhibition of cholinesterase activity, β -amyloid aggregation and Ca^{2+} overload. *Bioorganic & Medicinal Chemistry* 20:6513-6522.
- Wess, J.; Eglén, R.M.; Gautam, D. *Nat. Rev. Drug Disc.* 2007, 6, 721.
- Wehrfritz AP, Ihmsen H, Schmidt S, Müller C, Filitz J, Schüttler J, and Koppert W (2010) Interaction of physostigmine and alfentanil in a human pain model. *British Journal of Anaesthesia* 104:359-368.
- Weggen S., Eriksen J. L., Das P., Sagi S. A., Wang R., Pietrzik C. U., Findlay K. A., Smith T. E., Murphy M. P., Bulter T., Kang D. E., Marquez-Sterling N., Golde T. E., Koo E. H. (2001). A subset of NSAIDs lower amyloidogenic $A\beta_{42}$ independently of cyclooxygenase activity. *Nature* 414, 212–216.1038/35102591.
- WHO, International Agency for Research on Cancer, World Cancer Report 2008.
- Whitehouse PJ, Price DL, Struble RG, Clark AW, Coyle JT, and Delon MR (1982) Alzheimer's disease and senile dementia: loss of neurons in the basal forebrain. *Science* 215:1237-1239.

- Whitcomb, D.C. and Lowe, M.E. (2007) Human Intestinal Digestive Enzymes. *Digestive Diseases and Sciences*, 52, 1-17.
- Winston JT, Strack P, Beer-Romero P, Chu CY, Elledge SJ, Harper JW. The SCFbeta-TRCP-ubiquitin ligase complex associates specifically with phosphorylated destruction motifs in IkappaBalpha and beta-catenin and stimulates IkappaBalpha ubiquitination in vitro. *Genes Dev.* 1999;13:270-83.
- Witt, O, Deubzer, HE, Milde, T & Oehme, I. (2008). HDAC family: What are the cancer relevant targets? *Cancer letters*, Epub ahead of print.
- Wyss-Coray, T., Yan, F., Lin, A., Lambris, J., Alexander, J., Quigg, R. & Masliah, E. 2002, "Prominent neurodegeneration and increased plaque formation in complement-inhibited Alzheimer's mice", *Proc Natl Acad Sci U S A*, vol. 99, no. 16, pp. 10837.
- Xue L, Ko M-C, Tong M, Yang W, Hou S, Fang L, Liu J, Zheng F, Woods JH, Tai H-H, and Zhan C-G (2011) Design, Preparation, and Characterization of High-Activity Mutants of Human Butyrylcholinesterase Specific for Detoxification of Cocaine. *Molecular Pharmacology* 79:290-297.
- Yan XB, Wang SS, Hou HL, Ji R, Zhou JN. Lithium improves the behavioral disorder in rats subjected to transient global cerebral ischemia. *Behav Brain Res.* 2007; 177:282–289.
- Yang, XJ & Seto, E. (2007). HATs and HDACs: from structure, function and regulation to novel strategies for therapy and prevention. *Oncogene*, 26, 5310-5318.
- Youdim, M. B.; Amit, T.; Bar-Am, O.; Weinreb, O.; Yogev-Falach, M. *Neurotoxic. Res.* 2006, 10, 181–192.
- Yuskaitis, C.J., and Jope, R.S. (2009). Glycogen synthase kinase-3 regulates microglial migration, inflammation, and inflammation-induced neurotoxicity. *Cell Signal* 21, 264-273.
- Zhang H., Barcelo J.M., Lee B., Kohlhagen G., Zimonjic D.B., Popescu N.C. and Pommier Y. (2001) Human mitochondrial topoisomerase I, *Proc. Natl. Acad. Sci. USA.* 98: 10608-10613.
- Zhang, L., Song, L., Terracina, G., Liu, Y., Pramanik, B. & Parker, E. 2001, "Biochemical characterization of the gamma-secretase activity that produces beta-amyloid peptides", *Biochemistry*, vol. 40, no. 16, pp. 5049.
- Zilka, Ferencik, M. & Hulin, I. 2006, "Neuroinflammation in Alzheimer's disease: protector or promoter?", *Bratisl Lek Listy*, vol. 107, no. 9, pp. 374-83.
- Zhou, G., Ruperto, V.B.; Duffy, R.A.; Lachowicz, J.E. *Bioorg. Med. Chem. Lett.* 2002, 12, 795-798.